
**An Evaluation and Analysis of
Three Dynamic Watershed
Acidification Codes (MAGIC,
ETD, and ILWAS)**

**E. A. Jenne
L. E. Eary
L. W. Vail
D. C. Girvin**

**A. M. Liebetrau
L. F. Hibler
T. B. Miley
M. J. Monsour**

January 1989

**Work Supported by
the U.S. Environmental Protection Agency
under a Related Services Agreement
with the U.S. Department of Energy
Contract DE-AC06-76RLO 1830**

**Pacific Northwest Laboratory
Operated for the U.S. Department of Energy
by Battelle Memorial Institute**



Although the research described in this article has been funded wholly or in part by the United States Environmental Protection Agency (EPA), it has not been subjected to EPA review and therefore does not necessarily reflect the views of EPA and no official endorsement should be inferred.

DISCLAIMER

This report was prepared as an account of work sponsored by an agency of the United States Government. Neither the United States Government nor any agency thereof, nor Battelle Memorial Institute, nor any of their employees, makes any warranty, expressed or implied, or assumes any legal liability or responsibility for the accuracy, completeness, or usefulness of any information, apparatus, product, or process disclosed, or represents that its use would not infringe privately owned rights. Reference herein to any specific commercial product, process, or service by trade name, trademark, manufacturer, or otherwise does not necessarily constitute or imply its endorsement, recommendation, or favoring by the United States Government or any agency thereof, or Battelle Memorial Institute. The views and opinions of authors expressed herein do not necessarily state or reflect those of the United States Government or any agency thereof.

PACIFIC NORTHWEST LABORATORY
operated by
BATTELLE MEMORIAL INSTITUTE
for the
UNITED STATES DEPARTMENT OF ENERGY
under Contract DE-AC06-76RLO 1830

Printed in the United States of America
Available from
National Technical Information Service
United States Department of Commerce
5285 Port Royal Road
Springfield, Virginia 22161

NTIS Price Codes
Microfiche A01

Printed Copy

Pages	Price Codes
001-025	A02
026-050	A03
051-075	A04
076-100	A05
101-125	A06
126-150	A07
151-175	A08
176-200	A09
201-225	A10
226-250	A11
251-275	A12
276-300	A13

AN EVALUATION AND ANALYSIS OF THREE
DYNAMIC WATERSHED ACIDIFICATION CODES
(MAGIC, ETD, AND ILWAS)

E. A. Jenne	A. M. Liebetrau
L. E. Eary	L. F. Hibler
L. W. Vail	T. B. Miley
D. C. Girvin	M. J. Monsour

January 1989

Work Supported by
the U.S. Environmental Protection Agency
under a Related Services Agreement
with the U.S. Department of Energy
Contract DE-AC06-76RLO 1830

Pacific Northwest Laboratory
Richland, Washington 99352

ABSTRACT

The U.S. Environmental Protection Agency is currently using the dynamic watershed acidification codes MAGIC, ILWAS, and ETD to assess the potential future impact of acidic deposition on surface water quality by simulating watershed acid neutralization processes. The reliability of forecasts made with these codes is of considerable concern. The present study evaluates the process formulations (i.e., conceptual and numerical representation of atmospheric, hydrologic, geochemical and biogeochemical processes), compares their approaches to calculating acid neutralizing capacity (ANC), and estimates the relative effects (sensitivity) of perturbations in the input data on selected output variables for each code. Input data were drawn from three Adirondack (upstate New York) watersheds: Panther Lake, Clear Pond, and Woods Lake. Code calibration was performed by the developers of the codes. Conclusions focus on summarizing the adequacy of process formulations, differences in ANC simulation among codes and recommendations for further research to increase forecast reliability.

SUMMARY

The need to assess the impact of acidic deposition on surface water quality has led to the development of dynamic codes that simulate watershed acidification processes. The U.S. EPA is currently using the dynamic codes MAGIC (Model of Acidification of Groundwater in Catchments), ETD (Enhanced Trickle-Down), and ILWAS (Integrated Lake Watershed Acidification Study). Because public policy decisions may be partially based on the results of simulations made with these codes, it is vital to evaluate the reliability of code forecasts by analyzing the underlying models, studying the behavior and sensitivity of the codes, and field testing the codes.

An initial step in evaluation of the reliability of these codes is taken in the present study, which includes: 1) a review and comparison of features of the codes and the formulations used to simulate hydrologic and chemical processes occurring in watersheds, 2) a comparison of forecasts of acid neutralization capacity (ANC) generated by various watershed processes in response to alternative future deposition scenarios, and 3) a statistical analysis of the sensitivity of these codes to changes in the values of selected input variables. Because of the relative abundance of data available for calibration, three Adirondack watersheds were selected for this study: Panther Lake, Clear Pond, and Woods Lake. Calibration was performed by the developers of the individual codes.

The present study permits specific statements relative to the adequacy and merit of process representations contained in the underlying models and general conclusions concerning the types of acidification and recovery studies to which the individual codes may be applicable. However, the analyses reported here do not allow an explicit assessment of the forecast reliability of these codes.

The MAGIC and ILWAS codes contain process-oriented formulations based on principles of thermodynamic equilibria and kinetics for the following geochemical and biogeochemical processes: 1) silicate mineral weathering, 2) anion adsorption, 3) cation exchange, 4) aluminum hydroxide dissolution

and speciation, 5) carbonic acid equilibria, and 6) organic acid speciation. The process formulations are much less extensive in the MAGIC code than the ILWAS code. The additional process detail in the ILWAS code has the advantages of allowing more measurement data in the calibration process and more interpretation of the relative importance of various biogeochemical processes. However, the MAGIC code has the advantage of requiring fewer input data, thereby requiring the estimation of values for fewer variables, and less time to calibrate.

The ETD code, in contrast to the MAGIC and ILWAS codes, integrates watershed processes by expressing their effects on the ANC mass balance. This approach is based on the role of ANC as the prime indicator of surface water acidification. Limitations inherent in this code include the absence of reactions of important geochemical components (e.g., Al, N), process detail (e.g., specific base cations), and the choice of kinetic (rather than equilibrium) expressions for base-cation exchange reactions. These limitations preclude both the use of available characterization data in code calibration (thus reducing the confidence in the calibration) and the interpretation of differences in the relative importance of the major acidification processes among watersheds.

Single variable perturbations ($\pm 20\%$) of selected hydrologic variables of the ILWAS and ETD codes indicated that the numerical formulations in these codes were consistent with their respective conceptual models and that the qualitative responses were in accord with expected behavior. However, these tests do not assess the adequacy of the code's conceptual representation of the complex processes controlling hydrologic flow paths within a watershed.

The relative ANC contributions from individual processes (in MAGIC and ILWAS) or aggregated geochemical processes (in ETD) were generally similar among the codes and indicate that the displacement of base cations (Ca, Mg, K, and Na) from cation-exchange sites and the supply of base cations by weathering reactions are the dominant processes buffering acidic components in the calibrated watersheds compared to SO_4^{2-} adsorption. There were, however, significant differences among the codes in the calculated net flux of ANC from the watersheds during the

calibration years. In the acidic Woods Lake watershed, SO_4^{2-} adsorption provided an ANC flux similar to that of weathering. However, the weathering flux was considerably lower for this watershed than for the other two watersheds. The ratio of ANC produced from base-cation exchange versus that from weathering was found to be a useful means of examining the consequences of code formulation and visualizing the relative magnitude and variation of the dominant sources of ANC for watersheds in different degrees of acidification. The use of a hydrogen exponent in the weathering reaction formulation (tested only for MAGIC) had little impact on the flux of ANC from weathering during a 50-year forecast period. This was a consequence of the small forecasted changes in soil pH (<0.14 pH units). However, inclusion of the H^+ dependency in the calibration and simulations is a desirable feature where pH changes of a few tenths are possible.

Sensitivity analysis with these complex codes is somewhat problematic due to the absence of information on the dependence structure of input variables and the absence of a reliable basis for determining the extent to which input variables can be perturbed without invalidating the "in calibration" state. Meaningful comparisons among these codes are also difficult because of major differences in their process formulations. Using ANC as the primary response variable, it was found for the MAGIC code that the input variable with the greatest influence on ANC was the weathering rate (grouped for both soil layers). The weathering rate explained at least 99% of the variability in lake ANC in the two non-acidic lakes. The weathering rate was also important for the acidic Woods Lake, but soil depth, SO_4^{2-} maximum adsorption capacity, and SO_4^{2-} half-saturation constant all had a significant effect on output ANC for Woods Lake. For the ETD code, the set of variables with the greatest influence on ANC varied significantly between watersheds. These variables included the hydrolysis rate constant for the lake, (a) hydrolysis fraction rate constant for the lake, (a) hydrogen ion reference concentration for

(a) Weathering variables.

lake, (a) snow melt rate, soil porosity, soil depth, and soil sulfate partition coefficient. With the ILWAS code, 82% to 86% of the ANC variability was explained by layer thickness, sulfate wet deposition factor, and annual evaporation adjustment factor.

The MAGIC code is particularly well suited to data-limited applications on a seasonal or annual time scale. Its temporal discretization of months to years precludes its application to episodic phenomena. The minimal computing and calibration requirements of the MAGIC code make it feasible to perform multiple calibrations and to carry out multiple simulations to evaluate this source of forecast uncertainty. This code can also provide valuable information during the planning stage of watershed manipulation experiments when there is minimal data. The ILWAS code, because of its emphasis on comprehensive coverage of processes that contribute to the net alkalinity budget of a watershed, is particularly suited to data-intensive research studies, such as those of the EPA Watershed Manipulation Project. This code will also provide a useful function in the EPA Watershed Manipulation Project by integrating the various ANC-generating processes in a manner not readily accomplished by examination of individual field data; application of this code may assist in the prioritization of further data collection efforts. Of the three codes studied, the minimal temporal discretization and high level of process detail makes the ILWAS code the more appropriate code for study of episodic events. However, the ILWAS code requires a much greater calibration effort than the more highly temporally and spatially aggregated MAGIC code. The most appropriate application of the ETD code appears to be to data-limited regional studies where the dominant sources of ANC are base exchange, weathering, and sulfate adsorption, i.e., watersheds where Al, nitrogen, and organic acid reactions do not contribute significant ANC.

Although this study has identified limitations of the individual watershed acidification codes in making long-term forecasts, it is concluded that forecasts made with these codes may be useful in the development of national policy for limiting the emissions of acidic

(a) Weathering variables.

deposition precursors. This requires that adequate attention be given to the inherent limitations of each code and quality of the data used in its calibration. It is recommended that the forecast reliability of these codes be evaluated by a series of studies:

1. to test the capability of these codes to predict recovery of acidified watersheds for which multi-year monitoring is available - Any lack of match between simulations and observed data can be resolved by considering uncertainties of the input data, the adequacy of process formulations, or the appropriateness of process implementation.
2. to test the predictive capability of these codes at intensively studied watersheds where the acidic deposition is being manipulated - Alternative hypotheses can be tested for any lack of match between code simulations and observational data.

To the extent that these three watersheds are representative of sensitive watersheds in the northeastern United States, it is concluded that emphasis in future data collection should be placed on the characterization of base exchange and selectivity coefficients and collection of data appropriate to calculation of weathering rates.

ACKNOWLEDGMENTS

The Acid Rain Watershed Modeling Group of the Pacific Northwest Laboratory is pleased to acknowledge the interest and encouragement received from D. H. McKenzie and P. J. Wigington of the U.S. Environmental Protection Agency. We particularly wish to acknowledge the valuable technical assistance, support, and technical reviews of B. J. Cosby and G. M. Hornberger of the University of Virginia; N. Nikolaidis and J. Schnoor of the University of Iowa; S. A. Gherini and R. K. Munson of Tetra Tech, Inc.; and K. W. Thornton and D. E. Ford of FTN Associates. Special thanks go to S. S. Lepel and M. Cross for their careful and fast typing. Thanks are also extended to R. W. Smith and J. W. Cary for their technical review and to J. R. Weber for editing this report.

GLOSSARY OF SYMBOLS

Al-org	dissolved organically complexed aluminum
ANC	acid neutralizing capacity
(aq)	aqueous species
atm	atmosphere
°C	degrees Celsius
cal	calorie
cm	centimeter
eq	equivalent
in.	inch
g	gram
(g)	gas, gaseous species
ΔH_r	enthalpy of reaction
ha	hectare
J	Joules
k	rate constant
K	equilibrium constant
kg	kilogram
kJ	kilojoules
keq	kiloequivalents
km	kilometers
L	liter
m	meter
mbar	millibar
μ eq	microequivalent
meq	milliequivalent
μ g	microgram
mg	milligram
mm	millimeter
M	moles per liter
mmol	millimole
mol	mole
mth	month

n.c.	not considered
R	ideal gas constant
sec	second
TIC	total inorganic carbon
TOC	total organic carbon
u.s.	user-supplied data
yr	year
[]	concentration of dissolved species
()	activity of dissolved species
%	percent

CONTENTS

ABSTRACT	iii
SUMMARY	v
ACKNOWLEDGMENTS	xi
GLOSSARY	xiii
1.0 INTRODUCTION	1.1
2.0 COMPARISONS OF PROCESS FORMULATIONS FOR MAGIC, ETD, AND ILWAS WATERSHED ACIDIFICATION CODES	2.1
2.1 CONCEPTUAL MODELS	2.1
2.1.1 The MAGIC Code	2.5
2.1.2 The ETD Code	2.6
2.1.3 The ILWAS Code	2.6
2.2 NUMERICAL METHODS	2.7
2.2.1 Discretization	2.8
2.2.2 Solution Techniques	2.9
2.3 ATMOSPHERIC PROCESSES	2.9
2.3.1 Meteorology	2.9
2.3.2 Deposition Chemistry	2.11
2.4 HYDROLOGIC PROCESSES	2.13
2.4.1 Canopy Hydrology	2.15
2.4.2 Snowmelt, Sublimation, and Evapotranspiration	2.16
2.4.3 Hillslope Hydrology	2.19
2.4.4 Lake Hydrology	2.23
2.4.5 Energy Balance	2.23
2.5 GEOCHEMICAL PROCESSES	2.24
2.5.1 ANC Conventions	2.26

2.5.2	Carbonic Acid Equilibria	2.31
2.5.3	Aluminum Chemistry	2.34
2.5.4	Organic Acid Chemistry	2.38
2.5.5	Mineral Weathering	2.42
2.5.6	Cation Exchange	2.47
2.5.7	Anion Retention	2.51
2.6	BIOGEOCHEMICAL PROCESSES	2.55
2.6.1	Sulfate Reduction	2.56
2.6.2	Nitrification	2.57
2.6.3	Nutrient Uptake	2.58
2.6.4	Other Biogeochemical Processes Included in the ILWAS Code	2.59
2.7	SUMMARY	2.62
3.0	ANC GENERATING PROCESSES IN MAGIC, ILWAS, AND ETD CODES	3.1
3.1	APPROACH	3.1
3.2	THE MAGIC CODE	3.4
3.3	THE ETD CODE	3.19
3.4	THE ILWAS CODE	3.24
3.5	DISCUSSION OF RESULTS	3.27
3.6	SUMMARY	3.36
4.0	BEHAVIORAL ANALYSIS WITH HYDROLOGIC VARIABLES	4.1
4.1	RESULTS	4.2
4.1.1	Snowmelt	4.2
4.1.2	Sublimation	4.3
4.1.3	Evapotranspiration	4.6
4.1.4	Subsurface Flow	4.8

4.2	CONCLUSIONS	4.9
5.0	SENSITIVITY ANALYSIS	5.1
5.1	THE MAGIC CODE	5.3
5.2	THE ETD CODE	5.13
5.3	THE ILWAS CODE	5.22
5.4	SUMMARY AND CONCLUSIONS	5.28
6.0	CONCLUSIONS	6.1
6.1	COMPARISON OF CODES	6.1
6.2	FORECAST RELIABILITY	6.6
6.3	RECOMMENDATIONS	6.8
7.0	REFERENCES	7.1
APPENDIX A - INPUT DATA REQUIRED FOR THE MAGIC, ETD, AND ILWAS WATERSHED ACIDIFICATION CODES		A.1
APPENDIX B - ANNUAL-AVERAGE FLOW-WEIGHTED ANC BUDGETS FROM MAGIC CODE FORECASTS FOR CLEAR POND, PANTHER LAKE, AND WOODS LAKE WATERSHEDS		B.1
APPENDIX C - ANNUAL-AVERAGE FLOW-WEIGHTED ANC BUDGETS FROM ETD CODE FORECASTS FOR CLEAR POND, PANTHER LAKE, AND WOODS LAKE WATERSHEDS		C.1
APPENDIX D - ANNUAL-AVERAGE FLOW-WEIGHTED ANC BUDGETS FROM ILWAS CODE FORECASTS FOR CLEAR POND, PANTHER LAKE, AND WOODS LAKE WATERSHEDS		D.1
APPENDIX E - SINGLE VARIABLE PERTURBATION BEHAVIOR ANALYSIS		E.1

FIGURES

2.1	Buffer Intensities of Four Acid/Base Systems Pertinent to Watersheds	2.41
3.1	MAGIC Code, Variation in R Forecast for the Three Watersheds for Base-Case and Type-A Deposition Scenarios (n = 0)	3.10
3.2	MAGIC Code, Variation in R Forecast for the Three Watersheds for Base-Case and Type-B Deposition Scenarios (n = 0)	3.11
3.3	MAGIC Code, Variation in R Forecast for the Three Watersheds for Base-Case and Type-A Deposition Scenarios (n = 0.5)	3.12
3.4	MAGIC Code, Variation in R Forecast for Woods and Panther Lake Watersheds for Base-Case and Type-B Deposition Scenarios (n = 0.5)	3.13
3.5	MAGIC Code, 50-yr ANC Forecasts for Woods Lake and Panther Lake, Using Both Type-A and -B Deposition Scenarios (n = 0, 3-yr Linear Ramp)	3.17
3.6	ETD Code, Variation in R for Panther Lake, Clear Pond, and Woods Lake for Base-Case and Type-A Deposition Scenarios	3.23
3.7	ILWAS Code, Variation in R (3-Yr Annual Average) for Woods Lake, Panther Lake, and Clear Pond: Base-Case and Type-A Deposition Scenarios (n = 0.5)	3.25
3.8	Coefficients of Variation of Basin Outflow ANC Among the Three Codes	3.37
E.1	Variation in ANC and Sulfate Concentrations with Perturbation of the Porosity Variable, PORE6, in the Groundwater Compartment	E.3
E.2	Variation in Flow from the Unsaturated Compartment to the Groundwater Compartment with Zero Precipitation for 30 Days, Constant Precipitation for 30 Days, Followed by Zero Precipitation for the Remaining Time	E.4

TABLES

2.1	Codes Reviewed in This Study	2.2
2.2	Major Processes Incorporated Into the Codes	2.3
2.3	Meteorological Data Required by the Codes	2.10
2.4	Chemical Constituents in Wet and Dry Deposition Considered by the MAGIC, ETD, and ILWAS Codes	2.12
2.5	Expressions Used to Describe Surface Hydrology in the MAGIC, ETD, and ILWAS Codes	2.16
2.6	Chemical Constituents Included in Soil Solutions and Surface Water for the MAGIC, ETD, and ILWAS Codes	2.25
2.7	Definitions of Acid Neutralizing Capacity (ANC) Used by the MAGIC, ETD, and ILWAS Codes	2.28
2.8	Equilibrium Constants (K_{sp}) for $Al(OH)_3(s)$ Solubility for the MAGIC and ILWAS Codes	2.35
2.9	Aluminum Complexation and Organic Acid Dissociation Reactions Used in the MAGIC and ILWAS Codes	2.39
2.10	Weathering Rate Expressions Used in the MAGIC, ETD, and ILWAS Codes	2.43
2.11	Cation Exchange Relationships Used in the MAGIC, ETD, and ILWAS Codes	2.49
2.12	Expressions for Anion Retention in the MAGIC, ETD, and ILWAS Codes	2.53
2.13	Biogeochemical Processes Used in the MAGIC, ETD, and ILWAS Codes	2.57
3.1	MAGIC Code, Forecast of Annual Average Fluxes of ANC from Individual Processes for Panther Lake, All Deposition Scenarios ($n = 0$)	3.6
3.2	MAGIC Code, Forecast of Annual Average Fluxes of ANC from Individual Processes for Woods Lake, All Deposition Scenarios ($n = 0$)	3.7
3.3	MAGIC Code, Forecast of Annual Average Fluxes of ANC from Individual Processes for Panther Lake, All Deposition Scenarios ($n = 0.5$)	3.8

3.4	MAGIC Code, Forecast of Annual Average Fluxes of ANC from Individual Processes for Woods Lake, All Deposition Scenarios (n = 0.5)	3.9
3.5	MAGIC Code, 1982-1984 Average ANC Budget for Base-Case Deposition Scenario for Panther, Clear (1984-1986), and Woods Watersheds (n = 0.5)	3.18
3.6	ETD Code, Forecasts for 3-Yr Averages of Annual Average Fluxes of ANC from Cation Exchange and Weathering for Each Compartment for Panther Lake, Clear Pond, and Woods Lake: Base-Case and $\pm 20\%$ Deposition Scenarios (n = 0.5)	3.20
3.7	ETD Code, 1982-1984 Average ANC Budget for the Base-Case Deposition Scenario for Panther, Clear (1984-1986), and Woods Watersheds	3.21
3.8	ILWAS Code, Average ANC Fluxes from Cation Exchange and Weathering for All Type-A Deposition Scenarios for Panther and Woods Lakes (n = 0.5)	3.26
3.9	ILWAS Code, 1982-1984 Average ANC Budget for the Base-Case Deposition Scenario for Panther and Woods Watersheds	3.28
3.10	Estimated Time (t_{BE}) Required to Deplete Stored Base Cations Assuming No Replenishment of Exchange Cations Via Weathering and Constant Base-Exchange (BE) Flux	3.31
3.11	Comparison of Annual Average (1982-1984) ANC of Basin Outflow for Panther, Woods, and Clear Watersheds as Predicted by ILWAS, MAGIC, and ETD	3.35
4.1	Hydrologic Variables Considered in the Behavioral Analyses of the ETD Code	4.3
4.2	Effect of $\pm 20\%$ Changes in Hydrologic Variables on Flow-Weighted Annual-Average ANC Concentrations Forecasted by the ETD Code for Woods Lake	4.4
4.3	Effect of $\pm 20\%$ Changes in Hydrologic Variables on Flow-Weighted Annual-Average ANC Concentrations Forecasted by the ETD Code for Panther Lake	4.5
4.4	Hydrologic Variables Considered in the Behavioral Analyses of the ILWAS Code	4.5
4.5	Effect of $\pm 20\%$ Changes in Hydrologic Variables on Flow-Weighted Annual-Average ANC Concentrations Forecasted by the ILWAS Code for Woods Lake	4.6

4.6	Effect of $\pm 20\%$ Changes in Hydrologic Variables on Flow-Weighted Annual-Average ANC Concentrations Forecasted by the ILWAS Code for Panther Lake	4.7
5.1	Values of the Relative Standard Deviation (W) and the Number of Standard Deviations (K) for the Calibration Region of Output Variables for the MAGIC Code	5.5
5.2	Input Variable Calibration Values and Domains for the Lower Soil Layer for the MAGIC Code	5.6
5.3	Effect of Increase of Input Variable on Output Variables in the MAGIC Code	5.8
5.4	Correction Matrix and Regression Analysis Results for the MAGIC Code	5.10
5.5	Input Variables and Domains for the ETD Code	5.14
5.6	Regression Analysis Results for the ETD Code	5.17
5.7	Significant Correlations Among "In Calibration" Input Values for the ETD Code (Woods Lake)	5.21
5.8	Input Variables and Domains of the ILWAS Code for Panther Lake	5.23
5.9	Regression Analysis Results for the ILWAS Code for Panther Lake	5.24
5.10	Correlation Matrix for the ILWAS Code for Panther Lake	5.24
5.11	Input Variables and Domains for the ILWAS Code for Woods Lake	5.26
5.12	Regression Analysis Results for the ILWAS Code for Woods Lake	5.27
5.13	Correlation Matrix for the ILWAS Code for Woods Lake	5.27
B.1	MAGIC Code, 1982-1984 Average ANC Budgets for Panther Lake: Base-Case, $\pm 20\%$ Type-A, and $\pm 20\%$ Type-B Deposition Scenarios. Acid Dependent Weathering Coefficient = 0.0	B.1
B.2	MAGIC Code, 1982-1984 Average ANC Budgets for Panther Lake: Base-Case, $\pm 20\%$ Type-A, and $\pm 20\%$ Type-B Deposition Scenarios. Acid Dependent Weathering Coefficient = 0.5	B.2
B.3	MAGIC Code, 1991-1993 Average ANC Budgets for Panther Lake: Base-Case, $\pm 20\%$ Type-A, and $\pm 20\%$ Type-B Deposition Scenarios. Acid Dependent Weathering Coefficient = 0.0	B.3
B.4	MAGIC Code, 1991-1993 Average ANC Budgets for Panther Lake: Base-Case, $\pm 20\%$ Type-A, and $\pm 20\%$ Type-B Deposition Scenarios. Acid Dependent Weathering Coefficient = 0.5	B.4

B.5	MAGIC Code, 1984-1986 Average ANC Budgets for Clear Pond: Base-Case, ±20% Type-A, and ±20% Type-B Deposition Scenarios. Acid Dependent Weathering Coefficient = 0.0	B.5
B.6	MAGIC Code, 1984-1986 Average ANC Budgets for Clear Pond: Base-Case, ±20% Type-A, and ±20% Type-B Deposition Scenarios. Acid Dependent Weathering Coefficient = 0.5	B.6
B.7	MAGIC Code, 1994-1996 Average ANC Budgets for Clear Pond: Base-Case, ±20% Type-A, and ±20% Type-B Deposition Scenarios. Acid Dependent Weathering Coefficient = 0.0	B.7
B.8	MAGIC Code, 1994-1996 Average ANC Budgets for Clear Pond: Base-Case, ±20% Type-A, and ±20% Type-B Deposition Scenarios. Acid Dependent Weathering Coefficient = 0.5	B.8
B.9	MAGIC Code, 1982-1984 Average ANC Budgets for Woods Lake: Base-Case, ±20% Type-A, and ±20% Type-B Deposition Scenarios. Acid Dependent Weathering Coefficient = 0.0	B.9
B.10	MAGIC Code, 1982-1984 Average ANC Budgets for Woods Lake: Base-Case, ±20% Type-A, and ±20% Type-B Deposition Scenarios. Acid Dependent Weathering Coefficient = 0.5	B.10
B.11	MAGIC Code, 1991-1993 Average ANC Budgets for Woods Lake: Base-Case, ±20% Type-A, and ±20% Type-B Deposition Scenarios. Acid Dependent Weathering Coefficient = 0.0	B.11
B.12	MAGIC Code, 1991-1993 Average ANC Budgets for Woods Lake: Base-Case, ±20% Type-A, and ±20% Type-B Deposition Scenarios. Acid Dependent Weathering Coefficient = 0.5	B.12
B.13	MAGIC Code, 1982, 1983, 1984 Average ANC Budgets for Panther Lake: Base-Case, ±20% Type-A, and ±20% Type-B Deposition Scenarios. Acid Dependent Weathering Coefficient = 0.5	B.13
B.14	MAGIC Code, 1984, 1985, 1986 Average ANC Budgets for Clear Pond: Base-Case Deposition Scenario. Acid Dependent Weathering Coefficient = 0.5	B.14
B.15	MAGIC Code, 1982, 1983, 1984 Average ANC Budgets for Woods Lake: Base-Case Deposition Scenario. Acid Dependent Weathering Coefficient = 0.5	B.15
C.1	ETD Code, 1982-1984 Average ANC Budgets for Panther Lake: Base Case and ±20% Deposition Scenarios	C.1
C.2	ETD Code, 1991-1993 Average ANC Budgets for Panther Lake: Base Case and ±20% Deposition Scenarios	C.2

C.3	ETD Code, 1984-1986 Average ANC Budgets for Clear Pond: Base Case and $\pm 20\%$ Deposition Scenarios	C.3
C.4	ETD Code, 1994-1996 Average ANC Budgets for Clear Pond: Base Case and $\pm 20\%$ Deposition Scenarios	C.4
C.5	ETD Code, 1982-1984 Average ANC Budgets for Woods Lake: Base Case and $\pm 20\%$ Deposition Scenarios	C.5
C.6	ETD Code, 1991-1993 Average ANC Budgets for Woods Lake: Base Case and $\pm 20\%$ Deposition Scenarios	C.6
C.7	ETD Code, 1982, 1983, and 1984 Average ANC Budgets for Panther Lake: Base Case Deposition Scenarios	C.7
C.8	ETD Code, 1984, 1985, and 1986 Average ANC Budgets for Clear Pond: Base Case Deposition Scenarios	C.8
C.9	ETD Code, 1982, 1983, and 1984 Average ANC Budgets for Woods Lake: Base Case Deposition Scenarios	C.9
D.1	ILWAS Code, 1982-1984 Average ANC Budget for Panther Lake: Base Case and $\pm 20\%$ Deposition Scenarios	D.1
D.2	ILWAS Code, 1991-1993 Average ANC Budget for Panther Lake: Base Case and $\pm 20\%$ Deposition Scenarios	D.2
D.3	ILWAS Code, 1982-1984 Average ANC Budget for Woods Lake: Base Case and $\pm 20\%$ Deposition Scenarios	D.3
D.4	ILWAS Code, 1991-1993 Average ANC Budget for Woods Lake: Base Case and $\pm 20\%$ Deposition Scenarios	D.4
D.5	ILWAS Code, 1982 Average ANC Budget Storage for Panther Lake: Base Case Deposition Scenario	D.5
D.6	ILWAS Code, 1983 ANC Budget for Panther Lake: Base Case Deposition Scenario	D.6
D.7	ILWAS Code, 1984 ANC Budget Storage for Panther Lake: Base Case Deposition Scenario	D.7
D.8	ILWAS Code, 1982 ANC Budget Storage for Woods Lake: Base Case Deposition Scenario	D.8
D.9	ILWAS Code, 1983 ANC Budget Storage for Woods Lake: Base Case Deposition Scenarios	D.9
D.10	ILWAS Code, 1984 ANC Budget Storage for Woods Lake: Base Case Deposition Scenario	D.10

1.0 INTRODUCTION

Acidic deposition can adversely affect sensitive watersheds because of the resulting acidification of soils and surface waters. Acidification has been defined as a decrease in the acid neutralizing capacity (ANC) of surface waters and a decrease in the base saturation of soils over time (NAS 1984). The amount of deposition required to cause acidification may vary among watersheds because of complex and interrelated meteorological, hydrological, and biogeochemical processes. The United States Environmental Protection Agency (EPA) is responsible for estimating the number of watersheds that may become acidic in the future at current and at reduced acidic deposition levels. Therefore, the EPA is carrying out research to determine which watershed characteristics are most important in predicting the impact of acidic deposition on surface water chemistry and biology.

Because of the complexities of acidification processes and the years, or decades, that may pass before acidification becomes evident, dynamic codes of watershed acidification processes, applied in conjunction with extensive field monitoring and research studies, are a promising tool to simulate future acidic deposition on watersheds. The combination of mathematical code simulations and extensive research may allow the consequences from current or reduced acidic deposition levels to be assessed. Because policy decisions may be partially based on the results of these code simulations, it is important to evaluate these codes. Assessment of reliability of forecasts made with these codes will require testing them on watersheds with multi-year monitoring data.

The present Pacific Northwest Laboratory study is part of a larger effort to evaluate and apply these codes to investigate watershed acidification and recovery. The work reported here represents an evaluation of three dynamic codes of watershed response to acidic deposition: MAGIC (Model of Acidification of Groundwater In Catchments), ETD (Enhanced Trickle-Down), and ILWAS (Integrated Lake-Watershed Acidification Study). Although other codes of watershed acidification have been developed (e.g., Christophersen, Seip, and Wright 1982; Booty and Kramer 1984), this study is restricted to the three codes identified above, which are now being

used by the EPA as part of their Direct-Delayed Response (DDRP) and Watershed Manipulation (WMP) projects.

Satisfactory calibration of watershed codes is essential for making reliable forecasts. The watershed codes used in this study were previously calibrated by their developers for three intensively studied watersheds located in the Adirondacks (Panther Lake, Woods Lake, and Clear Pond). Earlier investigations of these watersheds, which provided the data used to calibrate these codes, were funded by the Electric Power Research Institute (Goldstein et al. 1985).

The code evaluation reported here consists of

- an in-depth review and comparison of the formulations used in the codes to represent important physical and chemical processes occurring in watersheds
- a comparison of code predictions resulting from changes in selected variables that affect various hydrological and geochemical processes
- a statistical analysis of the sensitivity of the output of the codes to perturbations in the values of important input parameters.

This report provides a basic reference for the three codes. It includes an initial understanding of the underlying process models, evidence of the need for extensive field data for calibration, an initial indication of the respective predictive capabilities and limitations, and discussions of the relative importance of various processes and variables that affect acidification forecasts for selected watersheds. Although each of these activities provides information valuable in evaluating these codes, it is beyond the scope of this report to validate^(a) the three codes under study or to draw conclusions concerning their forecast reliability. Testing of the predictive capability of these codes for a variety of watersheds for

(a) Model validation, in its broadest sense, refers to those steps taken to develop adequate confidence in the predictive capability of the model in question and its accompanying code.

which multi-year data is available will be necessary to assess the reliability of their acidification and recovery forecasts. Nevertheless, the information presented here provides an initial framework for evaluating the application of the codes to EPA monitoring and research studies of specific watersheds and for risk assessment.

The scale of this study and its potential importance to other EPA-funded studies has made it desirable to present the results obtained to date. There is a real need to interpret further the significance of these results in the context of the published literature.

The report begins (Section 2.0) with detailed comparisons of the three codes studied: their differing conceptual models, numerical methods, and algorithms for simulating atmospheric, hydrologic, geochemical, and biological processes. Section 3.0 investigates the consequences of differing formulations of ANC generating processes in each of these codes. The effects of perturbing hydrologic variables (snowmelt, sublimation, evapotranspiration, and subsurface flow) are examined in Section 4.0. Finally, a sensitivity analysis (Section 5.0) evaluates the relative effect of selected input variables on selected output variables for each code. The general conclusions and recommendations for further study of watershed acidification codes are found in Section 6.0.

2.0 COMPARISONS OF PROCESS FORMULATIONS FOR MAGIC, ETD, AND ILWAS WATERSHED ACIDIFICATION CODES

L. E. Eary, E. A. Jenne, L. W. Vail, and D. C. Girvin

Numerical codes of watershed acidification have been developed to integrate current understanding of the interrelated meteorological, hydrological, geochemical, and biogeochemical processes that affect acid neutralization on a watershed scale. The intended use of the codes is to predict the responses of watersheds to various scenarios of future and past acid deposition. This section reviews the three dynamic codes listed in Section 1.0, the MAGIC, ETD, and ILWAS codes, in major discussions of conceptual models, numerical methods, and atmospheric, hydrologic, geochemical, and biogeochemical processes. Each section includes a code-by-code comparison of the underlying assumptions, process formulations, computational methods, and data requirements. The primary authors and main characteristics of the three codes are listed in Table 2.1. In addition to the references listed in Table 2.1, Church and Turner (1986) provide a few descriptions of previous applications of the codes.

2.1 CONCEPTUAL MODELS

The impact of acid deposition on a watershed is affected by

- the amounts of deposition of acid and acid-forming constituents
- residence time and flow routing of the acidified waters in the watershed (i.e., the hydrologic characteristics)
- the extent to which deposited acids are neutralized by geochemical and biogeochemical processes (Church and Turner 1986).

Each of the codes reviewed here incorporates these factors and processes through explicit or implicit formulations (Table 2.2). However, conceptualizing the processes operating in complex ecosystems into mathematical codes is imperfect because of limited understanding of the processes and of the relationships among those processes. For instance, the effect of a specific process within a group of related processes may not be thought important enough to include in a watershed code, but in aggregate the

TABLE 2.1. Codes Reviewed in This Study

<u>Code</u>	<u>Primary Authors</u>	<u>Institution</u>	<u>Initial Application</u>	<u>Main Characteristics/ Predictive Time Scale</u>
MAGIC/ TOPMODEL (a)	B. J. Cosby G. M. Hornberger	University of Virginia	Stream-drained forested catchment (Cosby, Hornberger, and Galloway 1985; Cosby et al. 1985)	Lumped-parameter code of equilibrium soil processes/year- decade
ETD/ PEN (b)	J. Schnoor N. Nikolaidis	University of Iowa	Midwest seepage lakes (Schnoor and Stumm 1985; Schnoor, Nikolaidis, and Glass 1986) and Adirondack lakes (Nikolaidis 1987)	Rate-limited ANC mass balance/day-season- decade
ILWAS	S. Gherini R. Munson C. Chen	Tetra Tech Inc.	Adirondack water- sheds (Chen et al. 1983; Gherini et al. 1985)	Equilibrium and rate- controlled soil, canopy, and biogeochemical processes/day-season- decade

(a) TOPMODEL (Hornberger et al. 1985) is a surface hydrology code that operates as a companion to the MAGIC code by providing the hydrologic parameters required to run the MAGIC code.

(b) The PEN code is used to estimate evaporation coefficients for the ETD code if field data are not available.

TABLE 2.2. Major Processes Incorporated into the Codes (Parentheses indicate limited treatment of process.)

	<u>MAGIC/TOPMODEL</u>	<u>ETD/PEN</u>	<u>ILWAS</u>
<u>Atmospheric Processes</u>			
- Dry deposition	X	X	X
- Wet deposition	X	X	X
<u>Hydrological Processes</u>			
- Snow sublimation		X	X
- Evapotranspiration	(X) ^(a)	X	X
- Interception storage	(X) ^(a)	X	X
- Snowmelt		X	X
- Overland flow		X	X
- Soil freezing		X	X
- Macropore flow		X	X
- Unsaturated subsurface flow		X	X
- Saturated subsurface flow		X	X
- Stream flow		X	X
- Lake stratification			X
- Lake ice formation			X
<u>Geochemical Processes</u>			
- Carbonic acid chemistry	X	X	X
- Aluminum chemistry	X		X
- Organic acid chemistry	X		X
- Weathering	X	X	X
- Anion retention	X	X	X
- Cation exchange	X	X	X
<u>Biogeochemical Processes</u>			
- SO ₄ ²⁻ reduction in lake	(X) ^(b)	X	X
- Nitrification in soil	(X) ^(b)		X
- Nutrient uptake	(X) ^(b)		X
- Canopy interactions	(X) ^(a)		X
- Litter decay	(X) ^(a)		X
- Root respiration	(X) ^(a)		X

- (a) Cosby, B. J. (written review comments, 1988) considers that canopy interactions and root decay and respiration are implicitly included in the MAGIC code by use of a dry deposition factor and by designation of CO₂ partial pressure in soils and surface waters.
- (b) Sulfate reduction, nitrification, and uptake of ions can be simulated with the MAGIC code by specifying uptake rates of SO₄²⁻ and NH₄⁺ for various hydrologic compartments.

group of processes may be sufficiently important to include in the code. Thus, lumping or aggregation of acid-neutralizing processes by areal extent or depth, or across processes, may result from inadequate understanding of the processes involved or because the additional accuracy that might be gained by considering each possible process may not improve the predictive accuracy of the codes.

Events and processes important to watershed acidification occur over several orders of magnitude of scale in space and time. For example, soil depths occur at spatial scales of centimeters to meters, while watersheds occur at spatial scales of 10s to 100s of square kilometers. Cation exchange occurs at temporal scales of seconds to hours while significant changes in weathering rates occur over decades. Two of the central problems in modeling watershed acidification are 1) to identify procedures for aggregating or disaggregating data for processes occurring on different scales and 2) to assess the reliability of forecasts made with models where the scales of the process represented may not be consistent.

The conceptual limitations of the codes and the aggregation methods used to parameterize the codes also require that many of the important variables that are incorporated in the process formulations be derived empirically through calibration procedures. Calibration is the iterative process of adjusting the values of code variables to obtain agreement between the values of code predictions and field data from monitored watersheds. However, the selection of values for calibrated variables is not a totally unguided effort. In many cases, values from well-studied watersheds, such as the three Adirondack watersheds used in this report or experimental data, are used to guide the calibration procedure and provide bounds for the calibrated variables.

The codes differ primarily in the aggregation methods and mathematical formulations used to represent the natural factors and processes affecting watershed hydrology and chemistry. The specific processes incorporated in the codes are listed in Table 2.2, and this listing provides a generalized depiction of the aggregation of processes used in the codes. However, the formulations used to represent these processes differ

significantly among the codes. These differences are the primary focus of discussion in this section.

2.1.1 The MAGIC Code

A two-soil-layer version of the original one-soil-layer MAGIC code (Cosby, Hornberger, and Galloway 1985; Cosby et al. 1985) was used in this study. The MAGIC code is a relatively simple, process-based code typically used to predict average annual watershed response to long-term deposition of acidic precipitation (Table 2.2). This code was not designed to simulate variations in water chemistry of less than a month in duration. However, it can approximate seasonal variation in water chemistry through input of monthly data on deposition chemistry and meteorological conditions. The MAGIC code uses lumped parameters of soil and soil solution properties and spatially discretized representations of topography to drive the companion hydrology code TOPMODEL. The TOPMODEL code is run in conjunction with the MAGIC code to describe watershed hydrologic properties. In the MAGIC code, both equilibrium and rate-controlled formulations are used to represent geochemical processes. For example, concentrations of aqueous aluminum and carbonic acid species are controlled by the solubilities of aluminum hydroxide and $\text{CO}_2(\text{g})$, respectively, and SO_4^{2-} by adsorption to soil minerals. Rate expressions are used to describe the individual rates of base cation resupply and loss caused by mineral weathering and uptake by vegetation, respectively. Mass balances for the major cations and anions, and the effects of aqueous aluminum and organic acid species on the acid neutralizing capacity (ANC) of surface waters, are incorporated into the code. The primary goal of the developers of the MAGIC code was to describe surface water chemistry through well-understood physical and chemical processes that could be aggregated over an entire watershed. The MAGIC code has been used for predicting average annual stream chemistry for a small (5.15 km^2) forested catchment, White Oak Run, Virginia, that has little or no overland flow and an intermittent snowpack (Cosby et al. 1985). It has also been used to simulate the recovery of a small area of a Norwegian watershed from which acid deposition was excluded (Wright and Cosby 1987).

2.1.2 The ETD Code

The ETD code (Nikolaidis 1987), similar to the MAGIC code, is a lumped-parameter code, but is based entirely on the concept of ANC mass balance. Hence, various chemical processes in the ETD code (Table 2.2), such as mineral weathering, anion adsorption and desorption, and cation exchange, are incorporated into the code as either consuming or producing ANC (Schnoor and Stumm 1985). Rate expressions are used to describe mineral weathering, cation exchange, and SO_4^{2-} reduction reactions, whereas equilibrium expressions are used to describe carbonic acid chemistry and SO_4^{2-} adsorption and desorption. The ETD code specifically emphasizes rates of mineral weathering and SO_4^{2-} reduction, but does not explicitly include any aqueous aluminum, NO_3^- , or organic acid chemistry. Mass balance calculations for individual ions were not incorporated into the precursor trickle-down code (Schnoor, Nikolaidis, and Glass 1986) from which the ETD code was derived (Nikolaidis 1987). The ETD code, however, contains mass balances for SO_4^{2-} , Cl^- , and ANC. This code was developed as an intermediate complexity code that could predict seasonal and long-term changes in the acidity of lakes receiving acid deposition based on a single master variable, ANC (Schnoor and Stumm 1985; Schnoor, Nikolaidis, and Glass 1986). The original application of the precursor trickle-down code was to seepage lakes of the midwestern United States (Schnoor, Nikolaidis, and Glass 1986). The ETD code has had limited usage, but has been applied recently to three Adirondack lakes (Nikolaidis 1987).

2.1.3 The ILWAS Code

The ILWAS code is the most process-oriented of the three codes and, consequently, the most complex of the codes considered in this report. This code uses both equilibrium and rate-limited expressions that describe mass balances for 18 chemical constituents to represent the effects of geochemical and biogeochemical processes on water chemistry (Table 2.2). Many of the formulations used to represent geochemical processes are analogous to those used in the MAGIC code, but are more extensive. Mass balances for the major cations and anions and the effects on water chemistry of aqueous aluminum and organic acids are also incorporated in

the code. In contrast to the other two codes, the ILWAS code also explicitly incorporates the effects of numerous biogeochemical processes on water chemistry (Table 2.2). The ILWAS code was designed to describe episodic, seasonal and long-term changes in water chemistry caused by acidic deposition. Because the controls of watershed chemistry are extremely complex and involve numerous interrelated hydrologic, geochemical, and biogeochemical processes that can vary in importance on a seasonal basis, the ILWAS code incorporates detailed descriptions of the majority of the processes thought to affect water chemistry (Chen et al. 1983; Gherini et al. 1985). Although this approach allows detailed consideration of numerous geochemical and biological processes involved in affecting water chemistry, it also requires a correspondingly large amount of data on the watershed, making calibration of the code more difficult. The primary application of the ILWAS code has been to drainage-type watersheds in the Adirondack lake region of New York State (Gherini et al. 1985), and to seepage lakes in Wisconsin (Knauer et al. 1984).

2.2 NUMERICAL METHODS

All three codes approach the forecasting of watershed acidification by solving a transient initial- and boundary-value problem. The initial conditions for these codes include the chemical compositions of the soil, exchange complexes, soil solution, and surface waters, and the flow routing determined by the hydrologic submodels. The boundary conditions include the meteorological conditions, precipitation amounts, and deposition chemistry. Predictions of future acidification require that synthetic data (e.g., a multiyear record of precipitation chemistry) be generated to represent future boundary conditions.

Many important watershed properties, such as slope, soil depth, hydraulic conductivity, and canopy cover, vary spatially. The codes account for spatial variability through discretization of areal and vertical properties of the watershed. The numerical solution techniques rely on standard Eulerian integration methods.

2.2.1 Discretization

Spatial discretization in the MAGIC code consists of two areally homogeneous subsurface compartments and a surface water compartment. The TOPMODEL code, which provides the hydrologic data to the MAGIC code, includes the effects on watershed hydrology of canopy interception and storage, litter layer storage, and flow through both unsaturated and saturated subsurface compartments (Hornberger et al. 1985). Areal representation of a watershed in the TOPMODEL code requires discretizing the watershed into numerous compartments to provide a spatial description of watershed topography, thereby allowing representation of the effects of variable flow contributions from the saturated subsurface zone compartment. The specification of compartments in the TOPMODEL code, which performs the flow routing for the MAGIC code, actually refers to saturated and unsaturated zones rather than to differences in soil genesis or chemical composition, as is presumed in the MAGIC code.

Discretization in the ETD code consists of a snowpack compartment, a lake compartment, and three subsurface compartments that are labeled by Nikolaidis (1987) as "soil," "unsaturated," and "ground water" compartments. The various compartments serve to control the hydrological and chemical fluxes in the watershed, where the "ground water" compartment is simultaneously a hydrologic source and sink for the lake, whereas the "soil" and "unsaturated" compartments are sources only for the lake. All three subsurface compartments are actually variably saturated. As with the MAGIC code, the lake, snow, and subsurface portions of the watershed are each considered to be areally homogeneous.

In the ILWAS code, vertical discretization includes the canopy, a snow layer, stream segments, and up to 10 subsurface layers for each subcatchment that is specified as part of areal discretization (Chen et al. 1983). The ILWAS code provides for up to 20 subcatchments and associated stream segments in addition to the lake. The lake can be divided into as many as 80 stratified layers, including ice and snow layers.

2.2.2 Solution Techniques

Both the MAGIC and ILWAS codes use standard Eulerian numerical integration techniques in which the various snow, soil, and lake compartments, which are specified as part of the spatial discretization scheme, are treated as continuously stirred batch reactors. The fluxes of chemical constituents leaving a compartment are calculated from the difference between the amount entering and the rates of the reactions occurring within the compartment during each time step. In the ETD code, all time-dependent processes are formulated as first-order differential equations. The ETD code solves these equations using a predictor-corrector integration routine. This routine is not self-starting; a Runge-Kutta algorithm is used to start calculations at the beginning of each time step.

The TOPMODEL code uses 1-day time steps for calculations of hydrologic flow routing in the watershed, but the MAGIC code uses monthly or yearly time steps in its numerical scheme. Thus, hydrologic data derived from the TOPMODEL code need to be averaged on a monthly or yearly basis before they can be used in the MAGIC code. Both the ETD and ILWAS codes use 1-day time steps to calculate hydrologic flow routing and rate-limited chemical processes.

2.3 ATMOSPHERIC PROCESSES

2.3.1 Meteorology

Because watershed acidification codes must account for fluxes of chemical constituents into a watershed, they require data on characteristic meteorological conditions. The specific meteorological data used in the codes are listed in Table 2.3. Each code requires precipitation quantity and air temperature data. The TOPMODEL, ETD, and ILWAS codes require daily meteorological data. The MAGIC code uses monthly or yearly average values derived by TOPMODEL. Precipitation quantity is used to drive the hydrologic submodels and to calculate the fluxes of chemical constituents deposited on the watershed. Air, water, and soil temperatures are used to correct temperature-dependent constants (e.g., evaporation rates,

TABLE 2.3. Meteorological Data Required by the Codes

<u>Meteorological Data</u>	<u>MAGIC/TOPMODEL</u>	<u>ETD/PEN</u>	<u>ILWAS</u>
Interval for data measurement	Monthly ^(a) yearly	Daily	Daily
Precipitation	m ^(b)	mm ^(b)	cm ^(b)
Relative humidity or dewpoint		%	%
Min. air temperature	°C		°C
Max. air temperature	°C		°C
Avg. air temperature		°C	
Mean daylight hours	%	% ^(b)	
Cloud cover (fraction) (unitless) ^(c)		(unitless)	
Atmospheric pressure			mbars
Wind speed		m•sec ⁻¹	m•sec ⁻¹

(a) TOPMODEL runs with a daily time step.

(b) Per averaging-time interval.

(c) Average values per month required.

equilibrium constants, and reaction rate constants) used in the hydrologic, geochemical, and biogeochemical submodels. Air temperatures also are used to establish whether precipitation falls as rain or snow. In both the ETD and ILWAS codes, precipitation is designated as snow if temperatures are less than 0°C. Specifically for the ILWAS code, if the minimum (T_{min}) and maximum (T_{max}) daily temperatures are below and above 0°C, respectively, then the rainfall amount (P_r) is calculated from the following expression:

$$P_r = P(T_{max} - 0^\circ\text{C}) / (T_{max} - T_{min}) \quad (2.1)$$

where P is the total amount of precipitation. The remainder of the precipitation is assumed to be present as snow (P_s):

$$P_s = P - P_r \quad (2.2)$$

The ETD code also includes a utility code named PEN (Table 2.1). This code is used to calculate evapotranspiration rates given pertinent meteorological data if measured rates are not available.

2.3.2 Deposition Chemistry

In each of the codes, the deposition chemistry is coupled with the quantity of deposition to determine the fluxes of chemical constituents into a watershed over the period of a modeling exercise. The fluxes of chemical constituents deposited as dry deposition need to be specified separately. The constituents considered as part of deposition chemistry by each of the models are listed in Table 2.4. Both the MAGIC and ILWAS codes require data on the major elemental chemistry of the deposition, whereas the ETD code uses only ANC , SO_4^{2-} , and Cl^- . For the MAGIC code, monthly or yearly average values of constituent concentrations in wet deposition are required. The ETD and ILWAS codes use daily or monthly average values, respectively. The fluxes of chemical constituents deposited in wet deposition can be easily determined from measurements of the chemical composition of rainfall and snowfall. Dry deposition is less easily measured, but can be estimated by combining measured airborne concentrations and deposition velocities of the S- and N-bearing gases, such as $\text{SO}_x(\text{g})$ and $\text{NO}_x(\text{g})$. Because quantitative data are unavailable for most watersheds, the dry deposition of a chemical constituent often is approximated by:

$$C_{di} = D_i \cdot C_{wi} \quad (2.3)$$

where C_{di} , D_i , and C_{wi} are the dry deposition amount, dry deposition factor, and wet deposition amount for constituent i . Because of measurement difficulties, considerable uncertainty exists for the dry deposition factors. The MAGIC code requires that the fluxes of various constituents

TABLE 2.4. Chemical Constituents in Wet and Dry Deposition Considered by the MAGIC, ETD, and ILWAS Codes

Constituent	MAGIC		ETD		ILWAS	
	Wet	Dry ^(a)	Wet	Dry	Wet	Dry
SO _x (g)		(X) ^(b)				X
NO _x (g)		(X) ^(b)				X
H ⁺					X	X
Al(total)					X	X
Ca ²⁺	X	X			X	X
Mg ²⁺	X	X			X	X
K ⁺	X	X			X	X
Na ⁺	X	X			X	X
NH ₄ ⁺	X	X			X	X
SO ₄ ²⁻	X	X	X	X	X	X
NO ₃ ⁻	X	X			X	X
Cl ⁻	X	X			X	X
F ⁻	X	X				
PO ₄ ³⁻					X	X
ANC			X	X	X	X
TOC ^(c)			X		X	X
TIC ^(d)					X	X
H ₄ SiO ₄ ⁰					X	X
Units	$\mu\text{eq}\cdot\text{L}^{-1}$		$\text{meq}\cdot\text{m}^{-3}$	$\text{meq}\cdot\text{m}^{-3}$	$\text{meq}\cdot\text{L}^{-1}$	$\text{meq}\cdot\text{m}^{-3}$
Interval	monthly or yearly avg.		- daily -		- monthly avg. -	

(a) The MAGIC code requires that dry deposition be expressed by means of a dry deposition factor.

(b) Cosby, B. J. (written communication, 1988) considers that SO_x(g) and NO_x(g) are implicitly included by means of the dry deposition factor.

(c) Total organic carbon.

(d) Total inorganic carbon.

in dry deposition be specified by using dry deposition factors as shown in Equation 2.3. The ETD and ILWAS codes allow measured rates of dry deposition to be used, or, alternatively, deposition factors can be entered in the model input data according to Equation 2.3.

The MAGIC code also requires a period of estimated background data on wet and dry deposition quantities for the constituents listed in Table 2.4 for the region of study. Typically, Cosby et al. (1985) have used 140 years of background data. This background level of chemical deposition is used to establish the initial base cation concentrations in soil solution and on exchange sites in the watershed (Cosby, Hornberger, and Galloway 1985; Cosby et al. 1985). A historical trend in $\text{SO}_2(\text{g})$ emission is used by the MAGIC code to scale the resulting increase in acidic deposition that occurred during the backcast period, resulting in presumed perturbations to the initial conditions. The historical trends used by Cosby et al. (1985) in studies of acid deposition effects at White Oak Run, Virginia, were based on records of $\text{SO}_2(\text{g})$ emission for the eastern United States (OTA 1984).

2.4 HYDROLOGIC PROCESSES

All three of the codes discussed in this report provide formulations of hydrologic and chemical processes. The hydrologic response of a watershed is independent of the chemical state of the watershed. However, the chemical response is strongly dependent on the hydrologic state of the watershed. Therefore, it is necessary to simulate the hydrologic flowpaths within a watershed to understand its response to acidic deposition.

The hydrologic formulations used within these codes vary significantly in their relative complexity. The ILWAS code is the most complex, principally as a result of its greater discretization. The ETD code's hydrologic formulation is intermediate in complexity between that of the ILWAS and MAGIC codes. The MAGIC code does not include any hydrologic process formulations. The aggregated flowpath estimates used in MAGIC are provided by a separate code, TOPMODEL.

The hydrologic process representations used in these codes are generally consistent with the state-of-the-art of watershed modeling. It must be noted, however, that watershed modeling is generally performed on watersheds larger than those typically considered in acid rain studies. Additionally, watershed hydrological modeling is typically concerned with forecasting outflow hydrographs, not predicting flowpaths within the watershed. Highly aggregated watershed models usually can provide accurate forecasts of watershed outflow. It is important to consider the time scales of hydrologic phenomena. The outflow from a small watershed may vary significantly over a period of less than one day. However, meteorological inputs to the codes (e.g., precipitation and air temperature) are aggregated to daily (or larger) averages. The flowpaths for 1 inch of rainfall occurring over a 1-hour period will generally be different from the flowpaths of 1 inch of rainfall occurring over a 24-hour period, even if the daily outflows are the same. Thus, small watersheds tend to accentuate the significance of small time scales of hydrologic and geochemical variables.

The accuracy with which predictions of hydrologic flowpaths can be made is limited by spatial variability of hydraulic properties throughout the watershed and typically a paucity of characteristic data. Although using multiple signals during calibration (i.e., using chemical signals as well as the hydrograph, rather than only the hydrograph) can reduce the uncertainty in flowpath predictions (de Grosbois, Hooper, and Christopherson 1988), the codes will typically remain overparameterized (Hooper et al. 1988). Our review of the literature and the codes leads to the inference that the reliability of estimating hydrologic flow paths typically limits the reliability of forecasts made with watershed acidification codes. The spatial variability of a watershed contributes to the uncertainty in flow path estimation, limiting the predictive reliability of all three watershed acidification codes.

All three codes discussed in this report contain unmeasurable variables. One might expect that more sparsely parameterized process representations in the codes contain variables that are unmeasurable due to process aggregation. However, variables in more densely parameterized

codes may also be unmeasurable or require significant aggregation of limited observations.

2.4.1 Canopy Hydrology

The quantity of precipitation that is intercepted by the foliage of a forest canopy is referred to as "interception storage." Precipitation that passes through the canopy (including stem flow) is called "throughfall." The ETD code does not consider interception storage. In the MAGIC/TOPMODEL code combination, the modeler specifies the portion of precipitation that bypasses canopy interception as throughfall before reaching maximum interception storage, such that

$$P_t = \{f_d + \delta_{I_n, I_n} (1 - f_d)\}P \quad (2.4)$$

where I_n = the amount of water intercepted

I_n = the maximum interception storage

f_d = the fractional direct throughfall

δ = the Kronecker delta (i.e., $\delta_{I,J} = 1$ when $I = J$) and
($\delta_{I,J} = 0$ when $I \neq J$)

P = precipitation

P_t = throughfall.

Once the maximum value of interception (I_n) is reached, all precipitation (P) is treated as throughfall (P_t). Seasonal variation in the maximum interception storage (I_n) is not considered in the TOPMODEL code. The ILWAS code uses an expression similar to Equation 2.4 to describe canopy hydrology, but allows the maximum interception storage to vary seasonally in proportion to the user-specified monthly leaf area index, L_{mon} , according to

$$I_n = (L_{mon}/L_{max})D_{max} \quad (2.5)$$

where L_{max} is the maximum leaf area index for the year, and D_{max} is the potential interception storage for the month having the maximum leaf area index.

TABLE 2.5. Expressions Used to Describe Surface Hydrology in the MAGIC, ETD, and ILWAS Codes in Length Units^(a)
(For the ETD code, wet and dry refer to melting caused by rainfall and by air, respectively.)

<u>Code</u>	<u>Condition</u>	<u>Snowmelt</u>	<u>Evapotranspiration</u>
MAGIC/ TOPMODEL		$(C_1 + C_2 P_t)(T_a - T_c)$	$P_{ET}(S/S_{max})^{C_3}$
ETD/PEN	dry	$C_4(1.8T_a)^{1.25}$	$C_5 P_{ET} + C_1 P_{ET}$
	wet	$1.8(0.007P_t + 0.074)T_a + 0.05$	
ILWAS		$(T_a - T_c)\{(C_5 + C_6) [0.4 + \sin(0.0087B)] + 0.0039\}$	$P_{ET}(\theta/\theta_{fc})$

(a) where $C_1 - C_6$ = constants
 P_t = throughfall
 T_a = air temperature, °C
 T_c = incipient snow formation temperature, °C
 P_{ET} = potential evapotranspiration
 S = root zone storage
 S_{max} = maximum root zone storage
 C_5, C_1 = pan correction coefficients for soil and lake compartments
 θ = volumetric soil moisture content
 θ_{fc} = θ at field capacity

2.4.2 Snowmelt, Sublimation, and Evapotranspiration

The formulations used in the three codes for the surface hydrologic processes of snowmelt, sublimation, and evaporation flow are given in Table 2.5, and are briefly discussed here.

Snowmelt

Snowmelt can be caused by rain or air temperatures that are above 0°C. However, melting snow will not drain from a snowpack until the snowpack has reached its field capacity. Each code uses an empirical expression that relates the snowmelt rate to the air temperature and, in the ETD code, to the presence or absence of rainfall (Table 2.5). The ILWAS code also includes a variable that represents the aspect of the subcatchment to account for differences in melting rates for north- versus south-facing slopes (Table 2.5). In each of the code formulations, the coefficients

that describe the rate of snowmelt are often determined through calibration procedures. The redistribution of solutes in the snowpack by freezing and thawing is not included in any of the codes. However, the ETD and ILWAS codes allow the user to represent the effect of these processes by increasing the concentration of the snowmelt over the remaining snowpack. In both the ILWAS and ETD codes, the concentrations of ions, C_i , in the snowpack are calculated using the following expression:

$$C_i = M_i/V_s \quad (2.6)$$

where M_i is the mass of ion i in the snow and V_s is the equivalent water volume of the snow. As snow melts, the solutes contained in the melted volume are removed, and the melted volume also may leach solutes from the unmelted snow, resulting in higher solute concentrations in the first melt water (Chen et al. 1983). The leaching of constituents from snow as the snow melts is included in the ETD and ILWAS codes by the differential equation

$$d(C_i V_s)/dt = -C_i + K C_i V_s \quad (2.7)$$

where K is a leaching coefficient. The solution to Equation 2.7 describes an exponential decrease in solute concentration in melt water as the snow melts.

Sublimation

A snowpack can also decrease by sublimation. Because solutes do not leave the snowpack with the vapor phase, the sublimation of snow increases the concentration of salts in the remaining snow. The ETD code estimates the sublimation rate as an empirical function of the potential evapotranspiration rate. The ILWAS code uses annual average sublimation rates that are estimated for open and forested areas. The MAGIC/TOPMODEL code combination does not include any effects of sublimation on snow chemistry. The inclusion of snow leaching and sublimation and one-day time steps makes the ETD and ILWAS models more able to simulate the episodic

increases in solute concentration often observed in spring melt waters in comparison with the MAGIC code, which does not include these processes.

Evapotranspiration

The actual amount of water lost by evapotranspiration from a watershed is expressed as a function of the potential evapotranspiration rate in all three codes (Table 2.5). The potential evapotranspiration is the rate of moisture decrease in a saturated soil and canopy for a given set of environmental conditions, such as air temperature, elevation, latitude, wind speed, and humidity. In the TOPMODEL code, the potential evapotranspiration rate, P_{ET} , for the watershed is expressed as

$$P_{ET} = (1 - C)d^2 \cdot e^{0.62T} \quad (2.8)$$

where C is a calibration coefficient, d is hours of daylight, and T is the air temperature in degrees C. The actual evapotranspiration rate is a function of P_{ET} and the amount of water stored in the soil root zone (Table 2.5). In the ETD code, actual evaporation is estimated to be a function of the potential evapotranspiration rate for the lake and soil compartments of the watershed (Table 2.5). The values of P_{ET} in the ETD code are calculated in the separate PEN code by using van Bavel's formula (van Bavel 1966) to estimate the daily potential evapotranspiration. The evapotranspiration rate in the ILWAS code is a function of both the volumetric soil-moisture content and the potential evapotranspiration rate (Table 2.5) and is described by

$$P_{ET} = C \cdot T \cdot C_E(100 - H)^{\frac{1}{2}} \quad (2.9)$$

where C = calibration constant

T = temperature, °C

C_E = a local microclimatological parameter (determined through calibration)

H = the relative humidity.

2.4.3 Hillslope Hydrology

The components of hillslope discharge summarized from Whimkey and Kirkby (1978) are:

- Infiltration excess overland flow. When rainfall intensity or snowmelt rate exceeds the infiltration capacity of the watershed soil, overland flow may occur. If this occurs over a significant portion of the watershed, overland flow will likely dominate the watershed's total discharge. Overland flow is rarely observed in vegetated and soil-covered slopes, except when the watershed's soil infiltration capacity has been decreased as a result of freezing soil conditions.
- Saturation overland flow. Once soils have become saturated from either prior vertical percolation or downslope movement of water in saturated zones of the hillslope, further precipitation or snowmelt will result in overland flow. "Saturation overland flow" occurs when all the soil beneath a site has saturated, while "infiltration excess overland flow" occurs when the soil is not entirely saturated. The area contributing to saturation overland flow will grow as rainfall or snowmelt continues and gradually recedes once rainfall or snowmelt ceases. Neither saturation overland flow or infiltration excess overland flow allow the rainfall or snowmelt an opportunity to interact geochemically with the soil.
- Return flow. Subsurface flow may return to the surface during or after a rainfall or snowmelt event. This is often the result of the convergence of flows from other portions of the hillslope, creating an increased saturated thickness. Return flow provides a wide range of residence times within different soil horizons.
- Saturated subsurface flow. Generally, saturated subsurface flow is significantly slower than overland flow. Saturated subsurface flow may occur at different layers of a stratified soil column. For instance, water infiltrating through the soil

surface may perch and flow laterally over a clay lens, while the soils below the clay lens remain unsaturated. Upper soil layers are generally likely to be more permeable to water movement than deeper saturated soil layers.

- Unsaturated subsurface flow. Water flowing through unsaturated soil is generally dominated by the force of gravity and, therefore, moves almost entirely in the vertical direction. Unsaturated flow is generally very slow. A hillslope with deep unsaturated soils will be very slow to react to a rainfall or snowmelt event, because the water must travel slowly down the unsaturated soil column before reaching a faster-responding saturated zone. The hydraulic conductivity of an unsaturated soil is a nonlinear function of moisture content.
- Ground-water flow. Saturated flow of water in the deepest portions of the slope's soil is distinguished from saturated subsurface flow in that this flow is slower to respond to rainfall or snowmelt than saturated subsurface flow. Water from ground-water flow will have the longest residence times and generally the highest ANC.

The representation of each of these components of hillslope hydrology by each of the three codes are discussed in the following sections.

Infiltration Excess Overland Flow

The TOPMODEL code does not consider surface-controlled infiltration (i.e., infiltration-excess overland flow), however, the ETD and ILWAS codes do provide explicit representations of this phenomena.

The ETD code controls surface infiltration through specification of the saturated vertical hydraulic conductivity of the uppermost subsurface compartment. This hydraulic conductivity is not a function of the soil moisture content in the compartment but is reduced during soil-freezing conditions by an empirical frost index, which is a function of air temperature.

The ILWAS code controls surface infiltration through specification of the unsaturated vertical hydraulic conductivity of the upper subsurface layer. This hydraulic conductivity is a function of both soil moisture content and temperature and is reduced during soil-freezing conditions.

Saturation Overland Flow

The ETD and ILWAS codes simulate the occurrence of saturation overland flow only when the upper subsurface compartment has become fully saturated. However, lower subsurface compartments are not required to be saturated.

The TOPMODEL code requires the entire subsurface compartment to be saturated. However, the fine resolution of spatial discretization in the TOPMODEL topographic input provides a more reliable estimate of saturation overland flow in watersheds with significant variations in areas contributing to overland flow than is possible with the coarser spatial discretization of the two other codes.

Return Flow

With the limited exception of the ILWAS code, none of the codes represent return flow. The ILWAS code can represent return flow if several subcatchments are provided between the top of the watershed and the lake. However, even the ILWAS code cannot represent return flow within a single subcatchment.

Saturated Subsurface Flow

Saturated subsurface flow may be the most important of the six components of hillslope discharge particularly when it occurs in the upper soil horizons. This flow component is the most difficult to represent accurately because of the extreme variability of hydraulic properties throughout a watershed. All three codes use a form of Darcy's law to describe saturated subsurface flow. Both the ETD and ILWAS codes allow lateral flow in subsurface compartments which are only partially saturated, where the lateral flow in each compartment is conceptualized as being composed of saturated and totally unsaturated zones. Lateral flow is estimated using Darcy's Law by assuming that the hydraulic gradient is

equal to the average catchment slope. In the ILWAS code, this slope is adjusted for the depth of the saturated zone and surface water elevation. (This elevation correction is important only in areas of slight slope.) The TOPMODEL code only provides for lateral flow in the saturated portion of each subsurface computational element.

The MAGIC/TOPMODEL code combination allows a specified portion of the water entering the top soil layer by infiltration to move to the lower layer by macropore flow, thus bypassing the requirement that the amount of water must exceed the field capacity of the top soil layer before flow to the lower layer is permitted. Macropore flow is considered to include those paths where the water can move down a "saturated pipe," such as where a root has decayed, to a lower soil horizon. This treatment results in water moving into the lower layer without becoming geochemically altered by contact with the upper soil layer. Macropore flow is not considered in either the ETD or the ILWAS codes.

Unsaturated Subsurface Flow

The ILWAS code is the only one of the three codes which attempts to represent unsaturated flow phenomena. Flow in unsaturated soils is predominately vertical. In the ILWAS code, vertical flow in a soil layer is assumed to be zero at and below the field capacity. At higher moisture contents, the vertical flow is estimated to be proportional to the degree of saturation of the soil layer. This simplified approach cannot accurately represent wetting and drying fronts in soils. However, this is probably an insignificant limitation when compared to other uncertainty resulting by the spatial variability of hydraulic properties.

Ground-Water Flow

Similar to saturated subsurface flow, all three codes use a form of Darcy's Law to describe ground-water flow. The ground-water compartment in the ETD code was developed to represent conditions in seepage lakes. In contrast to other subsurface compartments in the ETD and ILWAS codes, where the hydraulic gradient is estimated to be the average slope of the catchment, the ground-water compartment of ETD uses a separate flow specified by the user.

2.4.4 Lake Hydrology

Cooling of a lake surface in the fall often causes strong density-driven mixing to occur in the lake. This "fall overturn" can rapidly turn a stratified lake into a well-mixed lake. The MAGIC and ETD codes consider the lake to be perfectly mixed. The ILWAS code considers stratification within the lake, and up to 80 horizontal layers can be specified in the lake discretization. The mixing of solutes and the flow of heat between layers is taken into account by considering both diffusive and advective flow. The ILWAS code also simulates the formation of ice on the lake through calculations of the energy balance in the lake and the latent heat of ice formation. Because snowmelt often occurs before the ice cover on a lake has completely thawed, snowmelt flowing over or just under the ice cover of a lake could result in a significantly lower ANC than snowmelt that had mixed thoroughly with the lake waters. The MAGIC and ETD codes do not include any explicit representation of lake ice effects.

2.4.5 Energy Balance

Soil temperature is important because it influences chemical processes and infiltration. If the soil is frozen, surface infiltration will be severely limited. The ILWAS code computes the temperature of each soil layer by considering both thermal conduction between layers and the advection of energy between layers caused by the vertical movement of water. Alternatively, the user of the ILWAS model can specify soil temperatures on a daily or monthly basis. In the ETD code, an annual variation in soil temperature for all three compartments with a maximum temperature of 22.5°C and a minimum temperature of -0.5°C. These temperatures in the ETD code are assumed to be independent of air temperature and are only used to estimate the CO₂(g) partial pressure in each subsurface compartment. The MAGIC model uses monthly average temperatures for each of the soil layers and the lake.

The vertical distribution of the temperature in a lake may influence both the hydrologic routing through the lake and mixing within a lake as a result of fall overturn. Neither the MAGIC/TOPMODEL or ETD codes

considers the effects of thermal energy in the lake. The ILWAS code computes the temperature of each lake layer by considering the following:

- long-wave radiation that is absorbed by the lake surface
- short-wave radiation that can penetrate below the surface
- long-wave radiation back to the atmosphere
- evaporative heat transfer
- convective heat transfer between the atmosphere and the lake surface
- diffusive transport between lake layers.

The diffusive coefficient for transport between lake layers is calculated as a function of wind speed and three empirical constants that are determined by calibration.

2.5 GEOCHEMICAL PROCESSES

The geochemical processes important for neutralizing acidic deposition and for controlling the chemical compositions of soil and surface waters (NAS 1984) include

- carbonic acid equilibria
- aluminum hydroxide dissolution and aqueous speciation
- mineral weathering
- anion retention
- cation exchange
- buffering by organic acid dissociation.

All three codes use different formulations to represent these processes. However, the ETD code does not include aluminum, nitrogen, or organic acid chemistry. Because of differences in representations of the geochemical processes, the three codes also consider different suites of chemical constituents. The chemical constituents included in the codes are listed in Table 2.6. The MAGIC and ILWAS codes use similar lists of major cations and anions. The ILWAS code also includes organically complexed species of aluminum. Although the soil mineralogies of acid-sensitive regions are dominated by silicate minerals, only the ILWAS code includes

TABLE 2.6. Chemical Constituents Included in Soil Solutions and Surface Water for the MAGIC, ETD, and ILWAS Codes

<u>Chemical Constituent</u>	<u>MAGIC</u>	<u>ETD</u>	<u>ILWAS</u>
ANC	X	X	X
Ca ²⁺	X		X
Mg ²⁺	X		X
K ⁺	X		X
Na ⁺	X		X
NH ₄ ⁺	X		X
H ⁺	X	X	X
Al ³⁺	X		X
Al(OH) _n ³⁻ⁿ (n = 1 to 4)	X		X
Al(F) _n ³⁻ⁿ (n = 1 to 6)	X		X
Al(SO ₄) _n ³⁻²ⁿ (n = 1 to 2)	X		X
Al-R ^(a)			X
SO ₄ ²⁻	X	X	X
NO ₃ ⁻	X		X
Cl ⁻	X	X	X
F ⁻	X		X
H ₂ PO ₄ ⁻			X
H ₄ SiO ₄ (aq)			X
CO ₂ (g)	X	X	X
CO ₂ (aq)	X	X	X
H ₂ CO ₃ (aq)	X	X	X
HCO ₃ ⁻	X	X	X
CO ₃ ²⁻	X	X	X
HR ⁱ , R ⁱ⁻ (b)			X
H ₂ R ⁱⁱ , HR ⁱⁱ⁻ , R ⁱⁱ²⁻ (b)	X		X
H ₃ R ⁱⁱⁱ , H ₂ R ⁱⁱⁱ⁻ (b) HR ⁱⁱⁱ²⁻ , R ⁱⁱⁱ³⁻			X

(a) Al-R refers to the various organic complexes of aluminum.

(b) Rⁱ, Rⁱⁱ, and Rⁱⁱⁱ refer to monoprotic, diprotic, and triprotic organic acids, respectively.

dissolved silica in its simulations of solution chemistry. The ETD code includes the smallest number of constituents, which is consistent with the emphasis of this code on ANC mass balance (Table 2.6).

2.5.1 ANC Conventions

The continuous deposition of strong acids on a watershed will eventually cause a change in the pH of the soil and surface waters if the neutralizing capacity of the system is exceeded. The pH, however, quantifies only the activity of the free H⁺ ions in solution (pH = -log (H⁺)). The pH itself is not an indication of the capacity of a solution to resist changes in the H⁺ ion activity that might be caused by the addition of a strong acid or base because the pH does not account for the association of H⁺ ions with other solution species, such as CO₃²⁻ and aluminum ions. The amount of acid or base that must be added to a solution to cause an incremental change in pH is described by the buffer intensity, as follows (van Breeman and Wielemaker 1974; Stumm and Morgan 1981):

$$\beta = -dC_A/d(\text{pH}) = dC_B/d(\text{pH}) \quad (2.10)$$

where dC_A and dC_B are the incremental amounts of acid or base in molar or molal concentration units required to cause an incremental change in pH. The integral of the buffer intensity over a certain pH range provides the general definition of the ANC of the solution, i.e.,

$$\text{ANC} = \int \beta \cdot d(\text{pH}) \quad (2.11)$$

The ANC is independent of temperature and pressure (Stumm and Morgan 1981) and is an important measure of water quality in acid rain studies because it indicates the capacity of surface waters to resist changes in pH caused by the deposition of strong acids.

The ANC of a solution can be defined by the integral of the buffer intensity as in Equation 2.11 or equivalently by the summed concentrations of the H⁺ ion acceptors minus the H⁺ ion donors (Stumm and Morgan 1981), i.e.,

$$\text{ANC} = \Sigma [\text{H}^+ \text{ ion acceptors}] - \Sigma [\text{H}^+ \text{ ion donors}] \quad (2.12)$$

Based on the principle of electroneutrality and Equation 2.12, ANC can be expressed alternatively as the sum of the nonhydrogen-containing cations, $[M_i]$, minus the sum of the strong acid anions, $[A_j]$ (Stumm and Morgan 1981; Gherini et al. 1985), as

$$\text{ANC} = \Sigma |z_i| [M_i] - \Sigma |z_j| [A_j] \quad (2.13)$$

where z_i and z_j are the charges of cation M_i and anion A_j , respectively. The primary H^+ ion acceptors in most natural systems include carbonate, bicarbonate, and hydroxyl species, and the primary H^+ donor is the H^+ ion itself. Consequently, the carbonate ANC (ANC_c) can be defined as (from Equation 2.12)

$$\text{ANC}_c = [\text{HCO}_3^-] + 2[\text{CO}_3^{2-}] + [\text{OH}^-] - [\text{H}^+] \quad (2.14)$$

Complexities in the definition of ANC for soil and surface waters arise from the presence of noncarbonate alkalinity. The primary components of noncarbonate alkalinity include weak organic acids and hydrolyzable metal ions such as Al^{3+} , and the ANC conventions in the codes account for these components differently. The ANC conventions used in the MAGIC and ILWAS codes are given in Table 2.7 excluding Al-sulfate and Al-fluoride ion pairs, which are generally subordinate species in most surface and ground waters.

Organic acids produce noncarbonate alkalinity by becoming protonated at pH conditions that are dependent on the dissociation constants of the organic acids. For instance, the protonation of a generic monoprotic organic acid RCOO^- can be written as



The ILWAS code considers the contributions of mono- and triprotic organic acids to ANC, whereas the MAGIC code includes a single diprotic organic acid (Table 2.7).

The conventions used by the MAGIC and ILWAS codes to account for the effects of hydrolyzed aluminum species on ANC are subtly different. An explanation of this difference is facilitated by a brief discussion of equilibria for the Al-H₂O system. Aluminum hydroxides are commonly considered to be the solubility-controlling solids for dissolved aluminum in acidic watersheds (Driscoll et al. 1984; Nordstrom and Ball 1986). The dissolution of Al(OH)₃(s), which can be described as

TABLE 2.7. Definitions of Acid Neutralizing Capacity (ANC) Used by the MAGIC, ETD, and ILWAS Codes (Brackets indicate concentration in molar or molal units, and R', R'', and R''' represent mono-, di-, and triprotic organic acids, respectively.)

<u>Code</u>	<u>Units</u>	<u>ANC Definition</u>
MAGIC	eq • L ⁻¹	$\text{ANC} = [\text{HCO}_3^-] + 2[\text{CO}_3^{2-}] + [\text{OH}^-] + [\text{HR}''] + 2[\text{R}'^{2-}] + [\text{Al}(\text{OH})_4^-] - [\text{H}^+] - 3[\text{Al}^{3+}] - [\text{Al}(\text{OH})_2^+] - 2[\text{AlOH}^{2+}]$
ETD ^(a)	meq • m ⁻³	ANC = function (cation exchange, weathering, SO ₄ ²⁻ adsorption, SO ₄ ²⁻ reduction, partial pressure of CO ₂ gas)
ILWAS	eq • L ⁻¹	$\text{ANC} = [\text{HCO}_3^-] + 2[\text{CO}_3^{2-}] + [\text{OH}^-] + [\text{H}_2\text{R}'''] + 2[\text{HR}'''] + 3[\text{R}'''] + [\text{R}'] + [\text{AlOH}^{2+}] + 2[\text{Al}(\text{OH})_2^+] + 3[\text{Al}(\text{OH})_3^0] + 4[\text{Al}(\text{OH})_4^-] + 3[\text{AlR}'''] + [\text{AlR}'^{2+}] + 2[\text{Al}(\text{R}')_2^+] + 3[\text{Al}(\text{R}')_3^0] - [\text{H}^+]$

(a) The ETD code operates on the principle of ANC mass balance.



with $\log K_{\text{sp}} = 8.77$ at 25°C for natural gibbsite (May et al. 1979), exerts a pH buffering effect because of the consumption of H^+ ions. This effect is diminished above about pH 6.5 because of the resulting increase in hydrolysis of the aqueous aluminum species. However, for the pH range of 5.0 to 6.5 found in many lakes subject to acidic deposition, $\text{Al(OH)}_3(\text{s})$ dissolution and Al^{3+} hydrolysis reactions consume H^+ ions and, thus, can contribute a small amount to the total ANC. The stepwise hydrolysis reactions that follow illustrate the ability of aqueous aluminum species to act as H^+ acceptors:



where the equilibrium constants at 25°C (K_1 to K_4) are from May et al. (1979).

In the definition of ANC used by the ILWAS code (Table 2.7), the hydrolyzed aluminum species are considered as H^+ ion acceptors that contribute to the total ANC. This definition is consistent with the general definition of ANC given in Equation 2.12. The convention of the ILWAS code also is consistent with the most common analytical methods for ANC, which involve the titration of a solution sample with a strong acid to an endpoint (Stumm and Morgan 1981). Generally, methods for determining ANC yield only a total value and do not distinguish between the different sources of ANC, such as those resulting from the protonation of aqueous aluminum species. Driscoll and Bisogni (1984) report a small but measurable contribution of aluminum species to total ANC in Adirondack lakes, indicating the need to consider the aqueous Al species as proton acceptors.

In the definition of ANC used by the MAGIC code, the positively charged aluminum species are treated as H⁺ ion donors and Al(OH)₄⁻ is treated as an H⁺ ion acceptor (Table 2.7). This definition is not rigorously consistent with the general definition of ANC (Equation 2.12) and leads to the following relationship between ANC for the MAGIC (ANC_M) code and for the ILWAS (ANC_I) code

$$\text{ANC}_I = \text{ANC}_M + 3[\text{Al}_t] \quad (2.21)$$

where [Al_t] is the total monomeric aluminum concentration in solution. For most natural waters, this difference in definitions does not result in a large difference in the numerical values of ANC calculated in the MAGIC and ILWAS codes because of the low solubility of Al(OH)₃(s). For instance, in a solution with pH 5.5 that is saturated with respect to atmospheric CO₂(g) (CO₂(g) = 10^{-3.48} atm) and natural gibbsite (Equation 2.16), the contribution of bicarbonate to total ANC is 46.6 μmol•L⁻¹ (log K = -1.45 for CO₂(g) = CO₂(aq) and log K = -6.35 for CO₂(aq) + H₂O = HCO₃⁻ + H⁺ at 25°C). For this solution, the contribution of the aluminum hydrolysis species to total ANC can be calculated as a function of H⁺ ion concentration using the equilibrium constants given above for Equations 2.16 to 2.20 as

$$[\text{Al}_t] = 10^{8.77}/[\text{H}^+]^3 (1.0 + 10^{-4.98}/[\text{H}^+] + 10^{-18.13}/[\text{H}^+]^2 + 10^{-16.76}/[\text{H}^+]^3 + 10^{-22.16}/[\text{H}^+]^4) \quad (2.22)$$

where unit values for activity coefficients are assumed. From Equation 2.22, [Al_t] is equal to only 0.241 μmol•L⁻¹ at pH 5.5, indicating an insignificant contribution of dissolved aluminum to total ANC compared to the carbonate ANC (46.6 μmol•L⁻¹). However, [Al_t] increases to 1.65 μmol•L⁻¹ at pH 5.0 and to 26.15 μmol•L⁻¹ at pH 4.5 because of the increased solubility of gibbsite. Obviously, at the lower pH values, the contribution of [Al_t] to total ANC becomes much more significant. For most modeling applications involving lakes with pH values that range from 5.0 to 6.5, the differences in ANC calculated by the MAGIC and ILWAS codes

will not be greatly different and should be comparable to analytical measurements of ANC. However, significant differences in ANC emerge between the two codes for pH less than about 5.0, depending on the equilibrium constant used for gibbsite solubility. In such cases, the different definitions of ANC used in the MAGIC and ILWAS codes should be considered when comparing results between these codes and, in the case of the MAGIC code, when comparing code calculations of ANC to analytical measurements of ANC.

An explicit definition of ANC is not shown in Table 2.7 for the ETD code because this code operates totally on ANC mass balance. Equilibrium relationships and mass balances for specific H⁺ ion acceptors are not explicitly considered in this code in a manner that allows ANC to be calculated according to a mathematical relationship involving concentrations of chemical constituents, such as Equation 2.12. Instead, reactions are written with ANC as a reactant or a product so that specific geochemical processes add or subtract from the total ANC present in the system (Schnoor and Stumm 1985).

2.5.2 Carbonic Acid Equilibria

In most slightly acidic surface waters, carbonate ANC is the major component of positive ANC (Equation 2.14) (Stumm and Morgan 1981). All three codes treat the dissolution of CO₂(g) in water and the resulting carbonic acid speciation as an equilibrium process. Equilibrium in the CO₂(g)-H₂O system can be described by the following reactions:



The fully protonated $\text{H}_2\text{CO}_3(\text{aq})$ species does not contribute to ANC; thus, the codes all describe the formation of HCO_3^- directly from $\text{CO}_2(\text{aq})$, as shown in Equation 2.24. The equilibrium constants for the reactions described in Equations 2.23 to 2.26 are dependent on temperature. All three codes use very nearly equivalent functions to describe the dependence of the equilibrium constants on temperature. These temperature functions are as follows:

$$\log K_{c1} = (2386)/T + (0.01563)T - 14.018 \quad (2.27)$$

$$\log K_{c2} = (-3404)/T + (0.03280)T + 14.844 \quad (2.28)$$

$$\log K_{c3} = (-2902)/T + (0.02380)T + 6.498 \quad (2.29)$$

$$\log K_w = (-4471)/T + (0.01706)T + 6.0875 \quad (2.30)$$

where T is temperature in degrees K. The sources of these functions include Harned and Davis (1943) for K_{c1} and K_{c2} , Harned and Scholes (1941) for K_{c3} , and Harned and Owen (1958) for K_w .

Average monthly temperatures for the different soil layers are specified by the user in the MAGIC code. The ILWAS code calculates soil temperatures as a function of conductive and advective heat flow, as indicated in Section 2.4.5, or user-supplied soil temperatures can also be used. Although air temperatures are input to the ETD code, they are used only for the temperature-dependent hydrologic variables. Temperatures for the geochemical variables are calculated internally in the ETD code by means a sinusoidal function that allows temperatures to vary from -0.5° to 22.5°C over the year.

In an open system that does not include soil minerals, the concentration of HCO_3^- in solution is a function of the $\text{CO}_2(\text{g})$ partial pressure (assuming fugacity is equal to the partial pressure of $\text{CO}_2(\text{g})$), pH, and temperature. Because an increase in $\text{CO}_2(\text{g})$ partial pressure results in an equal increase in both HCO_3^- and H^+ concentrations (Equation 2.24), no net increase in ANC results. If soil minerals are added to the open system, then ANC does become sensitive to changes in $\text{CO}_2(\text{g})$ partial pressure, as shown by Reuss and Johnson (1985). This effect is caused by the exchange of H^+ ions for the base cations located on the surface exchange

sites of the soil minerals. Because the H^+ ion concentration in soil solution is buffered by cation exchange reactions, an increase in $CO_2(g)$ partial pressure produces an increase in ANC through the resulting increase in the HCO_3^- concentration (see Equation 2.24) (Reuss and Johnson 1985). Both the MAGIC and ILWAS codes include the combined effects of $CO_2(g)$ partial pressure and cation exchange on ANC by using equilibrium expressions for $CO_2(g)$ - H_2O reactions and for specific reactions that describe the exchange of the major cations (i.e., Ca^{2+} , Mg^{2+} , Na^+ , K^+ , Al^{3+} , and H^+) on the surfaces of the soil minerals. The ETD code does not use specific reactions to account for the combined effects of $CO_2(g)$ partial pressure and cation exchange on ANC, but uses a lumped parameter of base cation exchange rate to account for the total increase in ANC resulting from exchange processes. Specific formulations for exchange reactions are discussed in a later section.

To determine the distribution of the carbonate species, each of the codes requires that the partial pressure of $CO_2(g)$ be specified in the soil and surface waters in a manner that depends on the vertical discretization scheme. In the MAGIC code, the partial pressure of $CO_2(g)$ is specified by the user for each of the two soil layers and for the lake. Partial pressures in soils are not often reported, but generally range from $10^{-3.48}$ atm (atmospheric) to $10^{-6.52}$ atm (Lindsay 1979). Cosby, Hornberger, and Galloway (1985) recommend values in the range of $10^{-3.8}$ to $10^{-1.8}$ atm for the upper and lower soil layers used in the MAGIC code, respectively, and $10^{-3.18}$ atm, which is equivalent to two times atmospheric $CO_2(g)$, for the lake compartment. In the input data file for the ETD code, a single value of $CO_2(g)$ partial pressure, which is indicated by Nikolaidis (1987) to be relevant for all the soil compartments, is specified by the user, along with a constant that defines the level of $CO_2(g)$ supersaturation with respect to atmospheric $CO_2(g)$ for the lake. The values commonly used for Adirondack watersheds have been $10^{-2.9}$ atm for soil $CO_2(g)$ and 1.5 times atmospheric CO_2 for the degree of supersaturation in the lake (Nikolaidis 1987). However, in the ETD FORTRAN code, the $CO_2(g)$ partial pressures in the soil, unsaturated, and ground-water compartments are reset to 3, 3, and 10 times atmospheric $CO_2(g)$,

respectively. The purpose of overriding the values input by the user for the soil are not clear. In both the MAGIC and ETD codes, the CO₂(g) partial pressures specified for soil and lake compartments are held constant throughout a simulation. Also, ideal gas behavior for CO₂(g) is assumed in the MAGIC and ETD codes, so that the CO₂(g) fugacity is assumed to be equivalent to the CO₂(g) partial pressure. However, the treatment of CO₂(g) in the ILWAS code is more complex. Partial pressures of CO₂(g) for each soil layer must be specified for layers 2 through 10. The concentration of dissolved CO₂(aq) is determined from its partial pressure and Henry's law,

$$[\text{CO}_2(\text{aq})] = K_H \cdot P(\text{CO}_2(\text{g})) \quad (2.31)$$

However, the partial pressures of CO₂(g) specified for the soil layers may not be constant during an ILWAS code simulation because of biogeochemical processes that produce CO₂(g). These processes, which include litter decay and root respiration, can be simulated by the ILWAS code and are discussed in more detail below. The effects of these processes on ANC in the soil solution, plus the loss of CO₂(g) from soil layers and the lake by advection, gas transfer, and diffusion, are also simulated by the ILWAS code.

2.5.3 Aluminum Chemistry

Acidic deposition can result in the mobilization of aqueous Al species in natural watersheds because of increased dissolution of Al(OH)₃(s) phases, such as gibbsite under acidic conditions (Driscoll et al. 1984; Bache 1986). In some acidified waters, concentrations of dissolved aluminum can reach levels that are toxic to fish (Baker and Schofield 1980; Driscoll et al. 1980). Aluminum solid phases and aqueous species also form a weak acid/base system that can be an important buffer in the weakly acidic waters often found in watersheds receiving acid deposition. Both the MAGIC and ILWAS codes consider the buffering effects of aluminum solid phase solubility and aqueous speciation in their calculation schemes of water quality. The ETD code does not include any aluminum chemistry.

The solubility-controlling solid for dissolved aluminum is assumed to be a form of $\text{Al}(\text{OH})_3(\text{s})$ in both the MAGIC and ILWAS codes. The solubility products (K_{sp}) for the $\text{Al}(\text{OH})_3(\text{s})$ phases used as solubility controls for dissolved aluminum in the MAGIC and ILWAS codes are listed in Table 2.8. However, aluminum concentrations in streamwaters have not always agreed with the solubility versus pH relationship expected for $\text{Al}(\text{OH})_3(\text{s})$ (Cronan et al. 1986; Hooper and Shoemaker 1985; Sullivan et al. 1986). To account for variations in aluminum concentrations that are not caused by pH or complexation, the user of the MAGIC code can specify different solubility products for different forms of aluminum-hydroxide solids. The values of these solubility products are determined during calibration.

The list of solubility products values suggested for use in the MAGIC code by Cosby and others (Cosby, Hornberger, and Galloway 1985; Cosby et al. 1985) includes all of the $\text{Al}(\text{OH})_3(\text{s})$ phases that are likely to be

TABLE 2.8. Equilibrium Constants (K_{sp}) for $\text{Al}(\text{OH})_3(\text{s})$ Solubility for the MAGIC and ILWAS Codes where $K_{sp} = (\text{Al}^{3+})/(\text{H}^+)^3$ (Parentheses indicate activity.)

Code	$\text{Al}(\text{OH})_3(\text{s})$ Phase	Log K_{sp} at 25°C	Temperature Dependence (log K_{sp})
MAGIC	Synthetic gibbsite	8.11	
	Natural gibbsite	8.77	
	Microcrystalline gibbsite	9.35	$16.61(T - 298)/T + 9.35^{(a,b)}$
	Amorphous $\text{Al}(\text{OH})_3(\text{s})$	16.86	
ILWAS	Unspecified $\text{Al}(\text{OH})_3(\text{s})$ or rate-controlled dissolution/precipitation ^(c)	8.18	$(9262)/T + (6.6513)T - 38.19$

(a) van't Hoff expression with $\Delta H_f = 64.54 \text{ kJ} \cdot \text{mol}^{-1}$ at 298°K and gas constant $R = 8.314 \text{ kJ} \cdot \text{deg}^{-1} \cdot \text{mol}^{-1}$.

(b) Using thermodynamic data from Wagman et al. (1982): $\Delta H_f = 95.1 \text{ kJ} \cdot \text{mol}^{-1}$ which gives $\log K_{sp} = 16.67(T-298)/T + 9.35$.

(c) $-d[\text{Al}(\text{OH})_3(\text{s})]/dt = k([\text{Al}^{3+}]_{\text{eq}} - [\text{Al}^{3+}])$ where $[\text{Al}^{3+}]_{\text{eq}}$ and $[\text{Al}^{3+}]$ represent the equilibrium and actual Al^{3+} concentrations ($\text{mol} \cdot \text{L}^{-1}$) in soil solution, and k is specific rate constant (day^{-1}).

found in a watershed (Table 2.8). However, from thermodynamic considerations, it is unlikely that more than one aluminum hydroxide solid could affect dissolved aluminum concentrations to a significant extent. The precipitation of poorly crystalline aluminum silicates, organic complexing, or disequilibrium conditions are more likely explanations for dissolved aluminum concentrations that deviate from aluminum hydroxide solubility.

In the ILWAS code, the solubility product for $\text{Al}(\text{OH})_3(\text{s})$ is fixed at a single value close to that determined by May et al. (1979) for synthetic gibbsite (Table 2.8). This value is not specified by the user, although a minor modification of the FORTRAN code would make this possible. The ILWAS code allows the user to account for the possibility that surface waters and soil solutions may not be in equilibrium with the solubility of $\text{Al}(\text{OH})_3(\text{s})$ through the optional use of a rate expression for $\text{Al}(\text{OH})_3(\text{s})$ dissolution and precipitation. This expression describes the rate of dissolution or precipitation as a linear function of the distance from equilibrium with respect to $\text{Al}(\text{OH})_3(\text{s})$ solubility (Table 2.8). The user can adjust the rate constant in the rate expression during code calibration to improve matches of code results to measured data.

Cronan et al. (1986) have reported that dissolved aluminum concentrations may be controlled by adsorption onto solid-phase humic substances at pH values below about 5.2, compared to solubility by aluminum hydroxide at higher pH. None of the codes includes the adsorption of aqueous aluminum to humic substances, although it should be noted that sorption reactions involving aluminum and organic materials are not well known. The kinetic controls in the ILWAS code and the selection of different $\text{Al}(\text{OH})_3(\text{s})$ solubility products for different soil layers allow much latitude in the calibration process for matching code predictions of dissolved aluminum concentrations to observed data. However, it is possible that in organic-rich, low-pH systems where aluminum is affected by sorption processes, aluminum calibrations may be achieved for incorrect reasons because they contain only dissolution and precipitation controls for aluminum. For these systems, predicted values of dissolved aluminum and pH, which is

strongly affected by $\text{Al}(\text{OH})_3(\text{s})$ solubility at low pH, may be significantly in error when compared to observed data.

The temperature dependence of $\text{Al}(\text{OH})_3(\text{s})$ solubility is incorporated into the MAGIC code by use of the van't Hoff equation, which is expressed as

$$d\ln(K)/dT = \Delta H_r/R \cdot T^2 \quad (2.32)$$

where K is an equilibrium constant, ΔH_r is the enthalpy of reaction at 298°K, R is the ideal gas constant ($8.314 \text{ J} \cdot \text{deg}^{-1} \cdot \text{mol}^{-1}$), and T is in °K. Integration of Equation 2.32 between temperature limits of 298°K and another temperature, T , and assuming $d\Delta H_r/dT = 0$ gives

$$\log K_T = \Delta H_r/2.303R \left\{ (T - 298)/T \cdot 298 \right\} - \log K_{298} \quad (2.33)$$

From Equation 2.33, the equilibrium constant, K_T , at the new temperature can be approximated from the value at 298°K (25°C), given by K_{298} . Cosby, Hornberger, and Galloway (1985) cite Hem (1968) and Robie and Waldbaum (1968) as sources of the thermodynamic data used to calculate a ΔH_r of $60.5 \text{ kJ} \cdot \text{mol}^{-1}$ for $\text{Al}(\text{OH})_3(\text{s})$ solubility, giving the temperature correction shown in Table 2.8. The earlier data currently in the MAGIC code should be replaced with the more recent value of ΔH_r ($95.1 \text{ kJ} \cdot \text{mol}^{-1}$) from Wagman et al. (1982). This change would result in a stronger temperature dependence for $\text{Al}(\text{OH})_3(\text{s})$ solubility than presently incorporated in the MAGIC code (Table 2.8). For example, $\log K_{sp}$ at 25°C is 9.35 for microcrystalline gibbsite (Table 2.8), but at 15°C is 8.98 using the ΔH_r in the MAGIC code, compared to 8.77 using the ΔH_r from Wagman et al. (1982). In view of the range of values shown in Table 2.8, the different ΔH_r values produce significantly different $\log K_{sp}$ values for a small temperature difference. The ILWAS code does not use a van't Hoff expression to describe the temperature-dependence of $\text{Al}(\text{OH})_3(\text{s})$, but uses a polynomial-type equation, which produces $\log K_{sp}$ values consistent with a ΔH_r of $95.1 \text{ kJ} \cdot \text{mol}^{-1}$ (Table 2.8).

The solubility of $\text{Al}(\text{OH})_3(\text{s})$ also is a function of pH and anion concentrations because of Al^{3+} hydrolysis and complexation. The hydrolysis, complexation, and organic acid dissociation reactions that are included in the MAGIC and ILWAS codes to describe aqueous aluminum speciation are listed in Table 2.9. The equilibrium constants for the hydrolysis and inorganic complexation reactions in these two codes are nearly the same, with a few exceptions. One exception is the third hydrolysis constant describing the formation of $\text{Al}(\text{OH})_3(\text{aq})$. The ILWAS code contains a very low value for the third hydrolysis constant because in the study by May et al. (1979), which is the data source for the hydrolysis constants, evidence of a neutral species was not conclusive. In the MAGIC code, equilibrium constants for some of the hydrolysis and inorganic complexation reactions are corrected for temperature using van't Hoff expressions (Table 2.9). However, the small ΔH_r values cited by Cosby, Hornberger, and Galloway (1985) for the first and fourth hydrolysis reactions result in almost no dependence on temperature of the equilibrium constants for these reactions. Other data from Wagman et al. (1982) and Naumov et al. (1974) indicate that the enthalpies for these reactions should be greater than those cited by Cosby et al. (1985), resulting in much greater temperature dependencies (Table 2.9). Temperature corrections for the complexation reactions of aluminum are not included in the ILWAS code. The different temperature-dependencies used in the MAGIC and ILWAS codes will lead to different predictions of the seasonal dynamics of dissolved aluminum concentration. Although the ILWAS code does not use temperature corrections for the aluminum hydrolysis and complexation reactions, whereas the MAGIC code does, the ILWAS formulations for the relatively more important process of $\text{Al}(\text{OH})_3(\text{s})$ solubility can be expected to provide a more accurate representation of seasonal aluminum dynamics than the formulations contained in the MAGIC code.

2.5.4 Organic Acid Chemistry

Both the MAGIC and ILWAS codes consider the effects of generic organic acids on solution chemistry. The constants for the dissociation of the organic acids included in the ILWAS code are listed in Table 2.9.

TABLE 2.9. Aluminum Complexation and Organic Acid Dissociation Reactions Used in the MAGIC and ILWAS Codes (The ETD code does not include similar reactions.)

Code	Reaction	Log K at 25°C for indicated value of n						Temperature dependence (van't Hoff)
		1	2	3	4	5	6	
MAGIC	$Al^{3+} + nH_2O = Al(OH)_n^{3-n} + nH^+$	-4.98	-16.13	-16.76	-22.16			n = 1, 4 ^a
	$Al^{3+} + nF^- = Al(F)_n^{3-n}$	7.62	12.76	17.63	19.73	26.92	26.87	n = 1-5 ^b
	$Al^{3+} + nSO_4^{2-} = Al(SO_4)_n^{3-2n}$	3.21	5.11					n = 1, 2 ^c
	$H_2R^{2-} = H_2-nR^{1-n} + nH^+$ (d)	u.s. (e)	u.s. (e)					
ILWAS	$Al^{3+} + nH_2O = Al(OH)_n^{3-n} + nH^+$	-4.99	-16.14	-24.13	-22.16			
	$Al^{3+} + nF^- = Al(F)_n^{3-n}$	7.66	12.76	17.63	19.73	26.92	26.87	
	$Al^{3+} + nSO_4^{2-} = Al(SO_4)_n^{3-2n}$	3.21	5.11					
	$HR' = H_1-nR'^{1-n} + nH^+$	-3.8,						
		-4.5						
	$H_3R^{3-} = H_3-nR^{1-n} + nH^+$	-4.8	-16.1	-19.35				
	$Al^{3+} + nR'^- = Al(R')_n^{3-n}$	7.81	14.67	26.15				
	$Al^{3+} + nR''^{3-} = Al(R'')_n^{3-3n}$	11.66						

(a) n=1: $\log K = 9.9915(T-298)/T - 4.98$ ($\Delta H_r = 9.668 \text{ kJ}\cdot\text{mol}^{-1}$) ($\Delta H_r = 49.6 \text{ kJ}\cdot\text{mol}^{-1}$ from Naumov (1974) and Wagman et al. 1982)

n=4: $\log K = -0.9968(T-298)/T - 22.16$ ($\Delta H_r = -9.639 \text{ kJ}\cdot\text{mol}^{-1}$) ($\Delta H_r = 171.7 \text{ kJ}\cdot\text{mol}^{-1}$ from Wagman et al. 1982)

(b) n=1: $\log K = 9.81(T-298)/T + 7.62$ ($\Delta H_r = 4.66 \text{ kJ}\cdot\text{mol}^{-1}$)

n=2: $\log K = 1.47(T-298)/T + 12.76$ ($\Delta H_r = 6.37 \text{ kJ}\cdot\text{mol}^{-1}$)

n=3: $\log K = 1.83(T-298)/T + 17.63$ ($\Delta H_r = 16.46 \text{ kJ}\cdot\text{mol}^{-1}$)

n=4: $\log K = 1.61(T-298)/T + 19.73$ ($\Delta H_r = 9.26 \text{ kJ}\cdot\text{mol}^{-1}$)

n=5: $\log K = 1.32(T-298)/T + 26.92$ ($\Delta H_r = 7.53 \text{ kJ}\cdot\text{mol}^{-1}$)

(c) n=1: $\log K = 1.68(T-298)/T + 3.21$ ($\Delta H_r = 9.58 \text{ kJ}\cdot\text{mol}^{-1}$)

n=2: $\log K = 2.25(T-298)/T + 5.11$ ($\Delta H_r = 12.84 \text{ kJ}\cdot\text{mol}^{-1}$)

(d) R', R'', R''' refer to monoprotic, diprotic, and triprotic organic acids, respectively.

(e) 'u.s.' means value specified by code user.

The MAGIC code has the option of including a diprotic organic acid for which the code user specifies two dissociation constants. The primary use of the diprotic organic acid in the MAGIC code is as an additional H⁺ ion acceptor that contributes to ANC (Table 2.7). The MAGIC code does not include any complexation of Al³⁺ by the organic acid. In the ILWAS code, two organic acids are included, one monoprotic and one triprotic. Complexation of Al³⁺ by the organic acids and the effects on ANC caused by protonation of organic acids are included in the ILWAS code (Table 2.9). An appreciable amount of organically complexed aluminum has been reported in Adirondack lake waters by Driscoll et al. (1984).

The importance of including detailed descriptions of aluminum and organic acid chemistry in codes of watershed acidification can be demonstrated by examining the acid buffer intensities exerted by different reactions. The acid buffer intensity, β_A , is defined in Equation 2.10 as the amount of acid or base in molar or molal concentration units required to cause an incremental change in pH. By differentiating (with respect to pH) the components listed in the definition of ANC from the ILWAS code (Table 2.7), the buffer intensities of the four major acid/base reactions important in natural watersheds can be expressed as follows (van Breeman and Wielemaker 1974):

$$\beta(\text{H}_2\text{O}) = 2.303([\text{H}^+] + [\text{OH}^-]) \quad (2.34)$$

$$\beta(\text{CO}_2\text{-H}_2\text{O}) = 2.303([\text{HCO}_3^-] + 4[\text{CO}_3^{2-}]) \quad (2.35)$$

$$\beta(\text{Al-H}_2\text{O}) = 2.303(9[\text{Al}^{3+}] + 4[\text{AlOH}^{2+}] + [\text{Al}(\text{OH})_2^+] + [\text{Al}(\text{OH})_4^-]) \quad (2.36)$$

$$\beta(\text{org}) = 2.303([\text{H}_2\text{R}^{1-}] + 4[\text{HR}^{2-}] + 9[\text{R}^{3-}]) \quad (2.37)$$

where only a single triprotic organic acid is considered. A plot of the individual buffer intensities as a function of pH is shown in Figure 2.1 for the following conditions: $\text{CO}_2(\text{g}) = 10^{-3.48}$ atm, $[\text{F}^-] = [\text{SO}_4^{2-}] = 0$, no organic acid complexing of aluminum, unit activity coefficients, total organic acid concentration = 10^{-5} M, and $\log K_{sp} = 8.77$ for $\text{Al}(\text{OH})_3(\text{s})$ solubility. Thermodynamic data for the aluminum hydrolysis species and

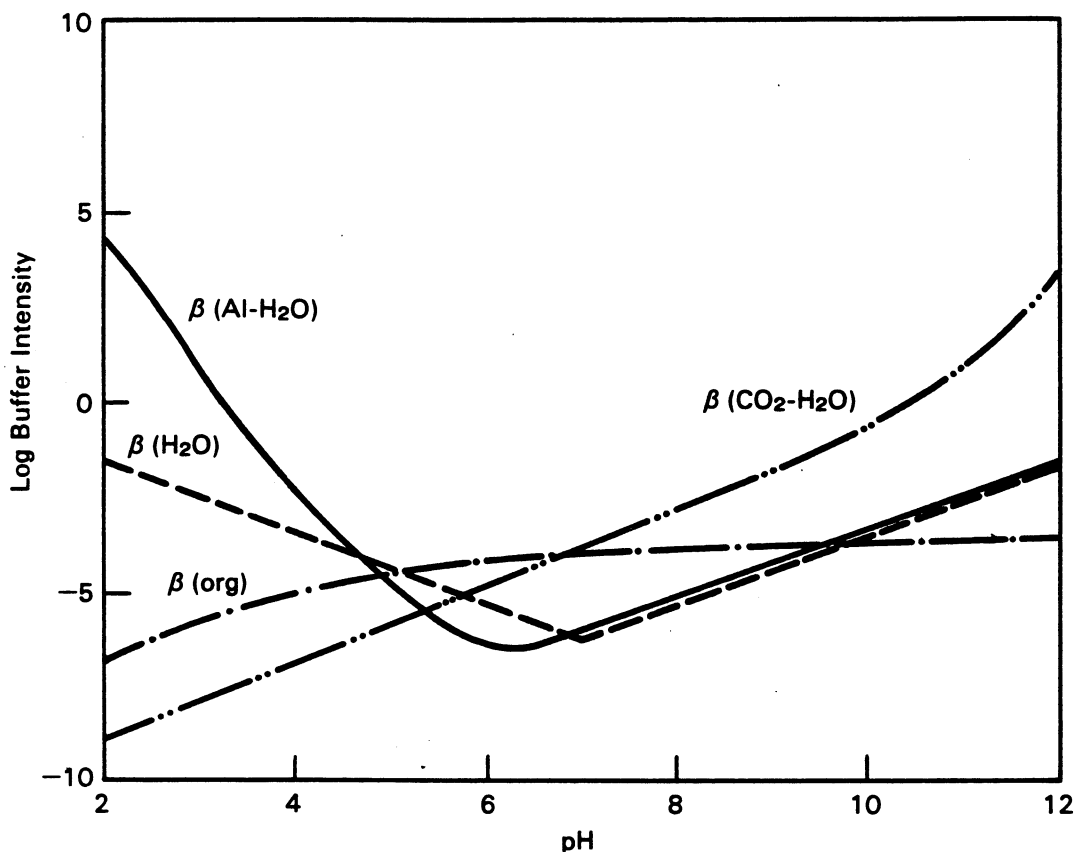


FIGURE 2.1. Buffer Intensities of Four Acid/Base Systems Pertinent to Watersheds. ($\text{CO}_2(\text{g}) = 10^{-3.48}$ atm, $[\text{F}^-] = [\text{SO}_4^{2-}] = 0$, no organic complexing of Al, unit activity coefficients, triprotic organic acid = 10^{-6} M, and $\log K_{sp} = 8.77$ for $\text{Al}(\text{OH})_3(\text{s})$ solubility.) Thermodynamic data are taken from Table 2.9 and Equations 2.27 to 2.30.

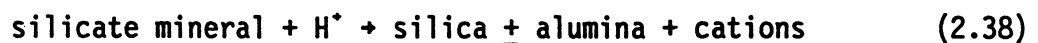
for dissociation of the triprotic organic acid are taken from Table 2.9 from the ILWAS code and for the $\text{CO}_2(\text{g})\text{-H}_2\text{O}$ system from Equations 2.27 to 2.30.

The importance of organic acid in providing acid buffering depends on its concentration and dissociation constants, but for the conditions described above, it can theoretically provide significant buffering capacity over the pH range of 5.0 to 6.5, as shown by the buffer intensity curves in Figure 2.1. Although the aluminum hydrolysis reactions provide some buffering at pH values between 5.0 and 6.5, they become most important below pH 5.0. Both the MAGIC and ILWAS codes include sophisticated

algorithms that quantitatively describe the buffering effects of organic acid protonation and aluminum hydrolysis on ANC by using well-established thermodynamic constraints. This approach reduces the amount of empiricism inherent in such codes. However, the ETD code does not contain these reactions, so it is more difficult to evaluate its adequacy in simulating the dynamics of ANC in surface waters.

2.5.5 Mineral Weathering

Geographic regions that are susceptible to acidification often have shallow soils and underlying exposed bedrock that consist predominantly of silicate minerals that formed under crustal conditions of high temperature and pressure. These high-temperature silicates are not thermodynamically stable at earth surface conditions and undergo weathering reactions that ultimately lead to assemblages of solids that are stable in surface environments. Weathering reactions involving silicate minerals can be thought of as the hydrolysis of basic salts (Johnson 1984) because most silicates consist of combinations of a weak acid (silicic acid) and strong bases (calcium, magnesium, potassium, sodium, and iron). Hydrolysis of a basic salt results in the production of excess OH^- ions or, conversely, the consumption of H^+ ions. The hydrolysis of aluminosilicate minerals can be described by the following generalized reaction (Lasaga 1984):



where the cations usually include calcium, potassium, sodium, magnesium, and iron. Experimental studies of aluminosilicate dissolution (Lasaga 1984) have found that weathering reaction rates depend on the H^+ ion activity (H^+) to some fractional power, n , such that

$$R = k \cdot (\text{H}^+)^n \quad (2.39)$$

where R is the dissolution rate and k is a specific rate constant for silicate hydrolysis that is dependent on the surface area of the reacting mineral. The expressions used to describe the kinetics of mineral weathering are listed in Table 2.10 for all three codes, and all are

TABLE 2.10. Weathering Rate Expressions Used in the MAGIC, ETD, and ILWAS Codes^(a)

Code	Concept	Rate Expression	Dependence $[H^+]$ (n _i)	Units
MAGIC	Bulk rates for specific cations and anions, i	$d[C_i]/dt = k_i [H^+]^n$	n.s.	$meq \cdot m^{-2} \cdot y^{-1}$
ETD	Bulk rate of ANC production	$d[ANC]/dt = \{k([H^+]/[H^+_{ref}])^n + k_g\} \cdot (S/S_{ref})^s (Q/Q_{ref})^q$	0.5	$eq \text{ ANC} \cdot m^{-2} \cdot d^{-1}$
ILWAS	Dissolution rates specified for i = 1 to 5 minerals	$dM_i/dt = -k_i M_i [H^+]^n$	0.1-0.5	$g \cdot sec^{-1}$

(a) where C_i = concentration of aqueous species i

$([H^+]/[H^+_{ref}])$ = ratio of hydrogen ion to reference hydrogen ion concentration

k = bulk rate constant for silicate hydrolysis (ETD)

k_i = specific rate constant for silicate hydrolysis

k_g = rate constant for ligand attack

M_i = mass of dissolving mineral i in soil layer

n = rate dependence on $[H^+]$

n.s. = recommended range not specified

$(Q/Q_{ref})^q$ = ratio of flow rate through soil to reference flow rate

$(S/S_{ref})^s$ = ratio of effective to total or reference surface area

t = time (d = day, y = year).

similar in form to Equation 2.39. In the ETD code formulation for weathering rate, the subscript "ref" associated with H^+ , S, and Q (Table 2.10) denotes reference values that are used to normalize the rate parameters to a base value that is determined through code calibration. All the codes express the functional dependence on H^+ ion in concentration rather than activity. For the dilute solutions in most watersheds, the use of H^+ ion concentration, as opposed to activity, will not cause any significant difference in rate calculations. None of the codes includes a temperature correction for the rate constants; however, the magnitudes of the rate constants are estimated by calibration procedures. Therefore, the lack of temperature corrections is unlikely to produce any significant error in the predictive accuracy of the codes, compared with the more important problem of determining representative values for the rate constants for specific watersheds.

The important step in silicate hydrolysis is the adsorption of H^+ ions onto active surface sites, which leads to the observed dependence on H^+ ion activity in solution (Lasaga 1981). The fractional order dependence on H^+ ion results from the presence of a range of active surface sites on silicate minerals that have different adsorption and reaction energetics (Lasaga 1981). Experimental studies with most of the common silicate minerals have found the dissolution rate dependence on H^+ ion to range from 0.5 to 1.0 in acidic solutions (Lasaga 1984). The authors of the ETD code suggest using a value of 0.5 for the fractional dependence on a normalized H^+ concentration (Nikolaidis 1987). For the ILWAS code, a range of 0.1 to 0.5 has been suggested by Chen et al. (1983). Although a H^+ dependence for weathering rate has been incorporated in the MAGIC code, a recommended range of values has not been reported, and Cosby and others have used a zero-order dependence on H^+ (Cosby, Hornberger, and Galloway 1985; Cosby et al. 1985).

Although the forms of the kinetic expressions for weathering rate are similar in each of the codes, the actual representations of mineral weathering processes are different. In the MAGIC code, the weathering rate is expressed as the rate of production of a specific cation or anion per unit area of the watershed (Table 2.10). Specific dissolving minerals

are not identified. Generally, when using the MAGIC code, no production of SO_4^{2-} , NH_4^+ , or NO_3^- and only a limited amount of Cl^- is assumed to result from weathering reactions (Cosby et al. 1985). The weathering of amphiboles and mica minerals may release small amounts of Cl^- to surface waters (Chen et al. 1983), but more important sources of Cl^- that are not considered in the models may include road salt, seawater spray in coastal areas, or fertilizers. The principal ions produced by weathering reactions are the basic cations. In using the MAGIC code, the production rates of specific cations are determined by adjusting the rate constants that control the individual weathering rates of the cations until agreement is reached with field observations of cation concentrations in the surface waters. In past usage, a zero-order dependence on H^+ concentration has been assumed (Cosby, Hornberger, and Galloway 1985; Cosby et al. 1985). The recommended calibration procedure (Cosby et al. 1985) suggests that the relative weathering rates should correspond to the relative abundances of the different base cations contained in minerals present in the soil layers. Because silica is not included in the MAGIC code, the stoichiometries of the dominant weathering minerals cannot be used to constrain relative rates of cation production. However, Cosby et al. (1985) have found that calibrations of the MAGIC code to field measurements of water chemistry at White Oak Run, Virginia, result in a narrow range of acceptable weathering rates for the basic cations.

In the ETD code, neither individual base cations nor reacting minerals are considered. Instead, the net result of all weathering reactions is directly linked to the rate of ANC production (Schnoor and Stumm 1985). In addition to a fractional dependence on H^+ , which is normalized to a reference H^+ concentration, the expression for mineral weathering in the ETD code also contains the option of including the effect on weathering caused by ligand attack (Table 2.10). This expression follows from the work of Furrer and Stumm (1986) and Zinder, Furrer and Stumm (1986), who have reported that the presence of ligands which complex the metal cation in oxide minerals increases the dissolution rate. Fractional dependencies of mineral weathering rate on the flow rate through the soil $(Q/Q_{r.e.f})^q$ and the ratio of effective to actual surface area $(S/S_{r.e.f})^s$ of

the weathering minerals are also contained in the weathering rate formulation incorporated in the ETD code, where the subscript "ref" refers to reference flow rate and reference surface area (Table 2.10), respectively. However, the actual use of these modifications is limited by lack of experimental and field data, so that in practice the exponents q and s are usually set to zero or the ratios are set to 1.0 (see Table 2.10) to cancel their effects of effective flow rate and effective surface area on the weathering rate (Nikolaidis 1987). The high level of detail in the mineral weathering expression of the ETD code leaves open the possibility of using experimentally derived data on mineral kinetics, which may be available in the future. However, methods for extrapolating laboratory weathering rate data to the field are not well established; thus, in the actual application of the ETD code to natural watersheds, the additional rate variables confound the calibration process because appropriate values are not known, as indicated by the fact that in practice these variables are set equal to 0 or 1 to cancel their effects. Additionally, the level of detail in the ETD rate expression for mineral weathering appears contradictory with the aggregation of all weathering processes by a single expression in ANC. In the actual application of the ETD code, the rate of ANC production caused by mineral weathering is determined by adjusting the magnitude of the hydrolysis rate constant until code results match field observations of ANC.

There are two unusual aspects in the mineral weathering coding of the ETD code. One is that mineral weathering is permitted in the unsaturated zone, the saturated or ground-water zone, and the lake sediments, but not in the uppermost soil zone (e.g., O, A, and B soil horizons). This treatment is based on the assumption that in the short term (e.g., < 50 years) weathering will have little effect on base saturation in the upper soil layers. Second, the ETD code assumes that Cl^- is a conservative substance that can be used to assess ANC and SO_4^{2-} mass balance during calibration procedures. However, this assumption requires the exclusion of internal sources of Cl^- in watersheds, such as mineral weathering or road-salt contamination, which may make calibration of the ETD code difficult for some watersheds.

In the ILWAS code, weathering rates are specified by the mass dissolution rates of specific minerals (Table 2.10). The rates of cation and anion production, including silica, and consumption of H^+ resulting from dissolution are determined from the stoichiometries of the reacting minerals and their dissolution reactions (Chen et al. 1983). In previous applications of the ILWAS code to Adirondack watersheds, where the soils often consist of glacial till derived from Precambrian shield regions in Canada and the anorthositic terrain of the Adirondacks, the dissolving minerals have included hornblende, sodic plagioclase, and potassium feldspar. These silicate minerals dissolve incongruently in slightly acidic solutions, and the reaction stoichiometries used by the ILWAS code to describe mineral weathering account for the formation of vermiculite and kaolinite (Gherini et al. 1985). The rate expression in the ILWAS code also involves the masses of the dissolving minerals in the soil layers. Although dissolution rates are more appropriately dependent on surface area, rather than on mass, the determination of the reactive surface area of a specific mineral in a soil matrix is extremely difficult. The mass of a mineral is more easily measured and its inclusion in the rate expression ensures a proportional dependence on the amount of the dissolving mineral present in the soil. The absolute rates of the dissolution reactions are determined by a calibration procedure that involves adjusting the hydrolysis rate constant for silicate mineral dissolution to match field observations of cation and silica concentrations in surface waters and/or soil solution. The inclusion of silica in the ILWAS code, as opposed to its absence in the other two codes, potentially provides a means for determining the total amounts of cation production and hydrogen ion consumption caused by silicate mineral weathering under ideal circumstances of correct reaction stoichiometries and reactive mineral masses. Thus, the ILWAS code contains the capability, where data are sufficient, to assess the relative importance of mineral weathering compared to cation exchange in affecting solution compositions.

2.5.6 Cation Exchange

Cation exchange reactions are similar to mineral weathering reactions involving silicates in that they consume H^+ ions and generate base cations

(Schnoor and Stumm 1985). In contrast to mineral weathering reactions, exchange reactions are rapid and the quantities of exchangeable cations present on soil minerals represent the degree to which soils can instantaneously respond to acidic deposition. The amounts of exchangeable base cations are usually significantly larger than the amounts present in soil solution (Reuss and Johnson 1986), and mineral weathering contributes to the resupply of base cations in soils. However, weathering rates are much slower than rates of cation exchange reactions, so that continued deposition of acid may eventually cause the depletion of exchangeable base cations in soils. Schnoor and Stumm (1985) have estimated that if weathering reactions did not replace the base cations on exchange sites of soils receiving acidic deposition, then the exchange capacity of the soils could be exhausted in 50 to 200 years.

The relationships used in each code to represent cation exchange reactions in soils are given in Table 2.11. Both the ILWAS and MAGIC codes use equilibrium-type relationships and selectivity coefficients, S , to describe cation exchange. In the ILWAS code, the reference cation is Ca^{2+} , so that the exchange reactions are written as the exchange of Ca^{2+} for other cations. For divalent-divalent exchange reactions, such as Mg^{2+} for Ca^{2+} , a Kerr-type relationship is used; for a monovalent-divalent exchange, such as H^+ for Ca^{2+} , a Gapon-type expression is used (Chen et al. 1983). The exchange of Al^{3+} for H^+ is not included in the ILWAS code. The cation exchange capacity (CEC) is designated as the sum of $\text{Ca}^{2+} + \text{Mg}^{2+} + \text{NH}_4^+ + \text{K}^+ + \text{Na}^+ + \text{H}^+$ cations present on the exchange sites (Table 2.11). When using the ILWAS code, measurements or estimates of the CEC, degree of base saturation, and selectivity coefficients are required for each of the soil layers. The selectivity coefficients can be determined from laboratory experiments or calculated from soil solution-composition and the concentrations of the adsorbed ions. Individual measurements of soil exchange properties must be aggregated to obtain values that are representative of a catchment (Chen et al. 1983). The values of these coefficients are evaluated and possibly modified during code calibration to achieve improved agreement between measured and predicted results for soil-solution composition.

TABLE 2.11. Cation Exchange Relationships Used in the MAGIC, ETD, and ILWAS Codes
 (n.c. means not considered, brackets indicate concentration, and parentheses indicate activities, BC refers to a base cation, and X⁻ (as in NaX) refers to a generic surface exchange site)

Code	Ref. Cation	CEC ($\text{meq} \cdot 100 \text{ g}^{-1}$)	Generalized Exchange Reaction	Formulation	Mass Balance Expression
MAGIC	Al^{3+}	$\text{AlX}_3 + \text{CaX}_2 + \text{MgX}_2 + \text{NaX} + \text{KX}$	$n\text{Al}^{3+} + 3\text{BC}^{+n}\text{X}_n =$ $n\text{AlX}_3 + 3\text{BC}^{+n}$ (n = 1, 2) (BC = Ca^{2+} , Mg^{2+} , Na^+ , K^+)	Gaines-Thomas $S_{\text{Al-BC}^+n} =$	$(\text{BC}^{+n})^3 [\text{AlX}_3]^n /$ $(\text{Al}^{3+})^3 [\text{BC}^{+n}\text{X}_n]^3$
ETD	n.c.	n.c.	n.c.	kinetic (a) $\text{Bex} =$	$k_{\text{ex}} \cdot M \cdot D \cdot [\text{H}^+] \cdot (\text{BS} - \text{BSd})$
ILWAS	Ca^{2+}	$\text{CaX}_2 + \text{MgX}_2 + \text{NH}_4\text{X} + \text{KX} + \text{NaX} + \text{HX}$	mono-divalent: $2\text{BC}^+ + \text{CaX}_2 = 2\text{BCX} + \text{Ca}^{2+}$ (BC = Na^+ , K^+ , H^+ , NH_4^+) di-divalent: $\text{Mg}^{2+} + \text{CaX}_2 = \text{MgX}_2 + \text{Ca}^{2+}$	Gapon $S_{\text{BC}^{1+}\text{-Ca}^{2+}} =$	$[\text{Ca}^{2+}] [\text{BCX}] /$ $[\text{CaX}_2] [\text{BC}^+]^2$
				Kerr $S_{\text{Mg}^{2+}\text{-Ca}^{2+}} =$	$[\text{Ca}^{2+}] [\text{MgX}_2] /$ $[\text{Mg}^{2+}] [\text{CaX}_2]$

(a) Bex refers to bulk cation exchange where k_{ex} is a second order rate coefficient, ($\text{m}^3 \cdot \text{eq}^{-1} \cdot \text{day}^{-1}$), M is the soil density ($\text{kg} \cdot \text{m}^{-3}$), D is the soil depth, $[\text{H}^+]$ is the hydrogen ion concentration ($\text{eq} \cdot \text{m}^{-3}$), and BS and BSd are the sum of bases and base depletion in the soil ($\text{meq} \cdot \text{kg}^{-1}$).

The MAGIC code uses Gaines-Thomas relationships to define selectivity coefficients for cation exchange (Cosby, Hornberger, and Galloway 1985), as shown in Table 2.11. The exchange reactions are described by the exchange of base cations with Al^{3+} (Cosby et al. 1986b), although they were described as base cation exchange reactions in previous literature accounts (Cosby, Hornberger, and Galloway 1985; Cosby et al. 1985). The use of Al^{3+} as the reference cation in the MAGIC code is conceptually equivalent to the use of Ca^{2+} as the reference cation in the ILWAS code. For example, the exchange of Ca^{2+} for H^+ in the ILWAS code is equivalent to the exchange of Ca^{2+} for Al^{3+} in the MAGIC code because the concentration of Al^{3+} in solution is determined in the MAGIC code from the pH and the solubility product for $\text{Al}(\text{OH})_3(\text{s})$ (Equation 2.16). Although the exchange relationships are conceptually equivalent in the MAGIC and ILWAS codes, differences in solubility products for $\text{Al}(\text{OH})_3(\text{s})$ can lead to different numerical results. The CEC in the MAGIC code is defined as the sum of $\text{Al}^{3+} + \text{Ca}^{2+} + \text{Mg}^{2+} + \text{Na}^+ + \text{K}^+$ (Table 2.11). Like the ILWAS code, the MAGIC code requires measurements or estimates of the CEC and either the fraction of base cation saturation or selectivity coefficients for up to two soil layers. Individual laboratory or field measurements from soil samples taken from more than two layers must be averaged together vertically and areally to obtain lumped values for the soil-exchange properties for the entire watershed. These values may be modified during code calibration but should fall within a reasonable range determined from individual field samples.

In the ETD code, an equilibrium relationship for cation exchange is not used. Instead, the bulk cation exchange is determined from a kinetic expression that is a function of H^+ concentration and the degree of base cation depletion in the soil layers, as shown in Table 2.11 (Nikolaidis 1987). The amount of ANC generation resulting from cation exchange is linked directly to the bulk cation exchange rate without requiring knowledge of the exchange behavior of specific cations in the soil. In using the ETD code, the magnitude of the rate coefficient for cation exchange rate is determined for the entire watershed by calibrating the code

results of ANC to match measured ANC values determined for soil solutions and/or the lake.

The equilibrium-based formulations for cation exchange used in the MAGIC and ILWAS codes allow the modeler to base his selection of exchange coefficients on experimental measurements that are representative of a specific site. Although cation exchange coefficients may vary over an entire watershed and may also be pH-dependent, the modeler can use whatever data are available to set up his input files. The selection of exchange coefficients is extremely important because it defines as an initial state the degree to which a watershed can quickly buffer acid deposition through rapidly occurring cation exchange reactions, and determines the amount of acid buffering resulting from exchange reactions relative to mineral weathering. The rate of depletion of the initial exchange capacity and degree to which it is replenished by weathering reactions are expected to be important indicators of future watershed acidification rates. In contrast, the cation exchange formulation used in the ETD model relates the rate of ANC generation to base saturation. Experimental measurements of base saturation for a watershed can be used to select representative initial values, but the important parameter is the rate coefficient (see Table 2.11), which governs the rate of cation depletion. Except for prior calibration experience, the modeler has no reference point to determine the rate coefficient and, in fact, has no way to separate the amounts of ANC generated by cation exchanged relative to mineral weathering because both relate a rate (that is, the rate of ANC generation) to calibrated parameters. Neither process can be related to experimental measurements that are specific to a watershed.

2.5.7 Anion Retention

Nitrate and sulfate are the principal strong acid anions that are present in acid deposition (Galloway, Likens, and Edgerton 1976; Bishoff, Paterson, and MacKenzie 1984). Increases in the concentrations of strong acid anions cause a direct reduction of ANC, as can be seen from the charge balance definition of ANC given in Equation 2.13. The soils of many forested watersheds are nitrogen-deficient. As a result, NO_3^- is

taken up in vegetation, where it may be reduced to NH_3 and incorporated into organic molecules (e.g., R-NH_2). This biochemical reaction requires the uptake of one H^+ ion, which is the equivalent of the release of one OH^- ion, thereby balancing the acid/base cycle for NO_3^- (Reuss and Johnson 1986). In past simulations by the MAGIC and ETD codes, it has been assumed that the majority of the NO_3^- in acidic deposition is taken up by plants and does not make a significant contribution to the reduction of ANC. This assumption is not valid if significant NO_3^- leaches from the soil before being taken up by plants. Nitrate leaching may be important during episodic periods such as spring snowmelt or heavy rainfall when accumulated NO_3^- and associated H^+ can be transported to the surface waters of a watershed over a period of only several hours or days (Reuss and Johnson 1986; Schofield, Galloway, and Hendry 1985; Tranter et al. 1987). During this time of the year, the residence time of the meltwater in the soil zones is too short to permit significant NO_3^- uptake by vegetation. Uptake also is slowed by cold weather dormancy of plants during early spring. Also, in geographic regions that receive NO_3^- deposition throughout the year in excess of vegetation requirements, such as in southern Scandinavia and northern Europe (van Breeman et al. 1982; van Breeman and Jordens 1983; Höfken 1983), NO_3^- leaching may significantly contribute to chronically lowered ANC values of surface waters. However, SO_4^{2-} is generally assumed to be the major anion in deposition that causes long-term annual average acidification of surface waters for most watersheds located in the eastern U.S.

Acidic deposition results in an increase in SO_4^{2-} concentration in soil solution and, consequently, a decrease in ANC, assuming the sum of base cations remains approximately constant. However, the concentration of SO_4^{2-} in soil solution is limited by the adsorption capacity of the soil minerals for SO_4^{2-} . Modeling and conceptual studies (Galloway, Norton, and Church 1983; Cosby et al. 1986b) have indicated that systems with high capacities to retain SO_4^{2-} in the soil will suffer less extensive and delayed rates of acidification. The expressions used in the MAGIC, ETD, and ILWAS codes to describe SO_4^{2-} adsorption are given in Table 2.12.

TABLE 2.12. Expressions for Anion Retention in the MAGIC, ETD, and ILWAS Codes (a)

Code	Sorbing Anions	Formulation	Expression	Units	
				Adsorbed Anion	Solution Anion
MAGIC	SO_4^{2-}	Langmuir	$[\text{As}] = 2[\text{A}_{\text{max}}][\text{A}] / \{[\text{A}_{1/2}] + 2[\text{A}]\}$	$[\text{As}]$: $\text{eq} \cdot \text{kg}^{-1}$ $[\text{A}_{\text{max}}]$: $\text{eq} \cdot \text{kg}^{-1}$	$[\text{A}]$: $\text{eq} \cdot \text{m}^{-3}$ $[\text{A}_{1/2}]$: $\text{eq} \cdot \text{m}^{-3}$
ETD	SO_4^{2-}	Linear	$[\text{As}] = \{1 + K_s M / \theta\} [\text{A}]$	$[\text{As}]$: $\text{eq} \cdot \text{m}^{-3}$ K_s : $(\text{eq} \cdot \text{kg}^{-1}) / (\text{eq} \cdot \text{m}^{-3})$ θ : $\text{m}^{-3} \cdot \text{kg}^{-1}$	$[\text{A}]$: $\text{eq} \cdot \text{m}^{-3}$
ILWAS	SO_4^{2-}	Linear	$[\text{As}] = [\text{A}] / K_s$	$[\text{As}]$: $\text{meq} \cdot \text{kg}^{-1}$	$[\text{A}]$: $\text{meq} \cdot \text{L}^{-1}$
	H_2PO_4^-	Linear	$[\text{As}] = [\text{A}] / K_s$	K_s : $\text{kg} \cdot \text{L}^{-1}$	
	$\text{H}_3\text{R}''''$	Nonlinear	$[\text{As}] = \alpha [\text{R}_t] / K_s$		

(a) where $[\text{A}]$ = equilibrium concentration of anion A in solution

$[\text{As}]$ = equilibrium concentration of sorbed anion A in soil

$[\text{A}_{\text{max}}]$ = maximum sulfate adsorption capacity of soil

$[\text{A}_{1/2}]$ = equilibrium concentration of anion A when $[\text{As}] = \frac{1}{2} [\text{A}_{\text{max}}]$

K_s = equilibrium adsorption constant

θ = amount of fluid in soil pore space

α = equilibrium constant for organic acid dissociation (total of 3 for triprotic acid)

$\text{H}_3\text{R}''''$ = a triprotic organic acid

R_t = total organic acid

M = soil density.

The MAGIC code uses a Langmuir-type expression (Cosby et al. 1986) to describe the adsorption of SO_4^{2-} as a nonlinear function of the equilibrium SO_4^{2-} concentration in soil solution that is independent of pH (Table 2.12). The important constants in this expression are the maximum SO_4^{2-} adsorption capacity, $[A_{\text{max}}]$, and the half-saturation constant for SO_4^{2-} , $[A_{1/2}]$, which is the concentration of SO_4^{2-} at which the amount of adsorbed SO_4^{2-} is equal to one half of $[A_{\text{max}}]$ (Cosby et al. 1986b). In the application of the MAGIC code to watersheds, these constants represent areally and vertically lumped variables that must be estimated over the entire watershed by aggregation of measured values or by calibration procedures. Cosby et al. (1986b) report that reasonable values of $[A_{\text{max}}]$ and $[A_{1/2}]$ can be determined from deposition history, average stream concentrations of SO_4^{2-} , and the rate of change of the SO_4^{2-} concentration in the watershed during the period of the calibration data. These authors also report that the response time for a system receiving SO_4^{2-} deposition is dependent more on the magnitude of $[A_{\text{max}}]$ than $[A_{1/2}]$, but that the overall response is a complex function of both parameters.

Both the ETD and ILWAS codes use linear relationships to describe the adsorption of SO_4^{2-} as a function of the equilibrium SO_4^{2-} concentration in soil solution (Table 2.12). An average value for the SO_4^{2-} adsorption constant, K_s , is required for each soil layer in both the ETD and ILWAS codes. The ILWAS code also uses a linear formulation for the adsorption of H_2PO_4^- and a nonlinear formulation for the adsorption of a triprotic organic acid (Table 2.12). The change in speciation of the adsorbing organic acid species with pH is incorporated into the adsorption equation by the appropriate dissociation constants (Table 2.12).

In general, the Langmuir-type formulation used in the MAGIC code is more descriptive of the adsorption characteristics of soils over a larger range of SO_4^{2-} concentrations than are linear relationships. Experimental studies of SO_4^{2-} adsorption onto oxide solids (Hingston, Posner, and Quirk 1972; Davis and Leckie 1980) and soils (Chao, Harward, and Fang 1962; Couto, Lathwell, and Bouldin 1979) have found that Langmuir-type expressions are required to adequately describe SO_4^{2-} adsorption. However, concentrations at which SO_4^{2-} adsorption becomes nonlinear may not be reached

in forest soils receiving acidic deposition. For example, anion adsorption experiments with soil from the Hubbard Brook Experimental Forest, New Hampshire, by Nodvin, Driscoll, and Likens (1986a, 1986b) showed that SO_4^{2-} concentration as a linear function of the amount adsorbed in solutions containing 0 to $146 \mu\text{mol}\cdot\text{liter}^{-1}$ SO_4^{2-} and 1:10 solid-to-solution ratios.

Perhaps more important than the question of using linear or nonlinear relationships to describe anion adsorption is the lack of pH dependence in the formulations used in the codes (Table 2.12). The adsorption capacity of the soils is strongly influenced by the amphoteric natures of the oxide minerals in soils, hence is pH-dependent (Schindler 1981). Experimental studies of SO_4^{2-} adsorption by soils have shown that pH is a master variable that controls adsorption capacity (Chao, Harward, and Fang 1962; Nodvin, Driscoll, and Likens 1986b). However, cation exchange capacities and weathering generally stabilize soil pH values. Thus, for simulation periods of less than 50 or 100 years, the dependence of SO_4^{2-} adsorption on pH may be of little importance. Also, the lack of available data on the pH dependence of SO_4^{2-} adsorption in watersheds prevents the actual application of such data in forecasts of watershed acidification. The aggregation process used in the three codes would require that the pH dependence be determined for the majority of the soils and horizons in a watershed. Both the MAGIC and ETD codes adjust the SO_4^{2-} adsorption parameters through the calibration process. Thus, it is not clear whether the capability to simulate the pH dependence of SO_4^{2-} adsorption would increase the accuracy of forecasts although it would be useful for carrying out sensitivity analyses.

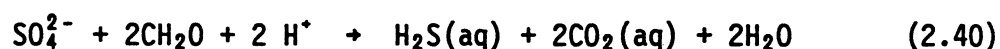
2.6 BIOGEOCHEMICAL PROCESSES

Biogeochemical processes are also important for controlling the response of a watershed to acidic deposition. The reduction of sulfate to sulfide and nitrification are redox processes that involve interaction with organic matter and catalysis by microorganisms. Other biogeochemical processes involve uptake of nutrients from soil layers by vegetation, canopy processes, and decomposition of organic matter with the subsequent return of nutrients to the soil. The ILWAS code includes explicit

representations of many biogeochemical processes in its code formulations, whereas the MAGIC and ETD codes have much less extensive capabilities. The incorporation of numerous biogeochemical process formulations in the ILWAS model does not necessarily equate to more accurate predictions. Representative data for many of the biogeochemical processes are available only for intensively monitored watersheds, such as the three Adirondack lakes studies under the ILWAS project (Gherini et al. 1985). For other less well-studied watersheds, the magnitudes of biogeochemical process variables can be obtained from the ILWAS project watersheds or estimated.

2.6.1 Sulfate Reduction

The reduction of SO_4^{2-} is predominantly an in-lake or wetlands process and can be described (Schnoor and Stumm 1985) in general terms by



The stoichiometry of this reaction shows that SO_4^{2-} reduction can result in a net consumption of H^+ ions, thereby increasing the ANC. All three codes have some capability to account for ANC increase in a lake, which would result from SO_4^{2-} reduction (Table 2.13). In the MAGIC code, a quasi-first-order rate expression is used to describe SO_4^{2-} reduction as a function of the amount of SO_4^{2-} input to the lake (Table 2.13). The user specifies a fraction of the total SO_4^{2-} coming into a lake that is reduced to sulfide during each year of code simulation. The removal of SO_4^{2-} from the lake is actually treated as an uptake rate in the formulations used in the MAGIC code (Cosby et al. 1985), but for calculating the lake ANC, this formulation is analogous to SO_4^{2-} removal by a reduction process.

In both the ILWAS and ETD codes, SO_4^{2-} reduction is described by first-order rate expressions with temperature-dependent rate constants (Table 2.13). In the ILWAS code, different rate constants can be used to simulate different rates of SO_4^{2-} reduction in each lake layer specified by the user. In the ETD code, however, reduction is considered to occur throughout the entire lake volume at an equivalent rate. In lakes that do not develop anoxic layers, SO_4^{2-} reduction may still occur in the lake

TABLE 2.13. Biogeochemical Processes Used in the MAGIC, ETD, and ILWAS Codes^(a)

Code	Sulfate Reduction (Lake)	Nitrification (Soil and Lake)	Nutrient Uptake (Soil)
MAGIC	$-d[SO_4^{2-}]/dt = k$	$-d[NH_4]/dt = k$	$-d[u_i]/dt = k$
ETD	$-d[SO_4^{2-}]/dt = k_T[SO_4^{2-}]$	-	-
ILWAS	$-d[SO_4^{2-}]/dt = [kA/V][SO_4^{2-}]$	$-d[NH_4]/dt = k\{[NH_4]/\{[NH_4]_{50} + [NH_4]\}\}$	$-d[u_i]/dt = u_i(bg) + u_i(lg) + u_i(fer)$

(a) where A = aquatic area
 k = temperature-dependent rate constant
 $k_T = k_{25} \cdot \theta^{T-25}$
 T = °C
 t = time
 $\theta = 1.02 - 1.09$
 V = lake volume

a = pH-dependent factor
 $k = a \cdot r_{max} \theta^{T-25}$
 $[NH_4]_{50}$ = conc. at which rate is 50% of maximum
 r_{max} = maximum rate at 25°C
 θ^{T-25} = temp. corr. factor

(bg) = bole growth
 (fer) = foliar exudation
 (lg) = leaf growth
 $[u_i]$ = conc. of chemical species i, taken up by vegetation

not develop anoxic layers, SO_4^{2-} reduction may still occur in the lake sediments. The ILWAS code can simulate this process by calculating the diffusive flux of SO_4^{2-} from the lake into the uppermost sediment layers where the SO_4^{2-} is reduced to $H_2S(aq)$.

2.6.2 Nitrification

The oxidation of NH_4^+ is another microbially mediated redox reaction. Nitrification results in a production of H^+ ions, as shown by the following general reaction



The MAGIC code has a limited capability to simulate the loss of NH_4^+ resulting from nitrification. It does so by using a zero-order rate expression that treats the loss of NH_4^+ from the soil as a nutrient uptake

process (Table 2.13). The user can specify an average amount of NH_4^+ lost by the combination of nitrification and uptake processes for a given year of code simulation. The ILWAS code includes the nitrification reaction for the soil and lake and uses a Michaelis-Menten expression (Chen et al. 1983) to describe the reaction rate (Table 2.13). The user specifies the rate constant for the nitrification rate in the soil and in the lake. The ETD code does not include any nitrogen chemistry.

2.6.3 Nutrient Uptake

During the growth of vegetation, equivalent amounts of strong acid anions and base cations may not be taken up (Reuss and Johnson 1986), resulting in a charge imbalance that is made up by H^+ and OH^- ions. The uptake of nutrients by vegetation and the resulting effects on soil ANC are included in the MAGIC and ILWAS codes.

In the MAGIC code, a zero-order rate expression is used to describe the fraction of specific chemical species (e.g., NO_3^- , NH_4^+ , SO_4^{2-}) taken up each year by vegetation (Table 2.13). The MAGIC code does not distinguish between the loss of nitrogen or sulfur species by plant uptake and redox reactions, but the user can specify the sum. Previous uses of the MAGIC code have included nutrient uptake only for N-containing species (Cosby et al. 1985), but uptake rates for other anions and cations can be specified.

The ILWAS code tracks the uptake of chemical species by various growth processes such as bole growth, leaf growth, and foliar exudation (Table 2.13). The rates of these growth processes are controlled by the net tree productivity ($\text{kg}\cdot\text{ha}^{-1}\cdot\text{yr}^{-1}$), which is specified for various canopy types. The user can specify monthly nutrient uptake rates to incorporate the seasonal pattern of tree growth into the nutrient uptake rates. The ILWAS code uses equivalent rate coefficients for NO_3^- and NH_4^+ and assumes that the rates of uptake of these species are directly proportional to their masses in soil solution (Chen et al. 1983).

2.6.4 Other Biogeochemical Processes Included in the ILWAS Code

The ILWAS code also includes formulations for the following biogeochemical processes: 1) canopy-induced changes in throughfall chemistry (canopy types include deciduous, coniferous, and open), 2) foliar exudation, 3) litter fall and decay, and 4) root respiration. Detailed descriptions of the formulations used for these processes in the ILWAS code are provided in Chen et al. (1983) and Gherini et al. (1985). Much of the following information is from these two references.

Canopy Throughfall Chemistry

The ILWAS code relies on user-supplied information about the area of each canopy type and the monthly leaf area indices to calculate the canopy interception storage volume and the volume of precipitation that falls through the canopy. The masses of chemical constituents in the canopy storage and throughfall are calculated from the wet deposition chemistry and the collection efficiency of the canopy for dry deposition. The deposition of various chemical constituents in the throughfall (D_{it}) resulting from dry deposition onto the canopy is calculated from the relationship

$$D_{it} = 0.01 \cdot E_f \cdot V_d \cdot C_{Ai} \cdot L_s \cdot A \quad (2.42)$$

where E_f = the collection efficiency

V_d = the deposition velocity in $\text{cm} \cdot \text{sec}^{-1}$

C_{Ai} = the concentration of constituent i in the air in $\mu\text{eq} \cdot \text{m}^{-3}$

L_s = the leaf area index (unitless)

A = the land surface area in m^2 .

Gaseous and ionic constituents such as $\text{SO}_x(\text{g})$, $\text{NO}_x(\text{g})$, and NH_4^+ are assumed to be oxidized to SO_4^{2-} and NO_3^- on the leaf surfaces. A rate expression, with a first-order dependence on NH_4^+ mass and a temperature-dependent rate constant, is used to calculate NH_4^+ oxidation on the leaf surfaces.

Foliar Exudation

The ILWAS code includes foliar exudation of chemical species onto the leaf surfaces although few data on the rates of foliar exudation are

available. The ILWAS code assumes that the foliar exudation rate for a chemical species i , X_i , is proportional to the leaf chemical composition, i.e.,

$$X_i = \alpha \cdot \gamma_i \cdot C_{Li} \cdot W_L \cdot L_s \cdot A/n \quad (2.43)$$

where α = effective leaf turnover rate in day^{-1}

γ_i = an ion amplification factor for species i

C_{Li} = the concentration of species i in the leaf in $\mu\text{eq}\cdot\text{g}^{-1}$

W_L = a factor for converting leaf dry weight to leaf area in $\text{g}\cdot\text{m}^{-2}$

n = the number of seconds in a day

L_s = the leaf area index (unitless)

A = the land surface area in m^2 .

The effective leaf turnover rate and amplification factors are calibration parameters that are determined through comparisons of code results with field observations. The ILWAS code uses the amounts of dry deposition and foliar exudation determined from the above expressions, wet deposition chemistry, and the canopy interception volume to calculate the concentrations of chemical species in the throughfall precipitation.

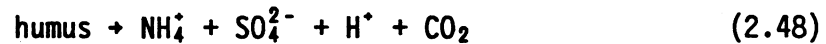
Litter Fall and Decomposition

The effects on soil chemistry of the fall and decay of leaf litter are also included in the ILWAS code. The rates of litter fall, L_f ($\text{kg litter}\cdot\text{m}^{-2}\cdot\text{mth}^{-1}$), and the weight fraction that is immediately leachable are input parameters that are specified for each canopy type. The immediate release of a chemical species to soil solution is determined from

$$X_{Fi} = C_{Li} \cdot F \cdot L_f \cdot A \cdot \Delta t \quad (2.44)$$

where X_{Fi} is the release rate for species i in $\mu\text{eq}\cdot\text{sec}^{-1}$, F is the fraction of leachable ions for one of the three canopy types (deciduous, coniferous, or open), and Δt is the time step in seconds used for numerical

calculations. The decay of the fallen litter is described by the rates of the four general reactions that follow:



The rates of these reactions are assumed to be directly proportional to the concentrations of the reactants, and the first-order rate constants are specified by the code user. The user also specifies the fractions of NH_4^+ and SO_4^{2-} that are released to soil solution by these decomposition reactions and the amounts of nitrogen, sulfur, and carbon present in the produced organic acid.

Root Respiration

The ILWAS code determines the production of $\text{CO}_2(\text{g})$ in the root zone by the following expression:

$$R = R_B + a \cdot R_A \cdot U_M \quad (2.49)$$

where R = the total root respiration rate in $\text{mg C} \cdot \text{cm}^{-2} \cdot \text{sec}^{-1}$

R_B and R_A = the basal and active metabolism rates, respectively, for tree growth in $\text{mg C} \cdot \text{cm}^{-2} \cdot \text{sec}^{-1}$

U_M = the fraction of total yearly uptake that occurs in a given month

a = a unit conversion factor.

The user specifies U_M , R_B , R_A , and root distribution as functions of depth for each canopy type. Root respiration and litter decay are the main sources of $\text{CO}_2(\text{g})$ in the soil zone. Some of the $\text{CO}_2(\text{g})$ may vent to the atmosphere, dissolve in the soil solution, or be moved spatially by fluid advection. The ILWAS code calculates the loss of $\text{CO}_2(\text{g})$ to the atmosphere by means of a simple diffusion equation, and the amount dissolved in the

soil solution by a Henry's law expression (see Equation 2.31). The advective transport of $\text{CO}_2(\text{g})$ is determined from the percolation rates of the fluid phase in the soil layers and from changes in moisture content, which cause liquid displacement of the $\text{CO}_2(\text{g})$ present in the gas phase in the void volume of the soil.

2.7 SUMMARY

The MAGIC and ILWAS codes contain all of the processes currently thought to be most important for affecting the chemical compositions of soil and surface waters in watersheds receiving acid deposition (NAS 1984), including carbonic acid equilibria, aluminum hydroxide dissolution and speciation, silicate mineral weathering, anion retention, cation exchange, and pH-buffering by organic acid dissociation. These two codes also contain similar suites of major cations and anions present in surface and soil waters, except that the ILWAS code also considers silica and organically complexed aluminum.

The primary differences between the MAGIC and ILWAS codes are in the formulations used to represent various processes and the level of detail contained within those formulations. Among the more important differences are the ANC conventions. The ILWAS code uses an ANC convention that is consistent with analytical methods for ANC determination, whereas the MAGIC code uses a slightly different convention. For most slightly acidic waters, the different conventions result in negligible differences in predicted ANC values. However, for waters with pH less than about 5.0, ANC values predicted by the two codes will be significantly different and should be kept in mind when comparing results.

The ILWAS code also contains formulations for complexing of aluminum by organic acids. This capability may be important for organic acid-rich waters, where total dissolved aluminum concentrations are higher than would be expected from $\text{Al}(\text{OH})_3(\text{s})$ solubility. Neither code includes aluminum adsorption to organic materials or pH-dependent relationships for SO_4^{2-} adsorption. The MAGIC, but not the ILWAS code, includes a pH-dependent relationship for cation exchange. However, these relationships

are not well known, making it difficult to assess their importance for predictive accuracy. The ILWAS code contains a more current representation of the temperature dependence of $\text{Al}(\text{OH})_3(\text{s})$ solubility than does the MAGIC code, which currently uses outdated thermodynamic data. The more complex representations of aluminum chemistry in the ILWAS code make it more suited for predicting the seasonal dynamics of aluminum concentrations compared to the MAGIC code.

The rate expressions for mineral weathering are grossly similar in form in both codes, but differ in detail. In the MAGIC code, weathering is specified by the user as the rate of production of an individual cation or anion per unit area of watershed. The composition of soil minerals can be used to guide the relative proportions of different ions produced by weathering reactions. In the ILWAS code, specific minerals present in the soil are dissolved according to the stoichiometry of the mineral. The inclusion of silica in the mineral stoichiometries provides a means for estimating the total amount of mineral weathering occurring in a watershed, assuming one has correct representations of the dissolution reactions. This permits the estimation of base cations from weathering to be separated from base cations supplied by cation exchange.

The ILWAS code also contains a number of biogeochemical processes that are not included in the other two codes and that potentially affect surface and soil water chemistry. The inclusion of these processes does not necessarily provide for better accuracy in predicting watershed acidification because data for many of the processes are available for only very intensively monitored watersheds. However, for watersheds where data are available, inclusion of the biogeochemical processes in the ILWAS code makes it more able to predict episodic and seasonal changes in soil and surface water chemistry. The inclusion of these processes in ILWAS also allows sensitivity analysis of the effect of forest fires or clear-cutting on watershed acidification.

In contrast to the other two codes, the ETD code does not include aluminum dissolution, cation exchange equilibrium, or organic acid buffering, and only considers a limited set of chemical species (i.e., ANC,

SO_4^{2-} , Cl^- , H^+ , and carbonic acid species). The lack of aluminum chemistry forces one to use a secondary code to determine aluminum concentrations after predictions of surface water chemistry are made, and it precludes using the ETD code to make any predictions in acidic systems (i.e., pH less than 5.0 to 5.5), where $\text{Al}(\text{OH})_3(\text{s})$ dissolution exerts a major effect on solution pH. The lack of nitrogen chemistry in the ETD code precludes its use in systems receiving a significant proportion of acidity in the form of nitrogen oxides and hydrates. Also, the rate formulations used to represent cation exchange in the ETD code do not allow the modeler to use available data on exchange coefficients to determine the relative importance of cation exchange versus mineral weathering for generating ANC because both are effectively calibrated variables. In large part, the formulations and the limited chemistry in the ETD code do not allow the modeler to use available data on soil chemistry to define the initial chemical state of a watershed.

Many of the differences in the codes also reflect the modeling approach of the code authors and the time scales for which the codes were intended to be used. For example, the MAGIC code incorporates nearly all of the major geochemical processes affecting watershed chemistry but does so with considerable temporal aggregation of variables. This approach is consistent with the MAGIC code's intended use of predicting average monthly to yearly changes in soil and surface water chemistry. Thus, the MAGIC code is very useful for making predictions of water chemistry for watersheds where detailed monitoring data are not available and for analyzing the effect of uncertainties in input data on predicted results. By contrast, the long time scales in the MAGIC code do not allow it to be used for predicting episodic events.

On the other hand, the high degree of process detail and short time step (generally one day) of the ILWAS code make it suitable for predicting episodic and seasonal events, and for conducting detailed numerical experiments to analyze the effects of different processes on soil and surface water chemistry. Although its input data sets are extensive, the ILWAS code can also be used for watersheds where monitoring data are

sparse. However, this requires that many variables, especially the biogeochemical ones, be estimated from the modeler's past experience or by analogy with well-studied watersheds. The ILWAS code also contains several output options that can be used for bookkeeping chores to track the mass balance relationships of all chemical constituents. This capability is helpful in analyzing code behavior in calibration, numerical experiments, and field testing of process representation.

In summary, the MAGIC and ILWAS codes are advanced models of the combined meteorological, hydrological, and biogeochemical processes that govern watershed acidification. In comparison, the ETD code appears to be less useful in predicting watershed acidification or for understanding acidification processes because it does not include many chemical processes and constituents accepted as being important in watershed acidification, and does not take advantage of measured soil chemistry characteristics to define an initial state from which calibration and modeling can be started. Although all three codes appropriately simulate discharge hydrographs, the state-of-science limitations in the modeling of flow routing limit the predictive capability of watershed acidification models.

Each of the codes incorporates to varying degrees process formulations that are consistent with theoretical and experimental studies of natural systems. Although the inclusion of a greater number of process representations in a watershed acidification code does not necessarily translate into increased predictive reliability, it improves the likelihood of reliable forecasts. Predictive reliability can only be assessed through comparison of code predictions to observed data from monitored watersheds and not solely from comparisons of process formulations or degrees of aggregation.

3.0 ANC GENERATING PROCESSES IN MAGIC, ILWAS, AND ETD CODES

D. C. Girvin, E. A. Jenne, L. E. Eary, and L. W. Vail

The evaluation of watershed response to acidic deposition and the ability of a specific watershed code to describe this response typically focuses on the acid neutralizing capacity (ANC) of surface waters. However, the conceptual and computational adequacy of a watershed acidification code cannot be readily evaluated by comparing measured surface water ANC with code simulations of the watershed response because a maximum period of only 1 to 2 years of data is likely to be available for testing after the calibration period. The critical examination of ANC generation by individual processes for short-term forecasts that are presented in this section establish the reasonableness of predictions of the ANC contributed by individual processes. However, this analysis cannot serve as a substitute for comparisons of model forecasts with multi-year field data in establishing the reliability of long-term forecasts using the watershed acidification codes considered here.

This section also assesses the relative importance of cation exchange and mineral weathering, the major watershed processes contributing to the neutralization of acidic deposition, and other acid neutralizing processes (e.g., SO_4^{2-} adsorption). Three watershed acidification codes MAGIC, ETD, and ILWAS have been used to examine the variation in forecasted ANC fluxes (mass/unit watershed area) from individual processes in the Panther Lake, Woods Lake, and Clear Pond watersheds for two deposition scenarios (three for MAGIC).

3.1 APPROACH

For Panther and Woods Lakes and Clear Pond, calibrated input data sets for the MAGIC code were received from B. J. Cosby and G. M. Hornberger (University of Virginia) and for the ETD code from N. P. Nikolaidis (University of Iowa). Calibrated input data sets for the ILWAS code were received from R. K. Munson and S. A. Gherini (Tetra Tech, Inc., Lafayette, CA) for Panther and Woods Lakes; the ILWAS code's calibrated

input data set for Clear Pond was not available. The input data sets for these three Adirondack watersheds contain daily values (ETD and ILWAS) or monthly (MAGIC) average values of observed data (see Table 2.1 for time-averaging intervals) and values of calibration variables. Based upon these calibrations, 12 to 15-year predictions or 50-year predictions (MAGIC only) were made for the deposition scenarios described below to examine the magnitude and variation in ANC generation for specific processes as a function of time and acid deposition amount. Some factors affecting this analysis are noted below.

The quantity of precipitation falling in a given period of time affects the ANC of immediately down-gradient surface waters. In the absence of long-term records of precipitation for these watersheds, the 2 years (Clear Pond) or 3 years (Panther and Woods) of available daily precipitation data were cycled during the 12- to 15-year prediction period for the ETD and ILWAS codes. Although year-to-year variations in ANC are of significant interest, the annual average ANC values reported below for the ETD and ILWAS codes have been averaged over the 3 years corresponding to the precipitation record cycle (1-1/2 cycle in the case of Clear Pond) in order to evaluate model response and compare models. Since monthly precipitation values are used by the MAGIC code, average values were derived from the 3 years of available daily precipitation data. These average monthly values were used for all years for which the MAGIC code was run.

The weathering rates in all three codes can depend on the H^+ concentration in the soil solution raised to a fractional power, n . In the original calibrated data sets received for the MAGIC code, this fractional power was set to zero ($n = 0$). That is, the weathering rates of silicate minerals in the three Adirondack watersheds considered here were assumed to be independent of H^+ ion concentration and, as a consequence, the weathering rates in MAGIC were constant during the forecast periods. This is the standard weathering scenario used by the authors of the MAGIC

code.(a) However, in calibrating the ETD and ILWAS codes for the watersheds considered here, n was set equal to 0.5 by the authors of these codes. To facilitate comparison between MAGIC and the other two codes, and to examine the difference in the weathering rates calculated by the MAGIC code, both cases $n = 0$ and $n = 0.5$ were examined. The MAGIC code was recalibrated for $n = 0.5$ by PNL, resulting in only relatively minor changes in calibration parameters (weathering rates, selectivity coefficients, and base saturation).

A major uncertainty in evaluating the probable impact of future reductions in sulfur emissions is the extent to which base cation deposition rates will vary as anthropogenic sulfur emissions are reduced. It is assumed that base-cation deposition fluxes are derived from local sources which may be unrelated to sources of sulfur. The three atmospheric deposition scenarios used (base case, Type A, and Type B) encompass this problem. In the first scenario, the deposition fluxes were maintained at the same values used for the calibration (base-case scenario). In the second scenario, the SO_4^{2-} and NO_3^- fluxes were increased or decreased by 20% relative to the base case, while the fluxes of base cations were held constant at base-case values. In concert with the change in anions, hydrogen ion was increased or decreased to maintain charge-balance in the precipitation; for the ETD code, only SO_4^{2-} was varied because NO_3^- is not an input to this code. This approach assumed that the dominant contributions to "acidic deposition" are sulfuric and nitric acid. Thus, since charge balance is maintained between cations and anions in the precipitation, no net change would result in the ANC of the precipitation, relative to the base case for the $\pm 20\%$ deposition scenario. However, for the $\pm 20\%$ deposition scenarios, changes have occurred in the concentrations of 1) the H^+ ion relative to base cations (in the precipitation) and base-cation sources, and 2) SO_4^{2-} relative to soil adsorption capacity. This is referred to as a $\pm 20\%$ Type-A deposition scenario. The $\pm 20\%$ perturbation of total acidic deposition can be visualized as a change of 40% in dry

(a) B. J. Cosby, personal communication 1987.

deposition only. This falls between the dry deposition uncertainty estimates of 50% (Sirois and Barrie 1988) and 30%(a).

In the third scenario, the flux of all constituents was increased or decreased by 20% relative to the base case ($\pm 20\%$ case, Type-B scenario). This scenario was included because it had been used previously in an unpublished study carried out on 10 northeastern United States watersheds for the U.S. EPA by the Pacific Northwest Laboratory in 1987. Only a limited test using the MAGIC code was included since this does not appear to be a realistic scenario. For each deposition scenario, the base-case calibration parameter set was used. For the MAGIC code, a 3-year linear ramp from the base-case deposition to the $\pm 20\%$ deposition values was used. For the ETD and ILWAS codes, the $\pm 20\%$ deposition values were imposed at the start of the calibration years and maintained at those values throughout the forecast period. Because of the time required for the simulation to adjust to changes in deposition scenario, the initial 3 years of an ILWAS code simulation were discarded.

The relative roles of cation exchange and mineral weathering in forecasting contributions to ANC budgets along with ANC production from other processes are examined below for each code: the MAGIC code in Section 3.2, the ETD code in Section 3.3, and the ILWAS code in Section 3.4. They are summarized and compared in Sections 3.5 and 3.6, respectively.

3.2 THE MAGIC CODE

The ANC contributed by cation exchange is not explicitly calculated in the MAGIC code. Therefore, it was obtained by difference from those processes whose fluxes are explicitly calculated by the MAGIC code, as follows:

$$\begin{aligned} \text{cation exchange} &= \text{net flux} - \text{base-cation weathering} - \text{base-cation} \\ &\quad \text{uptake by plants} - \text{anion uptake by plants} - \text{adsorption} \quad (3.1) \end{aligned}$$

(a) T. P. Meyers and B. B. Hicks, personal communication, September 1988.

These processes and fluxes are given for Panther and Woods Lakes in Tables 3.1 and 3.2 for $n = 0.0$ and in Tables 3.3 and 3.4 for $n = 0.5$. Because of the similarity between Panther Lake and Clear Pond watersheds, the flux data for Clear Pond watershed are not given. Scenarios are plotted versus forecast year in Figures 3.1 to 3.4.

Within each watershed, the variations in R (the ratio of ANC contributed by cation exchange to the ANC contributed by base-cation weathering for all scenarios, as noted in Tables 3.1 to 3.4 and Figures 3.1 to 3.4) are dominated by changes in cation exchange in the watershed soils. Where the weathering is constant with time ($n = 0$), the temporal variation in R within each watershed (Figures 3.1 and 3.2) results from variations in ANC contributed to the watershed by the exchange of Al^{3+} for base cations (Ca^{2+} , Mg^{2+} , K^+ , and Na^+) via cation exchange. Where $n = 0.5$ (Figures 3.3 and 3.4), the ANC flux due to weathering varies slightly with time (the maximum variation being 6% for Woods Lake) because of small changes ($\Delta pH \leq 0.1$ pH unit) in soil-solution pH. Thus, the change in R is still dominated by cation exchange. The greater divergence in $\pm 20\%$ R trajectories in Woods Lake as compared to Panther Lake watershed is due to the variation in gibbsite dissolution for Woods Lake (see last column of Tables 3.1-3.4). The difference in the ANC fluxes from weathering and exchange processes for the $n = 0$ and $n = 0.5$ cases were relatively small during the forecasts for all deposition scenarios, as can be seen in Tables 3.1 to 3.4. The reason for this is that the change in soil pH during the forecast period was less than 0.1 pH units. It should also be noted that for the 50-year MAGIC forecasts, described below, the difference in the $n = 0$ and $n = 0.5$ ANC fluxes from weathering and exchange processes was also relatively small, again because the change in soil pH during the forecast was ≤ 0.14 pH units. Because of these small changes in soil pH for all three watersheds and all deposition scenarios, the $n = 0$ weathering scenario originally used by the authors of MAGIC is a reasonably good approximation to the $n = 0.5$ weathering scenario, which we consider to be more representative of weathering processes as they occur in soils. However, experimental data for common silicate minerals indicates

TABLE 3.1.1. MAGIC Code, Forecast of Annual Average Fluxes of ANC from Individual Processes for Panther Lake, All Deposition Scenarios (n = 0; calculation normalized to terrestrial area)

Case	Deposition Scenario	Year	Net		NH ₄ Uptake	NO ₃ Uptake	SO ₄ Adsorption	Cation Exchange	R = $\frac{\text{Cation Exchange}}{\text{Weathering}}$	Atmospheric		
			Watershed Flux	Base Cation Weathering						Flux of Base Cations	Alt Gibbsite Dissolution	
			----- neq.m ⁻² .yr ⁻¹ -----									
Base	Base	1981	213.4	137.7	-28.8	+48.8	28.2	35.5	0.26	69.5	3.9	
Base	Base	1993	218.9	137.7	-28.1	+43.1	24.2	34.8	0.25	69.5	3.8	
-20%	Type A (SO ₄ + NO ₃)	1993	176.5	137.7	-28.1	-32.4	5.3	29.2	0.21	69.5	4.8	
+20%	Type A (SO ₄ + NO ₃)	1993	245.8	137.7	-28.1	53.8	43.8	38.6	0.28	69.5	3.7	
-20%	Type B (all constituents)	1993	192.9	137.7	-22.4	32.4	5.3	48.4	0.29	57.8	3.9	
+20%	Type B (all constituents)	1993	228.2	137.7	-33.9	53.8	43.8	27.9	0.28	81.1	3.7	

TABLE 3.2. MAGIC Code, Forecast of Annual Average Fluxes of ANC from Individual Processes for Woods Lake, All Deposition Scenarios (n = 0; calculation normalized to terrestrial area)

Case	Deposition Scenario	Year	Net Watershed Flux	Base Cation Weathering	NH4 Uptake	NO3 Uptake	SO4 Adsorption	Cation Exchange	R = $\frac{\text{Cation Exchange}}{\text{Weathering}}$	Atmospheric Flux of Base Cations	AIT Gibbsite Dissolution
			----- neq.m ⁻² .yr ⁻¹ -----								
Base	Base	1981	68.0	13.4	-27.6	42.6	25.7	13.9	1.04	55.7	25.4
Base	Base	1993	65.4	13.4	-27.6	42.7	23.7	13.2	0.99	55.7	27.6
-20%	Type A (SO4 + NO3)	1993	37.9	13.4	-27.6	34.2	16.6	7.3	0.54	55.7	20.9
+20%	Type A (SO4 + NO3)	1993	92.7	13.4	-27.6	51.2	36.6	19.1	1.43	55.7	34.9
-20%	Type B (all constituents)	1993	51.6	13.4	-22.1	34.2	16.6	15.5	1.16	46.6	22.1
+20%	Type B (all constituents)	1993	79.2	13.4	-33.1	51.2	36.6	11.1	0.83	64.9	33.4

TABLE 3.3. MAGIC Code, Forecast of Annual Average Fluxes of ANC from Individual Processes for Panther Lake, All Deposition Scenarios (n = 0.5; calculation normalized to terrestrial area)

Case	Deposition Scenario	Year	Net Watershed Flux	Base			S04 Adsorption	Cation Exchange	R = $\frac{\text{Cation Exchange}}{\text{Weathering}}$	AIT Gibbsite Dissolution
				Cation Weathering	NH4 Uptake	NO3 Uptake				
Base	Base	1991	213.0	151.1	-20.0	40.3	20.2	21.4	0.14	3.9
Base	Base	1993	211.2	151.1	-20.1	43.1	24.2	20.5	0.14	3.8
-20%	Type A (S04 + NO3)	1993	176.7	150.5	-20.1	32.4	5.3	16.6	0.11	4.0
-20%	Type A (S04 + NO3)	1993	245.6	152.4	-20.1	53.8	43.0	24.5	0.16	3.7
-20%	Type B (all constituents)	1993	193.1	150.9	-22.4	32.4	5.3	26.9	0.18	3.9
-20%	Type B (all constituents)	1993	229.2	152.1	-33.9	53.8	43.0	14.2	0.09	3.7

TABLE 3.4. MAGIC Code, Forecast of Annual Average Fluxes of ANC from Individual Processes for Woods Lake, All Deposition Scenarios (n = 0.5; calculation normalized to terrestrial area)

Case	Deposition Scenario	Year	Base				S04 Adsorption	Cation Exchange	R = $\frac{\text{Cation Exchange}}{\text{Weathering}}$	AIT Gibbsite Dissolution
			Net Watershed Flux	Cation Weathering	NH4 Uptake	NO3 Uptake				
Base	Base	1981	67.9	15.8	-27.6	42.6	25.7	11.4	0.72	25.4
Base	Base	1993	65.6	16.2	-27.6	42.7	23.7	10.6	0.65	27.5
-20%	Type A (S04 + NO3)	1993	37.9	15.7	-27.6	34.2	10.6	5.0	0.32	22.7
-20%	Type A (S04 + NO3)	1993	92.9	16.6	-27.6	51.2	36.6	16.1	0.97	34.7
-20%	Type B (all constituents)	1993	51.6	16.0	-22.1	34.2	10.6	12.9	0.81	22.0
-20%	Type B (all constituents)	1993	79.4	16.5	-33.1	51.2	36.6	0.2	0.50	33.2

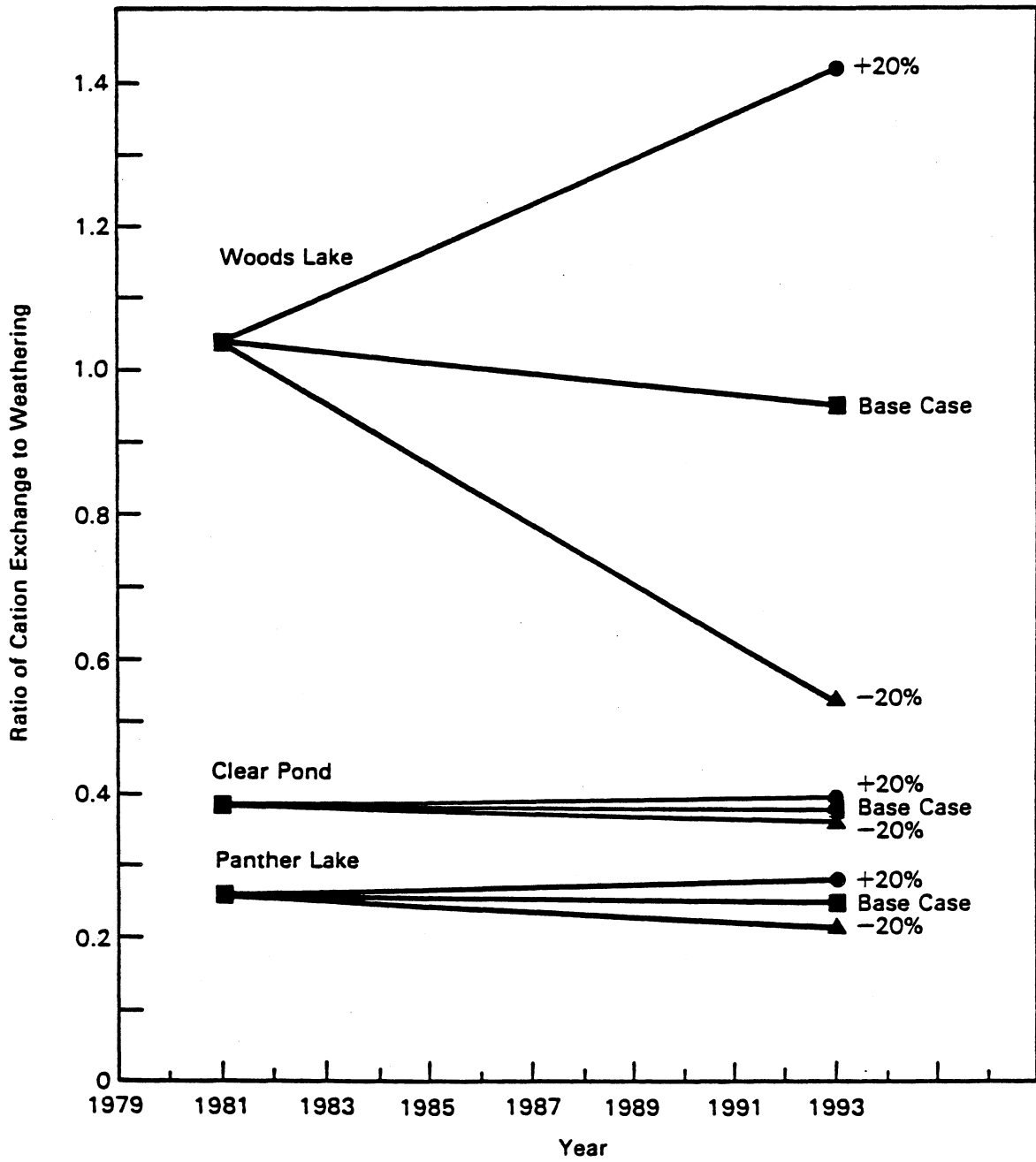


FIGURE 3.1. MAGIC Code, Variation in R Forecast for the Three Watersheds for Base-Case and Type-A Deposition Scenarios (n = 0) (For comparison with Panther and Woods Lakes, the 1984 and 1996 data points for Clear Pond have been plotted for 1981 to 1993.)

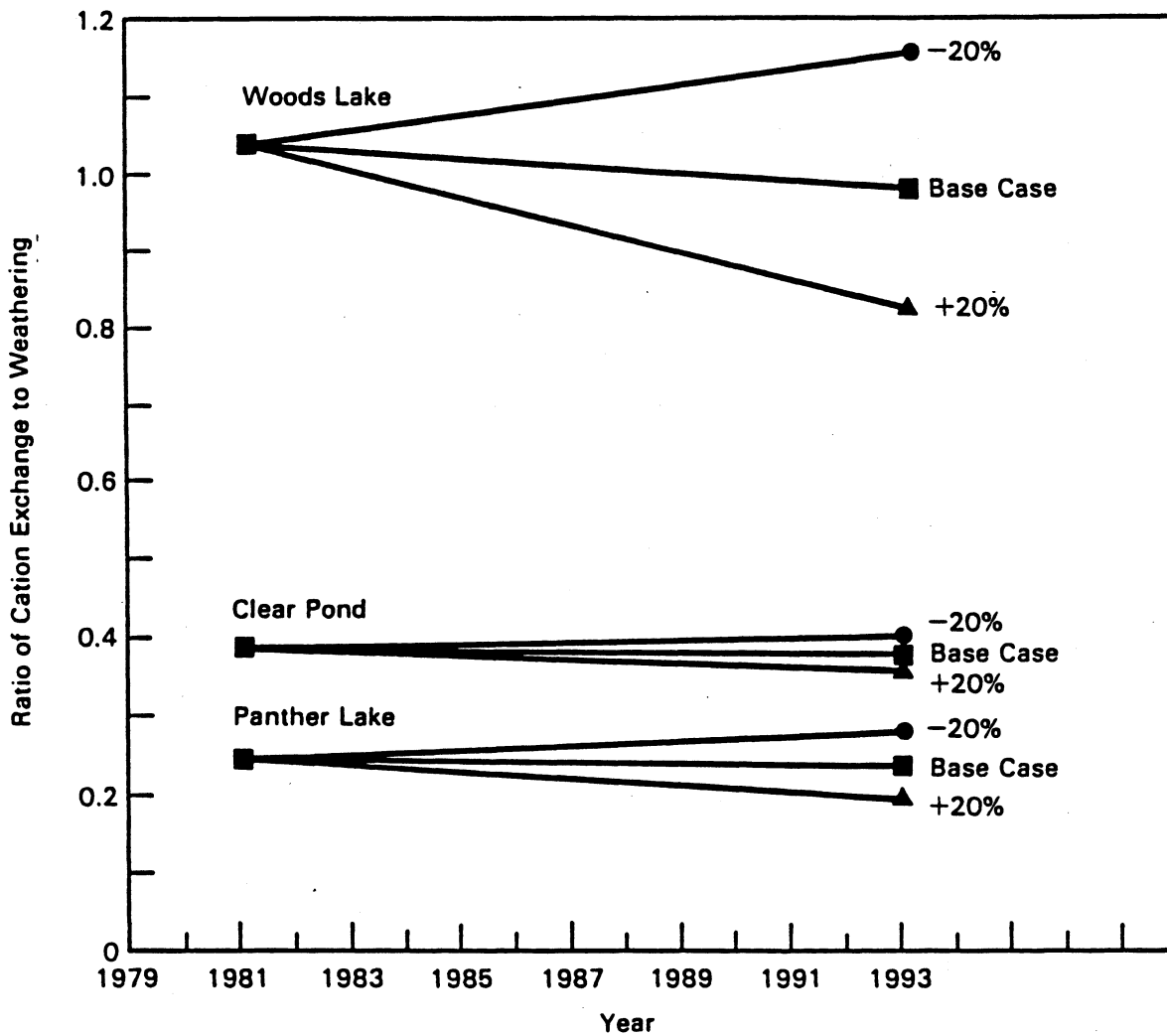


FIGURE 3.2. MAGIC Code, Variation in R Forecast for the Three Watersheds for Base-Case and Type-B Deposition Scenarios ($n = 0$) (For comparison with Panther and Woods Lakes, the 1984 to 1996 data points for Clear Pond have been plotted for 1981 to 1993.)

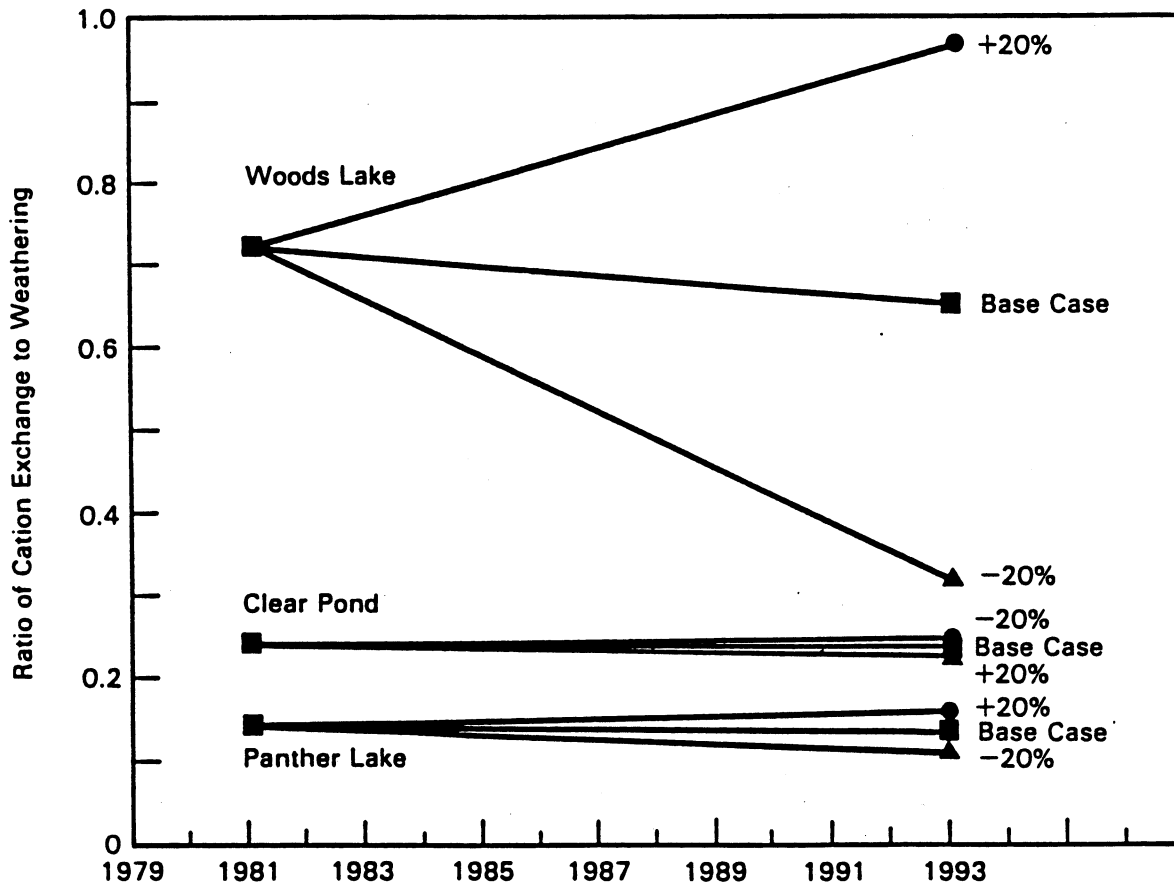


FIGURE 3.3. MAGIC Code, Variation in R Forecast for the Three Watersheds for Base-Case and Type-A Deposition Scenarios ($n = 0.5$) (For comparison with Panther and Woods Lakes, the 1984 to 1996 data points for Clear Pond have been plotted for 1981 to 1993.)

a fractional hydrogen ion dependence of dissolution reaction rates in acid solution of $0.5 \leq n \leq 1.0$ (Lasaga 1984; see discussion in Section 2.5.5).

The difference in the magnitude of R for Panther Lake (and Clear Pond) compared to that for Woods Lake (Figure 3.1) is because of the code structure and the calibration values selected for the base-cation weathering rates. For example, for the 1981 calibration year in Tables 3.1 and 3.2, in which the weathering for Panther Lake is 10 times greater than that for Woods Lake, the cation exchange for Panther Lake is only twice as great. The net result is that the value of R for Woods Lake is a factor of five greater than R for Panther Lake (Figure 3.1). Similar situations

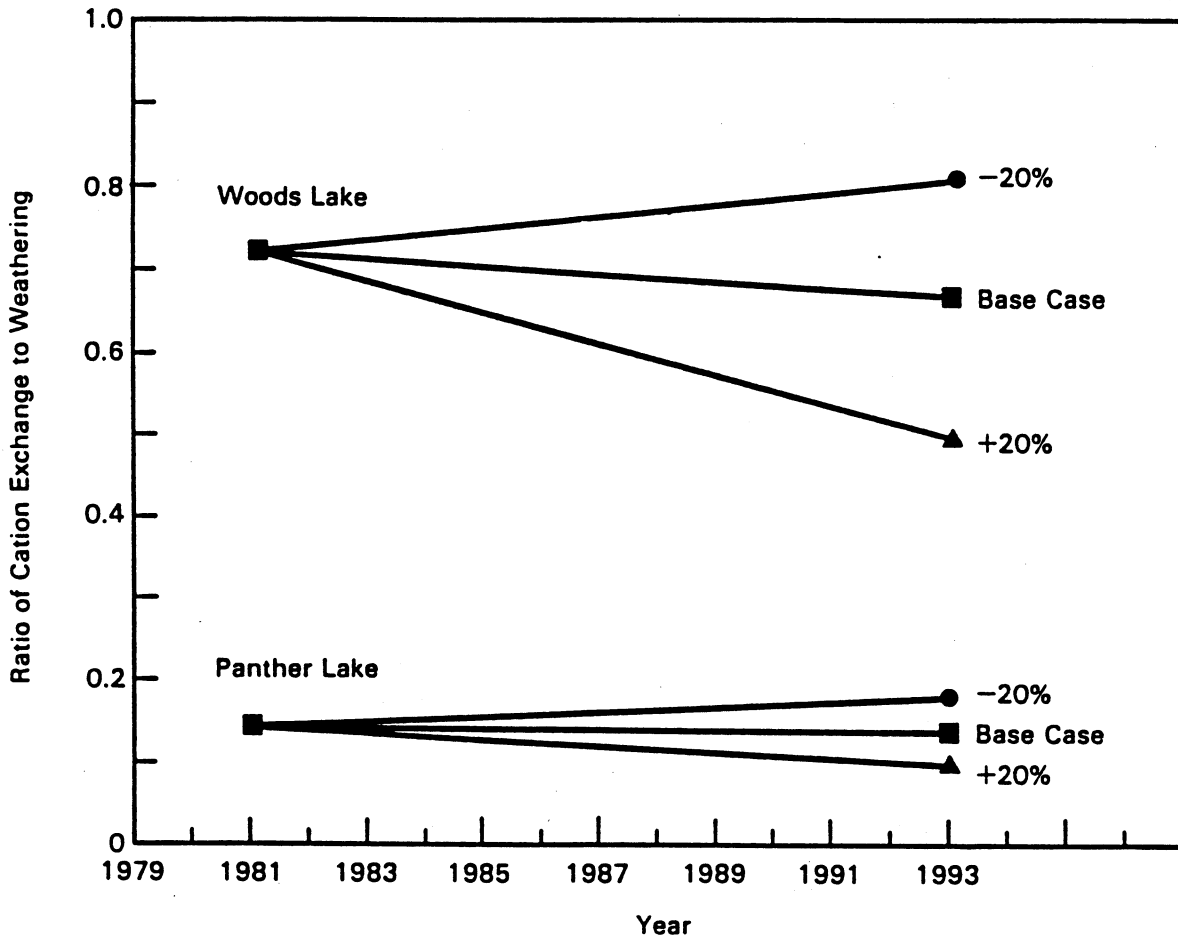
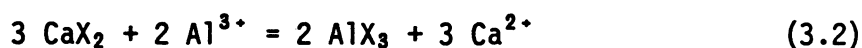


FIGURE 3.4. MAGIC Code, Variation in R Forecast for Woods and Panther Lake Watersheds for Base-Case and Type-B Deposition Scenarios (n = 0.5)

are found in Figures 3.2, 3.3, and 3.4. This increase in R for Woods Lake relative to Panther Lake is because the MAGIC code does not include Al^{3+} from gibbsite dissolution as a base cation; thus, Al is not included in the base cation (Ca^{2+} , Mg^{2+} , K^+ , and Na^+) weathering flux in Tables 3.1 to 3.4. This makes a significant difference for Woods Lake, where the flux of Al from gibbsite dissolution is a factor of two greater than the base-cation weathering flux (Tables 3.2 and 3.4). For Panther Lake, however, the Al flux is only 3% of the base-cation weathering flux (Tables 3.1 and 3.3). Thus, the weathering flux at Woods Lake relative to that at

Panther Lake drops by a factor of 10 because of the exclusion of Al from "weathering." The denominator in R is consequently less for Woods Lake than for Panther Lake.

The MAGIC code assumes that there is equilibrium with gibbsite and that an unlimited quantity of gibbsite is present. The formulation of cation exchange in the MAGIC code includes Al as one of the exchange ions (Al^{3+} , Ca^{2+} , Mg^{2+} , K^+ , and Na^+). Dissolved Al concentrations in the soil solutions are forecasted to be 55% to 85% higher in the Woods Lake than the Panther Lake watershed, depending on the deposition scenario. Therefore, exchange reactions, such as



where X denotes the soil exchange site, are driven to the right to a greater extent at Woods Lake than at Panther Lake. This increase in the numerator in R and the decrease in the denominator in R (described above) produces higher values of R for Woods Lake than Panther Lake and contributes to greater divergence in R for Woods Lake during the forecast period for the $\pm 20\%$ deposition scenarios (Figures 3.1 to 3.4).

Finally, it should be noted that the values of R are less for the cases of $n = 0.5$ than for $n = 0$. This difference results from the necessary recalibration of each watershed and the resulting increase in base-cation weathering and decrease in cation-exchange fluxes for $n = 0.5$ (compare Tables 3.1 through 3.4).

For Panther Lake and Clear Pond, the MAGIC code predicts the ANC of the basin outflow to be 107 and 65 $\text{meq}\cdot\text{m}^{-2}\cdot\text{yr}^{-1}$, respectively. The changes in cation exchange during the forecast period for the various scenarios are typically less than 6% of the basin outflow. This is reflected in the minor changes in R relative to the base case during the forecast period for all $\pm 20\%$ deposition scenarios (Figures 3.1 to 3.4). Given the accumulated error in all the experimental data used in these predictions and all of the assumptions and uncertainties inherent in any watershed code such as MAGIC, the changes with time or deposition scenario in R for Panther Lake and Clear Pond are of little significance. This is in sharp contrast to Woods Lake, which has a forecasted basin outflow ANC

of $-35 \text{ meq}\cdot\text{m}^{-2}\cdot\text{yr}^{-1}$. Variations in base cation exchange for Woods Lake are typically 20% during the forecast period for the $\pm 20\%$ deposition scenarios. Thus, the changes in R for Woods Lake are significant relative to the base case for all the $\pm 20\%$ deposition scenarios.

Perhaps the most important observation to be made from Figures 3.1 to 3.4 is the reversal in the slope of the forecasted value of R, depending upon whether only SO_4^{2-} and NO_3^- (Type A) or all constituents (Type B) are changed in a given deposition scenario. The same is true for both H^+ -independent and H^+ -dependent weathering ($n = 0, 0.5$). We suggest in the discussion below that deposition scenarios in which all constituents, cations and anions, vary by equal percentages (e.g., the cases shown in Figures 3.2 and 3.4) are not generally representative of the expected consequences of decreased emissions of acidic-deposition precursors.

For the Type-A +20% case deposition scenario, there is no increase in the atmospheric flux of base cations associated with the increased flux of SO_4^{2-} and NO_3^- (see last column in Tables 3.1 and 3.2). Thus, the increase in R (Figures 3.1 and 3.3) is plausible, because the additional acidic deposition decreases the soil-solution pH and thereby increases the dissolution rate of aluminosilicates and gibbsite. The associated increase in Al concentrations in the soil solutions displaces greater amounts of base cations from cation-exchange sites in the soils, causing the forecasted increase in R. A similar argument accounts for the observed decrease in R for the -20% Type-A scenario.

The response in R differs for Type-A and Type-B scenarios. Type-B scenarios (Figures 3.2 and 3.4) result in a decrease in R due to a reduced ANC contribution from cation exchange. This is because the Type-B scenarios does not represent, respectively, a +20% and -20% increase and a decrease in just "acidic" constituents but in all constituents, including base cations. Indeed, there is no net difference between the equivalents of strong acid anions and base cations among any of the Type-B scenarios. For the +20% case, the atmospheric flux of base cations to the watershed increases (see last column in Tables 3.1 and 3.2), but because weathering is constant (for $n = 0$) or changes only slightly (for $n = 0.5$), therefore,

the flux of base cations from exchange sites is decreased to compensate for the increased atmospheric flux of base cations. Thus, the ratio R decreases. The difference in the behavior of R between Type-A and -B deposition scenarios demonstrates the marked buffering effect of base cations in the precipitation.

The effect of using Type-A and -B deposition scenarios on the 50-year forecasts of lake ANC for Woods and Panther Lakes is shown in Figure 3.5. As can be seen for Woods Lake, the forecasted lake ANC for the -20% scenario would be $30 \text{ meq}\cdot\text{m}^{-3}$ less for the Type-B scenario than it would be for the Type-A scenario. Similarly, the +20% scenario results in a lake ANC value for the Type-B scenario of $30 \text{ meq}\cdot\text{m}^{-3}$ greater than for the Type-A scenario. By contrast, Panther Lake and Clear Pond show no significant differences in forecasted lake ANC for the Type-A and -B scenarios for either $\pm 20\%$ cases. Thus, we conclude that both the type of deposition scenario and the watershed have a major effect on forecasted ANC.

The Type-B scenario was included because of its prior use as noted in the Approach section. However, current emission controls on fossil fuel power plants result in minimal release of particulates. Furthermore, particulates tend to be deposited much closer to the source than are gases. Thus, it is assumed that base cations in atmospheric deposition are largely of local origin. Therefore, deposition scenarios in which only SO_4^{2-} and NO_3^- are varied, along with the equivalent change in H^+ to maintain electrical neutrality, are believed to more realistically represent changes in deposition chemistry that would result from applying mitigation technologies to minimize atmospheric $\text{SO}_x(\text{g})$ and $\text{NO}_x(\text{g})$ emissions.

The relative contribution of cation exchange, weathering, and SO_4^{2-} adsorption to ANC are affected by the choice of calibration parameters relating to these processes for the MAGIC code. Cation exchange and base-cation weathering contribute 86% of total ANC for Panther Lake and 99% for Clear Pond (Table 3.5). On the other hand, SO_4^{2-} adsorption is an important process for Woods Lake representing 49% of the total ANC from soil

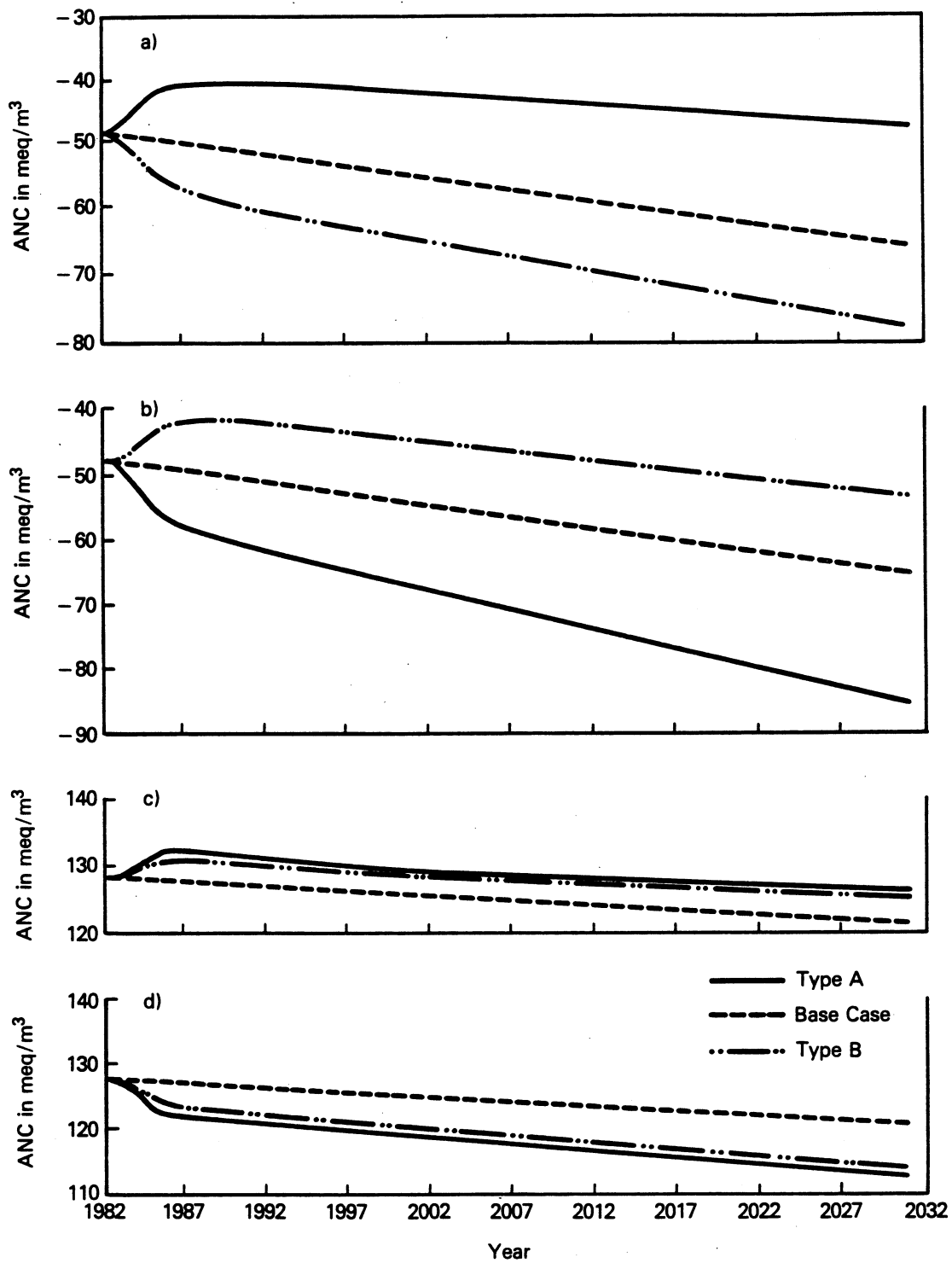


FIGURE 3.5. MAGIC Code, 50-yr ANC Forecasts for Woods Lake (a and b) and Panther Lake (c and d), Using Both Type-A and -B Deposition Scenarios ($n = 0$, 3-yr Linear Ramp): a) -20% Change, b) +20% Change, c) -20% Change, d) +20% Change

TABLE 3.5. MAGIC Code, 1982-1984 Average ANC Budget for Base-Case Deposition Scenario for Panther, Clear (1984-1986), and Woods Watersheds (n = 0.5; calculations normalized to terrestrial area)

	<u>Panther</u>	<u>Clear</u>	<u>Woods</u>
	- - - -	meq•m ⁻² •yr ⁻¹	- - - -
Atmospheric Inputs			
Terrestrial/Lake			
Wet	-107.5	-76.4	-103.0
Dry	0.0	0.0	0.0
Total	-107.5	-76.4	-103.0
Internal Sources			
Soil Solution			
NH ₄ Uptake (Nitrification)	-12.9	-9.2	-11.7
NO ₃ Uptake (Nitrate Reduction)	17.6	24.1	27.7
Net	4.7	14.9	16.0
Soil Processes			
Cation Exchange	21.3	24.7	13.7
SO ₄ Adsorption	27.9	-1.5	25.7
Weathering	151.1	98.1	15.8
Net	200.4	121.3	55.2
Lake			
NH ₄ Uptake (Nitrification)	-15.1	-4.8	-18.3
NO ₃ Uptake (Nitrate Reduction)	23.1	9.6	15.0
SO ₄ Reduction	0.0	0.0	0.0
Net	8.0	4.8	-3.3
Sum Internal Sources	213.0	141.0	67.9
Basin Outflow ^(a)	105.4	64.6	-35.1
Sum Atmospheric Input + Internal Sources ^(a)	105.6	64.7	-35.1
Basin Outflow of Al _T	3.9	2.2	25.5

(a) Values of basin outflow must agree with summed atmospheric input + internal sources since the cation exchange contribution to ANC is calculated by difference between them.

processes, because of the markedly less contribution from weathering. Sulfate adsorption contributes 14% to Panther Lake and is insignificant for Clear Pond.

Three additional observations can be made based upon the results for the MAGIC code given in Table 3.5. First, the lake is an insignificant source of ANC. Second, sulfate reduction in the lake is not invoked as a source of ANC for any of the watersheds. Third, total Al in the basin outflow contributes a significant amount of ANC for Woods Lake but not for Panther Lake and Clear Pond.

3.3 THE ETD CODE

The deposition chemistry that drives the ETD code is less extensive than that required by the MAGIC code. The ETD code requires the fluxes for the net ANC, SO_4^{2-} , and Cl^- (but not for NO_3^-), whereas the MAGIC code accepts the atmospheric fluxes for nine constituents (i.e., Ca^{2+} , Mg^{2+} , Na^+ , K^+ , NH_4^+ , Cl^- , NO_3^- , SO_4^{2-} , and F^-). Because the ETD code does not explicitly treat atmospheric base-cation fluxes, only Type-A deposition scenarios, in which SO_4^{2-} and the equivalent ANC are varied, can be considered. In addition, only H^+ -dependent weathering ($n = 0.5$) is considered.

The ANC fluxes for the ETD code were derived using the companion BUDGET code. This code calculates hydrologic, ANC, and SO_4^{2-} budgets using output from the ETD code. The ANC fluxes from cation exchange and weathering for Panther Lake, Clear Pond, and Woods Lake are given in Table 3.6 for the base case and the $\pm 20\%$ deposition scenarios. These fluxes are averaged over the 3-year periods at the beginning and end of the forecast period. The average values of R for these time periods, shown in the last column in Table 3.6, were calculated using the sum of the weathering in the unsaturated, ground-water and lake compartments. The majority of the weathering occurred in the unsaturated zone.

The ratios of cation exchange to weathering are essentially identical for Panther Lake and Clear Pond, with Woods Lake being only slightly higher. The base-cation weathering rate and the cation-exchange rate both

TABLE 3.6. ETD Code, Forecasts for 3-Yr Averages of Annual Average Fluxes of ANC from Cation Exchange and Weathering for Each Compartment for Panther Lake, Clear Pond, and Woods Lake: Base-Case and $\pm 20\%$ Deposition Scenarios (n = 0.5; calculations normalized to terrestrial area)

Watershed	Deposition Scenario	Years Averaged	Cation Exchange	Weathering			Ratio = $\frac{\text{Cation Exchange}}{\text{Sum Weathering}}$
			Soil	Unsaturated Zone	Ground Water	Lake	
- - - - neq.m ² .yr ⁻¹ - - - -							
Panther Lake	Base Case	1982-1984	94.8	161.8	14.8	22.3	0.47
	-20% SO ₄	1982-1984	84.8	155.7	14.8	22.2	0.44
	+20% SO ₄	1982-1984	103.7	168.5	14.8	22.4	0.51
	Base Case	1991-1993	91.8	163.6	14.4	22.3	0.46
	-20% SO ₄	1991-1993	82.7	157.8	14.5	22.2	0.43
	+20% SO ₄	1991-1993	101.2	169.4	14.4	22.4	0.49
Clear Pond	Base Case	1984-1988	76.1	132.6	0.3	17.5	0.51
	-20% SO ₄	1984-1988	67.8	123.6	0.3	17.4	0.47
	+20% SO ₄	1984-1988	85.2	141.7	0.3	17.7	0.53
	Base Case	1994-1998	71.8	136.3	0.3	17.3	0.46
	-20% SO ₄	1994-1998	62.9	126.1	0.3	17.2	0.44
	+20% SO ₄	1994-1998	79.8	146.9	0.3	17.5	0.48
Woods Lake	Base Case	1982-1984	34.9	46.5	10.7	4.5	0.57
	-20% SO ₄	1982-1984	31.8	44.8	10.7	4.2	0.53
	+20% SO ₄	1982-1984	39.1	49.3	10.6	5.8	0.68
	Base Case	1991-1993	33.8	46.9	10.1	4.4	0.55
	-20% SO ₄	1991-1993	30.2	44.2	10.8	4.1	0.52
	+20% SO ₄	1991-1993	37.8	49.9	10.1	4.9	0.58

TABLE 3.7. ETD Code, 1982-1984 Average ANC Budget for the Base-Case Deposition Scenario for Panther, Clear (1984-1986), and Woods Watersheds (calculation normalized to terrestrial area)

	<u>Panther</u>	<u>Clear</u>	<u>Woods</u>
	- - - - - meq•m ⁻² •yr ⁻¹ - - - - -		
Atmospheric Inputs			
Terrestrial/Lake/Snowpack			
Wet	-100.5	-99.3	-101.5
Dry	-37.9	-31.1	-29.9
Total	-138.4	-130.4	-131.4
Internal Sources			
Soil Compartment			
SO ₄ Adsorption	5.4	6.5	9.2
Cation Exchange	94.0	76.1	34.9
Net	99.4	82.6	44.1
Unsaturated Zone			
SO ₄ Adsorption	-0.2	-0.4	-0.1
Weathering	161.0	132.6	46.5
Net	160.8	132.2	46.4
Ground Water Compartment			
SO ₄ Adsorption	1.6	1.1	1.0
Weathering	14.8	0.3	10.7
Net	16.4	+1.4	11.7
Lake Compartment			
SO ₄ Reduction	16.1	15.4	15.1
Weathering	22.3	17.5	4.5
Net	38.4	32.9	19.6
Sum Internal Sources	315.0	249.1	121.8
Sum of Release from Storage	-8.0	1.5	3.3
Atmospheric Input + Internal Sources + Release from Storage	168.6	120.2	-6.3
Basin Outflow	<u>163.1</u>	<u>115.8</u>	<u>-10.0</u>
Difference	5.5	4.4	+3.7

depend on calibrated variables. For the ETD code, the flux of exchange cations from the soil and the flux of weathered cations from the unsaturated zone, ground-water, and lake compartments both decrease by a factor of approximately three in going from Panther Lake to Woods Lake (Table 3.6). Thus, the ratio R remains relatively constant among the watersheds in the ETD code. The variation in R forecast by the ETD code during the forecast period is small for all three watersheds (Figure 3.6).

For the ETD code, the ANC contribution from cation exchange and weathering dominates that from SO_4^{2-} adsorption and SO_4^{2-} reduction (lake) for all three watersheds (Table 3.7). The ANC budget in Table 3.7 is an average base-case deposition scenario for the period 1982-1984. The year-to-year variation for each source of ANC are relatively small (see Tables C.7 to C.15 in Appendix C). The ETD code is the only code of the three studied that was calibrated to invoke SO_4^{2-} reduction in the lake compartment of these three watersheds, although all codes have that capability. The sum of the SO_4^{2-} adsorption in the various compartments varies from 2% to 8% of the total ANC budget. Thus, for the ETD code, SO_4^{2-} adsorption plays a relatively minor role in neutralizing acidic deposition. The release from storage term in Table 3.7 represents the difference in the total mass of dissolved ANC within the watershed over the time period under consideration. At a given time, the total mass of dissolved ANC is equal to the sum over all compartments of the product [(ANC concentration) • (volume of water)]. The sum of these releases from storage should be zero by conservation of mass over multiple annual cycles. Considering yearly or 3-year averages (Table 3.7), the sum of the releases from storage differs slightly from zero for each watershed. The sum of the atmospheric input, internal sources, and release from storage should be identical to the basin output forecasted by the ETD code (Table 3.7). The lack of agreement shown in Table 3.7 as "Difference" indicates that the ANC mass balance in the ETD and/or Budget codes is not self-consistent. Because the annual average ANC flux from Woods Lake is low ($-10.0 \text{ meq}\cdot\text{m}^{-2}\cdot\text{yr}^{-1}$), the difference given in Table 3.7 for Woods Lake is a significantly greater fraction of the basin outflow ANC than it is for Panther Lake or Clear Pond. The absolute magnitude of this difference

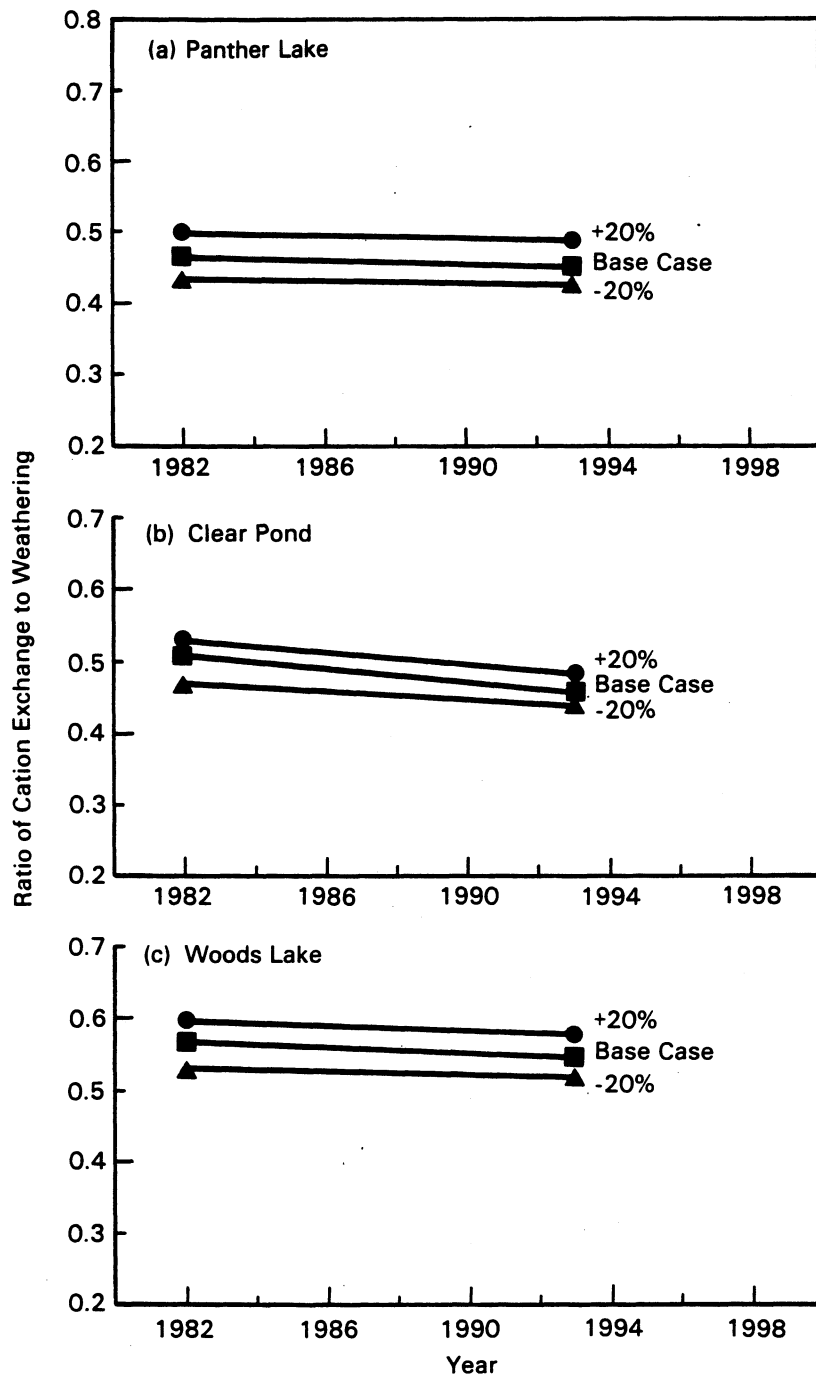


FIGURE 3.6. ETD Code, Variation in R for Panther Lake (a), Clear Pond (b), and Woods Lake (c) for Base-Case and Type-A Deposition Scenarios

(approximately $\pm 5 \text{ meq}\cdot\text{m}^{-2}\cdot\text{yr}^{-1}$) is a factor of 50 greater for ETD than it is for the other two models considered in this study. The inconsistency in the ANC budget of the ETD code may be due to the assignment (within the code) of the equivalent moisture depths to zero when the soil and unsaturated compartments reach a certain moisture content, and/or concurrently assigning the dissolved constituent masses to zero. In a recent modification of the ETD code, made subsequent to these simulations, the dissolved constituent masses are no longer set to zero as they were in the version of the code available for these simulations.(a) This change may have corrected the inconsistency in the ANC mass balance.

3.4 THE ILWAS CODE

The deposition chemistry that drives the ILWAS code is similar to that of the MAGIC code in that the atmospheric fluxes of Ca^{2+} , Mg^{2+} , Na^+ , K^+ , NH_4^+ , SO_4^{2-} , Cl^- , NO_3^- , and F^- must be specified to define the deposition scenario. The deposition fluxes of several additional constituents must also be specified, namely H_2PO_4^- , H_4SiO_4^0 , R' , R'' , R''' (see Table 2.6), Al_T , total inorganic carbon, SO_x , and NO_x . Only Type-A deposition scenarios are considered, covering $\pm 20\%$ changes in SO_4^{2-} and NO_3^- and the equivalent decrease or increase in the ANC of the deposition. The $\pm 20\%$ changes were made concomitantly for both wet and dry deposition. In addition, only H^+ -dependent mineral weathering rates ($n = 0.5$) were considered. These rates are for specific minerals (i.e., hornblende, plagioclase, K-feldspar, and gibbsite) having a specified stoichiometry. These weathering rates are calibrated in such a manner as to provide the best fit to all major constituents of these minerals.

Using the calibrated data sets for Panther and Woods Lakes, 15-year forecasts for the base case and the $\pm 20\%$ cases were run. (A calibrated data set was not available for Clear Pond from the authors of the ILWAS code.) The ANC fluxes from cation-exchange mineral weathering and other processes considered in the ILWAS code were calculated using CYCLE, a

(a) J. L. Schnoor, personal communication, July 5, 1988.

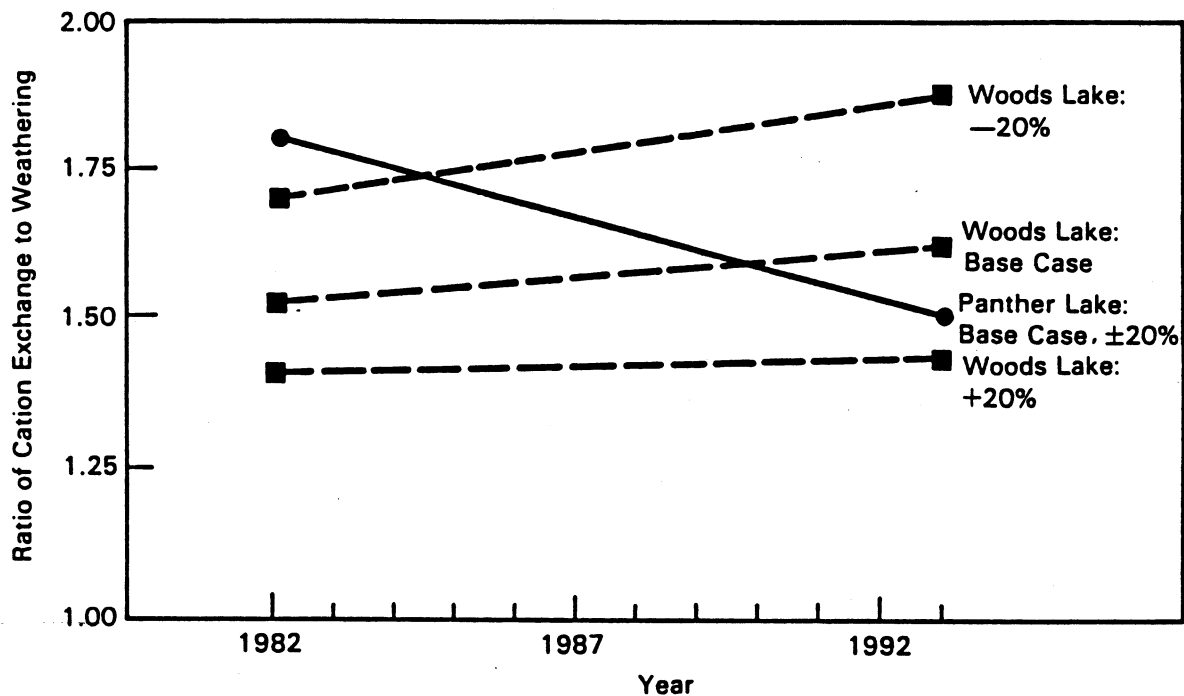


FIGURE 3.7. ILWAS Code, Variation in R (3-Yr Annual Average) for Woods Lake, Panther Lake, and Clear Pond: Base-Case and Type-A Deposition Scenarios (n = 0.5)

companion code that prepares an ANC budget from the output of each ILWAS code run. The annual average fluxes calculated for each watershed and deposition scenario are given in Table 3.8. The averages are taken over the second 3-year period (1982, 1983, 1984) and at the end of the forecast period (1991, 1992, 1993). Three-year averages were calculated because the same 3-year precipitation sequence that was used during the calibration years (1979, 1980, 1981) was repeatedly used during the forecast. Because there is significant variation in average annual ANC values within this sequence of deposition chemistry, 3-year average values were considered to provide the most meaningful comparison between beginning and ending time periods. It should be noted, however, that major yearly variations in ANC fluxes from cation exchange and weathering during the 3-year cycles do not occur, as can be seen from the actual yearly data shown in Tables D.5 to D.10 in Appendix D. The ratio R of the cation exchange to weathering is given in the last column of Table 3.8. The variation in

TABLE 3.8. ILWAS Code, Average ANC Fluxes from Cation Exchange and Weathering for All Type-A Deposition Scenarios for Panther and Woods Lakes (n = 0.5) (Average values for 3 yr; anion adsorption includes SO₄²⁻ and ionized organic compounds; calculation normalized to terrestrial area.)

Watershed	Deposition Scenario	Years	Cation Exchange	Mineral Weathering			R = $\frac{\text{Cation Exchange}}{\Sigma \text{ Weathering}}$	
				Hornblend	Plagioclase	K-feldspar		
Panther Lake	Base Case	1982-4	134	49.4	11.4	4.7	8.3	1.8
	-25%	1982-4	139	49.9	11.3	4.6	6.4	1.8
	+25%	1982-4	138	49.5	11.4	4.7	10.5	1.8
	Base Case	1991-3	112	50.6	11.7	5.1	9.3	1.5
	-25%	1991-3	107	50.0	11.5	4.9	6.7	1.5
	+25%	1991-3	117	51.0	11.8	5.1	11.6	1.5
	Base Case	1982-4	61	8.2	1.3	2.0	28.7	1.5
	-25%	1982-4	58.6	8.1	1.3	2.0	23.2	1.7
	+25%	1982-4	65.3	8.2	1.4	2.0	34.6	1.4
Woods Lake	Base Case	1991-3	64.8	8.6	1.4	2.1	27.7	1.6
	-25%	1991-3	63.2	8.6	1.4	2.1	21.5	1.9
	+25%	1991-3	66.7	8.7	1.4	2.1	34.5	1.4

this ratio during the forecast period for all scenarios is shown in Figure 3.7 for both watersheds.

The annual average ANC budget for Panther and Woods Lakes, as calculated by the ILWAS code, is given in Table 3.9 and summarizes all sources of ANC. The ANC fluxes from the canopy/trunk/leaf compartment is approximately canceled out by the ANC contributions from soil solution and soil organic matter. The net ANC contributed by lake processes is relatively small and no SO_4^{2-} reduction is invoked. The major contribution to the ANC budget is from the soil processes, with cation exchange and weathering contributing 90% of the ANC from the soil processes. Anion adsorption, consisting of SO_4^{2-} and humic acid adsorption, is a relatively insignificant source of ANC for both watersheds (i.e., 7% of the ANC from soil processes for Panther Lake and 3% for Woods Lake). The agreement of the basin output forecasted by the ILWAS code and the sum of the atmospheric input and the internal sources (Table 3.9) indicate that the mass balance in the ILWAS code is self-consistent. The ILWAS code provides a detailed summary of the ANC stored in each of the major compartments (Tables D.5 to D.10). The largest reservoirs of stored ANC for both Panther and Woods Lakes is that of soil cation exchange and soil organic matter. The cation exchange reservoir of ANC for Panther Lake ($1315 \text{ eq}\cdot\text{m}^{-2}$) is a factor of 70 greater than that of the soil organic matter. For Woods Lake, the cation exchange reservoir ($66.6 \text{ eq}\cdot\text{m}^{-2}$) is 26 times less than that of Panther Lake and only a factor of 3 greater than that of the particulate organic carbon. The quantity of ANC stored as soil organic carbon in both watersheds is virtually identical.

3.5 DISCUSSION OF RESULTS

This discussion focuses on a comparison among the three codes based on the information presented in the preceding sections. Comparisons logically begin with the representation and magnitude of the acidic deposition to the watersheds used by each model. All three models distinguish between the atmospheric deposition to the terrestrial and lake regions of the watersheds; however, we have presented these as a sum in Tables 3.5, 3.7 and 3.9. In the MAGIC code, the atmospheric flux of wet and dry ANC

TABLE 3.9. ILWAS Code, 1982-1984 Average ANC Budget for the Base-Case Deposition Scenario for Panther and Woods Watersheds (calculation normalized to terrestrial area)

	<u>Panther</u>	<u>Woods</u>
	- - - -	- - - -
	$\text{meq}\cdot\text{m}^{-2}\cdot\text{yr}^{-1}$	
Atmospheric Inputs		
Terrestrial/Lake		
Wet	-73.6	-75.0
Dry	-30.5	-25.3
Total	-104.1	-100.3
Internal Sources		
Canopy/Trunk/Leaf		
Release from Storage	-44.1	-83.0
Nitrate Reduction	220.7	259.3
Net	176.6	176.3
Soil Solution		
Release from Storage	1.2	0.3
Nitrification	-170.7	-194.7
Fulvic Acid Decay	5.6	4.3
Net	-163.9	-190.0
Soil Processes		
Cation Exchange	133.6	61.0
Anion Adsorption	16.2	3.2
Weathering	65.5	11.5
Gibbsite Dissolution	8.3	28.7
Net	223.6	104.4
Soil Organic Matter		
Release from Storage	-11.7	18.4
Fulvic Acid Formation	-11.7	-12.9
Net	-23.4	5.5
Lake Processes		
Release from Storage	0.3	-0.2
Nitrification	-21.8	-25.0
Fulvic Acid Decay	5.1	6.0
Gibbsite Precip.	-7.5	-10.4
Algal Growth	37.2	25.5
Net	13.3	-4.1
Sum Internal Sources	226.2	92.0
Basin Outflow	122.1	-8.3
Atmospheric Input + Internal Sources	122.1	-8.3

are treated identically. The wet and dry ANC fluxes can be entered separately; however, for the three watersheds being considered, the wet and dry ANC flux were summed by the authors of MAGIC and entered as "wet" deposition for each watershed. In the ETD and ILWAS codes, the total deposition has been partitioned into wet and dry components. This distinction is of little consequence because the sulfur and nitrogen species ($\text{SO}_{x(g)}$ and $\text{NO}_{x(g)}$) in the dry deposition are implicitly converted to SO_4^{2-} and NO_3^- by each code (the ETD code does not consider nitrogen species). The atmospheric flux of ANC used by the MAGIC and ILWAS codes differ by 3%. However, the ANC flux of the calibrated input files received from the authors of the ETD code for Panther and Woods Lakes is more acidic by a factor 1.3 than MAGIC and ILWAS and a factor of 1.7 more acidic than MAGIC for Clear Pond. Discussions with the authors of the ETD code have failed to identify the cause of this discrepancy. This additional flux of acid used by ETD is probably the major contributor to the difference in the basin outflow ANC between the ETD code and the MAGIC and ILWAS codes discussed at the end of this section (see Table 3.11).

Several differences in model calibration and formulation are evident from comparison of the ANC budgets (Tables 3.5, 3.7, 3.9, Appendixes B, C, and D). First, the net contribution of the lake to the ANC budget in the ETD code is consistently greater than that for the MAGIC and ILWAS codes. This is a result of 1) the positive ANC contribution from the ETD code for SO_4^{2-} reduction and mineral weathering in each of the lakes (calibration of the MAGIC and ILWAS codes for these watersheds do not invoke SO_4^{2-} adsorption, reduction, or weathering in the lake) and 2) the negative ANC contribution of the MAGIC and ILWAS code's lake nitrification reactions (the ETD code does not include nitrogen chemistry).

Second, the equivalents of "exchangeable" ANC or base exchange capacity allocated by the models to storage in the soils of each watershed vary for each model among watersheds and for a given watershed among models (Table 3.10). The ILWAS code consistently has the greatest reservoir of exchangeable base-cation ANC. For the MAGIC code, the difference in the exchangeable base-cation ANC storage among the watersheds is consistent with the difference in the assumed soil depth for Panther Lake, Clear

Pond, and Woods Lake of 24, 55, and 2.5 meters, respectively. For the ILWAS code, a similar variation between the reservoir of exchangeable base-cation ANC and soil depth holds for Panther and Woods Lakes. For the ETD code, the depths of the soil compartments for Panther Lake, Clear Pond, and Woods Lake are 0.63, 0.55 and 0.37 m, respectively. The difference in the reservoir of exchangeable base-cation ANC between Panther and Woods Lakes is consistent with the variation in soil depth; however, the exchange capacity for Clear Pond is not consistent with depth. In ETD, it should be noted, exchangeable base-cation ANC is derived from only the uppermost soil horizons and not, as is the case with MAGIC and ILWAS, from the entire depth of the till.

Third, estimates for each model of the time (t_{BE}) required for the stored exchangeable bases of the watershed soils to be depleted by acidic deposition can be derived from the base-exchange capacity and base exchange fluxes summarized in Table 3.10. This estimate assumes that 1) weathering reactions do not replace the base cations on soil exchange sites, 2) base exchange fluxes are held constant at the calibrated base-case values, and 3) base-cation export decreases linearly with decreasing base-cation saturation. The estimated base-exchange depletion times for Woods Lake are similar for all three models, however for Clear Pond there is a factor of 30 difference between times forecasted by the MAGIC and ETD codes. With the exception of the ETD code estimate for Clear Pond (265 years), these values of t_{BE} are significantly greater than the literature estimates that assume no replenishment from weathering reactions and are on the order of 50 to 200 (Schnoor and Stumm 1985). Finally, the assumption made above that no replenishment of exchange cations by weathering reactions occurs is correct for the ETD code, however the base-exchange flux decreases with time (Table 3.6), thus the times estimated by the ETD code represent lower limits. On the other hand, because weathering reactions do indeed replace the base cations on soil exchange sites in both the MAGIC and ILWAS codes and the base exchange fluxes decrease with time for both of these codes the base exchange depletion times will be in significant excess of the times given in Table 3.10 for both the MAGIC and ILWAS codes.

Fourth, differences in the magnitude and variation in the trajectory of R between the MAGIC (Figure 3.3) and ETD (Figure 3.6) codes during the 12- to 15-year forecasts are due to model structure and calibration values which affect both weathering and cation exchange fluxes. For all three water-sheds, the ETD code forecasts nearly equal values of R during the 15-year period (Figure 3.6). These R values differ from those forecast by the MAGIC code (Figure 3.3), due to inherent differences in the calibration of weathering and cation exchange fluxes between the two models, and are of little consequence. The magnitude and variation in the trajectory of R forecast by the MAGIC code for Woods Lake differed significantly from the predicted variation in R for Panther Lake. This difference is due to the major role played by the Al chemistry in the Woods Lake watershed (lake pH = 4.7) compared to Panther Lake watershed where Al is an insignificant component in the ANC budget (pH = 7.0). No change in R was forecast by the ETD code for Woods Lake relative to Panther Lake (Figure 3.6), because the ETD code does not explicitly treat Al chemistry. Thus, description of the weathering process for Woods Lake by the ETD code omits an apparently important acid neutralizing process.

The values of R predicted by the ILWAS code for Panther Lake are not affected by the $\pm 20\%$ change in Type-A deposition scenario (Figure 3.7). This is similar to the results obtained with the MAGIC and ETD codes where the $\pm 20\%$ change in deposition scenario had a relatively minor effect upon the value of R for Panther Lake and Clear Pond (Figures 3.1 to 3.4 and 3.6). The difference in R between Panther and Woods Lakes predicted by the ILWAS code for all scenarios (Figure 3.7) is related to the role Al plays in the ANC budget of Woods Lake. The predictions made by the MAGIC code for Woods Lake also showed significant variation with the deposition scenario (Figures 3.1 and 3.3), however the displacement relative to the base case of the $\pm 20\%$ trajectories for the MAGIC code are opposite to those in Figure 3.7. This is due to the fact that the ILWAS code includes Al in the base cation weathering flux, while the MAGIC code does not. An additional factor is that the ILWAS code does not include Al^{3+} as one of the exchangeable cations (Ca^{2+} , Mg^{2+} , Na^+ , K^+ , NH_4^+ , and H^+) but calculates the exchange of base cations with H^+ rather than Al^{3+} as in the MAGIC

code. Aluminum is a relatively minor contributor to weathering flux for Panther Lake, but it dominates the weathering flux for Woods Lake (Table 3.8). For the +20% scenario, the increase in the gibbsite weathering dominates over the increase in the H^+ -driven cation-exchange flux for Woods Lake (Table 3.8) causing R to decrease relative to the base case (Figure 3.7). The increase in R for the -20% scenario is dominated by the decrease in gibbsite weathering. It can be seen that these differences in the behavior of R between the MAGIC and ILWAS codes are due to differences in code formulation with respect to inclusion of Al chemistry. Both the MAGIC and ILWAS codes incorporate Al chemistry, which appears to be of major importance in the ANC budget of acid lakes ($pH < 5.0$) and acidic surface soil horizons, and thus predict variations in cation exchange and weathering fluxes associated with Al. This is a significant difference between these two models and ETD. Aluminum chemistry is quite important for acidic lakes, although the number of lakes with $pH < 5.0$ is relatively small. Aluminum chemistry is also important in surface soil horizons where the pH predicted by the MAGIC code in soil layer 1 for Panther, Woods, and Clear watersheds is 4.2 to 4.4, and by the ILWAS code in soil layers 1 and 2 for Panther and Woods Lakes is 4.0 to 4.5.

Fifth, the only source of base cations in the soil compartment of the ETD code is from time-dependent base-cation exchange as no weathering is included in the soil compartment. In addition, no cation exchange is included in the unsaturated soil, ground-water, and lake compartments, the only source of base cations in these compartments is weathering. In contrast, both the MAGIC and ILWAS codes include cation exchange and weathering processes in all soil compartments. However, this separation of processes among layers is not of major consequence since both process representations are totally calibrated variables. The ANC flux from weathering does differ from that of base-cation exchange in that weathering depends on a fractional power (e.g., square root) of the H^+ concentration while base-cation exchange depends linearly on H^+ . Further, the base-cation exchange flux decreases with time depending upon the difference between the total base cations in the soil ($CEC \cdot \% \text{ base saturation}$) and the base-cation depletion from the soil.

The average annual basin outflow ANC flux predicted by the three codes for each of the watersheds provides an overall basis of comparison among models. The specific intent here is to compare model simulations during the calibration period rather than forecast simulations because all models are bounded by observed dates during the calibration period. Because both ETD and ILWAS require a period of time to stabilize after the simulations are started, the second 3-year cycle of the simulation, rather than the first year, was used to avoid "start-up" biases in the 3-year averages. The annual average basin outflow ANC flux, averaged over the second 3-year cycle of the base case simulation, have been given for the three codes in Tables 3.5, 3.7 and 3.9 and summarized in Table 3.11. However, a comparison of these ANC fluxes ($\{ANC\}$) must take into account the difference between ANC_I (ILWAS) and ANC_M (MAGIC) due to a difference in the Al species considered as proton donors and acceptors (see Section 2.5.1). The ANC for the two models are related by the expression,

$$\{ANC\}_I = \{ANC\}_M + \{Al_T\}_M = \{ANC'\}_M \quad (3.3)$$

where the quantities in $\{ \}$ are ANC or total Al fluxes ($\text{meq} \cdot \text{m}^{-2} \cdot \text{y}^{-1}$). For Panther Lake and Clear Pond (pH 7.0) the Al_T term represents a small correction to $\{ANC\}_M$ (Table 3.11). However for Woods Lake (pH = 4.7) the Al_T term represents a significant adjustment to $\{ANC\}_M$. For both Panther and Woods Lakes $\{ANC\}_I$ and $\{ANC'\}_M$ are in reasonable agreement; a 9% and 17% difference for Panther Lake and Woods Lake, respectively. Unfortunately, for Clear Pond no comparison can be made because calibrated input files for the ILWAS code were not available from the authors.

Because the ETD code does not define ANC in terms of explicit chemical constituents no functional relationship, such as the one above, can be derived for relating ANC_E to that in either the MAGIC or ILWAS codes. The comparison of $\{ANC'\}_M$ and $\{ANC\}_E$ (Table 3.11) for all three watersheds shows that for two of the three watersheds there is significant disagreement; a 46% and 73% difference for Panther Lake and Clear Pond, respectively. For Woods Lake, $\{ANC\}_E$ is identical to that of the MAGIC code, however the lack of self-consistency in the mass balance in the ETD model

TABLE 3.11. Comparison of Annual-Average (1982-1984) ANC of Basin Outflow for Panther, Woods and Clear Watersheds as Predicted by ILWAS, MAGIC, and ETD (calculation normalized to terrestrial area)

Lake	Lake pH	ILWAS	MAGIC		ETD	
		$\{ANC\}_I$	$\{ANC\}_M$	$\{A\}_T$ in outflow	$\{ANC\}_M + \{A\}_T$	$\{ANC\}_E$
		----- meq·m ⁻² ·yr ⁻¹ -----				
Panther Lake	7.0	+122	+108	+3.9	+112	+163 (+169)
Woods Lake	4.7	-8.3	-35.0	+25.0	-10.0	-10.0 (-6.3)
Clear Pond (1984-1986)	7.0	-	+64.9	+2.2	+67.1	+116 (+120)

(see Section 3.3) yields an alternate estimate of the basin outflow ANC flux shown in parentheses in Table 3.11 (this value was equal to the sum of the atmospheric input, the internal sources, and the release from storage terms in Table 3.7). Thus, for Woods Lake we have either a 0% or 37% difference between the MAGIC and ETD codes. Since -6.3 represents the calculated value (which includes the problematic "release from storage" term), it will be used for Woods Lake. For the two watersheds where we have average annual ANC forecasts for all three models the mean, standard deviation and coefficient of variation (CV) of the ANC values were calculated and the CV values plotted in Figure 3.8. These CV values are similar for both Panther and Woods Lakes. The pairwise CV values calculated from the ANC values for the MAGIC and ILWAS codes, and the MAGIC and ETD codes are also given in Figure 3.8. The standard deviation for the pairwise CV values (two data points) were calculated using the expression $(X_1 - X_2)/(2)^{0.5}$, where X_i are the ANC values. The relatively small MAGIC-ILWAS CV values and the high MAGIC-ETD CV values for Panther and Woods Lakes show that the major source of CV variation in the three models arises from the ETD model estimates of basin outflow ANC. Although no

ILWAS ANC value is available for Clear Pond, the fact that the MAGIC-ETD CV values are of the same magnitude as that for Panther and Woods Lakes confirms the trend that ETD is consistently the dominant contributor to the standard deviation of the mean basin outflow ANC among the three models. The reason for this may be that the atmospheric flux of ANC to each of the watersheds was consistently more acidic for ETD than for the other two models as noted at the beginning of this section.

3.6 SUMMARY

The relative ANC contributions from individual (the MAGIC and ILWAS codes) or aggregated geochemical processes (the ETD code) were generally similar among the codes. However, relative changes in these ANC contributions occur with different atmospheric deposition scenarios because of differences in the process formulations and in aspects of the calibration of different codes for specific watersheds. The code comparisons can be summarized by the following points.

First, the displacement of base cations (Ca, Mg, K, and Na) from cation-exchange sites, either by H^+ (ILWAS) or Al^{3+} (MAGIC), and the supply of base cations by weathering reactions are the two dominant contributors to the neutralization of the atmospheric flux of acidic deposition. The single exception was for the Woods Lake watershed, where SO_4^{2-} adsorption was the dominant source of ANC forecasted by the MAGIC code. For all other watershed-code combinations, SO_4^{2-} adsorption (and SO_4^{2-} reduction in the lake compartment for the ETD code) was a relatively minor source of ANC for these three Adirondock watersheds.

Second, the ratio of base-cation exchange to weathering is a useful tool for examination of code formulation and visualization of the relative magnitude and variation of the dominant sources of ANC for watersheds in varying degrees of acidification.

Third, for the MAGIC code, the change in the flux of ANC from weathering during the 12- and 50-year forecast periods was not highly dependent upon the choice of n (exponential dependence of weathering rate on hydrogen ion concentration); that is, similar results were obtained for

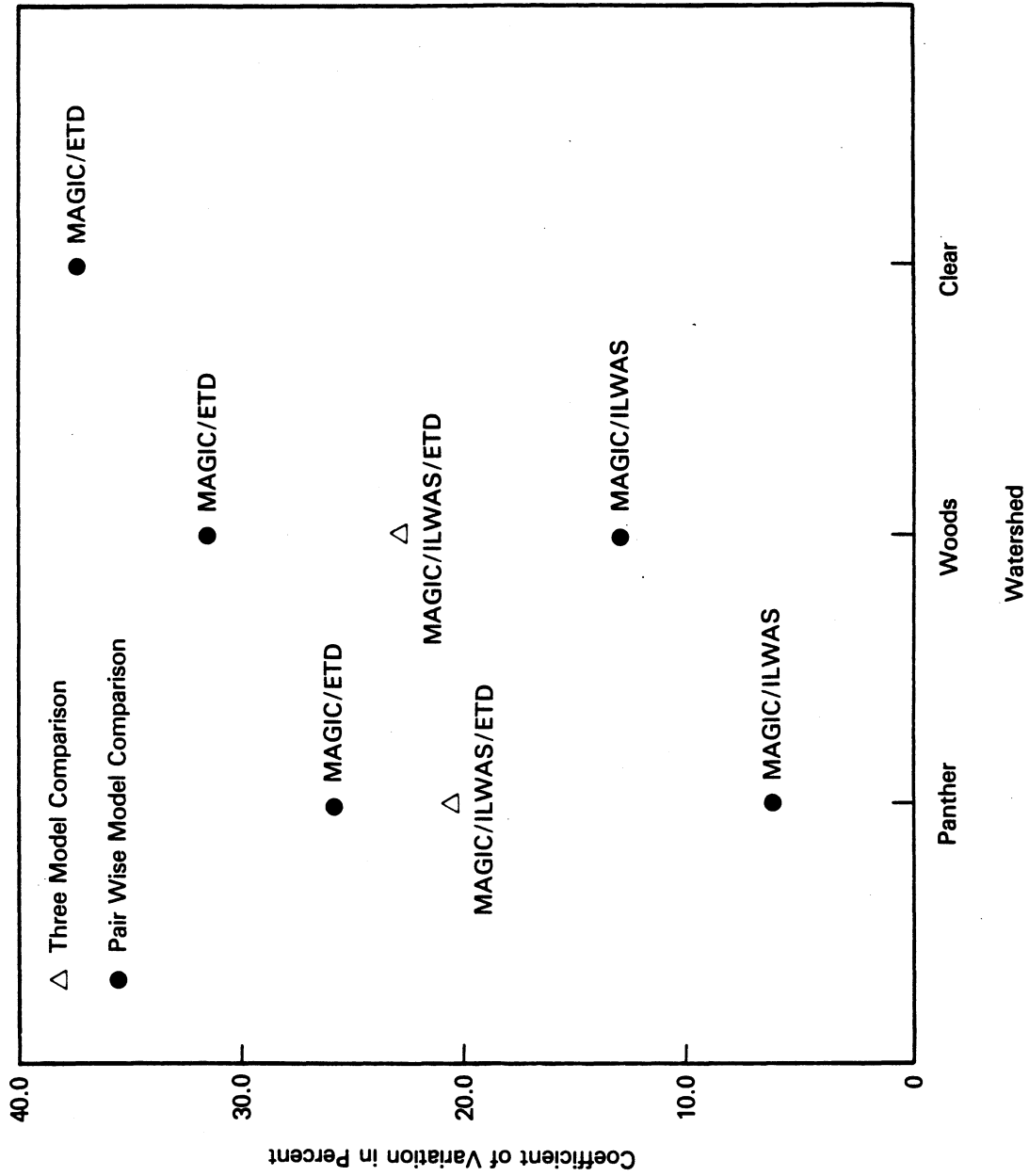


FIGURE 3.8. Coefficients of Variation (Standard Deviation • 100/Mean) of Basin Outflow ANC Among the Three Codes

$n = 0$ and $n = 0.5$ for each of the three Adirondack watersheds and the deposition scenarios considered. This is a consequence of the fact that the predicted change in soil pH during the forecast periods was < 0.14 pH units. However, for watersheds such as Panther and Woods Lakes and Clear Pond, where soils are dominated by silicate minerals, the use of $n = 0.5$ as an approximation of H^+ ion dependence is more representative of experimentally observed silicate weathering processes and is thus preferred over the use of $n = 0$. Additionally, a value of $n = 0.5$ would be more generally applicable, for example, in watersheds which are in rapid transition and for which changes in soil pH > 0.4 or 0.5 are expected or observed.

Fourth, the distinction between cation exchange and weathering in the ETD code is one of semantics only, since both are calibrated, rate-dependent sources of approximately equivalent amounts of ANC. The major distinctions are that cation exchange occurs in the soil compartment and varies linearly with H^+ while weathering occurs in the unsaturated and ground water compartments and varies with the square root of the H^+ concentration.

Fifth, an important difference in the MAGIC and ILWAS codes was found for Woods Lake where gibbsite dissolution influenced the cation weathering flux for the ILWAS code but not for the MAGIC code as a result of differences in definition of ANC.

Sixth, a significant deficiency in the formulation of the ETD code for acidic lakes ($pH < 5.0$) is its inability to treat the influence of Al chemistry upon watershed ANC.

Finally, two general observations are in order. First, if atmospheric inputs of base cations are largely of terrestrial origin and acid deposition is largely of anthropogenic origin, the Type-A scenarios (decreasing only SO_4^{2-} and NO_3^- and the equivalent quantity of H^+) more realistically represent changes in atmospheric deposition that would result from the application of mitigation technologies to minimize atmospheric $SO_{x(g)}$ and $NO_{x(g)}$ emissions than do Type-B scenarios. Second, to the extent that these three watersheds are representative of sensitive

watersheds in the northeastern United States, it can be concluded that emphasis in data collection should be placed on the characterization of 1) base-exchange fractions and selectivity coefficients and 2) weathering rates, as opposed to the characterization of SO_4^{2-} adsorption. This assumes that the objective is to increase the reliability of forecasts with dynamic watershed acidification codes by bounding the range of code calibration parameters for the dominant sources of ANC with field data.

4.0 BEHAVIORAL ANALYSIS WITH HYDROLOGIC VARIABLES

L. W. Vail, L. F. Hibler, and E. A. Jenne

Hydrologic behavior analyses were performed to test the numerical implementation of the hydrologic conceptual model imbedded in each code. These analyses did not assess the adequacy of each code's conceptual model to represent the complex processes controlling hydrologic flow paths in an actual watershed. These analyses were carried out by evaluating the change in the forecasted basin output ANC resulting from a 20% change in selected hydrologic input variables. (See Appendix E for the tabulated data and additional discussion of these behavior analyses.) Calibration data sets, for both Woods and Panther lakes, were provided for the ILWAS code by S. A. Gherini and R. K. Munson of Tetra Tech, Inc., Lafayette, California; for ETD code by N. D. Nikolaidis of the University of Connecticut; and for the MAGIC code by B. J. Cosby and G. M. Hornberger of the University of Virginia. Clear Lake was not included in the behavior analysis because calibration data sets for this watershed were unavailable from Tetra Tech, Inc., for the ILWAS code.

Hydrologic behavior analyses were not performed on the MAGIC/TOPMODEL codes. The "current conditions" employed by the MAGIC code are actually the results of a forecast begun 150 years in the past. These simulated "current conditions" (e.g., lake outflow ANC) are used for calibration of the model, whereas the ETD and ILWAS codes' "current conditions" are explicitly specified as input variables. Therefore, changing hydrological input variables in the MAGIC code would result in a change in the geochemical "current conditions." Thus, in order to match the "current conditions," the geochemical input variables must also be recalibrated if the values of hydrologic input variables are changed. This recalibration would confound any comparison between predictions from the original calibration data set and predictions from the modified data set, since the modified data set would include a new set of "recalibrated" geochemical variables.

For Woods and Panther Lakes, a 15-year period was simulated by replicating the 3 years of available meteorological data five times. To remove the between-year effect of the meteorological data, the flow-weighted annual-average ANC concentrations for the final 3 years of behavior analysis simulations were compared with the final 3 years of the base-case simulation. The behavior analysis was intended to test the following hypothesis:

A change in the value of a hydrologic input variable that increases the predicted fraction of the total basin discharge that passes through subsurface layers, especially the deeper layers, will result in an increase in the forecasted ANC of the basin outflow.

4.1 RESULTS

This section considers the effect on forecasted ANC of basin outflow to changes in hydrologic variables governing snowmelt, sublimation, evapotranspiration, and subsurface flow for both the ETD and ILWAS codes. Summaries of the results of changes in selected hydrologic variables of both models are also given in the tables for Woods Lake and Panther Lake.

4.1.1 Snowmelt

Both the ETD and ILWAS codes provide melt-rate variables. The melt rate of the snowpack in the ETD code is specified by the variable KAPPA (see Table 4.1 for all variables considered in the analysis of the ETD code). Increasing KAPPA causes the snowpack to melt more rapidly, while decreasing KAPPA causes the snowpack to melt less rapidly. A rapid snowmelt may flush H^+ and NO_3^- formed under the snow cover (Peters and Driscoll 1987; Rascher, Driscoll, and Peters 1987). With a slower melt rate, the water melted from the snowpack percolates deeper into the soil, resulting in a higher forecasted ANC. This phenomenon is observed with the ETD code for both Woods and Panther Lakes (see Tables 4.2 and 4.3, respectively). Similarly for the ILWAS code (whose variables are found in Table 4.4), a decrease in the melt-rate variables, OSMRAT and FSMRAT, resulted in a higher forecasted ANC (see Tables 4.5 and 4.6). However, the magnitude

TABLE 4.1. Hydrologic Variables Considered in the Behavioral Analyses of the ETD Code

<u>Variable</u>	<u>Compartment</u>	<u>Description</u>
CBED	Ground water	Hydraulic conductivity (lake bed)
KAPPA	Snow	Melt rate
KPAN2	Snow	Pan evaporation correction coefficient
KPAN3	Soil	Pan evaporation correction coefficient
KPAN5	Lake	Pan evaporation correction coefficient
KPERC3	Soil	Vertical hydraulic conductivity correction coefficient
KPERC4	Unsaturated	Vertical hydraulic conductivity correction coefficient
KLAT3	Soil	Horizontal hydraulic conductivity correction coefficient
KLAT4	Unsaturated	Horizontal hydraulic conductivity correction coefficient

of the change in forecasted ANC resulting from a 20% change in these variables was significantly greater for the ETD code than for the ILWAS code. For Panther Lake for instance, a 20% increase in the ILWAS code's melt-rate variable resulted in a change in forecasted ANC from 131 to 130 $\mu\text{eq}\cdot\text{L}^{-1}$, whereas a 20% increase in the ETD code's melt-rate variable resulted in a change from 155 to 139 $\mu\text{eq}\cdot\text{L}^{-1}$. By contrast, the ILWAS melt-rate variables affect both the magnitude and timing of the ANC depression that is induced by the spring snowmelt, but have little effect on forecasted flow-weighted annual-average ANC.

4.1.2 Sublimation

Sublimation concentrates the solutes present in the snowpack. When a snowpack containing acidic deposition has experienced significant sublimation, the H^+ concentration will be increased in the runoff as a result of the decreased volume. More importantly, the initial melt of a snowpack may remove a high percentage of the total acidity contained in the

TABLE 4.2. Effect of $\pm 20\%$ Changes in Hydrologic Variables on Flow-Weighted Annual-Average ANC Concentrations Forecasted by the ETD Code for Woods Lake (last 3 yr of a 15-yr simulation)

Variable	Base Value	Change from Base Value		
		-20%	0%	+20%
		- - - - $\mu\text{eq}\cdot\text{L}^{-1}$ - - - -		
(a)	-		-10.5	
KAPPA	1.14	-5.2		-11.4
KPAN2	1.01	-9.2		-5.7
KPAN3	1.55	-10.9		-9.9
KPAN5	1.64	-10.6		-10.5
KPAN2/KPAN3/KPAN5	1.01/1.55/1.64	-9.3		-4.8
KPERC3	0.0131	-12.7		-8.2
KPERC4	0.0117	-10.5		-10.5
KPERC3/KPERC4	0.0131/0.0117	-12.7		-8.1
KLAT3	243	-6.5		-12.7
KLAT4	14.8	-9.6		-11.2
CBED	0.32	-10.9		-10.3
KLAT3/KLAT4/CBED	243/14.8/0.32	-5.5		-12.8

(a) All variables are at their base values.

snowpack (Rascher, Driscoll, and Peters 1987). If such a snowmelt follows extensive sublimation, a major acid pulse may occur. However, increased sublimation also reduces the total volume of the snowpack, thereby reducing the likelihood of significant overland or shallow saturated subsurface flow being generated during snowmelt events resulting in a greater fraction of the total basin discharge coming from the deeper high-ANC subsurface compartments.

The results suggest that for both the ETD and ILWAS codes, the variables controlling sublimation of the snowpack are not well suited for use as calibration parameters (except to achieve a hydrologic water balance) because they have insignificant or ambiguous impacts on forecasted ANC. For Woods Lake, the ETD code shows an increase in predicted ANC from an

TABLE 4.3. Effect of $\pm 20\%$ Changes in Hydrologic Variables on Flow-Weighted Annual-Average ANC Concentrations Forecasted by the ETD Code for Panther Lake (last 3 yr of a 15-yr simulation)

Variable	Base Value	Change from Base Value		
		-20%	0%	+20%
(a)	-	$\mu\text{eq}\cdot\text{L}^{-1}$		
		- - - -	155	- - - -
KAPPA	1.14	165		139
KPAN2	0.177	154		153
KPAN3	1.55	153		157
KPAN5	1.54	150		160
KPAN2/KPAN3/KPAN5	0.177/1.55/1.54	148		161
KPERC3	0.000431	156		156
KPERC4	0.000417	155		155
KPERC3/KPERC4	0.000431/0.000417	156		156
KLAT3	4.52	157		155
KLAT4	4.98	158		155
CBED	4.58	154		158
KLAT3/KLAT4/CBED	4.52/4.98/4.58	159		157

(a) All variables are at their base values.

TABLE 4.4. Hydrologic Variables Considered in the Behavioral Analyses of the ILWAS Code

Variable	Description
OSMRAT	Melt-rate coefficient for open area
FSMRAT	Melt-rate coefficient for forested area
SNOSBO	Open area sublimation rate
SNOSBF	Forested area sublimation rate
ECOEFF	Annual evaporation adjustment factor
PERM	Horizontal hydraulic conductivity
SMI	Vertical hydraulic conductivity

TABLE 4.5. Effect of $\pm 20\%$ Changes in Hydrologic Variables on Flow-Weighted Annual-Average ANC Concentrations Forecasted by the ILWAS Code for Woods Lake (last 3 yr of a 15-yr simulation)

<u>Variable</u>	<u>Base Value</u>	<u>Change from Base Value</u>		
		<u>-20%</u>	<u>0%</u>	<u>+20%</u>
		----- $\mu\text{eq}\cdot\text{L}^{-1}$ -----		
(a)	-		-10.13	
OSMRAT/ FSMRAT ^(b)	0.075	-9.56		-10.64
SNOSBO/ SNOSBF ^(b)	0.005	-10.14		-10.12
ECOEFF	0.700	-7.97		-11.88
PERM	[10,120] ^(c)	-16.72		-3.00
SMI	[10,120]	-10.30		-10.02

(a) All variables are at their base values.

(b) Values for open and forested areas were equal.

(c) Brackets indicate the range (minimum and maximum) of the specified input variable in the data set. The Woods Lake data set included seven subcatchments, each with about five soil layers.

increase or decrease in KPAN2 (see Table 4.2). For Panther Lake, the ETD code shows a negligible increase in ANC resulting from either a decrease or an increase in KPAN2 (see Table 4.3). In the ETD code, the variable KPAN2 controls the evaporation from the snowpack (sublimation). The sublimation variables for the ILWAS code are SNOSBO and SNOSBF. An increase or decrease in these variables resulted in an ANC change of less than 1% (Tables 4.5 and 4.6).

4.1.3 Evapotranspiration

Increased evapotranspiration from the upper soil horizons decreases the fraction of the total basin output coming from these relatively low-ANC layers. The ETD code provides three variables for calibrating the evapotranspiration from snowpack (KPAN2), soil (KPAN3), and lake (KPAN5).

TABLE 4.6. Effect of $\pm 20\%$ Changes in Hydrologic Variables on Flow-Weighted Annual-Average ANC Concentrations Forecasted by the ILWAS Code for Panther Lake (last 3 yr of a 15-yr simulation)

Variable	Base Value	Change from Base Value		
		-20%	0%	+20%
		- - - - $\mu\text{eq}\cdot\text{L}^{-1}$ - - - -		
(a)	-	130.94		
OSMRAT/ FSMRAT ^(b)	0.070	131.94		130.31
SNOSBO/ SNOSBF ^(b)	0.005	130.71		131.18
ECOEFF	0.540	123.24		139.54
PERM	[5,150] ^(c)	94.86		157.12
SMI	[5,150]	127.09		133.49

- (a) All variables are at their base values.
- (b) Values for open and forested areas were set equal.
- (c) Brackets indicate the range (minimum and maximum) of the specified input variable in the data set. The Panther Lake data set included five subcatchments, each with about five soil layers.

The KPAN2 variable can affect the magnitude and time of arrival of the spring snowmelt depression in lake pH. The KPAN3 variable has a limiting effect on the fraction of basin discharge coming from the upper (low-ANC) soil layer. The KPAN5 variable has an unambiguous effect of increasing solute concentration in the lake. Thus, an increase in the KPAN3 variable increases the evapotranspiration of moisture from the "soil" compartment, which increases the forecasted ANC for both Woods Lake and Panther Lake (Tables 4.2 and 4.3). Similarly, decreasing KPAN3 decreases the forecasted ANC.

In the ILWAS code, the variable ECOEFF adjusts the annual evapotranspiration for the terrestrial portion of the watershed. Increasing the annual evaporation from a watershed with an acidic lake decreases the

forecasted ANC (Table 4.5), whereas decreasing the evaporation from a watershed with an alkaline lake increases its forecasted ANC (Table 4.6).

Evaporation from the lake tends to concentrate the dissolved constituents. Therefore, increasing the evaporation rate from a lake with positive ANC should make the lake more alkaline, whereas increasing the evaporation from an acidic lake should result in a decrease in forecasted ANC. This hypothesis was confirmed for Panther Lake with the ETD code, as shown in Table 4.3. For the low-ANC Woods Lake (Table 4.2), an insignificant change in lake alkalinity was observed with a change in the evaporation variable. The ILWAS code variable ECOEFF has no impact on lake evaporation.

4.1.4 Subsurface Flow

Flow within the various subsurface layers is controlled by the vertical and horizontal hydraulic conductivities. In the ETD code, the KPERC3 and KPERC4 variables are coefficients for the vertical hydraulic conductivity of the soil and unsaturated compartments, respectively, whereas KLAT3, KLAT4, and CBED are coefficients for the horizontal hydraulic conductivity in the soil, unsaturated, and ground water compartments, respectively. In the ILWAS code, the variables SMI(I) and PERM(I) define the vertical and horizontal hydraulic conductivity for each subsurface layer 1.

An increase in hydraulic conductivity in the deeper, less-weathered layers should result in an increased portion of the basin discharge moving through the deeper, base cation-rich layers, thereby increasing the forecasted ANC. Both the ILWAS and ETD codes yield results consistent with this hypothesis.

Increases in the vertical hydraulic conductivity variable for the soil compartment (KPERC3) in the ETD code yield the expected result of increased ANC. For both lakes, the ETD code is insensitive to changes in the vertical hydraulic conductivity for the unsaturated compartment (KPERC4). However, interpretation of results obtained when the lateral hydraulic conductivities were perturbed are slightly more complicated. For Woods Lake, increasing either of the lateral hydraulic conductivity

variables (KLAT3 or KLAT4) resulted in a decrease in forecasted ANC. This resulted from an increased portion of the total flow entering the lake without contacting lower layers. For Panther Lake, the KLAT4 and KLAT3 behave similarly to that observed for Woods Lake (i.e., an increase in KLAT4 produced a decrease in lake ANC). Increasing CBED increases lake ANC, a situation which is also consistent with the hypothesis.

As shown in Tables 4.5 and 4.6 for both Woods and Panther Lakes, an increased vertical conductivity (all subsurface layers being perturbed simultaneously by the same factor) also increased the annual average ANC calculated by the ILWAS code. These tables also show that an increased horizontal hydraulic conductivity resulted in an increase in the forecasted ANC.

4.2 CONCLUSIONS

Calibration methods are employed to select acceptable values of hydrologic variables that cannot be directly measured. The calibrated values of such variables are defined by adjusting these variables to match observed data. It is important to understand the effect of changes in calibration variables both to guide calibration and to qualitatively assess the significance of such changes on forecasts.

The procedure for calibrating the ILWAS and ETD codes involves adjusting the evapotranspiration rate to match annual cumulative basin outflow. The initial stage in calibrating these codes involves adjusting the value of the appropriate evapotranspiration variable to provide a match between simulated and measured annual basin discharge. Then, the hydraulic conductivity values are adjusted to further calibrate the models to the available chemistry data. Increasing the horizontal conductivity variables (KLAT3, KLAT4, and CBED in the ETD code, or PERM(I) in the ILWAS code) in upper compartments tends to decrease forecasted ANC. However, increasing the horizontal conductivity in the lower layers tends to increase forecasted ANC. Increasing the movement of water to deeper soil layers by increasing the vertical hydraulic conductivity variables (KPERC3

and KPERC4 in the ETD code or SMI in the ILWAS code) also tends to increase forecasted ANC.

It was found that the two codes' qualitative response to 20% perturbations in selected hydrologic variables was consistent with the initial hypothesis that increasing the predicted fraction of total basin discharge passing through subsurface layers also increases the forecasted ANC of basin outflow.

These analyses tested the numerical implementation of the hydrologic conceptual model imbedded in each code rather than assessing the adequacy of each code's conceptual model to represent the complex processes controlling hydrologic flow paths in an actual watershed. The 20% perturbations are much less than the confidence range within which many of these hydrologic variables can be measured or estimated; e.g., uncertainty in hydraulic conductivity measurements typically exceeds an order of magnitude. Therefore, the direction of change from the base case in Tables 4.1 to 4.4 should be considered rather than the magnitude of the change. A formal sensitivity analysis of these variables and selected geochemical variables is presented in Section 5.0.

These results show that numerical formulations in both the ILWAS and ETD codes are consistent with their respective conceptualizations. These results also provide useful information on the selection of hydrologic variables for use in code calibration to achieve improved agreement between simulated and measured hydrologic and geochemical data. For example, increasing the vertical conductivities of the deeper soil layers, which are generally less weathered and more alkaline than upper layers, results in an increase in the ANC of the drainage from the soil layers to the surface water.

5.0 SENSITIVITY ANALYSIS

A. M. Liebetrau, T. B. Miley, M. J. Monsour, and L. F. Hibler

The MAGIC, ETD, and ILWAS codes are being used to predict the changes in lake chemistry resulting from an increase or decrease in acidic deposition and to predict when lakes of low ANC (sensitive lakes) will become acidic. For this application, it is necessary to know the relative importance of input variables for forecasting the ANC of sensitive lakes. This sensitivity information will assist modelers with the prioritization of data collection needs and with calibration of the three codes.

The three codes were applied to three Adirondack lakes (Panther Lake, Woods Lake, and Clear Pond) to determine which of the input variables have the greatest effect on selected code output variables. The watershed data sets used in this study, which are from investigations funded by the Electric Power Research Institute (EPRI) (Goldstein, Chen, and Gherini 1985), are some of the most extensive watershed data available.

The sensitivity analyses involved a two-stage approach that consisted of an initial screening, followed by a regression analysis. The initial screening provided the basis for choosing the input variables to be included in the sensitivity analysis. The screening consisted of evaluating the results of the behavioral analysis described in Chapter 4.0 to obtain the initial list of variables to be considered for the sensitivity analysis. For the selected variables, runs of each code were made to determine the approximate ranges over which to conduct the sensitivity analysis. The major response variable for each code was selected to be flow-weighted annual average surface water ANC.^(a) At the second stage, a response surface or regression equation was fitted to predicted ANC values using the Statistical Analysis System (SAS) computer software package (SAS 1985). This regression analysis was used to identify the input variables that were most important for explaining changes in ANC.

(a) For convenience, flow-weighted annual-average surface water ANC is referred to as lake ANC or, more simply, as ANC.

The number of input and output variables and the complexity of the three codes vary considerably, as is reflected by the computer time required to run the codes. The MAGIC code is the simplest of the three codes and, for a 140-year (hindcast) simulation, has a run time of less than one minute on the VAX 11/780. For a 15-year forecast, the ETD code requires about an hour of run time on the same computer. The run time for the ILWAS code depends on the number of catchments and soil layers used and, for a 15-year forecast, was more than 2 hours for the selected watersheds (see Tables 4.5 and 4.6 for the number of catchments and subsurface layers used). Thus, there was no difficulty in obtaining a sufficient number of runs for sensitivity analysis with the MAGIC code. However, for the other two codes it was more difficult to determine the relative importance of the input variables because of limitations on the number of runs that could be performed. Because of the long run-times for the ETD and ILWAS codes, the runs obtained from the initial screening were used when possible, together with the subsequent runs that were made specifically for the sensitivity analysis. This strategy required a decision, based on the initial screening, as to which input variables to consider further for the sensitivity analysis. By considering only those input variables that showed an important effect on output ANC during the initial screening, the number of runs required for sensitivity analysis was minimized.

A Latin hypercube sampling (LHS) strategy (Iman and Conover 1980; Iman and Conover 1982; Liebetrau and Doctor 1987), augmented as described in the next paragraph, was used to generate input samples for the ETD and ILWAS codes, and full-factorial sampling designs were used to generate input samples to the MAGIC code. An LHS design has certain desirable statistical properties, especially when only a limited number of simulated observations (code runs) can be generated. For example, an LHS design ensures that the range of each input variable is "covered" by the selected sampling values. On the other hand, an ideal LHS design would reflect the dependence structure of the code input variables. Because of a limited understanding of the dependence structure of the input variables and because a large number of runs were possible with the MAGIC code, a full

factorial sampling design was used to generate input samples for this code.

One important reason for using a LHS design is to ensure that, regardless of the sample size, the sample points span the range of each input variable in the design. A suitable factorial design can also span the range of each variable. However, a full factorial design consists of the sample points generated by all combinations of (fixed) levels of each variable. A corresponding LHS design with a smaller sample size also spans the range of each input variable, but does (can) not cover the input space with the same density as the factorial design. Because we are dealing with model fitting, i.e., with model response, where no statistical errors are considered, both sampling designs can be expected to produce similar linear approximations to the response surface over the selected input region. For this reason, LHS designs were supplemented with "in calibration" points (see below) used for the initial screening when practicable to maximize the coverage of the input space.

5.1 THE MAGIC CODE

The MAGIC code matches the measured surface water chemistry values via a hindcast of 140 years. Thus, in calibrating the code for a particular lake, the input variables are varied until the output variables match the corresponding measured hydrologic and chemical values. The values of the input variables so obtained are called the calibration values, and with these input values the code is said to be calibrated for the lake in question. For convenience, the values of the output variables that correspond to the (input) calibration values are also called calibration values. The authors of the MAGIC code provided the calibrated data sets for the three lakes considered in this study.

The output variables under consideration in the MAGIC code are Ca^{2+} , SO_4^{2-} , ANC, Mg^{2+} , Na^+ , K^+ , NH_4^+ , Cl^- , NO_3^- , F^- . As determined from the initial screening, the most sensitive of these ten variables were found to be ANC, SO_4^{2-} and Ca^{2+} . A sensitivity analysis to assess the relative importance of input variables was conducted using only ANC.

A major problem in conducting a sensitivity analysis is the necessity that the code remain "in calibration" when the input variables are perturbed. Thus, a calibration region "centered" about the vector of calibration values was determined for the ten output variables of MAGIC. All input samples used for sensitivity analyses were required to lie within the determined calibration region. The calibration region was determined from calibration intervals, one for each output variable, each centered at its calibration value. Each calibration interval is of the form

$$Y (1 \pm K W/\sqrt{2}) \quad (5.1)$$

where Y is the measured (calibration) value of the variable, W is the relative standard deviation, and K is the number of standard deviations. Because lake water analyses from the Eastern Lake Survey (Linthurst et al. 1986) were used to calibrate the three watersheds selected for this study, data from the survey were also used to establish the calibration intervals for each output variable. In Equation 5.1, the $\sqrt{2}$ appears because variance estimates determined from the Eastern Lake Survey data are based on samples of size two.

Table 5.1 contains a list of values used for W and K. For a given run of MAGIC, an output variable was determined to remain "in calibration" if its value fell in the interval determined by Equation 5.1. Taken together, the calibration intervals for the ten output variables constitute a calibration region. The code is "in calibration" for a given run if each output value falls in its calibration interval. Because of their relative importance, a smaller value of K was chosen for ANC, SO_4^{2-} , and Ca^{2+} than for the other variables.

An important purpose of this sensitivity analysis was to provide information on the sensitivity of multi-decade forecasts of lake acidification to important watershed (model) variables. Because these forecasts are watershed-specific, watershed-specific calibration regions were established for the three watersheds under study. This procedure results in considerably smaller intervals than were used in the sensitivity analysis by Cosby et al. (1986a).

TABLE 5.1. Values of the Relative Standard Deviation (W) and the Number of Standard Deviations (K) for the Calibration Region of Output Variables for the MAGIC Code

<u>Variable</u>	<u>W</u>	<u>K</u>
Ca ²⁺	0.05	1.5
SO ₄ ²⁻	0.05	1.5
ANC	0.10	1.5
Mg ²⁺	0.05	2
Na ⁺	0.05	2
K ⁺	0.05	2
NH ₄ ⁺	0.05	2
Cl ⁻	0.05	2
NO ₃ ⁻	0.10	2
F ⁻	0.05	2.5

The calibration region determined for the output variables was used to constrain the domains of the input variables about their calibration values, which is an inverse problem. Although subsequent analysis (see Section 3) has shown SO₄²⁻ sorption to be of secondary importance for ANC generation in these watersheds, the input variables initially considered to be the most important for the MAGIC code were maximum SO₄²⁻ adsorption capacity (A_{max}), the half-saturation constant for SO₄²⁻ adsorption (A_{1/2}), soil depth (SD), and the nine weathering rates (R_i) (one for each of the nine elements considered in the MAGIC code) for each of the two soil layers. It was assumed that strong positive correlations exist among the weathering rates. Therefore, for the sensitivity analysis, the nine weathering rates were always changed by the same percentage. This procedure forced linear relationships among the weathering rates that effectively reduced the number of input variables from 24 to 8. (Since four of the rates are zero, as noted in Table 5.2, only five of the weathering rates are actually used.)

The initial runs of the MAGIC code, in which all input variables were changed simultaneously, indicated that for all three watersheds, the input variables of the upper layer had very little effect on the output (less

TABLE 5.2. Input Variable Calibration Values and Domains for the Lower Soil Layer for the MAGIC Code

Variable ^(a)	Calibration Values			Domain ^(b)
	Panther Lake	Clear Pond	Woods Lake	
SD	23.8	54.4	1.68	±15
A _{1/2}	150	150	150	±27
A _{max}	0.667	0.052	7.14	±10
R _{Ca}	115	73.7	11.0	±8
R _{Mg}	27.6	11.9	1.18	±8
R _{Na}	19.5	16.5	0.81	±8
R _K	0.97	0.99	0.8	±8
R _F	5.8	0.5	1.8	±8

- (a) The calibration values of weathering rates for NH₄, SO₄, Cl, and NO₃ were zero for all three watersheds.
 (b) Expressed as a percentage of calibration value.

than a 1.0% change) when compared to the input variables of the lower layer (at least a 10% change). Therefore, only the variables in the second soil layer were considered in the sensitivity analysis, and the number of input variables was further reduced from 8 to 4. It must be recognized that the relative importance of input variables from the upper layer may be different for other watersheds. The observation that input variables of the upper layer did not affect output may have been a consequence of the greater amount of flow routed through layer 2 than layer 1 (approximately 5:1 for Panther Lake and 3:1 for Woods Lake).

By varying one input variable at a time and keeping the others fixed, a domain was determined for each input variable throughout which corresponding values of the output variables remained in the established calibration region. For each lake, Table 5.2 contains the calibration value of each output variable and the domain of each input variable about its calibration value. The listed input variable domains were used for all three watersheds. For each input variable, values for sensitivity analyses were restricted to lie within the domain established for that variable. For example, the values of soil depth (SD) used for sensitivity

analysis ranged from 20.2 to 27.4 at Panther Lake and from 46.2 to 62.6 at Clear Pond. Input variable domains (and hence also sensitivity analysis results) are clearly watershed-specific.

The steps used to obtain the runs for sensitivity analysis for the MAGIC code are described in the following paragraph. The steps were carried out for each watershed. Three values of each of the four input variables (SD, $A_{1/2}$, A_{max} , R) were selected from the domains given in Table 5.2. For each variable, the selected values were its calibration value, a high value (relative to its base value) and a low value. Values were determined by selecting fixed-run-percentage deviations from the appropriate base value, so actual design values varied from one watershed to another. The MAGIC code was run for all 81 (3^4) possible combinations of these input values. To adequately cover the domain of each variable, this process was repeated three times with differing high and low values. For example, for the variable SD (soil depth), the design values were selected as 5-, 10-, and 15-percent deviations (both positive and negative) from the base value for the watershed in question. In this way, a total of 241 (243 minus the two duplicates of the base-value design point) runs of the MAGIC code were generated for each of the three watersheds.

Table 5.3 shows the response of each output variable to a small increase in each input variable. Results generated by examining the deviations of a single input-output variable pair at a time; all other variables were fixed at their base values. Only the effect of an increase in each input variable from its base value is tabulated, since decreasing an input variable merely changes the sign of the corresponding table entry.

Many of the behavioral patterns summarized in Table 5.3 are common to all three watersheds. Each of the six output variables ANC , SO_4^{2-} , Mg^{2+} , Na^+ , Cl^- , and F^- shows the same response pattern for all three lakes. The variable ANC is negatively correlated with SO_4^{2-} half saturation ($A_{1/2}$) and positively correlated with other input variables. The variable SO_4^{2-} is positively correlated with $A_{1/2}$, unchanged by weathering rate (R_i), and negatively correlated with soil depth (SD) and SO_4^{2-} maximum adsorption capacity (A_{max}). The variables Mg^{2+} and Na^+ are both positively

TABLE 5.3. Effect of Increase of Input Variable on Output Variables in the MAGIC Code

Lake	Input Variable	Effect on Output Variable ^(a)										
		ANC	SO ₄ ²⁻	Ca ²⁺	NO ₃ ⁻	NH ₄ ⁺	Mg ²⁺	Na ⁺	K ⁺	Cl ⁻	F ⁻	
Panther Lake	Soil depth (SD)	+	-	-	+	+	-	-	-	0	0	
	SO ₄ ²⁻ maximum capacity (A _{max})	+	-	-	0	0	-	-	0	0	0	
	SO ₄ ²⁻ half saturation (A _{1/2})	-	+	+	0	0	+	+	0	0	0	
	Weathering rate (R _i)	+	0	+	0	0	+	+	+	0	+	
Clear Pond	Soil depth	+	-	-	-	-	-	-	-	0	0	
	SO ₄ ²⁻ maximum capacity	+	-	-	0	0	-	-	-	0	0	
	SO ₄ ²⁻ half saturation	-	+	+	0	0	+	+	0	0	0	
	Weathering rate	+	0	+	0	0	+	+	+	0	+	
Woods Lake	Soil depth	+	-	-	0	0	-	-	-	0	0	
	SO ₄ ²⁻ maximum capacity	+	-	-	0	0	-	-	-	0	0	
	SO ₄ ²⁻ half saturation	-	+	-	0	0	+	+	+	0	0	
	Weathering rate	+	0	+	0	0	+	+	+	0	+	

(a) where + = increase (>0.5% change)
 0 = no change (<0.5% change)
 - = decrease (>0.5% change)

correlated with $A_{1/2}$ and R_i and negatively correlated with A_{max} and SD. The variable Cl^- shows no change in response to any of the input variables and F^- is affected only by weathering rates, exhibiting a positive correlation. For each lake, the variables NO_3^- and NH_4^+ both exhibit the same response pattern. They are positively correlated with SD for Panther Lake, negatively correlated with SD for Clear Pond, and unresponsive to SD at Woods Lake. These two variables are unresponsive to changes in the remaining three input variables for all three lakes. With the exception of response to $A_{1/2}$ in Woods Lake, Ca^{2+} and K^+ also exhibit the same response pattern for all three lakes: both respond positively to R_i , and negatively to SD and A_{max} . When interpreting these results, it should be kept in mind that Woods Lake is acidic (pH 4.7), with an ANC of $-49 \mu eq \cdot L^{-1}$, while Panther Lake (pH 7.0) and Clear Pond (pH 7.0) have ANC values of $127 \mu eq \cdot L^{-1}$ and $102 \mu eq \cdot L^{-1}$, respectively.

From the 241 MAGIC runs for each watershed, the runs chosen for detailed sensitivity analysis were those for which the output fell in the pre-established calibration region. The 241 runs were generated from orthogonal statistical designs (each level of each variable is paired with each level of every other variable), so it would not be expected that all the points generated would fall in the calibration region unless the input variables were mutually independent. When the out-of-calibration runs were eliminated, 116 runs remained for Panther Lake, 192 runs remained for Clear Pond and 147 runs remained for Woods Lake. From these numbers and from Table 5.2, it is clear that the calibration regions are watershed-specific.

For each lake, the correlations among the main output variable (ANC) and the four input variables calculated from the sensitivity analysis data are given in Table 5.4. For these data, ANC is positively correlated with the weathering rates (R_i). While the correlation is significant for all three lakes, it is especially high for Panther Lake ($R = 0.989$) and Clear Pond ($R = 0.997$). The variable ANC is uncorrelated with the other input variables except at Woods Lake, where it is positively correlated with A_{max} ($R = 0.26$) and negatively correlated with $A_{1/2}$ ($R = -0.37$). It must

TABLE 5.4. Correlation Matrix and Regression Analysis Results for the MAGIC Code

Lake	Input Variable	ANC	SD	A _{1/2}	A _{max}	R _i
Panther Lake ^(a)	ANC	1	-0.005	-0.06	0.06	0.989**
	SD		1	0.62**	-0.51**	-0.001
	A _{1/2}			1	0.13	-0.001
	A _{max}				1	0.02
	R _i					1
Clear Pond ^(b)	ANC	1	0.30**	0.007	0.02	0.997**
	SD		1	0.26**	-0.21**	0.23**
	A _{1/2}			1	0.03	0.02
	A _{max}				1	0.01
	R _i					1
Woods Lake ^(c)	ANC	1	0.12	-0.37**	0.26**	0.40**
	SD		1	0.59**	-0.30**	0.01
	A _{1/2}			1	0.18*	0.03
	A _{max}				1	-0.08
	R _i					1

* p < 0.05

** p < 0.01

Numbers in parentheses in equations (a), (b), and (c) are estimated standard errors for corresponding parameter estimates.

$$(a) \text{ ANC} = 188.29 * R_i + 25.2 * \text{SD} + 26.72 * A_{max} - 13.24 * A_{1/2} - 71.14$$

(0.75) (0.97) (1.01) (0.45) (1.69)

Fit: $R^2 = 0.998$

Influential Variables (Percent of Variability Explained): R_i(0.98), A_{1/2}(0.02)

$$(b) \text{ ANC} = 141.91 * R_i + 9.1 * \text{SD} + 4.25 * A_{max} - 1.78 * A_{1/2} - 58.76$$

(0.10) (0.07) (0.09) (0.03) (0.14)

Fit: $R^2 = 0.9999$

Influential Variables (Percent of Variability Explained): R_i(0.99)

$$(c) \text{ ANC} = 22.89 * R_i + 35.02 * \text{SD} + 34.39 * A_{max} - 20.21 * A_{1/2} - 121.22$$

(0.4) (0.41) (0.43) (0.21) (0.77)

Fit: $R^2 = 0.989$

Influential Variables (Percent of Variability Explained): A_{max}(0.42), A_{1/2}(0.31), R_i(0.24)

be emphasized that these relationships are observed for data within the calibration region and they do not necessarily extend to larger regions.

Although it is beyond the scope of this analysis to determine the relationships among the MAGIC input variables, it is possible to identify the significant correlations exhibited among them in the sensitivity analysis data. From the correlation matrices in Table 5.4, it can be seen that SD is positively correlated with $A_{1/2}$ and negatively correlated with A_{max} for each lake. Soil depth is uncorrelated with weathering rate (R_i) except at Clear Pond, where a positive correlation exists ($R = 0.23$). Indeed, except for the positive correlation with SD for Clear Pond, the weathering rates are uncorrelated with any of the other input variables. Grouped weathering rate(s), which all changed proportionately, were found to be essentially independent of the other input variables for these additional runs, supporting the earlier finding that, with the exception of the positive correlation with weathering rate at Clear Pond, soil depth is independent of the other input variables.

To estimate the sensitivity of ANC to changes in the four input variables, a linear model was fit to various functions of the input variables. A separate model was fit for each lake (watershed) using all observations that fell into the predetermined calibration region for that lake (116 observations for Panther Lake, etc.). The GLM (General Linear Models) procedure from the SAS computer software package (SAS 1985) was used to perform the necessary model fitting and residual analysis. For each watershed, the input values were expressed as a percentage of the appropriate calibration value. Of the models examined, the best fit for all three watersheds was obtained for a linear model that contained either the variables SD, A_{max} , $A_{1/2}$, and R_i , or the variables R_i , $SD \cdot A_{max}$, $SD \cdot A_{max} / A_{1/2}$ and $A_{max} / A_{1/2}$. Both models fit the data very well, explaining over 98% of the variability in ANC for all three lakes. The second model was examined because it contains variables that appear in the MAGIC code. However, since the fits are essentially equivalent, the first model was selected because it provides estimates of the sensitivity of ANC to the original input variables (whereas the second provides sensitivity estimates for certain functions of the original input variables). The

linear models based upon SD, A_{max} , $A_{1/2}$, and R_i are given in Table 5.4. As is to be expected from the correlation matrices, the weathering rate (R_i) is the dominant variable in the model for both Panther Lake and Clear Pond. Indeed, for these two lakes, a regression model that contains only the single input variable R_i explains at least 98% of the variability in ANC. For acidic Woods Lake, all four input variables contribute more or less equally to the variability in ANC and, in particular, R_i does not dominate as it does for the other two watersheds.

In summary, the MAGIC output variable (ANC) can be adequately described over the established calibration range by a linear model that contains the four input variables soil depth (SD), maximum capacity (A_{max}), half saturation ($A_{1/2}$) and weathering rate(s) (R_i). This result is hardly surprising because the input variables were restricted to a range about their base values over which ANC is essentially a linear function of each. However, the relationship of ANC to the four input variables is quite different for the acidic lake (Woods Lake) than it is for the two near-neutral lakes (Panther Lake, Clear Pond). At least 98% of the variability in ANC is explained by weathering rate (R_i) alone at Panther and Clear Lakes, whereas the four input variables contribute more-or-less equally to explanation of ANC variability at Woods Lake. Because ANC is linear in each input variable over the calibration range, the coefficients in the regression equations given in Table 5.4 can be used to estimate the sensitivity of the response variable ANC to each input variable. (a) For example, a 50% increase in weathering rate (relative to the base value $R_i = 1$) at Panther Lake results in a 63% increase in ANC.

-
- (a) If the calibration intervals for the input variables were so wide that ANC was not adequately estimated by a linear function, then output sensitivities could change significantly over the input region, and use of regression coefficients (or any other measure) to estimate "global" sensitivities would be problematical.

5.2 THE ETD CODE

As with the MAGIC code, the calibration values for ETD code input variables are obtained by manipulating them to match the values of the output variables with the measured water-chemistry values. Calibration values were provided by the authors of the ETD code (see Section 3.2.1) for each watershed. Because the available time series for precipitation data was limited to 2 years for Clear Pond and 3 years for Woods and Panther lakes, these time series data were cycled to provide a 15-year forecast. However, for consistency among watersheds, average values for the last 3 years of a 15-year forecast were taken as the output data for this study. The output variables of primary interest are the ANC and SO_4^{2-} concentrations of the lake; a sensitivity analysis was conducted using only ANC. When the calibration values are used as input to the code, the corresponding values of ANC and SO_4^{2-} are used as reference values.

Twenty-eight input variables were considered for the ETD code sensitivity analysis. Following the procedure described for the MAGIC code, output variables were determined to be "in calibration" when their observed values were within 20% of their reference values. Table 5.5 contains a list of the input variables and gives the calibration interval selected for each. For most variables, the calibration interval is expressed as a percentage of the appropriate calibration value. Except as noted, percentages used to define the input range of a given variable were the same for all three watersheds.

The calibration intervals for the ETD and ILWAS codes were selected to be somewhat wider than those selected for the MAGIC code, in part because of experience gained with the latter and in part because of the long run times for the ETD and ILWAS codes. The wider intervals were originally chosen so that a high percentage of sampling points selected (by LHS) for sensitivity analysis was defined to be "in calibration." Subsequently, the linearity of the response variable to each input variable was verified over the wider calibration range. Because of the long time required for a single run of the ETD code, it was not possible to use factorial designs (like those used with the MAGIC code) to

TABLE 5.5. Input Variables and Domains for the ETD Code

Input Variable Name	Compartment	Variable Identification	Calibration Interval ^(a)	Sampling Distribution
sulf ^(b)		sulfate wet deposition factor	± 20	U ^(c)
KAPPA		melt rate	0.5-2.0	T(1.423) ^(d)
KPAN2	Snow	pan evaporation correction coefficient	± 20	U
KPAN3	Soil	pan evaporation correction coefficient	± 20	U
KPAN5	Lake	pan evaporation correction coefficient	± 20	U
KPERC3	Soil	vertical hydraulic conductivity correction coefficient	± 20	U
KPERC4	Unsat	vertical hydraulic conductivity correction coefficient	± 20	U
PORE3	Soil	porosity	0.1-0.45	T(0.27) ^(e)
PORE4	Unsat	porosity	0.1-0.45	T(0.2) ^(f)
PORE6	GW	porosity	0.1-0.45	T(0.2) ^(f)
DEP3	Soil	soil depth	± 20	U
CBED	GW	hydraulic conductivity (lake bed)	± 20	U
KLAT3	Soil	horizontal hydraulic conductivity correction coefficient	± 20	U
KLAT4	Unsat	horizontal hydraulic conductivity correction coefficient	± 20	U
RE3	Soil	cation exchange reaction rate coefficient	± 20	U
K04	Unsat	ligand attachment rate constant	± 20	U
K05	Lake	ligand attachment rate constant	± 20	U
KP3	Soil	sulfate partition coefficient	± 20	U
K		sulfate reduction rate constant	± 20	U
KH4		hydrolysis rate constant	± 20	U
KH5	Lake	hydrolysis rate constant	± 20	U
KH6	GW	hydrolysis rate constant	± 20	U
MC4	Unsat	hydrolysis fraction rate constant	± 20	U
MC5	Lake	hydrolysis fraction rate constant	± 20	U
MC6	GW	hydrolysis fraction rate constant	± 20	U
HR4	Unsat	hydrogen ion reference concentration	± 20	U
HR5	Lake	hydrogen ion reference concentration	± 20	U
HR6	GW	hydrogen ion reference concentration	± 20	U

(a) Expressed as percentage of calibration value unless otherwise noted.

(b) Variable name assigned for this study.

(c) Uniform distribution over indicated calibration interval.

(d) Triangular distribution over the interval (0.5, 2.0) with mode at 1.423.

(e) Triangular distribution over the interval (0.1, 0.45) with mode at 0.27.

(f) Triangular distribution over the interval (0.1, 0.45) with mode at 0.20.

determine the calibration range. Thus, with the ETD code, there were no initial screening steps to determine variable ranges analogous to those for the MAGIC code. Instead, the regions were determined with the aid of runs conducted for the geochemical behavioral analysis reported in Section 3.

Data for the sensitivity analysis were generated using an LHS strategy (Iman and Conover 1980; Iman and Conover 1982; Liebetrau and Doctor 1987). Under this strategy, a probability distribution is assigned to each input variable and the range (calibration interval) of each is then divided into a preselected number, n , of equiprobable intervals determined in accordance with the assigned probability distribution. In this study, the range of each input variable was divided into $n = 40$ intervals. The next step was to generate a realization of each variable in each interval (a total of 40 realizations for each of 28 variables in this study). An initial input vector (a vector of input values, one for each input variable) for the ETD code was obtained by randomly selecting one of the 40 realizations available for each variable. A second input vector was obtained by randomly selecting one of the remaining 39 realizations of each variable. This step was repeated until $n = 40$ input vectors had been determined. Finally, values of ETD code output variables were determined for each input vector. This required 40 runs of the code.

The distribution assigned to each input variable is given in Table 5.5. Realizations of 24 of the input variables were generated from a uniform distribution over the calibration interval. In the case of KAPPA and PORE3-PORE6, where somewhat wider calibration intervals were assigned, realizations were generated from a triangular distribution. For each input variable, the same type of distribution (uniform, triangular) was used for each watershed. However, realizations differed among lakes in accordance with calibration values.

After the 40 input-output vectors were generated, they were screened (with the aid of the criterion described above) to eliminate those that were "out of calibration." To maximize the sampling coverage of the input space, the "in calibration" realizations generated by LHS were combined

with the "in calibration" geochemical behavioral analysis runs (see Section 3) to obtain the data set from which sensitivities were evaluated. This procedure resulted in data sets of sizes 94, 96, and 57 for Panther Lake, Clear Pond, and Woods Lake, respectively.

The STEPWISE procedure of the SAS statistical package (SAS 1985) was used to identify the input variables that have the greatest influence on the output (response) variable ANC. The influence of an input variable is measured by the percentage of the variability in the ANC data that it explains. Results are given in Table 5.6, which contains a list of "influential" variables together with a predictive equation for ANC based upon them. After the influential variables were identified, a predictive equation was obtained by fitting a linear model that involved only the "influential" variables and the response variable. Note that the number of input variables is not the same for the three watersheds.

For Panther Lake, the most influential variables (identified in Table 5.5), listed in decreasing order of importance^(a), were found to be

K05(18), HR5(10),

KPERC3(5), PORE4(4), MC4(4), PORE3(4), KPAN3(3), KAPPA(3), PORE6(3),
RE3(1)

The numbers in parentheses give the percentage of the total variability in ANC that is attributable to or explained by the named variable. The influence of the input variables given in Table 5.5 that are not listed in Table 5.6 is insignificant. For Clear Pond, the most influential variables, in decreasing order of importance^(a), were found to be

KH5(31), MC5(22), HR5(15)

KAPPA(8), PORE3(7)

KPAN3(2), sulf(1), KPERC3(1), K(1), KP3(1), KH4(1), PORE6(1)

(a) Variables listed on the same line have approximately the same influence (in terms of percentage of variance explained) on ANC.

TABLE 5.6. Regression Analysis Results for the ETD Code

Panther Lake (*)

$$\begin{aligned} \text{ANC} = & 128.60 + 250.49 * \text{K05} - 30224216.70 * \text{HR5} + 6511.31 * \text{KPERC3} + 37.08 * \text{PORE4} - 36.15 \\ & (46.56) \quad (8605956.53) \quad (2256.96) \quad (12.09) \quad (16.97) \\ * \text{MC4} - & 79.54 * \text{PORE3} + 17.09 * \text{KPAN3} - 7.76 * \text{KAPPA} + 43.97 * \text{PORE6} - 3132077.36 * \text{RE3} \\ & (17.20) \quad (6.17) \quad (3.17) \quad (15.08) \quad (2011804.62) \end{aligned}$$

Fit

$$R^2 = 0.56$$

Influential Variables (percent of total variability explained)

K05(18), HR5(10)
KPERC3(5), PORE4(4), MC4(4), PORE3(4), KPAN3(3), KAPPA(3), PORE6(3), RE3(1)

5.17

Clear Pond

$$\begin{aligned} \text{ANC} = & 60.82 + 536.11 * \text{KH5} + 83.50 * \text{MC5} - 379018272.60 * \text{HR5} - 11.20 * \text{KAPPA} - 39.06 * \text{PORE3} \\ & (30.15) (*) \quad (6.17) \quad (35468126.32) \quad (1.38) \quad (6.34) \\ + & 9.55 * \text{KPAN3} - 14.34 * \text{sulf} - 585.58 * \text{KPERC3} + 8805.29 * \text{K} - 79626.42 * \text{KP3} + 19.24 \\ & (2.78) \quad (4.19) \quad (181.23) \quad (3544.37) \quad (43219.29) \quad (8.92) \\ * \text{KH4} + & 12.29 * \text{PORE6} \\ & (5.40) \end{aligned}$$

Fit

$$R^2 = 0.89$$

Influential Variables (percent of total variability explained)

KH5(31), MC5(22), HR5(15)
KAPPA(8), PORE3(7),
KPAN3(2), sulf(1), KPERC3(1), K(1), KP3(1), KH4(1), PORE6(1)

TABLE 5.6. (contd)

Woods Lake

$$\begin{aligned}
 \text{ANC} = & - 14.03 - 12.80 * \text{PORE3} + 7.99 * \text{MC5} - 30.81 * \text{DEP3} + 97550.49 * \text{KP3} - 5143546.98 * \text{HR6} \\
 & (3.16)^{(a)} \quad (2.84) \quad (5.56) \quad (30230.90) \quad (1561376.24) \\
 & + 2512.68 * \text{K} + 207.86 * \text{KH5} + 5.70 * \text{PORE4} + 16677277.31 * \text{RE3} + 6.51 * \text{MC4} - 1.32 * \text{KAPPA} \\
 & (825.43) \quad (40.10) \quad (2.06) \quad (5301668.37) \quad (2.68) \quad (0.61) \\
 & - 645780.09 * \text{HR5} + 135.76 * \text{K05} - 0.04 * \text{KLAT3} \\
 & (167847.22) \quad (74.80) \quad (0.01)
 \end{aligned}$$

Fit

5.18

$R^2 = 0.72$

Influential Variables (percent of total variability explained)

PORE3(9), MC5(9), DEP3(9), KP3(6)
 HR6(4), K(4), KH5(4), PORE4(3), RE3(3), MC4(3), KAPPA(3), HR5(2), K05(2), KLAT3(2)

(a) Numbers in parentheses are estimated standard errors for corresponding parameter estimates.

The influence of the remaining 15 variables is insignificant. For Woods Lake, the influential variables, listed in decreasing order of importance, are:

PORE3(9), MC5(9), DEP3(9), KP3(6)

HR6(4), K(4), KH5(4), PORE4(3), RE3(3), MC4(3), KAPPA(3), HR5(2),
K05(2), KLAT3(2)

It is clear that the input variables with the greatest influence on ANC differ considerably from one watershed to another. Indeed, of the variables that explain at least 4% of the variability in ANC, only PORE3 is common to all three watersheds. Variables that explain a smaller percentage of the variability have been ignored for this three-way comparison because their relative influence on ANC is so small that large changes in their order has little or no effect. Of the influential variables considered, the only additional one that is common to Panther Lake and Clear Pond is HR5. The influential variables common to Clear Pond and Woods Lake are KH5 and MC5. Except for PORE3, which is common to all three watersheds considered, there are no additional influential variables common to Panther Lake and Woods Lake.

For Panther Lake, the influence of K05 and HR5 is considerably greater than that of any other variables. Likewise, for Clear Pond, the influence of KH5, MC5, and HR5 dominates. For Woods Lake, however, the situation is somewhat different: there is no small subset of the variables whose influence is substantially greater than that of any other. Because so few of the influential variables are common to two or more of the watersheds, it is doubtful that one can infer from this sample of lakes which input variables will have the greatest influence on ANC for watersheds not included in this study.

To examine the sensitivity of the results presented in Table 5.6 to small perturbations in the values of input variables, the analyses described above were repeated using only those "in calibration" samples generated by LHS. In the case of Clear Pond (n = 33), the lists of the seven most influential variables and their order of importance agreed for both analyses. In the case of Panther Lake, the analysis based upon the

"in calibration" LHS samples (n = 33) identified the two most influential variables (K05, HR5) and one (MC4) of the three that explained 4% of the total variability in the full analysis. For Woods Lake, however, the analysis of LHS data did not confirm the results of the full analysis. There are two possible reasons for this outcome. First, since no variables were clearly more influential than others, small perturbations in input values could be expected to have a significant effect on the list of "influential" variables. Second, the response of ANC to changes in the input variables was more variable for Woods Lake than for the other two watersheds. Thus, the number of "in calibration" samples (n = 14) is so small that little reliance can be placed on the ranking obtained from the LHS data.

The samples for the behavioral analysis were generated so that the effect of each variable could be examined independently of others. Likewise, the input samples for the sensitivity analysis were generated independently for each input variable. As with the MAGIC code, however, it is possible to obtain some idea of the de facto correlation structure of the input variables to the ETD code by examining those samples that remain "in calibration" following the initial screening. For Panther Lake and Clear Pond, the ETD code was in calibration for nearly all samples generated both for behavioral and sensitivity analysis. It is to be expected, therefore, that observed correlations among the input variables would not be significantly different from zero. An examination of the correlation matrices of the influential input variables for these two watersheds verifies this conclusion. The situation is somewhat different for Woods Lake because the code remained in calibration for only two-thirds (approximately) of the total samples generated. The correlation matrix for the 14 influential variables for Woods Lake is given in Table 5.7. From this matrix, it can be seen that significant correlations exist both among certain variables within a given layer and among given variables in different layers. For example, PORE3 is correlated with DEP3, RE3, PORE4, HR5, and K. In addition, DEP3 is correlated with KH5 and MC5, PORE4 is correlated with KLAT3 and HR6, and HR5 is correlated

TABLE 5.7. Significant Correlations Among "In Calibration" Input Values for the ETD Code (Woods Lake)

Input Variable Name	KAPPA	PORE3	PORE4	DEP3	KLAT3	RES	K05
KAPPA	1.0						
PORE3	0.123	1.0					
PORE4	-0.019	0.281*	1.0				
DEP3	-0.050	-0.352***	0.065	1.0			
KLAT3	0.244*	0.073	0.352***	0.099	1.0		
RES	0.103	-0.254*	-0.050	-0.086	-0.005	1.0	
K05	0.126	-0.217	-0.041	0.053	0.058	-0.027	1.0
KP3	-0.182	-0.180	-0.135	-0.010	-0.306**	0.000	-0.242*
K	0.019	-0.278**	-0.060	0.095	0.209	0.000	-0.057
KH5	-0.013	0.101	-0.018	0.427***	0.121	-0.302**	-0.130
MC4	0.207	0.071	0.108	0.070	0.320**	-0.083	0.003
MC5	0.034	0.021	0.039	0.307***	-0.053	-0.081	-0.082
HR5	-0.126	-0.231*	-0.113	0.019	-0.144	0.000	0.041
HR6	-0.101	-0.094	-0.306**	-0.087	-0.490***	0.000	-0.125

Input Variable Name	KP3	K	KH5	MC4	MC5	HR5	HR6
KP3	1.0						
K	-0.330**	1.0					
KH5	-0.382***	0.128	1.0				
MC4	-0.018	0.031	0.129	1.0			
MC5	0.021	-0.118	0.452***	0.305***	1.0		
HR5	0.000	-0.108	0.316**	0.094	0.305***	1.0	
HR6	0.000	0.205	0.107	-0.288**	-0.055	0.000	1.0

* P < 0.1
 ** P < 0.05
 *** P < 0.01

with KH5 and MC5. Other significant correlations include: KLAT3 with KP3, MC4, and HR6; KP3 with K05, KH5, and K; MC4 with MC5 and HR6; and KH5 with MC5.

5.3 THE ILWAS CODE

Like the other two codes considered in this study, the ILWAS code was calibrated by manipulating the values of the input variables until the values of the output variables matched measured values for the watershed in question. Calibration values were provided for Panther and Woods Lakes by the authors of the ILWAS code. Calibration data were not available for Clear Pond, so this watershed was not included in the sensitivity analysis.

One of the major respects in which the ILWAS code differs from the ETD code is that the lakes under study are represented by 12 or 14 layers (12 for Panther Lake, 14 for Woods Lake) in the ILWAS code, whereas for the ETD code, it is assumed that the lakes are perfectly mixed. Thus, for comparative purposes, the flow-weighted annual averages of ANC and SO_4^{2-} for the upper layer of the lakes were analyzed. As with the ETD code, values averaged over the last 3 years of a 15-year forecast were used.

Because the ILWAS code has the capability to model several subcatchments and several subsurface lake layers, some physical parameters (e.g., weathering rates) can vary from one subcatchment/layer to another. To reduce the dimensionality of the problem (i.e., the number of input variables considered), these parameters were varied proportionally (all by the same percentage), just as was done with the weathering rates (R_i) for the MAGIC code. In this fashion, all variables in a group of functionally similar variables whose values could possibly differ from layer to layer (or subcatchment to subcatchment) were treated as a single representative variable for purposes of the sensitivity analysis.

For Panther Lake, the input variables, the number of variables in the group represented by each, and the calibration interval for each are given in Table 5.8. An initial screening of the input variables revealed that sulfate adsorption (CKS04), gibbsite dissolution rate (CKDAL), and the

TABLE 5.8. Input Variables and Domains of the ILWAS Code for Panther Lake

<u>Representative Input Variable</u>	<u>Number of Variables Represented</u>	<u>Variable Identification</u>	<u>Calibration Interval^(a)</u>
sulf	1	Sulfate wet deposition factor	± 20
CKMNR	100 ^(b)	Weathering rates for minerals	-50, +100
CKSO ₄	25 ^(c)	Sulfate adsorption constant	± 20
CKDAL	1	Gibbsite dissolution rate	± 20
PRMPRD	12 ^(d)	Primary productivity in lake	± 20
ECOEFF	1	Annual evaporation adjustment factor	± 20
SCOEFF	1	Seasonal evaporation adjustment factor	± 20
PERM	25 ^(c)	Horizontal hydraulic conductivity	± 10
SMI	25 ^(c)	Vertical hydraulic conductivity	± 10
THICK	25 ^(c)	Layer thickness	± 10

(a) Expressed as percentage of calibration value.

(b) Number of minerals + number of catchments + number of subsurface layers.

(c) Number of catchments + number of subsurface layers.

(d) Monthly values

primary productivity of the lake (PRMPRD) exhibited a negligible effect on the output variable ANC. Moreover, on the assumption that horizontal and vertical hydraulic conductivity (PERM, SMI) are positively correlated, it seems reasonable to vary these two variables proportionally. By assuming that horizontal and vertical hydraulic conductivity are linearly related, the two variables are effectively treated as one for purposes of this analysis.

With the aid of an LHS strategy, values of the remaining six variables were generated randomly over their calibration range. By combining the randomly generated "in calibration" values with those from the "in calibration" runs from the initial screening, a total of 20 samples were made available for sensitivity analysis. A preliminary regression analysis revealed that weathering rates (CKMNR) had a negligible effect on lake ANC, so this variable was dropped from the analysis. Results of the behavioral analysis show that in the ILWAS code, a decrease in the

weathering rate(s) is compensated for by an increase in the ANC production from cation exchange, and vice versa. Thus, a decrease in the weathering rates will not be reflected by a decrease in lake ANC until the exchangeable bases are significantly reduced, and this does not occur within the 15-year simulation period.

Results of the regression analysis for the five remaining input variables and their correlations are shown in Tables 5.9 and 5.10. These variables jointly explain approximately 97% of the total variability in

TABLE 5.9. Regression Analysis Results for the ILWAS Code for Panther Lake

$$\begin{aligned} \text{ANC} = & - 186.34 - 165.59 * \text{THICK} - 54.69 * \text{sulf} + 57.06 * \text{ECOEFF} \\ & (40.10) \quad (12.64) \quad (6.92) \quad (7.30) \\ & + 193.55 * \text{PERM/SMI} + 26.33 * \text{SCOEFF} \\ & (33.40) \quad (6.59) \end{aligned}$$

Fit

$$R^2 = 0.97$$

Influential Variables (percentage of total variability explained)

THICK(39), sulf(30), ECOEFF(17), PERM/SMI(6), SCOEFF(5)

TABLE 5.10. Correlation Matrix for the ILWAS Code for Panther Lake^(a)

<u>Variable</u>	<u>sulf</u>	<u>ECOEFF</u>	<u>SCOEFF</u>	<u>PERM/SMI</u>	<u>THICK</u>
sulf	1	-0.12	0.18	-0.06	-0.19
ECOEFF		1	0.07	-0.09	0.08
SCOEFF			1	-0.19	0.1
PERM/SMI				1	-0.08
THICK					1

(a) No correlations are significantly different from zero.

ANC over the selected input domain, so the influence of other variables (as measured by the percentage of variability in lake ANC they explain) is negligible. The influential variables, listed in order of importance, are

THICK(39), sulf(30), ECOEFF(17), PERM/SMI(6), SCOEFF(5)

The number in parentheses following each variable name is the percent of total variability in lake ANC that the variable explains. These results indicate that the thickness of the soil layer, the sulfate wet deposition factor, and the annual evaporation adjustment factor have the greatest effect on ANC at Panther Lake. The accompanying correlation matrix shows that no significant correlations among the input variables were observed in the samples generated for this analysis.

Because of the long run times required for the ILWAS code, the size of the sample used for this analysis is quite small, so the results of this analysis should be used with caution. These results should be verified with a more thorough analysis before they can be used with confidence to make substantive procedural or policy decisions.

The sensitivity analysis for Woods Lake was conducted in the same fashion as that for Panther Lake, with the following four exceptions. First, Woods Lake was divided into 14 layers, compared to 12 layers for Panther Lake. The output values of ANC and SO_4^{2-} used for the sensitivity analysis were those obtained for the uppermost layer. Second, the numbers of variables in groups of functionally similar variables (one variable per layer) are different for the two lakes. Thus, although the same 10 representative variables were used for both watersheds, these variables could represent different numbers of input variables. Third, the calibration range of the SO_4^{2-} wet deposition factor was taken to be the interval of values within 10% of the reference value for Woods Lake, whereas the interval of values within 20% of the reference value was used for Panther Lake. Finally, because the reference ANC value for Woods Lake is quite close to zero, the calibration interval for ANC was taken to be (-10,+20). The 10 representative input variables for Woods Lake, the number of variables in the group represented by each, and the calibration interval for each are given in Table 5.11.

TABLE 5.11. Input Variables and Domains for the ILWAS Code for Woods Lake

<u>Representative Input Variable</u>	<u>Number of Variables Represented</u>	<u>Variable Identification</u>	<u>Calibration Interval^(a)</u>
sulf ^(b)	1	Sulfate wet deposition factor	± 10
CKMNL	12 ^(c)	Weathering rates for minerals	-50, +100
CKSO ₄	3 ^(d)	Sulfate adsorption constant	± 20
CKDAL	1	Gibbsite dissolution rate	± 20
PRMPRD	12 ^(e)	Primary productivity in lake	± 20
ECOEFF	1	Annual evaporation adjustment factor	± 20
SCOEFF	1	Seasonal evaporation adjustment factor	± 20
PERM	3 ^(d)	Horizontal hydraulic conductivity	± 10
SMI	3 ^(d)	Vertical hydraulic conductivity	± 10
THICK	3 ^(d)	Layer thickness	± 10

(a) Expressed as a percentage of calibration value.

(b) Variable name added in this study.

(c) Number of minerals * number of catchments * number of subsurface layers.

(d) Number of catchments * number of subsurface layers.

(e) Monthly values.

The initial screening of the input variables for Woods Lake indicated that of the 10 variables originally considered, the SO₄²⁻ adsorption constants (CKSO₄) and the gibbsite dissolution rate (CKDAL) had an insignificant effect on ANC. It was also concluded that horizontal and vertical hydraulic conductivity (PERM, SMI) could be varied proportionally and by the same percentage as for Panther Lake. Values of the remaining seven variables were generated randomly from their calibration range. The randomly generated "in calibration" input vectors were combined with the "in calibration" input vectors from the initial screening to produce a total of 20 samples for the sensitivity analysis.

A preliminary regression analysis showed that weathering rates (CKMNL) and the seasonal evaporation adjustment factor (SCOEFF) had negligible effects on lake ANC, so these variables were dropped from the

analysis. Results of the regression analysis for the five remaining input variables and the accompanying correlation matrix are shown in Tables 5.12 and 5.13. These variables jointly explain approximately 90% of the total variability in lake ANC over the selected input domain. The influential variables, listed in order of importance, are

THICK(64), sulf(10), ECOEFF(8), PRMPRD(7), PERM/SMI(1)

The number in parentheses following a variable name is the percentage of total variability in lake ANC it explains. These results indicate that the thickness of the soil layer has the greatest effect on ANC at Panther Lake. To a lesser extent, lake ANC is influenced by the sulfate wet

TABLE 5.12. Regression Analysis Results for the ILWAS Code for Woods Lake

$$\begin{aligned} \text{ANC} = & - 165.32 + 65.71 * \text{THICK} - 31.07 * \text{sulf} + 21.52 * \text{ECOEFF} \\ & (41.19) \quad (6.98) \quad (10.90) \quad (5.56) \\ & + 27.72 * \text{PRMPRD} + 86.22 * \text{PERM/SMF} \\ & (6.03) \quad (32.09) \end{aligned}$$

Fit

$$R^2 = 0.90$$

Influential Variables (percent of total variability explained)

THICK(64), sulf(10), ECOEFF(8), PRMPRD(7), PERM/SMI(1)

TABLE 5.13. Correlation Matrix for the ILWAS Code for Woods Lake

<u>Variable</u>	<u>sulf</u>	<u>PRMPRD</u>	<u>ECOEFF</u>	<u>PERM/SMI</u>	<u>THICK</u>
sulf	1	0.26	-0.1	-0.06	-0.16
PRMPRD		1	-0.13	-0.46**	-0.07
ECOEFF			1	-0.26	0.04
PERM/SMI				1	-0.13
THICK					1

** p < 0.05

deposition factor, the annual evaporation adjustment factor, and primary productivity in the lake. While the first three influential variables, in order of importance for explaining lake ANC variability, are the same for both lakes, the relative importance of the thickness of the soil layer(s) is much greater at Woods Lake than at Panther Lake. The accompanying correlation matrix shows that no significant correlations (except possibly between PRMPRD and PERM/SMI) among the input variables were observed in the samples generated for this analysis. As with Panther Lake, the results for Woods Lake must be interpreted with caution because of the small sample size.

5.4 SUMMARY AND CONCLUSIONS

This section presents the results of a sensitivity analysis for the three computer codes--MAGIC, ETD, and ILWAS--used to model the acidification of watersheds. The MAGIC and ETD codes were applied to three Adirondack lakes (Panther Lake, Woods Lake, and Clear Pond) and the ILWAS code was applied to two (Panther Lake and Woods Lake). Woods Lake is acidic, but Panther Lake and Clear Pond are nearly neutral. In all cases, the response variable of interest is flow-weighted average annual acid neutralizing capacity, ANC.

For the MAGIC code and for the nonacidic watersheds (Panther Lake and Clear Pond), the input variable with the greatest influence on ANC was found to be the grouped weathering rate^(a). The weathering rate explained at least 99% of the variability in lake ANC in these cases. For Woods Lake, however, four input variables (the grouped weathering rate, soil depth, SO_4^{2-} maximum adsorption capacity, and SO_4^{2-} half-saturation constant) were found to have a significant effect on ANC. In this case, no variable was as dominant as weathering rate is for the other two lakes.

For the ETD code, the set of variables with the greatest influence on ANC was unique to the watershed under study. Input variables that explained more than 5% of the variability in ANC for Panther Lake were K05

(a) All changed proportionately, as with the MAGIC code (Section 5.1).

(ligand attachment rate constant for the lake) and HR5 (lake surface hydrogen ion reference concentration). Input variables that explained more than 5% of the variability in ANC for Clear Pond were KH5 (hydrolysis rate constant for lake), MC5 (hydrolysis fraction rate constant for lake), HR5 (hydrogen ion reference concentration for lake), KAPPA (melt rate), and PORE3 (soil porosity). Finally, input variables that explained more than 5% of the variability at Woods Lake were PORE3 (soil porosity), MC5 (hydrolysis fraction rate constant for lake), DEP3 (soil depth), and KP3 (soil sulfate partition coefficient). The only influential variables common to all three watersheds, PORE3 and KAPPA, explained a relatively small percent of the variability in ANC at each. For Woods Lake, there was no dominant input variable: PORE3, the variable with the greatest influence, explained only 9% of the variability in ANC.

It is interesting to note that although the ETD code is more sensitive to variables associated with mineral weathering in the lake than to the variables associated with weathering in the soil compartments, the quantity of ANC generated in the lakes is significantly less than that generated in the soil compartments (Tables 5.6 and 3.6). Table 3.6 shows that the weathering in the unsaturated zone is the largest source of ANC.

For the ILWAS code, the three most influential variables were THICK (layer thickness), sulf (sulfate wet deposition factor), and ECOEFF (annual evaporation adjustment factor) for both Panther and Woods Lakes. These three variables combined to explain approximately 86% of the variability in ANC for Panther Lake and 82% of the variability at Woods Lake. Given the differences in the two lakes (Woods Lake is acidic and Panther Lake is not), the behavior of the ILWAS code was surprisingly similar for the two watersheds. The absence of weathering rates as a main variable was somewhat unexpected. However, detailed examinations of the code output indicated that in some cases the code may compensate for ANC lost by the reduction in the value of one variable (e.g., weathering) by increasing the ANC generated by another (e.g., base exchange). The capability of the ILWAS code to compensate in this manner provides a desirable simulation of the interaction of natural processes.

It is difficult or impossible to identify factors common to all codes that relate to the effects of influential variables because of major differences in process formulations among the codes. For reasons explained in Chapter 3, it was not feasible to perform sensitivity analysis on hydrologic variables with the MAGIC code. Thus, there can be no reconciliation of differences in the effect of hydrologic variables because it is not possible to compare the results of the MAGIC code with those of the ILWAS and ETD codes. Also, the weathering rate variables are aggregated in the MAGIC code, whereas they are not aggregated in the ILWAS and ETD codes. Consequently, the effect of weathering on ANC is dispersed over a number of variables in the ILWAS and ETD codes, none of which is as influential as the (aggregated) weathering rate in the MAGIC code. It is difficult to configure the more complex codes to obtain results comparable to those from the MAGIC code or comparable to each other.

Because of underlying assumptions and limitations, the results of this sensitivity analysis must be interpreted with care. Strictly speaking, the results apply only over (a subset of) the calibration region defined for each code/watershed combination. Moreover, the results depend upon the "size" of the selected calibration region. If the region is too small, so that the effect on ANC of perturbations in the most influential variables is small relative to random variability, then the results are little more than meaningless random "noise." Without data to estimate the measurement variability of model output variables (i.e., the random noise), which must be the ultimate reference for judging significance, there is no objective way to decide when a calibration region is too small. If the region is so large, on the other hand, that the response variable (ANC in this case) is not a monotone function (preferably linear) of each input variable, then it is possible to obtain results that are quite misleading. If the calibration interval for each calibration region in this study had been doubled, for example, it is conceivable that quite different results would have been obtained.

Inferences about other watersheds or other time scales based on this study should be tested to ensure their validity. There is no assurance

that the selected watersheds are representative, that is, typical of some larger population of lakes (nor do we know that these watersheds are not representative). Thus, the validity of any conclusions based on this assumption must be tested. Likewise, extrapolations in time require validation. Except for rather simple linear models, there is no a priori guarantee that the influential variables at one time will be the same as those at another.

In some cases, classes of input variables that could reasonably be assumed to behave in a similar fashion were replaced by a single variable in order to reduce the number of input variables. The effect on results of these assumptions is untested. Even with "reduced" input vectors, the number of simulations that were possible in some cases was quite limited, especially for the ILWAS code. Sensitivity analysis results based upon small samples, like those obtained by extrapolation, must be tested before they can be used with confidence.

A final factor that affects the results of a sensitivity analysis is the dependence structure of the input variables. Ideally, a sensitivity analysis would be performed with samples obtained according to the "true" joint probability distribution of the input variables. In many cases, especially with complex codes such as ETD and ILWAS, the information needed to estimate this joint probability distribution is unavailable. Under these circumstances, it is customary either to hypothesize a covariance structure or to treat the input variables independently, as was done in this study. There is no way to estimate the effect on the sensitivity analysis of treating the variables independently, rather than using their "true" joint distribution.

6.0 CONCLUSIONS

6.1 COMPARISON OF CODES

It is important to note that the three watershed acidification codes studied were developed for different purposes and applications; hence, they contain notably different time scales and levels of detail in their process formulations. The MAGIC and ILWAS codes contain process-oriented formulations that are based on chemical equilibria and kinetics for all the geochemical processes currently thought to be important in watershed acidification: 1) silicate mineral weathering, 2) anion retention, 3) cation exchange, 4) aluminum hydroxide dissolution and aluminum speciation, 5) carbonic acid equilibria, and 6) organic acid speciation. These two codes also contain similar suites of all the major cations and anions present in most surface and soil waters, except that the ILWAS code also considers silica and organically complexed aluminum. Given sufficient thermodynamic data and measurements of soil exchange complexes, the calibration of the MAGIC and ILWAS codes to specific watersheds is focused on cation exchange, weathering, biogeochemical reactions, and various hydrologic variables.

The ILWAS code incorporates highly detailed representations of hydrological, geochemical, and biogeochemical processes compared, to the other two codes. This approach has two potential advantages in that it allows the user to attribute changes observed in model output (e.g., annual-average volume-weighted ANC) to specific input variables (e.g., weathering rates) and allows additional measured variables to be used in the calibration process. For example, the inclusion of silica theoretically limits the amount of base cations that can be derived from weathering reactions because of stoichiometric constraints. Also, the ILWAS code uses a time step of one day or less which makes it applicable to simulation and forecasting of episodic events.

The MAGIC code contains concise formulations of the major geochemical processes affecting watershed acidification but does not explicitly contain representations of canopy and organic matter decomposition processes. The process formulations incorporated in the MAGIC code are temporally aggregated to a much greater extent than those in the ILWAS code. This approach is

consistent with the intended use of the MAGIC code for forecasting average monthly or yearly changes in soil and surface water chemistry.

A disadvantage of the numerous processes and high level of temporal and spatial detail included in the ILWAS code is that a correspondingly large amount of measured or estimated data is required. This in turn necessitates a proportional increase in calibration effort. In contrast, the less dense parameterization in the MAGIC code has the advantage of requiring considerably less input data and calibration effort.

The ILWAS code also contains biogeochemical processes that are not explicitly incorporated in the other two codes (e.g., canopy effects, organic matter decomposition), and formulations for the complexing of Al by organic acids which may be important for waters rich in organic acids. The more complex representations of Al chemistry in the ILWAS code are expected to make it more suitable for predicting the seasonal dynamics of Al concentrations than the MAGIC code.

The ILWAS and MAGIC codes use different ANC conventions. The contributions of dissolved aluminum species are included in the ILWAS definition of ANC but not in the MAGIC definition. The ANC definitions for the two models are related by the expression,

$$\{\text{ANC}\}_I = \{\text{ANC}\}_M + \{\text{Al}_T\}_M = \{\text{ANC}'\}_M \quad (6.1)$$

where the quantities in { } are ANC or total Al fluxes ($\text{meq}\cdot\text{m}^{-2}\cdot\text{y}^{-1}$), and I and M denote the ILWAS and MAGIC codes, respectively. In Panther Lake and Clear Pond ($\text{pH} \sim 7$), the Al term represents a small correction to $\{\text{ANC}\}_M$ (Table 3.11). However, the difference in ANC conventions in the MAGIC and ILWAS codes is much more important in calculating ANC in acidic ($\text{pH} < 5.0$) waters where gibbsite dissolution and aluminum speciation are major sources of acid buffering, such as in Woods Lake ($\text{pH} = 4.7$) where $\{\text{Al}_T\}_M$ represents a significant adjustment to $\{\text{ANC}\}_M$. When cast in the same convention, $\{\text{ANC}\}_I$ and $\{\text{ANC}'\}_M$ for both Panther and Woods Lakes are in reasonably good agreement, differing by 9% and 17%, respectively.

The ETD code, in contrast to the MAGIC and ILWAS codes, focuses on chemical rate processes and aggregates these processes in terms of their summed effects on the ANC mass balance. This approach is based on the generally

accepted use of the ANC of surface waters as the prime indicator of acidification and has the advantage of requiring a lesser amount of measured data than the ILWAS code. However, this approach requires that the several rate variables for all chemical processes be determined through calibration procedures. Specifically, the use of rate formulations for both cation exchange and mineral weathering does not allow one to make objective evaluations of the relative contributions of these processes for affecting ANC because they both are effectively calibrated variables that are unconstrained by measurements other than the ANC of surface waters. The other two models allow one to use generally available data on cation exchange fractions in soil horizons to fix or at least estimate the extent of acid buffering caused by exchange reactions relative to mineral weathering. The inclusion of representative data on soil chemistry in the ILWAS and MAGIC codes provides more confidence in calibration values and, consequently, in the predictive reliability of these codes, compared to the ETD code.

Another limitation of the ANC mass balance approach used in ETD is that it considers only a limited set of chemical components (i.e., ANC, SO_4^{2-} , Cl^- , H^+ , and carbonic acid species), omitting important factors that affect water quality such as Al-precipitation and dissolution, base-cation-exchange equilibria, organic acid buffering, and nitrogen chemistry. Their absence results in a reduction in the use of soils characterization data for selecting initial values of input variables. More specifically, the lack of an Al chemistry submodel precludes using the ETD code to forecast the further acidification or recovery of acidic systems (i.e., pH less than 5.0 to 5.5), where $\text{Al}(\text{OH})_3(\text{s})$ dissolution exerts a major effect on solution pH. The organic-rich upper horizons in many forested watersheds can often be expected to have soil pH values less than 5.0. The lack of nitrogen chemistry in the ETD code precludes its use in systems receiving an important amount of acidity due to nitrogen compounds. The absence of these important geochemical variables limits the use of simulation results and the assessment of how individual processes are affected by acidic deposition or for interpreting response differences among watersheds. For example, the ETD code considers the affects of base cation exchange on ANC only for the uppermost soil horizons whereas weathering is calculated only for the lower two soil horizons. This separation of processes among the soil layers is not in and

of itself a significant limitation since the rates of both cation exchange and mineral weathering are totally calibrated variables. However, without mineral weathering in the uppermost soil horizon, there is no replenishment of base cations on soil exchange sites resulting from mineral weathering reactions. The rate of depletion of base cation on exchange sites is expected to be a major factor in controlling the rate of watershed acidification (Cosby et al. 1985); the absence of this process in the ETD code limits its capability for making multi-decade forecasts of watershed acidification.

Analyses of the geochemical processes simulated by the ILWAS and ETD codes for three Adirondack watersheds showed that base-cation exchange and weathering are generally the dominant ANC sources. In contrast, SO_4^{2-} adsorption generated quantities of ANC comparable to that generated by cation exchange and weathering by the MAGIC code for the acidic Woods Lake watershed. Sulfate adsorption was a minor source of ANC for both the ETD and ILWAS codes for all watersheds. Gibbsite dissolution was forecasted by both MAGIC and ILWAS codes to provide 32% and 28%, respectively, of the net ANC produced by soil processes in the Woods watershed. Forecasts of watershed acidification for different future deposition scenarios by all three models showed that soil processes clearly buffer basin output ANC, but a change of 20% in the acidic deposition flux is quickly reflected by a decrease in lake waters ANC. It was found that the accuracy with which these models forecast surface-water acidification at current acidic deposition loadings may be limited by the accuracy with which acidic and base-cation deposition can be estimated.

The net contribution of ANC sources in the lake (or stream) to the total ANC budget is consistently greater in the ETD code than in the MAGIC and ILWAS codes. For example, the ETD calibration results in a positive ANC contribution from SO_4^{2-} reduction and mineral weathering in each of the lakes, whereas the MAGIC and ILWAS codes calculate a negative ANC contribution from lake nitrification reactions. Overall, significant differences in the average-annual outflow flux of ANC are obtained for the three codes from each lake studied here (Table 3.11). These differences in the sources of ANC in the watersheds are the result of differences in the underlying philosophy of the conceptual models and in code calibration.

Differences in process formulation among the three models makes comparison of the results of the sensitivity analysis difficult. Using ANC as the primary response variable, it was found for the MAGIC code that the input variable with the greatest influence on ANC was the weathering rate (grouped for both soil layers). The weathering rate explained at least 99% of the variability in lake ANC in the two non-acidic lakes and was important for the acidic Woods Lake; however, the grouped weathering rate, soil depth, SO_4^{2-} maximum adsorption capacity, and SO_4^{2-} half-saturation constant all had a significant effect on output ANC. For the ETD code, the set of variables with the greatest influence on ANC varied significantly between watersheds: ligand attachment rate constant(a), hydrolysis rate constant(a), hydrolysis fraction rate constant(a), hydrogen ion reference concentration(a), snow melt rate, soil porosity, soil depth, and soil sulfate partition coefficient. With the ILWAS code, layer thickness, sulfate wet deposition factor, and annual evaporation adjustment factor together explain approximately 86% of the variability in ANC for Panther Lake and 82% of the variability at Woods Lake.

The results of any sensitivity analysis with these watershed acidification codes depends upon the "size" of the selected "in calibration region" within which the variables values are constrained to fall. If the region is too small, the results may not be meaningful because they are of the same magnitude as the random "noise." On the other hand, if the region is large enough that the response variable is not a monotone function of each input variable, then it is possible to obtain results that are quite misleading. Ideally, a sensitivity analysis would be performed with samples obtained according to the "true" joint probability distribution of the input variables, which would necessitate knowing the dependence structure of the input variables. Since the dependence structure of the input variables is not known, joint probabilities cannot be calculated but can only be hypothesized for such complex codes as ETD and ILWAS. Therefore, the input variables that were not varied proportionally were treated as though they were independent because of the lack of substantial information to do otherwise.

(a) Weathering rate variables.

In summary, the MAGIC and ILWAS codes are advanced models of the combined meteorological, hydrological, and biogeochemical processes that govern watershed acidification. The MAGIC code is most appropriately used for forecasting watershed acidification where detailed monitoring data are not available and for analyzing the effects of uncertainties in input data on predicted results. The extent of temporal aggregation in the MAGIC code precludes its application at a time scale of less than a month. The high degree of process detail and short time step (generally one day) of the ILWAS code make it suitable for forecasting both episodic and seasonal events, and for conducting detailed numerical experiments to analyze the effects of different processes on soil and surface water chemistry. Although the number of input variables in the ILWAS code are extensive, this code can also be used for watersheds where monitoring data are sparse. However, this requires that many variables, especially the biogeochemical ones, be estimated from the modeler's past experience or by analogy with intensively studied watersheds. The ILWAS code also contains several output options that can be used for bookkeeping chores to track the mass balance relationships of all chemical constituents. This capability is helpful in analyzing code behavior in numerical experiments and calibration exercises. In comparison, the ETD code appears less useful in predicting watershed acidification or for understanding acidification processes because it does not include many of the accepted chemical processes and constituents affecting acidification, and does not take advantage of measured soil chemistry characteristics to define an initial state from which calibration and modeling can be started.

6.2 FORECAST RELIABILITY

An adequate assessment of the forecast reliability of the three watershed acidification codes cannot be made using only the analyses of code formulations, behavior, and studies presented in this report. Although our results indicate that each of the codes incorporates to some degree process formulations that are consistent with theoretical and experimental studies of natural systems, the inclusion or exclusion of particular processes do not translate directly into forecast reliability. Similarly, the number of process representations in a code is not an indicator of the reliability of its

forecasts although the addition, and appropriate parameterization, of significant variables offers the opportunity of increased forecast reliability.

Forecast reliability also depends on the methods of determining the values of variables that control various processes, including both calibrated and experimentally measured variables, and the methods used to aggregate those variables in both spatial and temporal scales. The values of many highly aggregated variables that affect watershed chemistry must be determined empirically by adjusting the values of those variables by calibration to match measured hydrologic and biogeochemical data. This procedure makes the forecast reliability dependent upon the quality of the calibration. Consequently, it is difficult to determine whether a given calibration, based on past watershed response over a relatively brief period of one or more years, will provide a reliable forecast of future response. There is no unique set of input values yielding a given output value because in each code enough latitude is incorporated in the manipulation of variable values to allow numerous acceptable combinations of calibrated variable values, simulating the water quality data for a particular period of time for a given watershed. Discerning which set of calibration values is the most likely to provide reliable forecasts must be based on the modeler's experience in calibration of the model, the process formulations within the model, and knowledge of the relative importance of various acid-neutralizing processes occurring in a watershed. Although reported literature on acidification processes can provide guidance for the selection of the calibration values for some model variables (e.g., SO_4^{2-} adsorption), for other variables literature values are not applicable (e.g., weathering rates). Process evaluations indicate that using an exponent on H^+ in the weathering equations is expected to provide a small increase in forecast reliability.

Forecast reliability is also affected by the significant temporal and spatial variability in precipitation and acidic deposition that occurs within a watershed. Because meteorological and acidic deposition data are often sparse, the uncertainty in these data used in the calibration process may confound the field testing of watershed acidification codes and limit the reliability of any forecasts. Another factor affecting reliability is the necessary spatial aggregation of watershed hydrologic properties and soil

chemistry data. For example, our studies of hydrologic behaviors of the ILWAS and MAGIC (TOPMODEL) codes indicate that the relative quantity of water routed through the various flow paths has a very important affect on the chemistry of runoff waters, hence on lake chemistry. The uncertainty in the description of flow routing is due to spatial variability of hydrologic properties, such as layer depth, hydraulic conductivity, and topography, and is the prime component of uncertainty in predictive reliability of all three watershed acidification codes.

Ideally, the forecast reliability could be tested by calibrating the models using measured data from a prior period and then making blind predictions of watershed chemistry for a subsequent period, which can be compared with data for that subsequent period. This approach provides the best available estimate of forecast reliability. However, watershed acidification is a long-term process whose importance has been recognized only during the last two decades. No watersheds have been monitored over a long enough time to provide data that are adequate for testing the reliability of forecasts of watershed acidification codes over periods of 50 to 100 years. We conclude that testing of these codes at thoroughly characterized watersheds with multi-year monitoring data is essential in establishing their reliability. However, this approach will be constrained by the limited number of watersheds for which such data are available.

6.3 RECOMMENDATIONS(a)

The EPA needs an evaluation of the reliability of watershed acidification codes prior to the preparation of the 1990 assessment of the acid rain problem in the United States that has been mandated by Congress. Since it is highly probable that the acid rain issue will continue through the next decade, there is a clear need for a more definitive evaluation of the reliability of watershed acidification forecasts made with these codes than will be possible by early 1990. All of the hydrogeochemical processes known to be important in watershed acidification are represented, in varying degrees of

-
- (a) A draft copy of this report was initially submitted to EPA in March, 1988. Some of these recommendations for further research have been implemented since then.

aggregation, in one or more of the codes included in this study. However, the present study does not establish that the formulations which implement these processes, the mode of spatial aggregation of data, and the calibration approaches used are adequate for long-term acidification forecasting. In investigations underway at PNL, but not yet reported in the literature, instances of a significant lack of fit between simulations and observational data have been encountered. To resolve these process-related problems, short-term studies using available data are needed. To provide further evidence of the adequacy of process formulations and implementation and of the general reliability of these codes, longer term studies are needed. We recommend the following further research to establish the forecast reliability of these codes:

- Select watersheds with available multi-year data (meterological, depositional, hydrologic, and biogeochemical) and carry out the following studies:
 - Determine the capability of these codes to forecast the recovery of watersheds that have been acidified as a result of anthropogenic emissions;
 - Identify the instances of significant lack of fit between simulations and observational data in the foregoing simulations;
 - Determine the extent to which uncertainties in input data could account for the lack of fit ;
 - Determine the extent to which alternative calibrations would significantly improve the match between simulations and observed data, and develop calibration rules to guide future calibrations;
 - Where appropriate, evaluate possible modifications or alternatives of process formulations and implementation to improve the fit between simulations and observational data.
- Extend the code studies identified above to multi-year, intensively-studied watersheds where acidic deposition is being (or, preferably, is about to be) manipulated.

7.0 REFERENCES

- Bache, B. W. 1986. "Aluminum Mobilization in Soils and Waters." J. Geol. Soc. 143:699-706.
- Baker, J. P., and C. L. Schofield. 1980. "Aluminum Toxicity to Fish as Related to Acid Precipitation and Adirondack Surface Water Quality." In Proceedings of the International Conference on Ecological Impacts of Acid Precipitation, eds. D. Drablos and A. Tollan, pp. 292-293. SSNF Project, Oslo, Norway.
- Beven, K., and E. F. Wood. 1983. "Catchment Geomorphology and the Dynamics of Runoff Contributing Areas." J. Hydr. 65:134-158.
- Bischoff, W. D., V. L. Paterson, and F. T. Mackenzie. 1984. "Geochemical Mass Balance for Sulfur- and Nitrogen-Bearing Acid Components: Eastern United States." In Geological Aspects of Acid Deposition, ed. O. P. Bricker, pp. 1-21. Butterworth Publishers, Boston, Massachusetts.
- Booty, W. G., and J. R. Kramer. 1984. "Sensitivity Analysis of a Watershed Acidification Model." Phil. Trans. R. Soc. London B. 305:441-449.
- Chang, F. J., J. W. Deleur, and A. R. Rao. 1986. Implementation, Sensitivity Analysis and Application of the 'ILWAS' Model of Acid Precipitation Impacts to Panther Lake and Walker Branch Watersheds. Purdue University, Water Resources Research Center, West Lafayette, Indiana. Tech. Report No. 176.
- Chao, T. T., M. E. Harward, and S. C. Fang. 1962. "Adsorption and Desorption of Sulfate Ions in Soils." Soil Sci. Am Proc. 26:234-237.
- Chen, C. W., S. A. Gherini, R. J. M. Hudson, and J. D. Dean. 1983. The Integrated Lake-Watershed Acidification Study. Volume I: Model Principles and Application Procedures. Final Report EA-3221, Electric Power Research Institute, Palo Alto, California.
- Christopherson, N., H. M. Seip, and R. F. Wright. 1982. "A Model for Streamwater Chemistry at Birkenes, Norway." Water Res. Res. 18:977-996.
- Church, M. R., and R. S. Turner. 1986. Factors Affecting the Long-Term Response of Surface Waters to Acidic Deposition: State-of-the-Art-Science, Vol II. Rep. ORNL/M--152, Oak Ridge National Laboratory, Oak Ridge, Tennessee.
- Cosby, B. J., G. M. Hornberger, and J. N. Galloway. 1985. "Modeling the Effects of Acid Deposition: Assessment of a Lumped Parameter Model of Soil Water and Streamwater Chemistry." Water Res. Res. 21:51-63.

- Cosby, B. J., G. M. Hornberger, S. H. Rastetter, J. N. Galloway, and R. F. Wright. 1986. "Estimating Catchment Water Quality Response to Acidic Deposition using Mathematical Models of Soil Ion Exchange Processes." Geoderma. 38:77-95. [Cited in text as Cosby et al. 1986a.]
- Cosby, B. J., G. M. Hornberger, R. F. Wright, and J. N. Galloway. 1986. "Modeling the Effects of Acid Deposition: Control of Long-Term Sulfate Dynamics by Soil Sulfate Adsorption." Water Res. Res. 22:1283-1291. [Cited in text as Cosby et al. 1986b.]
- Cosby, B. J., R. F. Wright, G. M. Hornberger, and J. N. Galloway. 1985. "Modeling the Effects of Acid Deposition: Estimation of Long-Term Water Quality Responses in a Small Forested Catchment." Water Res. Res. 21:1591-1601.
- Couto, W., D. J. Lathwell, and D. R. Bouldin. 1979. "Sulfate Sorption by Two Oxisols and an Alfisol of the Tropics." Soil Sci. 127:108-116.
- Cronan, S. C., W. J. Walker, and P. R. Bloom. 1986. "Predicting Aqueous Aluminum Concentrations in Natural Waters." Nature 324:140-143.
- Davis, J. A., and J. O. Leckie. 1980. "Surface Ionization and Complexation at the Oxide/Water Surface. 3. Adsorption of Anions." J. Colloid Inter. Sci. 74:32-43.
- De Grosbois, E., R. P. Hooper, and N. Christophersen. 1988. "A Multi-signal Automatic Calibration Methodology for Hydrochemical Models: A Case Study of the Birkenes Model." Water Res. Res. 24:1299-1307.
- Driscoll, C. T., J. P. Baker, J. J. Bisogni, and C. L. Schofield. 1980. "Effect of Aluminum Speciation on Fish in Dilute Acidified Waters." Nature 284:161-164.
- Driscoll, C. T., J. P. Baker, J. J. Bisogni, and C. L. Schofield. 1984. "Aluminum Speciation and Equilibria in Dilute Acidic Surface Waters of Adirondack Region of New York State." In Geological Aspects of Acid Deposition, ed. O. P. Bricker, pp. 55-75. Butterworth Publishers, Boston, Massachusetts.
- Driscoll, C. T., and J. J. Bisogni. 1984. "Weak Acid/Base Systems in Dilute Acidified Lakes and Streams of the Adirondack Region of New York State." In Modeling of Total Acid Precipitation Impacts, ed. J. L. Schnoor, pp. 53-75. Butterworth Publishers, Boston, Massachusetts.
- Furrer, G., and W. Stumm. 1986. "The Coordination Chemistry of Weathering: I. Dissolution Kinetics of γ - Al_2O_3 and BeO." Geochem. Cosmochim. Acta 50:1847-1860.
- Galloway, J. N., G. E. Likens, and E. S. Edgerton. 1976. "Acid Precipitation in the Northeastern United States: pH and Acidity." Science 194:722-724.

- Galloway, J. N., S. A. Norton, and M. R. Church. 1983. "Freshwater Acidification from Atmospheric Deposition of Sulfuric Acid: A Conceptual Approach." Environ. Sci. Tech. 17:541A-545A.
- Gherini, S., L. Mok, R. J. Hudson, G. F. Davis, C. W. Chen, and R. A. Goldstein. 1985. "The ILWAS Model: Formulation and Application." Water, Air and Soil Pollution 26:425-459.
- Goldstein, R. A., C. W. Chen, and S. A. Gherini. 1985. "Integrated Lake-Watershed Acidification Study: Summary." Water, Air and Soil Pollution 26:327-337.
- Harned, H. S., and R. Davis. 1943. "The Ionization Constant of Carbonic Acid in Water and the Solubility of Carbon Dioxide in Water and Aqueous Salt Solutions from 0 to 50°C." J. Am. Chem. Soc. 65:2030-2037.
- Harned, H. S., and B. B. Owen. 1958. The Physical Chemistry of Electrolyte Solutions. 3rd ed. Reinhold, New York.
- Harned, H. S., and S. R. Scholes Jr. 1941. "The Ionization Constant of HCO_3^- from 0 to 50°C." J. Am. Chem. Soc. 63:1706-1709.
- Hem, J. D. 1968. "Graphical Methods for Studies of Aqueous Aluminum Hydroxide, Fluoride, and Sulfate Complexes." Geol. Surv. Water Supply Paper 1827-B, Washington, D.C.
- Hingston, F. J., A. M. Posner, and J. P. Quirk. 1972. "Anion Adsorption by Goethite and Gibbsite: I. The Role of the Proton in Determining Adsorption Envelopes." Soil Sci. 23:177-192.
- Höfken, K. D. 1983. "Input of Acidifiers and Heavy Metals to a German Forest Area Due to Wet and Dry Deposition." In Effects of Accumulation of Air Pollutants on Forest Ecosystems, eds. B. Ulrich and J. Pankrath, pp. 57-64. Reidel, Boston, Massachusetts.
- Hooper, R. P., and C. A. Shoemaker. 1985. "Aluminum Mobilization in an Acidic Headwater Stream: Temporal Variation and Mineral Dissolution Disequilibria." Science 229:463-465.
- Hooper, R. P., A. Stone, N. Christophersen, E. De Grosbois, and H. M. Seip. 1988. "Assessing the Birkenes Model of Stream Acidification Using a Multisignal Calibration Methodology." Water Res. Res. 24:1308-1316.
- Hornberger, G. M., K. J. Beven, B. J. Cosby, and D. E. Sappington. 1985. "Shenandoah Watershed Study: Calibration of a Topography Based, Variable Contributing Area Hydrological Model to a Small Forested Catchment." Water Res. Res. 21:1841-1850.

- Iman, R. L., and W. J. Conover. 1980. "Small Sample Sensitivity Analysis Techniques for Computer Models, with an Application to Risk Assessment." Comm. in Stat. A9(17):1749-1842.
- Iman, R. L., and W. J. Conover. 1982. "A Distribution-Free Approach to Inducing Rank Correlation Among Input Variables." Comm. in Stat. B11(3):311-334.
- Iman, R. L., and J. C. Melton. 1985. A Comparison of Uncertainty and Sensitivity Analysis Techniques for Computer Models. NUREG/CR-3904 (SAND 84-1461), U.S. Nuclear Regulatory Commission, Washington, D.C.
- Johnson, N. M. 1984. "Acid Rain Neutralization by Geologic Materials." In Geological Aspects of Acid Deposition, ed. O. P. Bricker, pp. 37-53. Butterworth Publishers, Boston, Massachusetts.
- Knauer, D. R., J. G. Bockheim, C. W. Chen, J. Slichinger, P. J. Garrison, S. A. Gherini, A. J. Prey, and D. A. Wentz. 1984. The Regional Inter-rated Lake Watershed Acidification Study at Round and East Eightmile Lakes, Wisconsin, 1981-1983. Electric Power Research Institute, Palo Alto, California.
- Krauskopf, K. B. 1967. Introduction to Geochemistry. McGraw-Hill, New York.
- Lasaga, A. C. 1981. "Rate Laws of Chemical Reactions." In Kinetics of Geochemical Processes, eds. A. C. Lasaga and R. J. Kirkpatrick, pp. 1-67. Mineralogical Society of America, Washington, D.C.
- Lasaga, A. C. 1984. "Chemical Kinetics of Water-Rock Reactions." J. of Geophys. Res. B 89:4009-4025.
- Lee, Sijin. 1987. Uncertainty Analysis for Long-Term Acidification of Lakes in Northeastern USA. Ph.D. thesis, University of Iowa, Ames, Iowa.
- Liebetrau, A. M., and P. G. Doctor. 1987. "The Generation of Dependent Input Variables to a Performance Assessment Simulation Code." In Proceedings of an NEA Workshop on Uncertainty Analysis for Performance Assessments of Radioactive Waste Disposal Systems, pp. 85-115. The Organization for Economic Cooperation and Development, Paris, France.
- Lindsay, W. L. 1979. Chemical Equilibria in Soils. John Wiley and Sons, New York.
- Linthurst, R. A., D. H. Landers, J. M. Eilers, D. F. Brakke, W. S. Overton, E. P. Meier, and R. E. Crowe. 1986. Characteristics of Lakes in the Eastern United States: Volume I: Population Descriptions and Physico-Chemical Relationships. EPA/600/4-86/007a, U.S. Environmental Protection Agency, Washington, D.C.

- May, H. M., P. A. Helmke, and M. L. Jackson. 1979. "Gibbsite Solubility and Thermodynamic Properties of Hydroxy-aluminum Ions in Aqueous Solutions at 25°C." Geochim. Cosmochim. Acta 43:861-868.
- National Academy of Sciences (NAS). 1984. Acid Deposition: Processes of Lake Acidification. National Academy Press, Washington, D.C.
- Naumov, G. B., B. N. Ryzhenko, and I. L. Khodakhovskiy. 1974. In Handbook of Thermodynamic Data, eds. I. Barnes and V. Speltz. Translation from Russian original transl. G. S. Soleimani. USGS-WRD-74-001, National Technical Information Service, Springfield, Virginia.
- Nikolaidis, N. 1987. Modeling the Direct Versus Delayed Response of Surface Waters to Acid Deposition in Northeastern United States. Ph.D. thesis, University of Iowa, Ames, Iowa.
- Nodvin, S. C., C. T. Driscoll, and G. E. Likens. 1986a. "The Effect of pH on Sulfate Adsorption by a Forest Soil." Soil Sci. 142:69-75.
- Nodvin, S. C., C. T. Driscoll, and G. E. Likens. 1986b. "Simple Partitioning of Anions and Dissolved Organic Carbon in a Forest Soil." Soil Sci. 142:20-28.
- Nordstrom, D. K., and J. W. Ball. 1986. "The Geochemical Behavior of Aluminum in Acidified Surface Waters." Science 232:54-56.
- Office of Technology Assessment (OTA). 1984. Acid Rain and Transported Air Pollutants: Implications for Public Policy. Rep. OTA-0-240, U.S. Congr. Office of Technology Assessment, Washington, D.C.
- Peters, N. E., and C. T. Driscoll. 1987. "Sources of Acidity During Snowmelt at a Forested Site in the West-Central Adirondack Mountains, New York." Forest Hydrology and Watershed Management. Proceedings of the Vancouver Symposium, August 1987, Actes Publ. #167.
- Rascher, C. M., C. T. Driscoll, and N. E. Peters. 1987. "Concentration and Flux of Solutes from Snow and Forest Floor During Snowmelt in the West-Central Adirondack Region of New York." Biogeochemistry 3:209-224.
- Reuss, J. O., and D. W. Johnson. 1985. "Effect of Soil Processes on the Acidification of Water by Acid Deposition." J. Environ. Qual. 14:26-31.
- Reuss, J. O., and D. W. Johnson. 1986. Acid Deposition and the Acidification of Soils and Waters. Springer-Verlag, New York.
- Robie, R. A., and D. R. Waldbaum. 1968. "Thermodynamic Properties of Minerals and Related Substances at 298.15°K (25°C) and One Atmosphere (1.013 bars) Pressure and at Higher Temperatures." U.S. Geol. Surv. Bull. 1259, Washington, D.C.

- SAS Institute, Inc. (SAS). 1985. SAS^R User's Guide: Statistics. Version 5 Edition. SAS Institute, Inc., Cary, North Carolina.
- Schindler, P. W. 1981. "Surface Complexes at Oxide-Water Interfaces." In Adsorption of Inorganics at Solid-Liquid Interfaces, eds. M. A. Anderson and A. T. Rubin, pp. 1-50. Ann Arbor Science Publishers, Ann Arbor, Michigan.
- Schnoor, J. L., and W. Stumm. 1985. "Acidification of Aquatic and Terrestrial Systems." In Chemical Processes in Lakes, ed. W. Stumm, pp. 311-338. John Wiley and Sons, New York.
- Schnoor, L., N. P. Nikolaidis, and G. E. Glass. 1986. "Lake Resources at Risk to Acidic Deposition in the Upper Midwest." J. Water Pollution Control Federation 58:139-148.
- Schofield, C. L., J. N. Galloway, and G. R. Hendry. 1985. "Surface Water Chemistry in the ILWAS Basins." Water, Air, and Soil Pollution 26:403-423.
- Sirois, A., and L. A. Barrie. 1988. "An Estimate of the Importance of Dry Deposition as a Pathway of Acidic Substances from the Atmosphere to the Biosphere in Eastern Canada." Tellus 40B:59-80.
- Stumm, W., and J. J. Morgan. 1981. Aquatic Chemistry: An Introduction Emphasizing Chemical Equilibria in Natural Waters. 2nd ed. John Wiley and Sons, New York.
- Sullivan, T. J., N. Christopherson, I. P. Muniz, H. M. Seip, and P. D. Sullivan. 1986. "Aqueous Aluminum Chemistry Response to Episodic Increases in Discharge." Nature 323:324-327.
- Tranter, M., T. D. Davies, P. Brimblecomb, and C. E. Vincent. 1987. "The Composition of Acidic Meltwaters During Snowmelt in the Scottish Highlands." Water, Air, and Soil Pollution 36:75-90.
- van Bavel, C. H. M. 1966. "Potential Evapotranspiration: The Combination Concept and Its Experimental Verification." Water Res. Res. 2:455-467.
- van Breeman, N., P. A. Burrough, E. J. Velthorst, H. F. van Dobben, T. de Witt, T. B. Ridder, and H. F. R. Reijnders. 1982. "Soil Acidification from Atmospheric Ammonium Sulfate in Forest Canopy Throughfall." Nature 229:548-550.
- van Breeman, N., and E. R. Jordens. 1983. "Effects of Atmospheric Ammonium Sulfate on Calcareous and Non-calcareous Soils of Woodlands in the Netherlands." In Effect of Accumulation of Air Pollutants on Forest Ecosystems, eds. B. Ulrich and J. Pankrath, pp. 171-182. Reidel, Boston, Massachusetts.

- van Breeman, N., and W. G. Wielemaker. 1974. "Buffer Intensities and Equilibrium pH of Minerals and Soils: I. The Contribution of Minerals and Aqueous Carbonate to pH Buffering." Soil Sci. Am. Proc. 38:55-60.
- Wagman, D. P., W. H. Evans, V. B. Parker, R. H. Schumm, I. Halow, S. M. Bailey, K. L. Churney, and R. L. Nuttall. 1982. The NBS Tables of Chemical Thermodynamic Properties. Selected Values for Inorganic and C₁ and C₂ Organic Substances in SI Units. J. Phys. Chem. Ref. Data 11, Supplement 2, Am. Chem. Soc. and Am. Inst. for Physics, New York.
- Whimkey, R. Z., and M. J. Kirkby. 1978. "Flow Within the Soil." In Hillslope Hydrology, ed. M. J. Kirkby. John Wiley and Sons, Chichester, England.
- Wright, R. F., and B. J. Cosby. 1987. "Use of a Process-Oriented Model to Predict Acidification at Manipulated Catchments in Norway." Atmos. Environ. 21:727-730.
- Zinder, B., G. Furrer, and W. Stumm. 1986. "The Coordination Chemistry of Weathering: II. Dissolution of Fe(III) Oxides." Geochim. Cosmochim. Acta 50:1861-1869.

APPENDIX A

INPUT DATA REQUIRED FOR THE MAGIC, ETD, AND ILWAS
WATERSHED ACIDIFICATION CODES

APPENDIX A

INPUT DATA REQUIRED FOR THE MAGIC, ETD, AND ILWAS WATERSHED ACIDIFICATION CODES

1. MAGIC Code Input Data Required (Because many of the input variables in the MAGIC code reside in matrices, they are not given specific variable names. The variables for MAGIC are listed in order of input below.)

Line #	Code	Column	Description	Units	Optimized	Measured
<u>Model Control, Hydrologic, Meteorologic, and Parameters</u>						
1			Catchment name			
2	1		Number of dissolved constituents on which mass balance is performed			X
	2		Number of soil parameters			X
	3		Number of stream/lake parameters			X
	4		Number of integration steps per year			X
3	1		Convergence criteria for mass balance calculations	seq.m-3		X
	2		Mean annual stream flow normalized by watershed area	m.yr-1		X
	3		Mean annual precipitation normalized by watershed area	m.yr-1		X
	4		Hindcast simulation period	yr		X
	5		Forecast simulation period	yr		X
	6		Starting year of hindcast simulation			X
	7		Number of soil layers (1 or 2)			X
	8		Shape factor; Generally =1, for vertical soil layers			X
4	1-5		Equivalent fractions for Ca, Mg, Na, K, and total base saturation for soil layer one			X
5	1-5		Equivalent fractions for Ca, Mg, Na, K, and total base saturation for soil layer two			X
6-17	1		Percentage of annual average streamflow for each month (Calculated from TOPMODEL output or hydrograph)			X
	2		Percentage of total annual precipitation for each month (Calculated from precipitation time series data)			X
	3		Overland flow for each month, % (Calculated from TOPMODEL output of daily overland flow)		X	
	4		Macroflow for each month, % (TOPMODEL optimization parameter)		X	

Appendix A (cont'd)

Line #	Column	Description	Units	Optimized	Measured
5		Horizontal drainage for each month, % (Calculated from TOPMODEL output of average saturation deficit and depth of soil layers)		X	
18	1	Annual average streamflow for year (must be 100%)			X
	2	Annual average precipitation per year (must be 100%)			X
	3	Annual average overland flow, % (Calculated from TOPMODEL output of daily overland flow)			X
	4	Annual average macropore flow, % (TOPMODEL optimization parameter)		X	
	5	Annual average horizontal drainage, % (Calculated from TOPMODEL output of average saturation deficit and soil depths)			X
<u>Deposition Chemistry</u>					
A.2	19-27	Concentrations in order Ca, Mg, Na, K, NH ₄ , SO ₄ , Cl, NO ₃ , and F	meq.m ⁻³		X
	1	Concentration in background precipitation			X
	2	Concentration in present day precipitation			X
	3	Dry deposition factor for background year			X
	4	Dry deposition factor for present day			X
<u>Soil Data</u>					
	28-41	Soil depths for layers 1 and 2	m		X
	1-2	Porosity for layers 1 and 2, fraction			X
	1-2	Bulk density for layers 1 and 2	kg.m ⁻³		X
	1-2	Cation exchange capacity for layers 1 and 2	meq.kg ⁻¹		X
	1-2	Sulfate half saturation concentration for layers 1 and 2	meq.m ⁻³	X	
	1-2	Sulfate maximum adsorption capacity for layers 1 and 2	meq.kg ⁻¹	X	
	1-2	Solubility product for gibbsite			X
	1-2	Selectivity coefficient for Al-Ca exchange for layers 1 and 2			X
	1-2	Selectivity coefficient for Al-Mg exchange for layers 1 and 2			X
	1-2	Selectivity coefficient for Al-Na exchange for layers 1 and 2			X
	1-2	Selectivity coefficient for Al-K exchange for layers 1 and 2			X
	1-2	Total organic acid in layers 1 and 2	mmol.m ⁻³		X

Appendix A (contd)

Line #	Column	Description	Units	Optimized	Measured
1-2		Logarithm of first acidity constant for organic acid in layers 1 and 2			X
1-2		Logarithm of second acidity constant for organic acid in layers 1 and 2			X
<u>Stream/Lake Parameters</u>					
42-48	1	Lake retention time	yr		X
	2	Lake area normalized to total watershed area			X
	3	Solubility product for gibbsite in stream/lake			X
	4	Total organic acid in stream/lake			X
	5	Logarithm of first acidity constant for organic acid in stream/lake			X
	6	Logarithm of second acidity constant for organic acid in stream/lake			X
<u>Uptake and Weathering Rates</u>					
49-66		Rates in order Ca, Mg, Na, K, NH ₄ , SO ₄ , Cl, NO ₃ , and F Soil layer 1, lines 49-57; layer 2, lines 58-66			
	1	Background uptake rate in starting year of hindcast, % of total amount		X	
	2	Present day uptake rate, % of total amount		X	
	3	Background weathering rate		X	
	4	Present day weathering rate		X	
	5	Fractional dependence of weathering rate in hydrogen ion concentration		X	
	6	Weathering rate constant for background year		X	
67-75	1	Background uptake rates in stream/lake, % of total amount			
	2	Present uptake rates in stream/lake, % of total amount			
75-87	1	Percent of total annual uptake occurring in each month in soil layer 1			
	2	Percent of total annual uptake occurring in each month in soil layer 2			
	3	Percent of total annual uptake occurring in each month in stream/lake			
88	1-3	Sum of monthly uptake rates (must equal 100%)			

Appendix A (contd)

Line #	Column	Description	Units	Optimized	Measured
<u>Additional Soil and Lake Data</u>					
89-100	1	Average monthly temperature in soil layer 1	°C		X
	2	Average monthly temperature in soil layer 2	°C		X
	3	Average monthly temperature in stream/lake	°C		X
101	1-3	Annual mean temperature in soil layer 1, layer 2, and stream/lake	°C		X
102-113	1-3	Monthly partial pressure of carbon dioxide in soil layer 1, layer 2, and stream/lake	atm.	X	
114	1-3	Annual average partial pressure of carbon dioxide in soil layer 1 (up to 100 times atmospheric), layer 2 (up to 40 times atmospheric), and stream/lake (generally 2 times atmospheric)		X	
<u>Factors for Scaling Hindcast Deposition Rates to Present Day</u>					
115-124		Deposition sequence name and scaling factors for chemical constituents in deposition			
125-end	1-5	Deposition ramps and ramp factors for wet and dry deposition and soil and lake uptake rates			

Appendix A (contd)

2. ETD Model Input Data Required (from Nikolaidis 1987).

Variable Name	Description	Units	Optimized	Measured
<u>Watershed hydrological and kinetic data</u>				
ALF1	Correction factor of the hydraulic gradient for lake seepage		X	
ALF2	Correction factor of the hydraulic gradient for the groundwater seepage		X	
AREA	Lake area	m ²		X
AREATT	Terrestrial area	m ²		X
BETA	Snowmelt fraction that flows to lake late due to land slope		X	
BL(1)	Lower limit of BETA			X
BU(1)	Upper limit of BETA			X
CBDRY	Groundwater zone conductivity	m-day ⁻¹		X
CBED	Hydraulic conductivity of lake bed	m-day ⁻¹		X
CF	Concentration factor for dissolved constituents in snowmelt		X	
CG	Bare ground frost coefficient			X
CS	Reduction in frost coefficient			X
CT	Thaw coefficient			X
D1	Fraction of surface water perimeter that recharges the lake		X	
DAY#	Initial Julian day of simulation			X
DEP3	Depth of soil zone			X
DEP4	Depth of unsaturated zone			X
DEPBR	Depth to bedrock			X
DIST	Characteristic distance of flow path in watershed			X
FI1	Initial frost index	°C		X
FIL	Limiting frost index	°C		X
FRAX	Fraction of transpiration from the unsaturated soil zone		X	
HC	Daily thaw rate	°C		X
HEI2	Initial equivalent water depth of snow			X
HEI3	Initial equivalent water depth of soil			X
HEI4	Initial equivalent water depth of unsaturated zone			X
HEI5	Initial equivalent water depth of lake			X
HEI6	Initial equivalent water depth of groundwater zone			X

Appendix A (contd)

Variable Name	Description	Units	Optimized	Measured
HR4	Reference H ⁺ concentration for unsaturated zone	meq·m ⁻³	X	
HR5	Reference H ⁺ concentration for lake	meq·m ⁻³	X	
HR6	Reference H ⁺ concentration for groundwater zone	meq·m ⁻³	X	
K	Rate constant for sulfate reduction	day ⁻¹	X	
KAPPA	Snow melt rate	in·day ⁻¹ ·°C ⁻¹	X	
KB	Transpiration coefficient	in·day ⁻¹		X
KH4	Hydrolysis rate constant for the unsaturated soil zone	eq·m ⁻² ·day ⁻¹	X	
KH5	Hydrolysis rate constant for the lake	eq·m ⁻² ·day ⁻¹	X	
KH6	Hydrolysis rate constant for the groundwater zone	eq·m ⁻² ·day ⁻¹	X	
KHL	Horizontal permeability of unsaturated zone			X
KHU	Horizontal permeability of soil			X
KLAT3	Lateral flow correction coefficient for soil		X	
KLAT4	Lateral flow correction coefficient for unsaturated soil zone		X	
K04	Rate constant for ligand attack for unsaturated zone	eq·m ⁻² ·day ⁻¹	X	
K05	Rate constant for ligand attack for lake	eq·m ⁻² ·day ⁻¹	X	
K06	Rate constant for ligand attack for groundwater zone	eq·m ⁻² ·day ⁻¹	X	
KP3	Partitioning coefficient for sulfate in soil		X	
KP4	Partitioning coefficient for sulfate in unsaturated zone		X	
KP6	Partitioning coefficient for sulfate in groundwater zone		X	
KPAN2	Pan correction coefficient for snow		X	
KPAN3	Pan correction coefficient for soil		X	
KPAN5	Pan correction coefficient for lake		X	
KPERC3	Vertical hydraulic conductivity coefficient for soil		X	
KPERC4	Vertical hydraulic conductivity coefficient for unsaturated soil zone		X	
KVL	Vertical permeability of unsaturated zone			X
KVU	Vertical permeability of soil			X
M3	Bulk density of soil	kg·m ⁻³		X
M4	Bulk density of unsaturated zone	kg·m ⁻³		X
M6	Bulk density of soil in groundwater zone			X
MC4	Fractional order dependence of hydrolysis rate for unsaturated zone			X
MC5	Fractional order dependence of hydrolysis rate for lake sediments			X
MC6	Fractional order dependence of hydrolysis rate for groundwater zone			X

Appendix A (contd)

Variable Name	Description	Units	Optimized	Measured
NDAYS	Duration of simulation	days		X
PC02	Partial pressure of atmospheric CO ₂ (g)	atm.		X
PERIC	Catchment perimeter	m		X
PERIL	Lake perimeter	m		X
PORE3	Effective porosity of soil zone			X
PORE4	Effective porosity of unsaturated zone			X
PORE6	Effective porosity of groundwater zone			X
QA4	Flow rate through unsaturated zone	m ³ .day ⁻¹		X
QA5	Flow rate through lake sediments	m ³ .day ⁻¹		X
QA6	Flow rate through groundwater zone	m ³ .day ⁻¹		X
QAR4	Reference flow rate through unsaturated zone	m ³ .day ⁻¹		X
QAR5	Reference flow rate through lake sediments	m ³ .day ⁻¹		X
QAR6	Reference flow rate through groundwater zone	m ³ .day ⁻¹		X
QC4	Fractional order dependence on flow rate for unsaturated zone			X
QC5	Fractional order dependence on flow rate for lake sediments			X
QC6	Fractional order dependence on flow rate for groundwater zone			X
R3	Base depletion in soil zone			X
RE3	Ion exchange reaction rate coefficient for soil zone	meq.kg ⁻¹		X
RQ3	Sum of bases in soil zone	m ³ .eq ⁻¹ .day ⁻¹	X	
SA4	Effective surface area of unsaturated zone	meq.kg ⁻¹		X
SA5	Effective surface area of sediments in lake	m ² .kg ⁻¹		X
SA6	Effective surface area of groundwater zone	m ² .kg ⁻¹		X
SAR4	Reference effective surface area of unsaturated zone	m ² .kg ⁻¹		X
SAR5	Reference effective surface area of lake sediments	m ² .kg ⁻¹		X
SAR6	Reference effective surface area of groundwater zone	m ² .kg ⁻¹		X
SBE	Stream bed elevation	m		X
SC4	Surface area fractional order rate constant for unsaturated zone			X
SC5	Surface area fractional order rate constant for lake sediments			X
SC6	Surface area fractional order rate constant for groundwater zone			X
SLOPE	Average slope of watershed			X
SPAN	Span of requested output intervals	days		X
SUPERX	Level of CO ₂ (g) supersaturation of lake water			X

Appendix A (contd)

Variable Name	Description	Units	Optimized	Measured
THETA	Temperature switch for sulfate reduction in lake	°C	X	X
YEAR0	Initial year of simulation			
<u>Watershed solution chemistry</u>				
A2	Initial alkalinity of snow	meq.m ⁻³		X
A3	Initial alkalinity of soil	meq.m ⁻³		X
A4	Initial alkalinity of unsaturated zone	meq.m ⁻³		X
A5	Initial alkalinity of lake	meq.m ⁻³		X
A6	Initial alkalinity of groundwater zone	meq.m ⁻³		X
C2	Initial chloride concentration in snow	meq.m ⁻³		X
C3	Initial chloride concentration in soil	meq.m ⁻³		X
C4	Initial chloride concentration in unsaturated zone	meq.m ⁻³		X
C5	Initial chloride concentration in lake	meq.m ⁻³		X
C6	Initial chloride concentration in groundwater zone	meq.m ⁻³		X
S2	Initial sulfate concentration in snow	meq.m ⁻³		X
S3	Initial sulfate concentration in soil	meq.m ⁻³		X
S4	Initial sulfate concentration in unsaturated zone	meq.m ⁻³		X
S5	Initial sulfate concentration in lake	meq.m ⁻³		X
S6	Initial sulfate concentration in groundwater	meq.m ⁻³		X
<u>Monthly meteorological data</u>				
PDAY1-PDAY12	Mean percent of monthly daylight hours			X
TMI-TM12	Mean monthly temperatures	°C		X
<u>Daily meteorological data</u>				
AD	Alkalinity of dryfall	meq.m ⁻²		X
EVAP	Evaporation amount	mm.day ⁻¹		X
PREC	Precipitation amount	mm.day ⁻¹		X
TEMP	Atmospheric temperature	°C		X

Appendix A (contd)

Variable Name	Description	Units	Optimized	Measured
TOC	Total organic carbon in precipitation	mg.l ⁻³		X
TSPAN	Span in meteorological input data	day		X
XA	Alkalinity of precipitation	mg.l ⁻³		X
XC	Chloride in precipitation	mg.l ⁻³		X
XS	Sulfate in precipitation	mg.l ⁻³		X

Appendix A (contd)

3. ILWAS Model Input Data Required (Parentheses after variable names indicate sizes of arrays. Parentheses after descriptions indicate suggested ranges [from Gherini et al. 1983].)

Variable Name	Description	Units	Optimized	Measured
<u>CONTROL VARIABLES (Input File 1)</u>				
<u>Simulation Identification</u>				
NAMERN	Identification name and information			
<u>Controls for Simulation and Data Reads</u>				
CANOPY	ON/OFF switch for canopy simulation			
CHANEL	ON/OFF switch for stream simulation			
CHECKS	ON/OFF switch for checking input data consistency			
LAKBIO	ON/OFF switch for lake biological simulation			
LAKEQ	ON/OFF switch for lake quality simulation			
LAKES	ON/OFF switch for lake simulation			
NLDOPS	Number of loops to repeat time-varying input data			
RCHANL	ON/OFF switch for stream data read			
RCNOPY	ON/OFF switch for canopy data read			
RIVERQ	ON/OFF switch for river quality simulation			
RLAKEQ	ON/OFF switch for lake quality data read			
RLAKES	ON/OFF switch for lake data read			
RRIVERQ	ON/OFF switch for river quality data read			
RSNOWQ	ON/OFF switch for snow quality data read			
RSNOWS	ON/OFF switch for snow hydrologic read			
RSOILQ	ON/OFF switch for soil quality data read			
RSOILT	ON/OFF switch for reading soil temperature data			
SNOWQ	ON/OFF switch for snow quality simulation			
SNOWS	ON/OFF switch for snow hydrologic simulation			
SOILQ	ON/OFF switch for soil quality simulation			

Appendix A (contd)

Variable Name	Description	Units	Optimized	Measured
<u>Print Options</u>				
IPRINT	Options for summary output, i.e., YEAR, MNTH, DAY, STEP, OFF			
JPRINT	ON/OFF switch for cycle chart outputs			
PLOTS	ON/OFF switch for requesting plot files			
<u>Simulation Period</u>				
BDAY	Beginning day of simulation			
BMNTH	Beginning month of simulation			
BYEAR	Beginning year of simulation			
EDAY	Ending day of simulation			
EMNTH	Ending month of simulation			
EYEAR	Ending year of simulation			
IYRREG	Julian day to begin hydrologic year			
<u>System Sizes</u>				
LAKCAT	Number of subcatchments adjacent to lake			
NCATCH	Number of subcatchments (1-20)			
NSEG	Number of stream segments (0-10)			
PERDAY	Time steps per day (1)			
<u>File Definition</u>				
MUNIT	File unit number for detailed hydrologic and chemistry summaries			
RHUNIT	File unit number for lake watershed data			
RMUNIT	File unit number for meteorological data			
RQUNIT	File unit number for rate coefficients			
RSUNIT	File unit number for precipitation and air chemistry			

Appendix A (contd)

Variable Name	Description	Units	Optimized	Measured
<u>Variable Manipulations for Plot Files (If PLOTS = ON)</u>				
IOPVAR	Variable identification for operation			
KP	Constituent name			
LM	Tributary number			
MOPN	Options for concentrations, i.e., VSUM, MULT, SBTR, DIVD, CHGS, CLOG, CONC, PCON, CALC			
MP	Soil layer number			
NAMEPL	Identification name for plot			
NOPNS	Number of mathematical operations			
NP	Lake element number			
NVAR	Number of variables to operate on			
PCONST	Constant for operation (if IOPVAR = CNST)			
POPNDX	Segment identification (prefix L for land subcatchment and R for river segment)			
<u>Plot File Content</u>				
IPLVAR	Variable identification name			
KPL	Constituent name			
LM	Tributary number			
LPL	Soil layer number			
LPUNIT	Unit number for plot file			
MPLT	Plot option: TSER for time series, TCUM for cumulative			
NFILES	Number of plot files (0-9)			
NPL	Lake element number			
NPLOTS	Number of files to be plotted (0-12)			
PLNDEX	Segment identification name (prefix L for land subcatchment and R for river segment)			
<u>Chemistry Output Control (If JPRINT = ON)</u>				
CPRINT	Option for cycle chart, i.e., OFF, STEP, DAY, MNTH, or YEAR			
DPRINT	Option for chemistry summary, i.e., OFF, STEP, DAY, MNTH, or YEAR			
ICYCLE	Constituents of cycle charts (18 ions maximum)			

Appendix A (contd)

Variable Name	Description	Units	Optimized	Measured
NCYCLE	Number of cycle charts			
NDTAIL	Option for output details, i.e., PART or FULL			
<u>LAKE-WATERSHED DATA (Input File 2)</u>				
<u>Interception and Evaporation Data</u>				
CIIMAX	Maximum coniferous canopy storage (0-0.3)	cm		X
DIIMAX	Maximum deciduous canopy storage (0-0.3)	cm		X
ECOEFF	Calibration parameter to adjust annual evaporation up (>1) or down (<1)		X	
LAIC(12)	Monthly coniferous canopy leaf index	cm ² .cm ⁻²		X
LAI0(12)	Monthly deciduous canopy leaf index	cm ² .cm ⁻²		X
LAI0(12)	Monthly open area leaf index	cm ² .cm ⁻²		X
OIMAX	Maximum open area interception storage (0-0.3)	cm		X
RH(12)	Mean monthly relative humidity (0-100)	%		X
WSCF	Wind speed amplification factor over the lake surface (1-3)			X
XLAT	Latitude of basin			X
XLON	Longitude of basin			X
<u>Subcatchment Data</u>				
BELVY	Average basin elevation	m		X
TAREA	Total basin area including lake	m ²		X
Data below are repeated for each subcatchment up to NCATCH subcatchments				
ASPECT	Aspect of subcatchment, degrees clockwise from north			X
DTSMAX	Average surface depression storage	cm		X
LAYERS	Number of soil layers in subcatchment			X
NN	Manning's n for overland flow (0.1-0.6)		X	
PCCONF	Percent coniferous canopy			X
PCDECD	Percent deciduous canopy			X

Appendix A (contd)

Variable Name	Description	Units	Optimized	Measured
PCOPEN	Percent unforested area			X
PRECWT	Precipitation weighting factor for subcatchment (0.0-1.3)			X
SCATCH	Subcatchment number			X
SCNDTH	Mean width	m		X
SSLOPE	Average surface slope	m·m ⁻¹		X
Data below are repeated for each soil layer for up to LAYERS times.				
ETWGT	Fraction of root distribution for soil layer (0-1)			X
PERM	Horizontal permeability (10 ¹ - 10 ⁸)	cm·day ⁻¹	X	
SCAREA	Surface area of the soil layer	m ²		X
SMI	Vertical permeability (10 ² - 10 ⁸)		X	
SOLTMP	Initial soil temperature	°C		X
THEFC	Field capacity (0-0.4)		X	
THETA	Initial soil moisture content (0-0.6)			X
THETS	Saturation moisture content (0.1-0.6)			X
THICK	Thickness of soil layer	cm		X
<u>Stream Data</u>				
NAMECH	Identification name			
Data below are repeated for each stream segment for up to NSEG times				
CONECR(2)	Upstream segment numbers (0-2)			X
CONECL(13)	Tributary subcatchment numbers (0-13)			X
DEPTH	Initial water depth	m		X
KR	Muskingum routing coefficient (1.0 - 102.3)	day		X
KX	Muskingum routing coefficient (0 - 0.5)	day		X
LENGTH	Length of river segment	m		X
RIVSEG	Stream segment number			X
SELEV1	Upstream bed elevation	m		X

Appendix A (contd)

Variable Name	Description	Units	Optimized	Measured
SELEV2	Downstream bed elevation	m		X
STGSAR(10)	Ten pairs of stage-surface area values	m ²		X
STW	Initial stream temperature	°C		X
<u>Lake Data</u>				
A1	Empirical coefficient to calculate diffusion as a function of wind speed			X
A2	Empirical coefficient to calculate diffusion as a function of wind speed			X
A3	Empirical coefficient to calculate diffusion as a function of wind speed			X
AREA	Lake surface area	m ²		X
CKTICE	Fraction of solutes retained in ice (θ.1)			X
CONECL(13)	Tributary subcatchments			X
CONECR(2)	Tributary stream segments (θ-2)			X
CONICE	Thermal conductivity of ice (θ.005)	cal.cm ⁻¹ .sec ⁻¹ .°C ⁻¹		X
D1	Lake elevation	m		X
DEPICE	Initial ice cover			X
DEPTH	Average lake depth	m		X
EDMAX	Secchi disc depth	m		X
ELMAX	Maximum lake elevation	m		X
ELMIN	Minimum lake elevation	m		X
ELOUT	Lake outlet elevation	m		X
GMIN	Minimum negative density gradient for lake mixing (θ.θ)	kg.m ⁻⁴		X
GSHW	Minimum diffusion coefficient	kg.m ⁻⁴		X
	Water column critical method	kg.m ⁻⁴		X
	Wind method	m ² .sec ⁻¹		X
NAMELA	Identification name			X
OUTMAX	Maximum flow rate at lake outlet	m ³ .sec ⁻¹		X
RIVSEG	Stream segment number			X
RT	Effective length of lake	m		X
SDZ	Lake element thickness (θ.2-1)	m		X
SELEV	Initial lake surface elevation	m		X
STGL0(21)	Pairs of stage-flow relationships	m ³ .sec ⁻¹		X

Appendix A (contd)

Variable Name	Description	Units	Optimized	Measured
VOL	Lake volume below ELMIN	m ³		X
WIDTH	Width of lake where the flow field is dominated by lake outlet	m		X
WOUT	Width of lake outlet	m		X
XQDEP	Depth at which XQPCT absorption occurs (0.1-1.0)	m		X
XQPCT	Fraction of solar radiation absorbed in XQDEP depth (0.1-0.9)			X
Physical data for each lake layer, D and AR2				
AR2	Surface area	m ²		X
D	Depth	m		X
IDEM	1 for wet bulb temperature, 0 for dew point temperature			X
PRECWT	Precipitation weighting factor for lake (0.0-1.3)			X
TEMP	Initial lake temperature	°C		X
TURB	Atmospheric turbidity (2-5)			X
<u>Snowpack Data</u>				
FSMRAT	Forested area snowmelt rate coefficient (0.05-0.1)	cm·C·day ⁻¹	X	
NAMESN	Identification name			
OSMRAT	Open area snowmelt rate coefficient (0.05-0.1)	cm·C·day ⁻¹	X	
PCSTOR	Moisture field capacity of snowpack	%		X
SNODEP	Initial snow depth	cm of water		X
SNOSBF	Forested area snow sublimation rate (0.005)	cm·day ⁻¹		X
SNOSBO	Open area snow sublimation rate (0.005)	cm·day ⁻¹		X
SNOTMP	Temperature below which precipitation is snow	°C	X	
<u>RATE COEFFICIENT DATA (Input File 3)</u>				
<u>Coefficients for Canopy Processes</u>				
ACCC(18)	Initial coniferous canopy accumulation of 18 ions	meq		X
ACCD(18)	Initial deciduous canopy accumulation of 18 ions	meq		X

Appendix A (contd)

Variable Name	Description	Units	Optimized	Measured
ACCO(18)	Initial open area canopy accumulation of 18 ions	meq		X
BETAC(12)	Monthly coniferous foliar exudation rate	day ⁻¹	X	
BETAD(12)	Monthly deciduous foliar exudation rate	day ⁻¹	X	
BETA0(12)	Monthly open area foliar exudation rate	day ⁻¹	X	
CHEIGT	Height of coniferous canopy	m		X
COLLEFC(2)	Coniferous canopy collection efficiencies for wet and dry surfaces		X	X
COLLEFD(2)	Deciduous canopy collection efficiencies for wet and dry surfaces		X	X
COLLEF0(2)	Open area canopy collection efficiencies for wet and dry surfaces		X	X
DEFFAC(18)	Dry deposition factors for loading adjustment for 18 ions		X	X
DHEIGT	Height of deciduous canopy	m		X
EXCAMP(18)	Coniferous foliar exudation amplification factor for 18 ions		X	
EXDAMP(18)	Deciduous foliar exudation amplification factor for 18 ions		X	
EXOAMP(18)	Open area foliar exudation amplification factor for 18 ions		X	
FLRIDE	Fluoride concentration	µg·L ⁻¹		X
GASDV(12)	Monthly gas deposition velocities (θ-θ.5)	cm·sec ⁻¹		X
GASUV(12)	Monthly NO ₂ (g) and SO ₂ (g) deposition velocities (θ-θ.5)	cm·sec ⁻¹		X
GFLD, GFLE	Growth factor for deciduous (GFLE), coniferous (GFLC), and open (GFLO) areas (-1 or 1)			X
GFL0	Coniferous long-term growth coefficient (1.0-1.2)			X
GROWC	Deciduous long-term growth coefficient (1.0-1.2)			X
GROWD	Open area long-term growth coefficient (1.0-1.2)			X
GROW0	ON: Internal calculation of deposition velocity OFF: Deposition velocity from input	yr ⁻¹		X
IVDGAS	Monthly coniferous litter fall rate	yr ⁻¹		X
LFC(12)	Coniferous leaf composition (18 constituents)(a)	kg·m ⁻² ·mth ⁻¹		X
LFCMPC(18)	Deciduous leaf composition (18 constituents)(a)	mg·g ⁻¹		X
LFCMPD(18)	Open area leaf composition (18 constituents)(a)	mg·g ⁻¹		X
LFCMP0(18)	Open area leaf composition (18 constituents)(a)	mg·g ⁻¹		X
LFD(12)	Monthly deciduous litter fall rate	kg·m ⁻² ·mth ⁻¹		X
LFD0(12)	Monthly open area litter fall rate	kg·m ⁻² ·mth ⁻¹		X
NAMECA	Identification name			X
OHEIGT	Height of open area canopy	m		X
PARTDV(12)	Monthly deposition velocity of particles (θ.2-θ.8)	cm·sec ⁻¹		X

Appendix A (contd)

Variable Name	Description	Units	Optimized	Measured
PRODD, PRODC,	Annual productivity for deciduous (PRODD), coniferous (PRODC), and			
PRODD	open (PRODD) areas (0-1.2)	kg·m ⁻² ·yr ⁻¹		X
RESPCM	Coniferous maintenance respiration rate	day ⁻¹	X	
RESPDM	Deciduous maintenance respiration rate	day ⁻¹	X	
RESPOM	Open area maintenance respiration rate	day ⁻¹	X	
STAND	Standing biomass (10-25)	kg·m ⁻²		X
TRCMPD(18)	Coniferous trunk composition (18 constituents)	mg·g ⁻¹		X
TRCMPD(18)	Deciduous trunk composition (18 constituents)	mg·g ⁻¹		X
TRCMPD(18)	Open area trunk composition (18 constituents)	mg·g ⁻¹		X
UDISTD(12)	Monthly uptake of coniferous trees	fraction·yr ⁻¹	X	
UDISTD(12)	Monthly uptake of deciduous trees	fraction·yr ⁻¹	X	
UDISTD(12)	Monthly uptake of open area	fraction·yr ⁻¹	X	
VNIH4	Nitrification rate in canopy (0.4)	day ⁻¹		X
ZHEIGT	Height of wind speed measurement	m		X
<u>Coefficients for Snowmelt Processes</u>				
CKMELT	Snowmelt leaching coefficient (0-4.0)		X	
NAMESQ	Identification name			
SNOTON(18)	Initial ion concentrations in snowpack	meq·L ⁻¹		X
<u>Coefficients for Soil Processes</u>				
ADSCAT(18)	Adsorbed ions (18 constituents) (a)			X
	Cations			
	Anions			
CEC	Cation exchange capacity	% CEC		
CKEA(5)	Cation exchange coefficient for H ⁺ in each soil layer	meq·100 g ⁻¹		X
CKDAL	Gibbsite solubilization rate constant (0.000001) (See also MALDH3, pg. B.17.)	meq·100 g ⁻¹		X
CKEMG(5)	Cation exchange coefficient for Mg in each soil layer	day ⁻¹	X	
CKENA(5)	Cation exchange coefficient for Na in each soil layer		X	
CKENH4(5)	Cation exchange coefficient for NH ₄ in each soil layer		X	

Appendix A (contd)

Variable Name	Description	Units	Optimized	Measured
CKFA0(5)	Anion adsorption coefficient for organic acid in each soil layer	L.kg ⁻¹	X	
CKMNR(5)	Weathering rate of minerals for each soil layer	yr ⁻¹	X	
CKP0(5)	Anion adsorption coefficient for phosphate in each soil layer	L.kg ⁻¹	X	
CKS0(5)	Anion adsorption coefficient for sulfate in each soil layer	L.kg ⁻¹	X	
CKVNH4	Specific nitrification rate (0.1)	day ⁻¹	X	
DNSITY	Soil density	g.cm ⁻³		X
FINES	Weight fraction of fine litter in top soil layer (0.10-0.20)			X
FBRATE	Fine-litter-to-humus breakdown rate (0.05)	yr ⁻¹	X	
FRLCH1	Fraction of leachable ions in litterfall (0-0.2)		X	
FRLCH2	Fraction of sulfate and ammonia that goes to soil solution when fine litter decomposes to humus (0.2-0.7)		X	
FRLCH3	Fraction of sulfate and ammonia that forms organic acid during humus decay (0.2-0.7)		X	
LBRATE	Litter breakdown rate (1-2)	yr ⁻¹	X	
MINERL	Four-letter mineral name abbreviation			
MNMWT	Mineral molecular weight	g.mol ⁻¹	X	
MNWT(18)	Weathered mineral reaction product, weathered	meq.mol ⁻¹	X	
NALOH3	Options for gibbsite dissolution, 1 for equilibrium with gibbsite, 2 for mass action limited rates		X	
NAME5Q	Identification name			
NMRLS	Number of dissolving soil minerals (1-6)			X
0A1C	Amount of C in organic acid (4.0-8.0)	eq C.eq acid ⁻¹	X	
0A1N	Amount of N in organic acid (0.05-0.20)	eq N.eq acid ⁻¹	X	
0A1S	Amount of S in organic acid (0.01-0.10)	eq S.eq acid ⁻¹	X	
0ARATE	Organic acid breakdown rate (0.05)	yr ⁻¹	X	
SLCOMP(5)	Percent dissolution by weight of minerals	%	X	
SOLION(18)	Dissolved ions in soil solution (18 constituents)(a)	meq.L ⁻¹	X	
TORT	Soil tortuosity		X	
WEXP(5)	Weathering rate dependence on H ⁺ ion for NMRLS (0.3-0.7)		X	
XLIT	Weight fraction of litter in top soil layer (0.005-0.010)		X	

Appendix A (contd)

Variable Name	Description	Units	Optimized	Measured
<u>Coefficients for River Processes</u>				
NAMERQ	Identification name			
SCONC(18)	Concentrations of 18 ions in river segments			X
<u>Coefficients for Lake Processes</u>				
CKDAL2	Gibbsite dissolution rate constant in lake		X	
DKRAT(2)	Decay rate of fulvic acid and nitrification in lake	day ⁻¹	X	
LAKION(18)	Concentrations of 18 ions in lake			X
MQSWZT	Option of ME for meq-L ⁻¹ or MG for mg-L ⁻¹			
NALOH3	Option for gibbsite dissolution in lake; 1 for equilibrium with gibbsite, 2 for mass action limited dissolution rate, and 3 for precipitation only		X	
NAMELQ	Identification name			
PRMPRD(12)	Primary productivity for each month	µg C·m ⁻² ·day ⁻¹	X	
<u>METEOROLOGICAL DATA (Input File 4)</u>				
<u>Daily Meteorological Data</u>				
AP	Atmospheric pressure	mbar		X
C	Fraction cloud cover			X
DP	Dew point or wet bulb temperature	°C		X
ID	Day			
IM	Month			
IY	Year			
PRECIP	Precipitation	cm		X
TMIN	Minimum air temperature	°C		X
TMAX	Maximum air temperature	°C		X
WIN	Wind speed	m·sec ⁻¹		X

Appendix A (contd)

Variable Name	Description	Units	Optimized	Measured
PRECIPITATION AND AIR QUALITY DATA (Input File 5)				
Precipitation and Air Chemistry				
AIRQ(18)	Concentrations of 18 constituents in air (air quality)(a)			X
ID	Day			
IM	Month			
IY	Year			
MASWZT	ME for $\mu\text{eq}\cdot\text{m}^{-3}$ or MG for $\mu\text{g}\cdot\text{m}^{-3}$			
MPSWZT	ME for $\text{eq}\cdot\text{L}^{-1}$ or MG for $\text{mg}\cdot\text{L}^{-1}$			
RAINQ(18)	Concentrations of 18 constituents in wet precipitation(a)			X

(a) The 18 constituents are SO_2 , NO_x , H^+ , NH_4^+ , Al_{monomeric}, Ca^{2+} , Mg^{2+} , K^+ , Na^+ , SO_4^{2-} , NO_3^- , Cl^- , F^- , $\text{H}_3\text{-n}(\text{PO}_4)^{n-}$, alkalinity, total inorganic carbon, H_4SiO_4 , and organic acids.

APPENDIX B

ANNUAL-AVERAGE FLOW-WEIGHTED ANC BUDGETS FROM
MAGIC CODE FORECASTS FOR CLEAR POND, PANTHER LAKE,
AND WOODS LAKE WATERSHEDS

APPENDIX B

ANNUAL-AVERAGE FLOW-WEIGHTED ANC BUDGETS FROM MAGIC CODE FORECASTS
FOR CLEAR POND, PANTHER LAKE, AND WOODS LAKE WATERSHEDS

TABLE B.1. MAGIC Code, 1982-1984 Average ANC Budgets for Panther Lake: Base-Case, $\pm 20\%$ Type-A, and $\pm 20\%$ Type-B Deposition Scenarios. Acid Dependent Weathering Coefficient = 0.0 ($\text{meq}\cdot\text{m}^{-2}\cdot\text{yr}^{-1}$ of terrestrial area)

	Deposition Scenarios				
	Base Case	-20% Type-A	+20% Type-A	-20% Type-B	+20% Type-B
<u>Atmospheric Inputs</u>					
<u>Terrestrial/Lake</u>					
Wet	-105.4	-92.6	-118.2	-98.5	-112.4
Dry	0.0	0.0	0.0	0.0	0.0
Net	-105.4	-92.6	-118.2	-98.5	-112.4
<u>Internal Sources</u>					
<u>Soil Solution</u>					
NH ₄ Uptake (nitrification)	-12.9	-12.9	-12.9	-12.0	-13.7
NO ₃ Uptake (nitrate reduction)	17.7	16.5	18.8	16.5	18.8
Net	4.8	3.6	5.9	4.5	5.1
<u>Soil Processes</u>					
Cation Exchange	33.1	33.1	33.3	36.6	29.8
SO ₄ Adsorption	27.5	20.0	35.0	20.0	35.0
Weathering	139.0	139.0	139.0	139.0	139.0
Net	199.7	192.0	207.3	195.5	203.8
<u>Lake</u>					
NH ₄ Uptake (nitrification)	-15.1	-15.1	-15.1	-14.1	-16.2
NO ₃ Uptake (nitrate reduction)	23.3	20.3	26.4	20.3	26.4
SO ₄ Reduction	0.0	0.0	0.0	0.0	0.0
Net	8.2	5.2	11.3	6.2	10.2
Sum of Internal Sources	212.7	200.8	224.6	206.2	219.1
Basin Output	107.3	108.2	106.4	107.8	106.7
Atm Input + Internal Sources	107.3	108.2	106.4	107.8	106.7
Total Al Outflow from Basin	3.9	3.9	3.9	3.9	3.9

TABLE B.2. MAGIC Code, 1982-1984 Average ANC Budgets for Panther Lake: Base-Case, $\pm 20\%$ Type-A, and $\pm 20\%$ Type-B Deposition Scenarios. Acid Dependent Weathering Coefficient = 0.5 ($\text{meq}\cdot\text{m}^{-2}\cdot\text{yr}^{-1}$ of terrestrial area)

	Deposition Scenarios				
	<u>Base Case</u>	<u>-20% Type-A</u>	<u>+20% Type-A</u>	<u>-20% Type-B</u>	<u>+20% Type-B</u>
<u>Atmospheric Inputs</u>					
<u>Terrestrial/Lake</u>					
Wet	-105.4	-92.6	-118.2	-98.5	-112.4
Dry	0.0	0.0	0.0	0.0	0.0
Net	-105.4	-92.6	-118.2	-98.5	-112.4
<u>Internal Sources</u>					
<u>Soil Solution</u>					
NH ₄ Uptake (nitrification)	-12.9	-12.9	-12.9	-12.0	-13.7
NO ₃ Uptake (nitrate reduction)	17.7	16.5	18.8	16.5	18.8
Net	4.8	3.6	5.9	4.5	5.1
<u>Soil Processes</u>					
Cation Exchange	21.2	21.1	21.3	24.6	17.6
SO ₄ Adsorption	27.5	20.0	35.0	20.0	35.0
Weathering	151.1	151.1	151.2	151.1	151.2
Net	199.8	192.2	207.5	195.7	203.8
<u>Lake</u>					
NH ₄ Uptake (nitrification)	-15.1	-15.1	-15.1	-14.1	-16.2
NO ₃ Uptake (nitrate reduction)	23.3	20.3	26.4	20.3	26.4
SO ₄ Reduction	0.0	0.0	0.0	0.0	0.0
Net	8.2	5.2	11.3	6.2	10.2
Sum of Internal Sources	212.8	201.0	224.7	206.4	219.1
Basin Output	107.4	108.3	106.5	107.9	106.7
Atm Input + Internal Sources	107.4	108.3	106.5	107.9	106.7
Total Al Outflow from Basin	3.9	3.9	3.9	3.9	3.9

TABLE B.3. MAGIC Code, 1991-1993 Average ANC Budgets for Panther Lake: Base-Case, ±20% Type-A, and ±20% Type-B Deposition Scenarios. Acid Dependent Weathering Coefficient = 0.0 (meq•m⁻²•yr⁻¹ of terrestrial area)

	Deposition Scenarios				
	Base Case	-20% Type-A	+20% Type-A	-20% Type-B	+20% Type-B
<u>Atmospheric Inputs</u>					
<u>Terrestrial/Lake</u>					
Wet	-105.4	-67.1	-143.8	-84.6	-126.3
Dry	0.0	0.0	0.0	0.0	0.0
Net	-105.4	-67.1	-143.8	-84.6	-126.3
<u>Internal Sources</u>					
<u>Soil Solution</u>					
NH ₄ Uptake (nitrification)	-12.9	-12.9	-12.9	-10.3	-15.4
NO ₃ Uptake (nitrate reduction)	17.7	14.1	21.2	14.1	21.2
Net	4.8	1.2	8.3	3.8	5.7
<u>Soil Processes</u>					
Cation Exchange	32.8	28.3	37.2	39.1	26.6
SO ₄ Adsorption	24.5	5.4	43.6	5.4	43.6
Weathering	139.0	139.0	139.0	139.0	139.0
Net	196.3	172.7	219.7	183.5	209.2
<u>Lake</u>					
NH ₄ Uptake (nitrification)	-15.2	-15.2	-15.2	-12.1	-18.5
NO ₃ Uptake (nitrate reduction)	25.3	18.0	32.6	18.0	32.6
SO ₄ Reduction	0.0	0.0	0.0	0.0	0.0
Net	10.1	2.8	17.4	5.9	14.2
Sum of Internal Sources	211.1	176.7	245.4	193.2	229.1
Basin Output	105.7	109.6	101.6	108.6	102.8
Atm Input + Internal Sources	105.7	109.6	101.6	108.6	102.8
Total Al Outflow from Basin	3.8	4.0	3.7	3.9	3.7

TABLE B.4. MAGIC Code, 1991-1993 Average ANC Budgets for Panther Lake: Base-Case, $\pm 20\%$ Type-A, and $\pm 20\%$ Type-B Deposition Scenarios. Acid Dependent Weathering Coefficient = 0.5 ($\text{meq}\cdot\text{m}^{-2}\cdot\text{yr}^{-1}$ of terrestrial area)

	Deposition Scenarios				
	Base Case	-20% Type-A	+20% Type-A	-20% Type-B	+20% Type-B
<u>Atmospheric Inputs</u>					
<u>Terrestrial/Lake</u>					
Wet	-105.4	-67.1	-143.8	-84.6	-126.3
Dry	0.0	0.0	0.0	0.0	0.0
Net	-105.4	-67.1	-143.8	-84.6	-126.3
<u>Internal Sources</u>					
<u>Soil Solution</u>					
NH ₄ Uptake (nitrification)	-12.9	-12.9	-12.9	-10.3	-15.4
NO ₃ Uptake (nitrate reduction)	17.7	14.1	21.2	14.1	21.2
Net	4.8	1.2	8.3	3.8	5.7
<u>Soil Processes</u>					
Cation Exchange	20.6	16.9	24.2	27.4	13.8
SO ₄ Adsorption	24.5	5.4	43.6	5.4	43.6
Weathering	151.4	150.5	152.2	150.9	152.0
Net	196.5	172.9	220.0	183.7	209.4
<u>Lake</u>					
NH ₄ Uptake (nitrification)	-15.2	-15.2	-15.2	-12.1	-18.5
NO ₃ Uptake (nitrate reduction)	25.3	18.0	32.6	18.0	32.6
SO ₄ Reduction	0.0	0.0	0.0	0.0	0.0
Net	10.1	2.8	17.4	5.9	14.2
Sum of Internal Sources	211.4	176.9	245.7	193.4	229.3
Basin Output	106.0	109.8	101.9	108.8	103.0
Atm Input + Internal Sources	106.0	109.8	101.9	108.8	103.0
Total AI Outflow from Basin	3.9	4.0	3.7	4.0	3.7

TABLE B.5. MAGIC Code, 1984-1986 Average ANC Budgets for Clear Pond: Base-Case, ±20% Type-A, and ±20% Type-B Deposition Scenarios. Acid Dependent Weathering Coefficient = 0.0 (meq•m⁻²•yr⁻¹ of terrestrial area)

	Deposition Scenarios				
	Base Case	-20% Type-A	+20% Type-A	-20% Type-B	+20% Type-B
<u>Atmospheric Inputs</u>					
<u>Terrestrial/Lake</u>					
Wet	-76.4	-56.9	-95.9	-63.1	-89.7
Dry	0.0	0.0	0.0	0.0	0.0
Net	-76.4	-56.9	-95.9	-63.1	-89.7
<u>Internal Sources</u>					
<u>Soil Solution</u>					
NH ₄ Uptake (nitrification)	-9.2	-9.2	-9.2	-9.0	-9.2
NO ₃ Uptake (nitrate reduction)	22.0	21.5	22.5	21.5	22.5
Net	12.7	12.3	13.2	12.5	13.2
<u>Soil Processes</u>					
Cation Exchange	33.8	33.8	34.0	37.0	30.8
SO ₄ Adsorption	-1.3	-13.1	10.5	-13.1	10.5
Weathering	89.0	89.0	89.0	89.0	89.0
Net	121.5	109.6	133.5	112.9	130.2
<u>Lake</u>					
NH ₄ Uptake (nitrification)	-4.8	-4.8	-4.8	-2.4	-7.4
NO ₃ Uptake (nitrate reduction)	11.7	6.0	17.5	6.0	17.5
SO ₄ Reduction	0.0	0.0	0.0	0.0	0.0
Net	7.0	1.2	12.7	3.5	10.1
Sum of Internal Sources	141.2	123.1	159.4	128.9	153.6
Basin Output	64.8	66.2	63.5	65.8	63.8
Atm Input + Internal Sources	64.8	66.2	63.5	65.8	63.8
Total Al Outflow from Basin	2.2	2.2	2.1	2.2	2.2

TABLE B.6. MAGIC Code, 1984-1986 Average ANC Budgets for Clear Pond: Base-Case, $\pm 20\%$ Type-A, and $\pm 20\%$ Type-B Deposition Scenarios. Acid Dependent Weathering Coefficient = 0.5 ($\text{meq}\cdot\text{m}^{-2}\cdot\text{yr}^{-1}$ of terrestrial area)

	Deposition Scenarios				
	<u>Base Case</u>	<u>-20% Type-A</u>	<u>+20% Type-A</u>	<u>-20% Type-B</u>	<u>+20% Type-B</u>
<u>Atmospheric Inputs</u>					
<u>Terrestrial/Lake</u>					
Wet	-76.4	-56.9	-95.9	-63.1	-89.7
Dry	0.0	0.0	0.0	0.0	0.0
Net	-76.4	-56.9	-95.9	-63.1	-89.7
<u>Internal Sources</u>					
<u>Soil Solution</u>					
NH ₄ Uptake (nitrification)	-9.2	-9.2	-9.2	-9.0	-9.2
NO ₃ Uptake (nitrate reduction)	22.0	21.5	22.5	21.5	22.5
Net	12.7	12.3	13.2	12.5	13.2
<u>Soil Processes</u>					
Cation Exchange	23.7	23.7	23.8	26.9	20.6
SO ₄ Adsorption	-1.3	-13.1	10.5	-13.1	10.5
Weathering	99.0	98.9	99.0	98.9	99.0
Net	121.4	109.5	133.3	112.7	130.1
<u>Lake</u>					
NH ₄ Uptake (nitrification)	-4.8	-4.8	-4.8	-2.4	-7.4
NO ₃ Uptake (nitrate reduction)	11.7	6.0	17.5	6.0	17.5
SO ₄ Reduction	0.0	0.0	0.0	0.0	0.0
Net	7.0	1.2	12.7	3.5	10.1
Sum of Internal Sources	141.1	122.9	159.2	128.7	153.4
Basin Output	64.7	66.0	63.4	65.6	63.7
Atm Input + Internal Sources	64.7	66.0	63.4	65.6	63.7
Total Al Outflow from Basin	2.2	2.2	2.1	2.2	2.2

TABLE B.7. MAGIC Code, 1994-1996 Average ANC Budgets for Clear Pond: Base-Case, $\pm 20\%$ Type-A, and $\pm 20\%$ Type-B Deposition Scenarios. Acid Dependent Weathering Coefficient = 0.0 ($\text{meq}\cdot\text{m}^{-2}\cdot\text{yr}^{-1}$ of terrestrial area)

	Deposition Scenarios				
	Base Case	-20% Type-A	+20% Type-A	-20% Type-B	+20% Type-B
<u>Atmospheric Inputs</u>					
<u>Terrestrial/Lake</u>					
Wet	-76.4	-54.5	-98.3	-61.4	-91.4
Dry	0.0	0.0	0.0	0.0	0.0
Net	-76.4	-54.5	-98.3	-61.4	-91.4
<u>Internal Sources</u>					
<u>Soil Solution</u>					
NH ₄ Uptake (nitrification)	-9.2	-9.2	-9.2	-9.0	-9.2
NO ₃ Uptake (nitrate reduction)	22.0	17.6	25.7	17.6	25.7
Net	12.7	8.3	16.5	8.5	16.5
<u>Soil Processes</u>					
Cation Exchange	33.4	31.4	35.3	35.0	31.8
SO ₄ Adsorption	-1.0	-11.2	9.3	-11.2	9.3
Weathering	89.0	89.0	89.0	89.0	89.0
Net	121.4	109.2	133.6	112.8	130.1
<u>Lake</u>					
NH ₄ Uptake (nitrification)	-4.8	-4.8	-4.8	-2.2	-7.7
NO ₃ Uptake (nitrate reduction)	11.7	9.2	14.9	9.2	14.9
SO ₄ Reduction	0.0	0.0	0.0	0.0	0.0
Net	7.0	4.5	10.1	7.1	7.2
Sum of Internal Sources	141.1	122.0	160.2	128.4	153.8
Basin Output	64.7	67.5	61.9	67.0	62.4
Atm Input + Internal Sources	64.7	67.5	61.9	67.0	62.4
Total Al Outflow from Basin	2.2	2.3	2.1	2.3	2.1

TABLE B.8. MAGIC Code, 1994-1996 Average ANC Budgets for Clear Pond: Base-Case, $\pm 20\%$ Type-A, and $\pm 20\%$ Type-B Deposition Scenarios. Acid Dependent Weathering Coefficient = 0.5 ($\text{meq}\cdot\text{m}^{-2}\cdot\text{yr}^{-1}$ of terrestrial area)

	Deposition Scenarios				
	Base Case	-20% Type-A	+20% Type-A	-20% Type-B	+20% Type-B
<u>Atmospheric Inputs</u>					
<u>Terrestrial/Lake</u>					
Wet	-76.4	-54.5	-98.3	-61.4	-91.4
Dry	0.0	0.0	0.0	0.0	0.0
Net	-76.4	-54.5	-98.3	-61.4	-91.4
<u>Internal Sources</u>					
<u>Soil Solution</u>					
NH ₄ Uptake (nitrification)	-9.2	-9.2	-9.2	-9.0	-9.2
NO ₃ Uptake (nitrate reduction)	22.0	17.6	25.7	17.6	25.7
Net	12.7	8.3	16.5	8.5	16.5
<u>Soil Processes</u>					
Cation Exchange	23.4	21.8	24.8	25.3	21.4
SO ₄ Adsorption	-1.0	-11.2	9.3	-11.2	9.3
Weathering	98.9	98.6	99.3	98.6	99.3
Net	121.3	109.1	133.4	112.7	130.0
<u>Lake</u>					
NH ₄ Uptake (nitrification)	-4.8	-4.8	-4.8	-2.2	-7.7
NO ₃ Uptake (nitrate reduction)	11.7	9.2	14.9	9.2	14.9
SO ₄ Reduction	0.0	0.0	0.0	0.0	0.0
Net	7.0	4.5	10.1	7.1	7.2
Sum of Internal Sources	141.0	121.9	160.0	128.3	153.7
Basin Output	64.6	67.4	61.7	66.9	62.3
Atm Input + Internal Sources	64.6	67.4	61.7	66.9	62.3
Total Al Outflow from Basin	2.2	2.3	2.1	2.3	2.1

TABLE B.9. MAGIC Code, 1982-1984 Average ANC Budgets for Woods Lake: Base-Case, $\pm 20\%$ Type-A, and $\pm 20\%$ Type-B Deposition Scenarios. Acid Dependent Weathering Coefficient = 0.0 ($\text{meq}\cdot\text{m}^{-2}\cdot\text{yr}^{-1}$ of terrestrial area)

	Deposition Scenarios				
	<u>Base Case</u>	<u>-20% Type-A</u>	<u>+20% Type-A</u>	<u>-20% Type-B</u>	<u>+20% Type-B</u>
<u>Atmospheric Inputs</u>					
<u>Terrestrial/Lake</u>					
Wet	-103.0	-91.2	-114.8	-96.2	-109.8
Dry	0.0	0.0	0.0	0.0	0.0
Net	-103.0	-91.2	-114.8	-96.2	-109.8
<u>Internal Sources</u>					
<u>Soil Solution</u>					
NH ₄ Uptake (nitrification)	-11.7	-11.7	-11.7	-10.9	-12.5
NO ₃ Uptake (nitrate reduction)	15.9	14.8	16.9	14.8	17.2
Net	4.2	3.1	5.2	3.9	4.8
<u>Soil Processes</u>					
Cation Exchange	13.7	13.3	14.1	16.0	11.3
SO ₄ Adsorption	25.6	19.2	32.0	19.2	32.0
Weathering	13.4	13.4	13.4	13.4	13.4
Net	52.7	45.9	59.5	48.7	56.7
<u>Lake</u>					
NH ₄ Uptake (nitrification)	-15.9	-15.9	-15.9	-14.7	-17.0
NO ₃ Uptake (nitrate reduction)	26.8	24.2	29.5	24.2	29.1
SO ₄ Reduction	0.0	0.0	0.0	0.0	0.0
Net	10.9	8.3	13.6	9.5	12.1
Sum of Internal Sources	67.8	57.3	78.2	62.0	73.6
Basin Output	-35.2	-33.9	-36.6	-34.2	-36.2
Atm Input + Internal Sources	-35.2	-33.9	-36.6	-34.2	-36.2
Total Al Outflow from Basin	25.6	24.4	26.7	24.7	26.4

TABLE B.10. MAGIC Code, 1982-1984 Average ANC Budgets for Woods Lake: Base-Case, ±20% Type-A, and ±20% Type-B Deposition Scenarios. Acid Dependent Weathering Coefficient = 0.5 (meq·m⁻²·yr⁻¹ of terrestrial area)

	Deposition Scenarios				
	<u>Base Case</u>	<u>-20% Type-A</u>	<u>+20% Type-A</u>	<u>-20% Type-B</u>	<u>+20% Type-B</u>
<u>Atmospheric Inputs</u>					
<u>Terrestrial/Lake</u>					
Wet	-103.0	-91.2	-114.8	-96.2	-109.8
Dry	0.0	0.0	0.0	0.0	0.0
Net	-103.0	-91.2	-114.8	-96.2	-109.8
<u>Internal Sources</u>					
<u>Soil Solution</u>					
NH ₄ Uptake (nitrification)	-11.7	-11.7	-11.7	-10.9	-12.5
NO ₃ Uptake (nitrate reduction)	15.9	14.8	16.9	14.8	17.2
Net	4.2	3.1	5.2	3.9	4.8
<u>Soil Processes</u>					
Cation Exchange	11.2	10.9	11.5	13.6	8.7
SO ₄ Adsorption	25.6	19.2	32.0	19.2	32.0
Weathering	15.8	15.8	15.9	15.8	15.9
Net	52.6	45.9	59.4	48.6	56.6
<u>Lake</u>					
NH ₄ Uptake (nitrification)	-15.9	-15.9	-15.9	-14.7	-17.0
NO ₃ Uptake (nitrate reduction)	26.8	24.2	29.5	24.2	29.1
SO ₄ Reduction	0.0	0.0	0.0	0.0	0.0
Net	10.9	8.3	13.6	9.5	12.1
Sum of Internal Sources	67.7	57.3	78.2	62.0	73.5
Basin Output	-35.3	-33.9	-36.6	-34.3	-36.3
Atm Input + Internal Sources	-35.3	-33.9	-36.6	-34.3	-36.3
Total Al Outflow from Basin	25.6	24.4	26.8	24.7	26.5

TABLE B.11. MAGIC Code, 1991-1993 Average ANC Budgets for Woods Lake: Base-Case, $\pm 20\%$ Type-A, and $\pm 20\%$ Type-B Deposition Scenarios. Acid Dependent Weathering Coefficient = 0.0 (meq \cdot m $^{-2}$ \cdot yr $^{-1}$ of terrestrial area)

	Deposition Scenarios				
	Base Case	-20% Type-A	+20% Type-A	-20% Type-B	+20% Type-B
<u>Atmospheric Inputs</u>					
<u>Terrestrial/Lake</u>					
Wet	-103.0	-67.5	-138.4	-82.6	-123.3
Dry	0.0	0.0	0.0	0.0	0.0
Net	-103.0	-67.5	-138.4	-82.6	-123.3
<u>Internal Sources</u>					
<u>Soil Solution</u>					
NH ₄ Uptake (nitrification)	-11.7	-11.7	-11.7	-9.4	-14.0
NO ₃ Uptake (nitrate reduction)	15.9	12.7	19.0	12.7	19.0
Net	4.2	1.0	7.3	3.3	5.0
<u>Soil Processes</u>					
Cation Exchange	13.3	7.5	19.1	15.7	10.9
SO ₄ Adsorption	23.9	10.6	37.1	10.6	37.1
Weathering	13.4	13.4	13.4	13.4	13.4
Net	50.6	31.4	69.6	39.7	61.4
<u>Lake</u>					
NH ₄ Uptake (nitrification)	-15.9	-15.9	-15.9	-12.7	-19.1
NO ₃ Uptake (nitrate reduction)	26.8	21.5	32.2	21.5	32.2
SO ₄ Reduction	0.0	0.0	0.0	0.0	0.0
Net	10.9	5.6	16.3	8.7	13.1
Sum of Internal Sources	65.7	38.0	93.2	51.7	79.5
Basin Output	-37.3	-29.5	-45.2	-30.9	-43.8
Atm Input + Internal Sources	-37.3	-29.5	-45.2	-30.9	-43.8
Total Al Outflow from Basin	27.4	20.8	34.4	21.9	33.1

TABLE B.12. MAGIC Code, 1991-1993 Average ANC Budgets for Woods Lake: Base-Case, $\pm 20\%$ Type-A, and $\pm 20\%$ Type-B Deposition Scenarios. Acid Dependent Weathering Coefficient = 0.5 ($\text{meq}\cdot\text{m}^{-2}\cdot\text{yr}^{-1}$ of terrestrial area)

	Deposition Scenarios				
	<u>Base Case</u>	<u>-20% Type-A</u>	<u>+20% Type-A</u>	<u>-20% Type-B</u>	<u>+20% Type-B</u>
<u>Atmospheric Inputs</u>					
<u>Terrestrial/Lake</u>					
Wet	-103.0	-67.5	-138.4	-82.6	-123.3
Dry	0.0	0.0	0.0	0.0	0.0
Net	-103.0	-67.5	-138.4	-82.6	-123.3
<u>Internal Sources</u>					
<u>Soil Solution</u>					
NH ₄ Uptake (nitrification)	-11.7	-11.7	-11.7	-9.4	-14.0
NO ₃ Uptake (nitrate reduction)	15.9	12.7	19.0	12.7	19.0
Net	4.2	1.0	7.3	3.3	5.0
<u>Soil Processes</u>					
Cation Exchange	10.6	5.2	16.0	13.3	8.1
SO ₄ Adsorption	23.9	10.6	37.1	10.6	37.1
Weathering	16.2	15.7	16.6	15.9	16.4
Net	50.7	31.4	69.7	39.7	61.6
<u>Lake</u>					
NH ₄ Uptake (nitrification)	-15.9	-15.9	-15.9	-12.7	-19.1
NO ₃ Uptake (nitrate reduction)	26.8	21.5	32.2	21.5	32.2
SO ₄ Reduction	0.0	0.0	0.0	0.0	0.0
Net	10.9	5.6	16.3	8.7	13.1
Sum of Internal Sources	65.8	38.0	93.4	51.8	79.7
Basin Output	-37.2	-29.5	-45.0	-30.8	-43.6
Atm Input + Internal Sources	-37.2	-29.5	-45.0	-30.8	-43.6
Total Al Outflow from Basin	27.3	20.8	34.3	21.9	32.9

TABLE B.13. MAGIC Code, 1982, 1983, 1984 Average ANC Budgets for Panther Lake: Base-Case Deposition Scenario. Acid Dependent Weathering Coefficient = $0.5 \text{ (meq}\cdot\text{m}^{-2}\cdot\text{yr}^{-1}$ of terrestrial area)

	Average ANC Budgets		
	<u>1982</u>	<u>1983</u>	<u>1984</u>
<u>Atmospheric Inputs</u>			
<u>Terrestrial/Lake</u>			
Wet	-105.4	-105.4	-105.4
Dry	0.0	0.0	0.0
Net	-105.4	-105.4	-105.4
<u>Internal Sources</u>			
<u>Soil Solution</u>			
NH ₄ Uptake (nitrification)	-12.9	-12.9	-12.9
NO ₃ Uptake (nitrate reduction)	17.7	17.7	17.7
Net	4.8	4.8	4.8
<u>Soil Processes</u>			
Cation Exchange	21.3	21.2	21.0
SO ₄ Adsorption	27.9	27.5	27.2
Weathering	151.1	151.1	151.2
Net	200.3	199.8	199.4
<u>Lake</u>			
NH ₄ Uptake (nitrification)	-15.1	-15.1	-15.1
NO ₃ Uptake (nitrate reduction)	23.0	23.3	23.6
SO ₄ Reduction	0.0	0.0	0.0
Net	7.9	8.2	8.5
Sum of Internal Sources	213.0	212.8	212.7
Basin Output	107.5	107.3	107.3
Atm Input + Internal Sources	107.6	107.4	107.3
Total Al Outflow from Basin	3.9	3.9	3.9
Cation Exchange Storage ($\text{eq}\cdot\text{m}^{-2}$)	50.9	50.9	50.9

TABLE B.14. MAGIC Code, 1984, 1985, 1986 Average ANC Budgets for Clear Pond: Base-Case Deposition Scenario. Acid Dependent Weathering Coefficient = $0.5 \text{ (meq}\cdot\text{m}^{-2}\cdot\text{yr}^{-1}$ of terrestrial area)

	Average ANC Budgets		
	<u>1984</u>	<u>1985</u>	<u>1986</u>
<u>Atmospheric Inputs</u>			
<u>Terrestrial/Lake</u>			
Wet	-76.4	-76.4	-76.4
Dry	0.0	0.0	0.0
Net	-76.4	-76.4	-76.4
<u>Internal Sources</u>			
<u>Soil Solution</u>			
NH ₄ Uptake (nitrification)	-9.2	-9.2	-9.2
NO ₃ Uptake (nitrate reduction)	24.1	24.1	24.1
Net	14.9	14.9	14.9
<u>Soil Processes</u>			
Cation Exchange	24.7	23.8	23.8
SO ₄ Adsorption	-1.5	-1.5	-1.5
Weathering	98.1	99.0	99.0
Net	121.3	121.3	121.3
<u>Lake</u>			
NH ₄ Uptake (nitrification)	-4.8	-4.8	-4.8
NO ₃ Uptake (nitrate reduction)	9.6	9.6	9.6
SO ₄ Reduction	0.0	0.0	0.0
Net	4.8	4.8	4.8
Sum of Internal Sources	141.0	141.0	141.0
Basin Output	64.6	64.6	64.6
Atm Input + Internal Sources	64.7	64.7	64.7
Total Al Outflow from Basin	2.2	2.2	2.2
Cation Exchange Storage ($\text{eq}\cdot\text{m}^{-2}$)	189.5	189.5	189.5

TABLE B.15. MAGIC Code, 1982, 1983, 1984 Average ANC Budgets for Woods Lake: Base-Case Deposition Scenario. Acid Dependent Weathering Coefficient = $0.5 \text{ (meq}\cdot\text{m}^{-2}\cdot\text{yr}^{-1}$ of terrestrial area)

	Average ANC Budgets		
	<u>1982</u>	<u>1983</u>	<u>1984</u>
<u>Atmospheric Inputs</u>			
<u>Terrestrial/Lake</u>			
Wet	-103.0	-103.0	-103.0
Dry	0.0	0.0	0.0
Net	-103.0	-103.0	-103.0
<u>Internal Sources</u>			
<u>Soil Solution</u>			
NH ₄ Uptake (nitrification)	-11.7	-11.7	-11.7
NO ₃ Uptake (nitrate reduction)	15.8	15.8	15.8
Net	4.2	4.2	4.2
<u>Soil Processes</u>			
Cation Exchange	11.3	11.2	11.1
SO ₄ Adsorption	25.7	25.6	25.5
Weathering	15.8	15.8	15.9
Net	52.8	52.6	52.5
<u>Lake</u>			
NH ₄ Uptake (nitrification)	-15.9	-15.9	-15.9
NO ₃ Uptake (nitrate reduction)	26.9	26.9	26.9
SO ₄ Reduction	0.0	0.0	0.0
Net	10.9	10.9	10.9
Sum of Internal Sources	67.9	67.7	67.6
Basin Output	-35.1	-35.3	-35.4
Atm Input + Internal Sources	-35.1	-35.3	-35.4
Total Al Outflow from Basin	25.5	25.6	25.7
Cation Exchange Storage ($\text{eq}\cdot\text{m}^{-2}$)	7.2	7.2	7.1

APPENDIX C

ANNUAL-AVERAGE FLOW-WEIGHTED ANC BUDGETS FROM
ETD CODE FORECASTS FOR CLEAR POND, PANTHER LAKE,
AND WOODS LAKE WATERSHEDS

APPENDIX C

ANNUAL-AVERAGE FLOW-WEIGHTED AND BUDGETS FROM ETD CODE FORECASTS
FOR CLEAR POND, PANTHER LAKE, AND WOODS LAKE WATERSHEDS

TABLE C.1. ETD Code, 1982-1984 Average ANC Budgets for Panther Lake:
Base Case and $\pm 20\%$ Deposition Scenarios ($\text{meq}\cdot\text{m}^{-2}\cdot\text{yr}^{-1}$ of
terrestrial area)

	Deposition Scenario		
	Base Case	-20%	+20%
<u>Atmospheric Inputs</u>			
<u>Terrestrial/Lake/Snowpack</u>			
Wet	-100.5	-84.3	-116.9
Dry	-37.9	-37.9	-37.9
Net	-138.4	-122.2	-154.8
<u>Internal Sources</u>			
<u>Soil Compartment</u>			
SO ₄ Adsorption	5.4	5.1	5.7
Cation Exchange	94.0	84.6	103.7
Net	99.4	89.7	109.4
<u>Unsaturated Zone</u>			
SO ₄ Adsorption	-0.2	-0.1	-0.2
Weathering	161.0	155.7	166.5
Net	160.8	155.6	166.3
<u>Groundwater Compartment</u>			
SO ₄ Adsorption	1.6	1.4	1.8
Weathering	14.8	14.8	14.8
Net	16.4	16.2	16.6
<u>Lake Compartment</u>			
SO ₄ Reduction	16.1	14.5	17.7
Weathering	22.3	22.2	22.4
Net	38.4	36.7	40.1
Sum of Internal Sources	315.0	298.2	332.4
Release from Storage	-8.0	-4.6	-11.7
Atm Input + Internal Sources + Release Storage	168.6	171.3	166.0
Basin Output	163.1	165.8	160.4

TABLE C.2. ETD Code, 1991-1993 Average ANC Budgets for Panther Lake: Base Case and $\pm 20\%$ Deposition Scenarios ($\text{meq}\cdot\text{m}^{-2}\cdot\text{yr}^{-1}$ of terrestrial area)

	<u>Deposition Scenario</u>		
	<u>Base Case</u>	<u>-20%</u>	<u>+20%</u>
<u>Atmospheric Inputs</u>			
<u>Terrestrial/Lake/Snowpack</u>			
Wet	-100.5	-84.3	-116.9
Dry	-37.9	-37.9	-37.9
Net	-138.4	-122.2	-154.8
<u>Internal Sources</u>			
<u>Soil Compartment</u>			
SO ₄ Adsorption	5.4	5.1	5.7
Cation Exchange	91.8	82.7	101.2
Net	97.2	87.8	106.9
<u>Unsaturated Zone</u>			
SO ₄ Adsorption	-0.2	-0.1	-0.2
Weathering	163.6	157.8	169.4
Net	163.4	157.7	169.2
<u>Groundwater Compartment</u>			
SO ₄ Adsorption	1.6	1.3	1.8
Weathering	14.4	14.5	14.4
Net	16.0	15.8	16.2
<u>Lake Compartment</u>			
SO ₄ Reduction	16.1	14.5	17.8
Weathering	22.3	22.2	22.4
Net	38.4	36.7	40.2
Sum of Internal Sources	315.0	298.0	332.5
Release from Storage	-8.9	-5.4	-12.6
Atm Input + Internal Sources + Release Storage	167.7	170.4	164.9
Basin Output	162.1	164.9	159.4

TABLE C.3. ETD Code, 1984-1986 Average ANC Budgets for Clear Pond:
Base Case and $\pm 20\%$ Deposition Scenarios ($\text{meq}\cdot\text{m}^{-2}\cdot\text{yr}^{-1}$ of
terrestrial area)

	Deposition Scenario		
	Base Case	-20%	+20%
<u>Atmospheric Inputs</u>			
<u>Terrestrial/Lake/Snowpack</u>			
Wet	-99.3	-82.2	-116.4
Dry	-31.1	-31.1	-31.1
Net	-130.4	-113.3	-147.3
<u>Internal Sources</u>			
<u>Soil Compartment</u>			
SO ₄ Adsorption	6.5	5.9	7.0
Cation Exchange	76.1	67.0	85.2
Net	82.6	72.9	92.2
<u>Unsaturated Zone</u>			
SO ₄ Adsorption	-0.4	-0.4	-0.4
Weathering	132.6	123.6	141.7
Net	132.2	123.2	141.3
<u>Groundwater Compartment</u>			
SO ₄ Adsorption	1.1	1.0	1.3
Weathering	0.3	0.3	0.3
Net	1.4	1.3	1.6
<u>Lake Compartment</u>			
SO ₄ Reduction	15.4	13.6	17.1
Weathering	17.5	17.4	17.7
Net	32.9	31.0	34.8
Sum of Internal Sources	249.1	228.4	269.9
Release from Storage	1.5	7.6	-4.4
Atm Input + Internal Sources + Release Storage	120.3	122.5	118.3
Basin Output	115.8	118.1	113.8

TABLE C.4. ETD Code, 1994-1996 Average ANC Budgets for Clear Pond: Base Case and $\pm 20\%$ Deposition Scenarios ($\text{meq}\cdot\text{m}^{-2}\cdot\text{yr}^{-1}$ of terrestrial area)

	Deposition Scenario		
	Base Case	-20%	+20%
<u>Atmospheric Inputs</u>			
<u>Terrestrial/Lake/Snowpack</u>			
Wet	-92.4	-76.5	-108.1
Dry	-29.3	-29.3	-29.3
Net	-121.7	-105.8	-137.4
<u>Internal Sources</u>			
<u>Soil Compartment</u>			
SO ₄ Adsorption	3.0	3.0	3.1
Cation Exchange	71.0	62.9	79.0
Net	74.0	65.9	82.1
<u>Unsaturated Zone</u>			
SO ₄ Adsorption	0.3	0.3	0.3
Weathering	136.3	126.1	146.9
Net	136.6	126.4	147.2
<u>Groundwater Compartment</u>			
SO ₄ Adsorption	1.2	1.1	1.4
Weathering	0.3	0.3	0.3
Net	1.5	1.4	1.7
<u>Lake Compartment</u>			
SO ₄ Reduction	16.5	14.6	18.4
Weathering	17.3	17.2	17.5
Net	33.8	31.8	35.9
Sum of Internal Sources	245.9	225.5	266.9
Release from Storage	-15.4	-8.2	-22.7
Atm Input + Internal Sources + Release Storage	109.0	111.3	106.8
Basin Output	104.8	107.2	102.6

TABLE C.5. ETD Code, 1982-1984 Average ANC Budgets for Woods Lake: Base Case and $\pm 20\%$ Deposition Scenarios ($\text{meq}\cdot\text{m}^{-2}\cdot\text{yr}^{-1}$ of terrestrial area)

	<u>Deposition Scenario</u>		
	<u>Base Case</u>	<u>-20%</u>	<u>+20%</u>
<u>Atmospheric Inputs</u>			
<u>Terrestrial/Lake/Snowpack</u>			
Wet	-101.5	-88.3	117.4
Dry	-29.9	-29.8	29.9
Net	-131.4	-118.1	-147.3
<u>Internal Sources</u>			
<u>Soil Compartment</u>			
SO ₄ Adsorption	9.2	8.6	9.9
Cation Exchange	34.9	31.0	39.1
Net	44.1	39.6	49.0
<u>Unsaturated Zone</u>			
SO ₄ Adsorption	-0.1	-0.1	-0.1
Weathering	46.5	44.0	49.3
Net	46.4	43.9	49.2
<u>Groundwater Compartment</u>			
SO ₄ Adsorption	1.0	0.7	1.3
Weathering	10.7	10.7	10.6
Net	11.7	11.4	11.9
<u>Lake Compartment</u>			
SO ₄ Reduction	15.1	13.8	16.7
Weathering	4.5	4.2	5.0
Net	19.6	18.0	21.7
Sum of Internal Sources	121.8	112.9	131.8
Release from Storage	3.3	1.4	4.9
Atm Input + Internal Sources + Release Storage	-6.5	-3.7	-10.6
Basin Output	-10.0	-7.2	-14.1

TABLE C.6. ETD Code, 1991-1993 Average ANC Budgets for Woods Lake: Base Case and $\pm 20\%$ Deposition Scenarios ($\text{meq}\cdot\text{m}^{-2}\cdot\text{yr}^{-1}$ of terrestrial area)

	<u>Deposition Scenario</u>		
	<u>Base Case</u>	<u>-20%</u>	<u>+20%</u>
<u>Atmospheric Inputs</u>			
<u>Terrestrial/Lake/Snowpack</u>			
Wet	-101.5	-88.3	-117.4
Dry	-29.9	-29.8	-29.9
Net	-131.5	-118.1	-147.3
<u>Internal Sources</u>			
<u>Soil Compartment</u>			
SO ₄ Adsorption	9.2	8.6	9.9
Cation Exchange	33.8	30.2	37.8
Net	43.0	38.8	47.7
<u>Unsaturated Zone</u>			
SO ₄ Adsorption	-0.1	0.0	-0.1
Weathering	46.9	44.2	49.9
Net	46.8	44.2	49.8
<u>Groundwater Compartment</u>			
SO ₄ Adsorption	0.5	0.3	0.7
Weathering	10.1	10.0	10.1
Net	10.6	10.3	10.8
<u>Lake Compartment</u>			
SO ₄ Reduction	15.2	13.9	16.9
Weathering	4.4	4.1	4.9
Net	19.6	18.0	21.8
Sum of Internal Sources	120.0	111.3	130.1
Release from Storage	5.8	4.1	7.5
Atm Input + Internal Sources + Release Storage	-5.6	-2.7	-9.8
Basin Output	-9.1	-6.1	-13.4

TABLE C.7. ETD Code, 1982, 1983, and 1984 Average ANC Budgets for Panther Lake; Base-Case Deposition Scenarios (meq•m⁻²•yr⁻¹ of terrestrial area)

	Average ANC Budgets		
	1982	1983	1984
<u>Atmospheric Inputs</u>			
<u>Terrestrial/Lake/Snowpack</u>			
Wet	-108.0	-92.6	-100.7
Dry	-42.7	-35.5	-35.2
Net	-150.7	-128.5	-135.9
<u>Internal Sources</u>			
<u>Soil Compartment</u>			
SO ₄ Adsorption	3.9	5.4	6.9
Cation Exchange	101.2	93.4	87.5
Net	105.1	98.8	94.4
<u>Unsaturated Zone</u>			
SO ₄ Adsorption	-3.4	0.9	2.1
Weathering	162.6	157.1	163.4
Net	159.2	158.0	165.5
<u>Groundwater Compartment</u>			
SO ₄ Adsorption	1.6	1.6	1.6
Weathering	14.9	14.8	14.8
Net	16.5	16.4	16.4
<u>Lake Compartment</u>			
SO ₄ Reduction	16.0	16.8	15.4
Weathering	22.7	22.0	22.1
Net	38.7	38.8	37.5
Sum of Internal Sources	319.5	312.0	313.8
Release from Storage	17.7	-26.9	-14.9
Basin Output	180.1	151.4	157.8
Atm + Internal Sources	186.3	156.6	163.0
Sum of Remaining Exchangeable Bases (eq•m ⁻²)	74.4	73.7	73.0

TABLE C.8. ETD Code, 1984, 1985, and 1986 Average ANC Budgets for Clear Pond: Base-Case Deposition Scenarios ($\text{meq}\cdot\text{m}^{-2}\cdot\text{yr}^{-1}$ of terrestrial area)

	Average ANC Budgets		
	<u>1982</u>	<u>1983</u>	<u>1984</u>
<u>Atmospheric Inputs</u>			
<u>Terrestrial/Lake/Snowpack</u>			
Wet	-106.3	-85.5	-106.3
Dry	-32.8	-27.5	-32.8
Net	-139.1	-113.0	-139.1
<u>Internal Sources</u>			
<u>Soil Compartment</u>			
SO ₄ Adsorption	9.9	-0.4	9.9
Cation Exchange	77.9	73.3	77.1
Net	87.8	72.9	87.0
<u>Unsaturated Zone</u>			
SO ₄ Adsorption	-1.2	1.1	-1.3
Weathering	134.8	127.2	136.0
Net	133.6	128.3	134.7
<u>Groundwater Compartment</u>			
SO ₄ Adsorption	1.1	1.3	1.1
Weathering	0.3	0.3	0.3
Net	1.4	1.6	1.4
<u>Lake Compartment</u>			
SO ₄ Reduction	14.2	17.6	14.2
Weathering	17.9	16.8	17.9
Net	32.1	34.4	32.1
Sum of Internal Sources	254.9	237.2	255.2
Release from Storage	14.3	-22.9	13.3
Basin Output	125.2	97.5	124.8
Atm + Internal Sources	129.9	101.4	129.4
Sum of Remaining Exchangeable Bases ($\text{eq}\cdot\text{m}^{-2}$)	17.9	17.3	16.6

TABLE C.9. ETD Code, 1982, 1983, and 1984 Average ANC Budgets for Woods Lake: Base-Case Deposition Scenarios ($\text{meq}\cdot\text{m}^{-2}\cdot\text{yr}^{-1}$ of terrestrial area)

	Average ANC Budgets		
	<u>1982</u>	<u>1983</u>	<u>1984</u>
<u>Atmospheric Inputs</u>			
<u>Terrestrial/Lake/Snowpack</u>			
Wet	-109.2	-80.5	-114.8
Dry	-32.6	-30.0	-27.3
Net	-141.8	-110.5	-142.1
<u>Internal Sources</u>			
<u>Soil Compartment</u>			
SO ₄ Adsorption	10.3	2.4	15.0
Cation Exchange	37.8	33.6	33.2
Net	48.1	36.0	48.2
<u>Unsaturated Zone</u>			
SO ₄ Adsorption	-2.3	0.4	1.7
Weathering	48.8	47.0	43.6
Net	46.5	47.4	45.3
<u>Groundwater Compartment</u>			
SO ₄ Adsorption	1.1	0.9	0.9
Weathering	10.8	10.6	10.5
Net	11.9	11.5	11.4
<u>Lake Compartment</u>			
SO ₄ Reduction	13.6	13.3	18.2
Weathering	4.7	4.2	4.7
Net	18.3	17.5	22.9
Sum of Internal Sources	124.8	112.4	127.8
Release from Storage	5.8	-3.5	7.4
Basin Output	-14.7	-5.0	-10.3
Atm + Internal Sources	-11.1	-1.6	-6.9
Sum of Remaining Exchangeable Bases ($\text{eq}\cdot\text{m}^{-2}$)	38.3	38.1	37.9

APPENDIX D

ANNUAL-AVERAGE FLOW-WEIGHTED ANC BUDGETS FROM
ILWAS CODE FORECASTS FOR CLEAR POND, PANTHER LAKE,
AND WOODS LAKE WATERSHEDS

APPENDIX D

ANNUAL-AVERAGE FLOW-WEIGHTED ANC BUDGETS FROM ILUS CODE FORECASTS
FOR CLEAR POND, PANTHER LAKE, AND WOODS LAKE WATERSHEDS

TABLE D.1. ILWAS Code, 1982-1984 Average ANC Budget for Panther Lake: Base Case and $\pm 20\%$ Deposition Scenarios ($\text{meq}\cdot\text{m}^{-2}\cdot\text{yr}^{-1}$ of terrestrial area)

	<u>Deposition Scenarios</u>		
	<u>Base Case</u>	<u>-20%</u>	<u>+20%</u>
<u>Atmospheric Inputs</u>			
<u>Terrestrial/Lake</u>			
Wet	-73.6	-48.1	-99.2
Dry	-30.5	-18.8	-42.2
Net	-104.1	-66.9	-141.4
<u>Internal Sources</u>			
<u>Canopy/Trunk/Leaf</u>			
Release from Storage	-44.1	-44.1	-44.1
Nitrate Reduction	220.7	207.8	232.2
Net	176.6	163.8	188.1
<u>Soil Solution</u>			
Release from Storage	1.2	0.9	1.6
Nitrification	-170.7	-167.1	-174.2
Fulvic Acid Decay	5.6	5.4	5.8
Net	-163.9	-160.9	-166.8
<u>Soil Processes</u>			
Cation Exchange	133.6	130.1	138.1
Anion Adsorption	16.2	3.5	29.0
Weathering	65.5	65.2	65.8
Gibbsite Dissolution	8.3	6.4	10.5
Net	223.6	205.1	243.4
<u>Soil Organic Matter</u>			
Release from Storage	-11.7	-11.7	-11.7
Fulvic Acid Formation	-11.7	-11.7	-11.7
Net	-23.4	-23.4	-23.4
<u>Lake</u>			
Release from Storage	0.3	0.7	0.5
Nitrification	-21.8	-20.9	-22.8
Fulvic Acid Decay	5.1	4.8	5.4
Gibbsite Precip.	-7.5	-6.2	-8.9
Algal Growth	37.2	34.0	37.3
Net	13.3	12.4	11.5
Sum of Internal Sources	226.2	197.0	252.9
Basin Output	122.1	130.0	111.6

TABLE D.2. ILWAS Code, 1991-1993 Average ANC Budget for Panther Lake: Base Case and $\pm 20\%$ Deposition Scenarios ($\text{meq}\cdot\text{m}^{-2}\cdot\text{yr}^{-1}$ of terrestrial area)

	<u>Deposition Scenarios</u>		
	<u>Base Case</u>	<u>-20%</u>	<u>+20%</u>
<u>Atmospheric Inputs</u>			
<u>Terrestrial/Lake</u>			
Wet	-73.6	-99.2	-48.1
Dry	-30.5	-42.2	-18.8
Net	-104.1	-141.4	-66.9
<u>Internal Sources</u>			
<u>Canopy/Trunk/Leaf</u>			
Release from Storage	-25.4	-25.4	-25.3
Nitrate Reduction	213.1	225.1	199.8
Net	187.7	199.7	174.5
<u>Soil Solution</u>			
Release from Storage	1.2	1.5	1.6
Nitrification	-158.9	-163.8	-153.8
Fulvic Acid Decay	5.1	5.3	4.9
Net	-152.6	-157.0	-147.9
<u>Soil Processes</u>			
Cation Exchange	111.8	117.1	107.4
Anion Adsorption	17.3	28.9	5.7
Weathering	67.2	67.9	68.5
Gibbsite Dissolution	8.9	11.6	6.7
Net	205.2	225.5	188.3
<u>Soil Organic Matter</u>			
Release from Storage	-17.1	-17.1	-17.1
Fulvic Acid Formation	-11.4	-11.4	-11.4
Net	-28.5	-28.5	-28.5
<u>Lake</u>			
Release from Storage	0.3	0.2	0.3
Nitrification	-20.4	-21.2	-19.5
Fulvic Acid Decay	4.6	4.8	4.3
Gibbsite Precip.	-8.2	-9.9	-6.6
Algal Growth	35.7	37.3	31.6
Net	12.0	11.2	10.1
Sum of Internal Sources	223.9	250.7	194.3
Basin Output	119.8	109.4	127.4

TABLE D.3. ILWAS Code, 1982-1984 Average ANC Budget for Woods Lake: Base Case and $\pm 20\%$ Deposition Scenarios ($\text{meq}\cdot\text{m}^{-2}\cdot\text{yr}^{-1}$ of terrestrial area)

	Deposition Scenarios		
	Base Case	-20%	+20%
<u>Atmospheric Inputs</u>			
<u>Terrestrial/Lake</u>			
Wet	-75.0	-49.5	-100.6
Dry	-25.3	-17.1	-33.4
Net	-100.3	-66.6	-134.0
<u>Internal Sources</u>			
<u>Canopy/Trunk/Leaf</u>			
Release from Storage	-83.0	-83.0	-83.0
Nitrate Reduction	259.3	244.6	272.7
Net	176.3	161.6	189.7
<u>Soil Solution</u>			
Release from Storage	0.3	0.3	0.4
Nitrification	-194.7	-191.5	-197.9
Fulvic Acid Decay	4.3	4.2	4.4
Net	-190.0	-187.0	-193.1
<u>Soil Processes</u>			
Cation Exchange	61.0	58.6	64.3
Anion Adsorption	3.2	-3.3	9.6
Weathering	11.5	11.4	11.6
Gibbsite Dissolution	28.7	23.2	34.6
Net	104.4	89.9	120.2
<u>Soil Organic Matter</u>			
Release from Storage	18.4	18.4	18.4
Fulvic Acid Formation	-12.9	-12.9	-12.9
Net	5.5	5.5	5.5
<u>Lake</u>			
Release from Storage	-0.2	-0.9	0.6
Nitrification	-25.0	-23.8	-26.0
Fulvic Acid Decay	6.0	5.7	6.3
Gibbsite Precip.	-10.4	-9.0	-10.5
Algal Growth	25.5	22.5	26.2
Net	-4.1	-5.5	-3.4
Sum of Internal Sources	92.0	84.5	118.9
Basin Output	-8.3	-2.1	-15.0

TABLE D.4. ILWAS Code, 1991-1993 Average ANC Budget for Woods Lake: Base Case and $\pm 20\%$ Deposition Scenarios ($\text{meq}\cdot\text{m}^{-2}\cdot\text{yr}^{-1}$ of terrestrial area)

	Deposition Scenarios		
	Base Case	-20%	+20%
<u>Atmospheric Inputs</u>			
<u>Terrestrial/Lake</u>			
Wet	-75.0	-48.4	-49.5
Dry	-25.3	-16.6	-16.9
Net	-100.3	-65.0	-66.4
<u>Internal Sources</u>			
<u>Canopy/Trunk/Leaf</u>			
Release from Storage	-83.0	-55.0	-83.0
Nitrate Reduction	248.0	925.3	230.9
Net	165.0	870.3	147.9
<u>Soil Solution</u>			
Release from Storage	0.4	1.1	0.4
Nitrification	-180.1	-91.8	-175.3
Fulvic Acid Decay	4.3	2.9	4.2
Net	-175.4	-87.8	-170.7
<u>Soil Processes</u>			
Cation Exchange	64.8	40.9	63.2
Anion Adsorption	2.9	6.8	-2.1
Weathering	12.2	8.1	12.1
Gibbsite Dissolution	27.7	23.3	21.6
Net	107.6	79.1	94.8
<u>Soil Organic Matter</u>			
Release from Storage	11.6	7.4	11.6
Fulvic Acid Formation	-13.0	-8.6	-13.0
Net	-1.4	-1.2	-1.4
<u>Lake</u>			
Release from Storage	0.1	1.9	0.1
Nitrification	-24.6	-14.0	-23.4
Fulvic Acid Decay	5.8	4.2	5.5
Gibbsite Precip.	-9.9	-6.9	-8.4
Algal Growth	24.5	8.7	21.5
Net	-4.1	-6.1	-4.7
Sum of Internal Sources	91.6	854.4	65.8
Basin Output	-8.7	-1.1	-0.8

TABLE D.5. ILWAS Code, 1982 Average ANC Budget Storage for Panther Lake; Base-Case Deposition Scenario (meq•m⁻²•yr⁻¹ of terrestrial area)

		<u>ANC Values</u>		
<u>Atmospheric Inputs</u>				
<u>Terrestrial/Lake</u>				
Wet		-85.8		
Dry		-32.8		
Net		-118.6		
<u>Internal Sources</u>			<u>Watershed Storage</u>	
<u>Canopy/Trunk/Leaf</u>				
Release from Storage	-46.6		Canopy	1.9391E+03
Nitrate Reduction	228.3		Trunk	5.3000E-01
Net	181.7		Leaf	0.0000E+00
<u>Soil Solution</u>				
Release from Storage	-4.1		Soil Solution	2.1901E+03
Nitrification	-182.5			
Fulvic Acid Decay	5.9			
Net	-180.6			
<u>Soil Processes</u>				
Cation Exchange	143.9		Cation Exchange	1.3146E+06
Anion Adsorption	15.0		Anion Adsorption	-1.3679E+04
Weathering	65.4			
Gibbsite Dissolution	7.7			
Net	232.0			
<u>Soil Organic Matter</u>				
Release from Storage	-1.9		Organic	1.8888E+04
Fulvic Acid Formation	-12.1			
Net	-14.0			
<u>Lake</u>				
Release from Storage	2.0		Lake	1.3016E+02
Nitrification	-24.4			
Fulvic Acid Decay	5.8			
Gibbsite Precip.	-7.0			
Algal Growth	37.3			
Net	13.6			
Sum of Internal Sources	232.7			
Basin Output	114.1			

**TABLE D.6. ILWAS Code, 1983 ANC Budget Storage for Panther Lake:
Base-Case Deposition Scenario ($\text{meq}\cdot\text{m}^{-2}\cdot\text{yr}^{-1}$ of
terrestrial area)**

		<u>ANC Values</u>		
<u>Atmospheric Inputs</u>				
<u>Terrestrial/Lake</u>				
Wet		-59.2		
Dry		-36.0		
Net		-95.2		
<u>Internal Sources</u>			<u>Watershed Storage</u>	
<u>Canopy/Trunk/Leaf</u>				
Release from Storage	-43.6		Canopy	1.9831E+03
Nitrate Reducation	216.7		Trunk	1.3000E+01
Net	173.1		Leaf	0.0000E+00
<u>Soil Solution</u>				
Release from Storage	4.3		Soil Solution	2.1858E+03
Nitrification	-188.5			
Fulvic Acid Decay	5.5			
Net	-158.7			
<u>Soil Processes</u>				
Cation Exchange	128.1		Cat Ex Storage	1.3145E+06
Anion Adsorption	17.5		Anion Ads Storage	-1.3696E+04
Weathering	65.5			
Gibbsite Dissolution	9.6			
Net	220.7			
<u>Soil Organic Matter</u>				
Release from Storage	-14.8		Organic Storage	1.8903E+04
Fulvic Acid Formation	-11.7			
Net	-26.5			
<u>Lake</u>				
Release from Storage	1.9		Lake Storage	1.2828E+02
Nitrification	-22.4			
Fulvic Acid Decay	5.4			
Gibbsite Precip.	-7.2			
Algal Growth	37.3			
Net	14.9			
Sum of Internal Sources	223.5			
Basin Output	128.2			

**TABLE D.7. ILWAS Code, 1984 ANC Budget Storage for Panther Lake:
Base-Case Deposition Scenario ($\text{meq}\cdot\text{m}^{-2}\cdot\text{yr}^{-1}$ of
terrestrial area)**

		<u>ANC Values</u>		
<u>Atmospheric Inputs</u>				
<u>Terrestrial</u>				
Wet		-76.8		
Dry		-22.7		
Net		-98.7		
<u>Internal Sources</u>			<u>Watershed Storage</u>	
<u>Canopy/Trunk/Leaf</u>				
Release from Storage	-42.8		Canopy	2.8258E+03
Nitrification	217.1		Trunk	2.7888E-01
Net	175.1		Leaf	8.8888E+00
<u>Soil Solution</u>				
Release from Storage	3.5		Soil Solution	2.1823E+03
Nitrification	-181.3			
Fulvic Acid Decay	5.4			
Net	-152.4			
<u>Soil Processes</u>				
Cation Exchange	128.8		Cation Exchange	1.3144E+06
Anion Adsorption	18.3		Anion Adsorption	-1.3712E+04
Weathering	65.6			
Gibbsite Dissolution	7.7			
Net	218.4			
<u>Soil Organic Matter</u>				
Release from Storage	18.5		Organic	1.8921E+04
Fulvic Acid Formation	-11.4			
Net	-38.8			
<u>Lake</u>				
Releases from Storage	-3.8		Lake	1.3128E+02
Nitrification	-18.6			
Fulvic Acid Decay	4.1			
Gibbsite Precip.	-8.1			
Algal Growth	37.2			
Net	11.5			
Sum of Internal Sources	222.6			
Basin Output	124.8			

**TABLE D.8. ILWAS Code, 1982 ANC Budget Storage for Woods Lake:
Base-Case Deposition Scenario (meq•m⁻²•yr⁻¹ of
terrestrial area)**

		<u>ANC Values</u>		
<u>Atmospheric Inputs</u>				
<u>Terrestrial/Lake</u>				
Wet		-87.0		
Dry		-28.0		
Net		-115.0		
<u>Internal Sources</u>			<u>Watershed Storage</u>	
<u>Canopy/Trunk/Leaf</u>				
Release from Storage	-82.1		Canopy	1.9447E+03
Nitrification	258.1		Trunk	5.5000E+01
Net	176.0		Leaf	0.0000E+00
<u>Soil Solution</u>				
Release from Storage	2.4		Soil Solution	1.7287E+02
Nitrification	-191.7			
Fulvic Acid Decay	4.3			
Net	-185.1			
<u>Soil Processes</u>				
Cation Exchange	59.4		Cation Exchange	6.6702E+04
Anion Adsorption	7.3		Anion Adsorption	-3.6986E+03
Weathering	11.5			
Gibbsite Dissolution	31.0			
Net	109.2			
<u>Soil Organic Matter</u>				
Release from Storage	19.0		Organic	2.0248E+04
Fulvic Acid Formation	-12.9			
Net	6.1			
<u>Lake</u>				
Release from Storage	0.0		Lake	4.5100E+00
Nitrification	-26.0			
Fulvic Acid Decay	6.3			
Gibbsite Precip.	-9.8			
Algal Growth	25.3			
Net	-4.2			
Sum of Internal Sources	102.1			
Basin Output	-13.0			
Atm Input + Internal Sources	-12.9			

**TABLE D.9. ILWAS Code, 1983 ANC Budget Storage for Woods Lake:
Base-Case Deposition Scenario (meq•m⁻²•yr⁻¹ of
terrestrial area)**

		<u>ANC Values</u>		
<u>Atmospheric Inputs</u>				
<u>Terrestrial/Lake</u>				
Wet		-83.8		
Dry		-24.2		
Net		-87.2		
<u>Internal Sources</u>			<u>Watershed Storage</u>	
<u>Canopy/Trunk/Leaf</u>				
Release from Storage	-82.6		Canopy	2.8277E+03
Nitrification	265.5		Trunk	1.5000E+01
Net	182.9		Leaf	8.0000E+00
<u>Soil Solution</u>				
Release from Storage	8.8		Soil Solution	1.7288E+02
Nitrification	-196.6			
Fulvic Acid Decay	4.3			
Net	-192.3			
<u>Soil Processes</u>				
Cation Exchange	51.4		Cation Exchange	6.8650E+04
Anion Adsorption	3.2		Anion Adsorption	-3.6998E+03
Weathering	11.5			
Gibbsite Dissolution	27.8			
Net	93.1			
<u>Soil Organic Matter</u>				
Release from Storage	17.3		Organic	2.8229E+04
Fulvic Acid Formation	-12.9			
Net	4.4			
<u>Lake</u>				
Release from Storage	2.4		Lake	2.1100E+00
Nitrification	25.9			
Fulvic Acid Decay	6.3			
Gibbsite Precip.	-11.5			
Algal Growth	24.7			
Net	-4.1			
Sum of Internal Sources	84.1			
Basin Output	-3.8			
Atm Input + Internal Sources	-3.8			

TABLE D.10. ILWAS Code, 1984 ANC Budget Storage for Woods Lake:
Base-Case Deposition Scenario ($\text{meq}\cdot\text{m}^{-2}\cdot\text{yr}^{-1}$ of
terrestrial area)

		<u>ANC Values</u>		
<u>Atmospheric Inputs</u>				
<u>Terrestrial/Lake</u>				
Wet		-75.3		
Dry		-23.5		
Net		-98.8		
<u>Internal Sources</u>			<u>Watershed Storage</u>	
<u>Canopy/Trunk/Leaf</u>				
Release from Storage	-84.3		Canopy	2.1107E+03
Nitrification	254.3		Trunk	1.4700E+00
Net	170.0		Leaf	0.0000E+00
<u>Soil Solution</u>				
Release from Storage	-1.4		Soil Solution	1.7430E+01
Nitrification	-195.8			
Fulvic Acid Decay	4.4			
Net	-192.8			
<u>Soil Processes</u>				
Cation Exchange	72.2		Cation Exchange	6.8578E+04
Anion Adsorption	-1.1		Anion Adsorption	-3.8988E+03
Weathering	11.6			
Gibbsite Dissolution	28.1			
Net	110.8			
<u>Soil Organic Matter</u>				
Release from Storage	18.9		Organic	2.0210E+04
Fulvic Acid Formation	-12.9			
Net	110.8			
<u>Lake</u>				
Release from Storage	-3.1		Lake	5.2500E+00
Nitrification	-23.0			
Fulvic Acid Decay	5.8			
Gibbsite Precip.	-9.8			
Algal Growth	28.3			
Net	-4.1			
Sum of Internal Sources	89.8			
Basin Output	-8.9			
Atm Input + Internal Sources	-8.9			

APPENDIX E

SINGLE VARIABLE PERTURBATION BEHAVIORAL ANALYSIS

APPENDIX E

SINGLE VARIABLE PERTURBATION BEHAVIOR ANALYSIS

Numerous approaches have been used to establish confidence in the behavior of mathematical models. With simple models, it is possible to compare algorithms in the actual code with equations derived from basic principles. This approach is impractical for the more complex watershed acidification models which may involve thousands of lines of code and hundreds of variables. An alternative approach taken in this report was to perturb the calibrated value of one variable at a time, using calibrated datasets provided by the authors of the models. The calibrated values were both increased and decreased, to test for potentially anomalous results. Some details of the approach used and resultant effects on forecasted surface water alkalinity and sulfate concentrations are given in this appendix. The results of these single variable perturbations are used in Sections 3.0, 4.0, and 5.0 of this report.

Those calibrated process-related variables that had previously been found to have an important impact (Cosby et al. 1986, Lee 1987, Nikolaidis 1987) on surface water alkalinity, or were judged to potentially have such an impact, were included in this analysis. Although soil depth is of obvious importance, perturbation of the depths of soil compartments is constrained by the definition of depths used in a model. In the ETD model, the depth of the unsaturated-plus-saturated compartment is defined as the difference between the defined soil depth and the depth to bedrock. The relative depths of the unsaturated and saturated compartment are defined by the effective water depth. Thus, in both the single variable perturbation behavior analysis and the sensitivity analysis, only the depth of the soil (DEP3) was varied. In the case of the MAGIC model, water flow is partitioned between two layers by the TOPMODEL hydrologic preprocessor. Thus, the depth of the soil layers can not be varied without recalibration of the MAGIC code which defeats the purpose of this type of analysis. The selected input variables were generally perturbed by the same percentage of their calibration value for all three lakes.

Selection of appropriate ranges over which to perturb individual variables is difficult. For measured input variables, the range of values reported in the literature was generally used to establish the perturbation values, in all other instances, the variables were perturbed by $\pm 20\%$ relative to their calibration values. Certain subsets of variables (representative variables) in the ETD model (HR4, HR5, HR6; KH4, DH5, KH6; and MC4, MC5, MC6) were perturbed simultaneously by the same percentage. This procedure forces all the variables in the subset to change proportionally (i.e., changes are linearly related) and effectively reduces the number of variables in the subset to one).

The interpretation of results of single variable perturbation behavior analysis is, of course, confounded by any covariance that may exist among variables. Only those variables that were observed to behave in a counter intuitive manner were investigated further. For example, the single variable behavior analysis showed that surface water alkalinity increased as a result both of increasing and decreasing the value of porosity of the groundwater compartment (PORE6), noncalibrated variable. Because this did not conform to expectations, additional perturbations of the value of PORE6 were performed as is shown in Figure E.1. The variability of meteorological data (i.e., precipitation, air temperature, evaporation potential, etc.) makes it difficult to interpret the response of the model to specific variables. Therefore to clarify the issue of the ETE code response to variations in PORE6, the foregoing approach was modified to examine the predicted response to a controlled moisture perturbation. All meteorological and deposition parameters were held constant for a period of time, then a single meteorological parameter (e.g., rainfall) would be perturbed from its initial zero value, and after a period of constant precipitation, the precipitation rate returned to its initial zero state. Figure E.2 shows the flow of water from the unsaturated zone compartment to the groundwater compartment in the ETD code where the watershed was subjected to a constant rate of precipitation (1 cm/day) for 30 days, and then the precipitation was allowed to return to its initial zero state. The next step was to examine the actual source code to

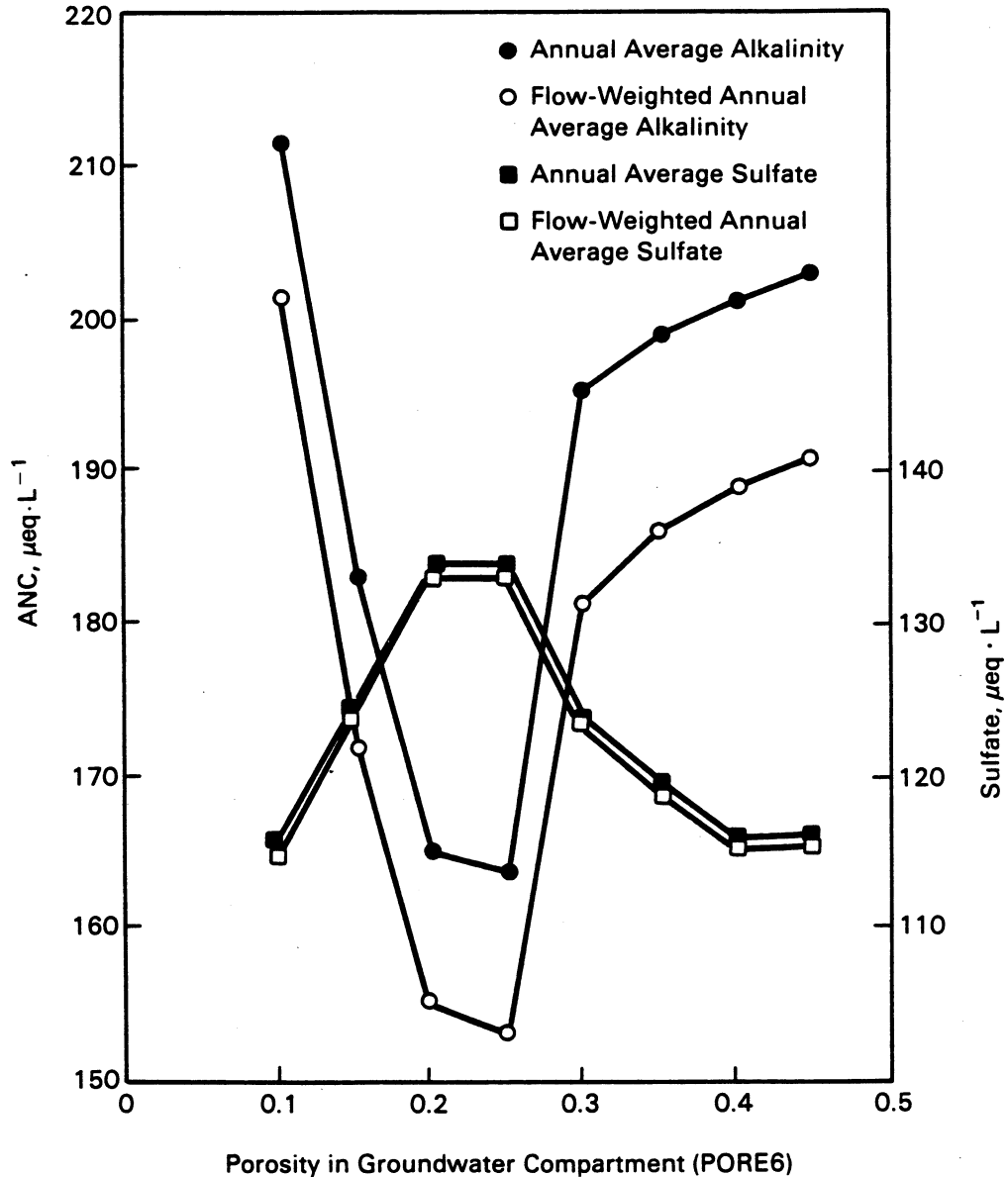


FIGURE E.1. Variation in ANC and Sulfate Concentrations with Perturbation of the Porosity Variable, PORE6, in the Groundwater Compartment

This set of plots revealed that when the soil and unsaturated zones reach some minimum moisture content, the concentrations of dissolved identify the algorithms in which PORE6 was used. It was found that these perturbations violated assumptions in the ETD code concerning water table in the groundwater compartment and lake stage relationships.

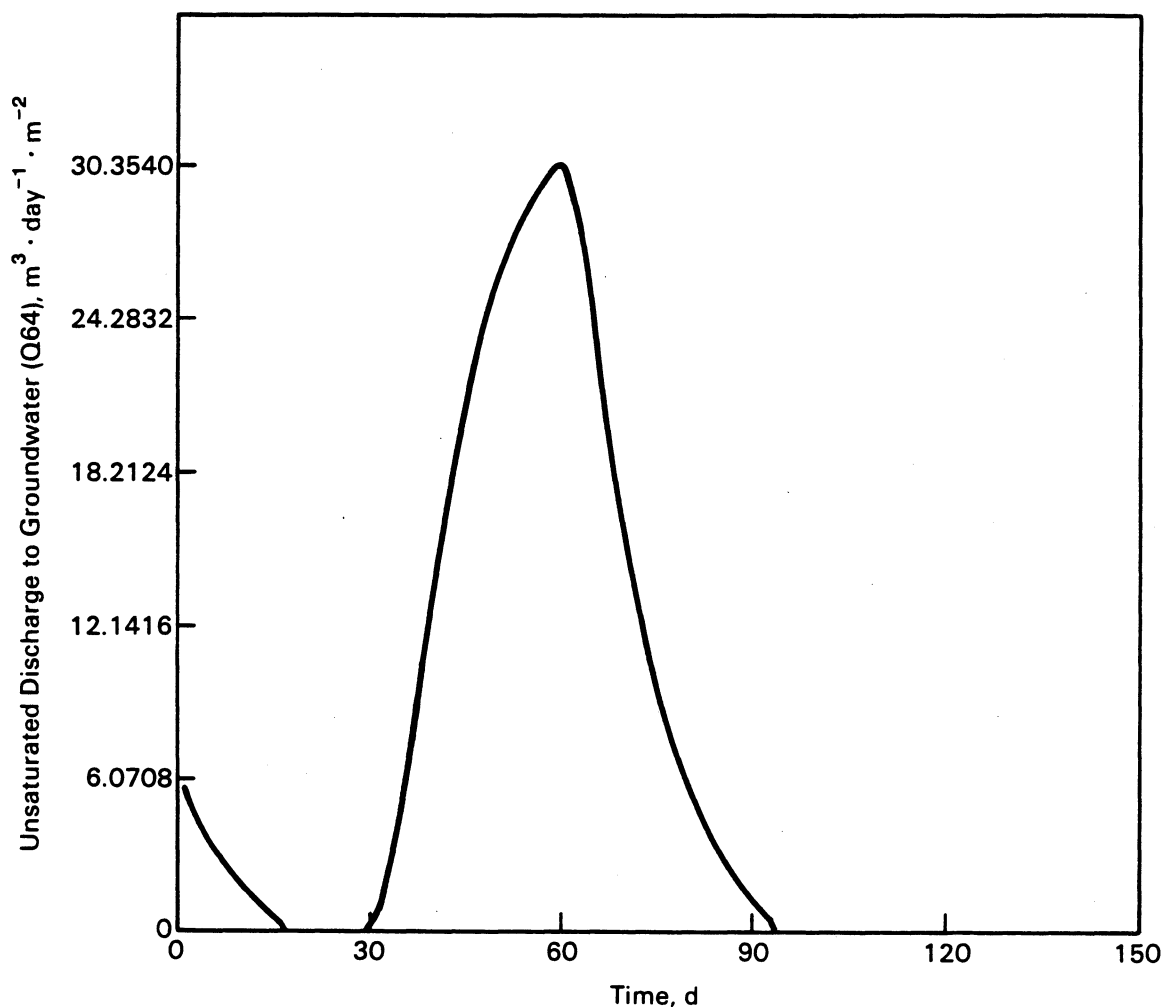


FIGURE E.2. Variation in Flow from the Unsatrated Compartment to the Groundwater Compartment with Zero Precipitation for 30 Days, Constant Precipitation for 30 Days, Followed by Zero Precipitation for the Remaining Time

constituents go to zero. When precipitation occurs, the concentrations of sulfate and alkalinity in the soil and unsaturated zones increase from zero with time. It would be more reasonable to initialize dissolved constituents to their concentrations when the equivalent moisture depth was set to zero. A letter from Dr. Jerry Schnoor, dated July 5, 1988, indicates that the code has been modified to accomplish this.

TABLE E.1. Single Variable Behavioral Analysis with ETD Model (flow-weighted annual-average surface-water alkalinity and sulfate concentrations: average of the last 3 yr of a 15-yr simulation)

Variable Description	Name	Range	Variable Value		Compartment(a)	Panther Lake		Woods Lake		Clear Pond	
			Panther	Woods		Alkalinity	Sulfate	Alkalinity	Sulfate	Alkalinity	Sulfate
Base Case	none	-	-	-	-	155	133	-10.5	147	114	126
Sulfate Deposition	none	±20%	1.0	1.0	1.0	157(152)(b)	129(147)	-7.0(-15.5)	133(163)	117(112)	112(141)
Hydraulic Conductivity (of bed and GW)	CBED	±20%	4.500E+0	3.200E-1	4.320E-1 GW	154(157)	133(129)	-10.9(-10.3)	146(147)	114(114)	126(126)
	DEP3	±20%	6.300E-1	3.604E-1	5.500E-1 Soil	159(152)	119(132)	-6.6(-12.5)	145(146)	123(126)	108(107)
H ⁺ Reference Concentrations	HR	±20%			(c)	103(148)	133(133)	-7.7(-12.9)	147(147)	128(106)	126(126)
H ⁺ Reference Concentration	HR4	±20%	1.000E-5	1.000E-6	1.000E-5 Unsat	156(154)	133(133)	-10.1(-10.9)	147(147)	115(114)	126(126)
H ⁺ Reference Concentration	HR5	±20%	1.000E-6	1.000E-5	1.000E-7 Lake	102(149)	133(133)	-8.5(-12.2)	147(147)	125(106)	126(126)
H ⁺ Reference Concentration	HR6	±20%	3.160E-7	1.000E-6	3.160E-6 GW	155(155)	133(133)	-10.2(-10.6)	147(147)	114(114)	126(126)
Sulfate Reduction Rate Constant	K	±20%	2.033E-3	2.033E-3	1.033E-3 Lake	152(157)	136(131)	-12.0(-9.1)	150(144)	113(116)	129(124)
Snow Melt Rate	KAPPA	±20%	1.142E+0	1.142E+0	1.142E+0 Snow	165(139)	130(137)	-5.2(-11.4)	141(144)	121(108)	133(127)
Hydrolysis Rate Constants	KH	±20%			(c)	142(167)	133(133)	-16.2(-5.9)	147(147)	97.2(130)	126(126)
	Hydrolysis Rate Constant KH4	±20%	7.000E-1	5.990E-2	4.000E-1 Unsat	153(156)	133(133)	-11.4(-9.8)	147(147)	113(115)	126(126)
Hydrolysis Rate Constant KH5	±20%	3.500E-1	6.000E-2	1.290E-1 Lake	144(166)	133(133)	-14.6(-7.1)	147(147)	97.2(129)	126(126)	
Hydrolysis Rate Constant KH6	±20%	2.000E-2	2.000E-2	5.000E-4 GW	154(155)	133(133)	-11.2(-10.0)	147(147)	114(114)	126(126)	
Lateral Flow Correction Coefficient	KLATS	±20%	4.528E+0	2.428E+2	5.478E+1 Soil	157(155)	134(120)	-6.5(-12.7)	151(140)	117(116)	127(107)

TABLE E.1. (contd)

Variable Description	Name	Range	Variable			Component (a)	Panther Lake		Woods Lake		Clear Pond	
			Panther	Woods	Clear		Alkalinity	Sulfate	Alkalinity	Sulfate	Alkalinity	Sulfate
Lateral Flow Correction Coefficient	KLAT4	±20%	4.979E+0	1.479E+1	5.579E+1	Unsat	158(155)	124(130)	-9.6(-11.2)	147(147)	115(121)	127(106)
Ligand Attachment Rate Constant	K04	±20%	1.000E-1	2.000E-2	1.100E-2	Unsat	154(155)	133(133)	-10.7(-10.4)	147(147)	114(114)	126(126)
Ligand Attachment Rate Constant	K05	±20%	2.000E-1	2.000E-2	1.100E-2	Lake	142(108)	133(133)	-11.5(-9.6)	147(147)	114(115)	126(126)
Sulfate Partition Coefficient	KP3	±20%	5.000E-5	6.000E-5	9.000E-5	Soil	154(155)	134(133)	-10.0(-10.3)	148(146)	114(114)	126(126)
Pan Correction Coefficient	KPAN2	±20%	1.700E-1	1.007E+0	1.700E-1	Snow	154(153)	132(137)	-9.2(-5.7)	142(142)	110(115)	131(127)
Pan Correction Coefficient	KPAN3	±20%	1.547E+0	1.547E+0	1.317E+0	Soil	153(157)	131(126)	-10.9(-9.9)	146(146)	112(124)	123(110)
Pan Correction Coefficient	KPAN5	±20%	1.538E+0	1.638E+0	1.038E+0	Lake	150(160)	129(130)	-10.6(-10.5)	142(151)	112(117)	123(130)
Hydraulic Conductivity Coefficient, Vertical	KPERC3	±20%	4.312E-3	1.312E-2	2.312E-2	Soil	150(156)	134(116)	-12.7(-8.2)	150(143)	123(113)	110(125)
Hydraulic Conductivity Coefficient, Vertical	KPERC4	±20%	4.174E-3	1.174E-2	2.174E-2	Unsat	155(155)	133(133)	-10.5(-10.5)	147(147)	114(114)	126(126)
Hydrolysis Rate, Fractional Order Dependence	MC	±20%				(c)	163(147)	133(133)	-11.0(-9.6)	147(147)	104(124)	126(126)
Hydrolysis Rate, Fractional Order Dependence	MC4	±20%	5.000E-1	5.000E-1	5.000E-1	Unsat	156(155)	133(133)	-11.1(-10.1)	147(147)	114(114)	126(126)
Hydrolysis Rate, Fractional Order Dependence	MC5	±20%	6.000E-1	5.000E-1	6.000E-1	Lake	162(148)	133(133)	-11.2(-9.9)	147(147)	104(124)	126(126)

□ ○

TABLE E.1. (contd)

Variable Description	Name	Range	Variable		Compartment(a)	Panther Lake		Woods Lake		Clear Pond	
			Panther	Woods		Alkalinity	Sulfate	Alkalinity	Sulfate	Alkalinity	Sulfate
Hydrolysis Rate, Fractional Order Dependence	MC6	±20%	5.000E-1	5.000E-1	5.000E-1 GW	155(155)	133(133)	-10.5(-10.6)	147(147)	114(114)	126(126)
	PORE3	0.1(0.45)	2.700E-1	2.700E-1	2.700E-1 Soil	178(147)	83(135)	3.5(-14.2)	113(154)	127(111)	76(127)
	PORE4	0.1(0.45)	2.000E-1	2.000E-1	2.000E-1 Soil	158(169)	116(129)	-12.0(-5.3)	141(147)	119(119)	108(126)
	PORE6	0.1(0.45)	2.000E-1	2.000E-1	2.000E-1 Unsat	208(191)	115(116)	-10.0(-13.0)	147(147)	114(110)	126(124)
Ion Exchange Rate Coefficient	RE3	±20%	4.500E-6	2.900E-7	3.000E-6 Soil	152(158)	133(133)	-12.9(-8.5)	147(147)	112(116)	126(126)

----- μeq.L⁻¹ -----

(a) GW = groundwater, Unsat = unsaturated
 (b) The first value is the result of the lower end of range and the value in parentheses is the upper end of the range.
 (c) This variable was changed in soil, unsaturated, and lake compartments simultaneously.

APPENDIX E REFERENCES

- Cosby, B. J., G. M. Hornberger, R. F. Wright, and J. N. Galloway. 1986. "Modeling the Effects of Acid Deposition: Control of Long-Term Sulfate Dynamics by Soil Sulfate Adsorption." Water Res. Res. 22:1283-1291.
- Lee, Sijin. 1987. Uncertainty Analysis for Long-Term Acidification of Lakes in Northeastern USA. Ph.D. thesis, University of Iowa, Ames, Iowa.
- Nikolaidis, N. 1987. Modeling the Direct Versus Delayed Response of Surface Waters to Acid Deposition in Northeastern United States. Ph.D. thesis, University of Iowa, Ames, Iowa.

DISTRIBUTION

<u>No. of Copies</u>		<u>No. of Copies</u>
	<u>OFFSITE</u>	
20	T. C. Strickland Environmental Research Laboratory Environmental Protection Agency 200 S.W. 35th St. Corvallis, OR 97333	T. Lee Dept. of Civil Engineering Madison and Washington Streets Engineering Building University of Iowa Iowa City, IA 52242
10	DOE/Office of Scientific and Technical Information J. B. Cosby Department Environmental Sciences University of Virginia Charlottesville, VI 22903 E. H. Dolacek L-383 Lawrence Livermore Laboratory Livermore, CA 94550 S. A. Gherini Tetra Tech, Inc. 3746 Mt. Diablo Blvd. Suite #300 Lafayette, CA 94549 L. F. Hankins National Bureau of Standards Washington, DC 20234 G. M. Hornberger Department Environmental Sciences University of Virginia Charlottesville, VI 22903	R. K. Munson Tetra Tech, Inc. 3746 Mt. Diablo Blvd. Suite #300 Lafayette, CA 94549 N. P. Nikolaidis The School of Engineering UTE Building, Room 376 191 Auditorium Road University of Connecticut Storrs, CT 06168 D. E. Phillips Argonne National Laboratory 9800 Cass Avenue Argonne, IL 60439 K. A. Rose Oak Ridge National Laboratory P.O. Box 2008 Oak Ridge, TN 37831 J. L. Schnoor Dept. of Civil Engineering Madison and Washington Streets Engineering Building University of Iowa Iowa City, IA 52242

No. of
Copies

K. W. Thorton
FTN Associates Ltd.
3 Innword Circle #220
Little Rock, AK 72211

ONSITE

DOE Richland Operations
Office

E. C. Norman

45 Pacific Northwest Laboratory

J. W. Cory
L. J. Criscenti
L. E. Eary
J. W. Falco
D. C. Girvin
M. J. Graham

No. of
Copies

Pacific Northwest Laboratory
(contd)

J. M. Hales
P. C. Hays
L. F. Hibler
E. A. Jenne (20)
A. M. Liebetrau
T. B. Miley
M. J. Monsour
R. G. Riley
R. L. Skaggs
R. W. Smith
J. A. Stottlemire
L. W. Vail
J. R. Weber
R. E. Wildung
Publishing Coordination
Technical Report Files (5)